Walking Molecules

Mark D. Symes

Degree of Doctor of Philosophy
School of Chemistry
University of Edinburgh
April, 2009

For my parents

Table of Contents

Abstract

Inspired by the motor protein kinesin, an ambitious and unprecedented mimic is proposed – a synthetic molecular motor that can walk. This thesis aims to explain the basic principles which define such walking molecules, with reference to both natural and synthetic systems. In light of these tenets, the rational design of the proposed synthetic kinesin analogue will then be expounded. The putative design envisages the use of a series of stimuli-induced binding events to cause a "walker unit" to process along a polypyridyl track in a unidirectional, hand-over-hand fashion. The chemistry behind the stepping mechanisms of both feet of the walker unit will be discussed in detail, along with a complete description of the synthesis of the track and walker unit to date. The future challenges and potential applications of the proposed system will be addressed.

Declaration

The scientific work described in this Thesis was carried out in the School of Chemistry at the University of Edinburgh between September 2005 and December 2008. Unless otherwise stated, it is the work of the Author and has not been submitted in whole or in part in support of an application for another degree or qualification at this or any other University or institute of learning.

Signed…….

Date…….

Meetings and Lectures Attended and Presentations Given

1. **Organic Research Seminars**, School of Chemistry, University of Edinburgh, UK, 2005-2008.
   Oral Presentations:
   a) *Towards Synthetic Kinesin Analogues: Molecular Machines that Can Walk*, March 2006.
   b) *A Protonmotive Palladium-Containing Molecular Shuttle and its Metastable Positional Isomers*, January 2007.
   c) *Towards Synthetic Kinesin Analogues: Molecular Machines that Can Walk*, March 2008.

2. **School of Chemistry Visiting Speaker Colloquia**, School of Chemistry, University of Edinburgh, UK, 2005-2008.

3. **RSC Perkin Division 34th Scottish Regional Meeting**, University of Strathclyde, UK, December, 2005.

4. **University of St. Andrews, UK**, July, 2006
   Oral presentation: *Towards Synthetic Kinesin Analogues: Molecular Machines that Can Walk.*

5. **The Young(-ish!) Giants of Chemistry: A Symposium Marking the Sixty-Fifth Birthday of Sir J. Fraser Stoddart**, University of Edinburgh, June, 2007
   Poster presentation: *A protonmotive palladium-based molecular shuttle.*

6. **NMR Methods**, eight-lecture course on advanced NMR techniques, School of Chemistry, University of Edinburgh, UK, June, 2007.

7. **2nd International Symposium on Macrocyclic and Supramolecular Chemistry**, Salice Terme, Italy, June, 2007
   Poster presentation: *A protonmotive palladium-based molecular shuttle.*

8. **RSC Perkin Division 35th Scottish Regional Meeting**, University of Glasgow, UK, December, 2007
   Poster presentation: *A traceless Cadiot-Chodkiewicz active-metal template route to rotaxanes.*

9. **3rd International Symposium on Macrocyclic and Supramolecular Chemistry**, Las Vegas, USA, July, 2008
   Poster presentation: *Cadiot-Chodkiewicz active template synthesis of rotaxanes and switchable molecular shuttles with weak intercomponent interactions.*

10. **RSC Discussion Group Meeting: Inorganic Reaction Mechanisms and Coordination Chemistry Symposium**, University of Edinburgh, June, 2008
    Oral presentation: *A protonmotive palladium-based molecular shuttle.*

11. **42nd Annual Universities of Scotland Inorganic Chemistry Conference**, University of Strathclyde, September, 2008
Oral presentation: *Protonmotive palladium-based molecular shuttles and walking molecules.*

12. **Special Symposium in Honour of David Reinhoudt**, School of Chemistry, University of Edinburgh, UK, November, 2008
Oral presentation: *Synthetic Kinesin Analogues: Molecular Machines that Can Walk.*

Acknowledgements

First and foremost, I must thank my supervisor, Professor David Leigh, for all his encouragement and support over the last three (and a bit) years, both academically and personally. His patience and enthusiasm have been, and continue to be, a real boon when times are tough.

I must also give special thanks to Dr. Paul Lusby, the brains behind the brawn of Team Walker. Without his ideas and his help, Chapters Three and Four of this thesis would not exist, and I would be a much poorer chemist for it.

As far as day-to-day supervision is concerned, there are two chemists to whom I owe an enormous debt of gratitude. The first is Dr. James Crowley, about whom it is no exaggeration to say that he taught me everything I know about practical synthetic chemistry. The second is Dr. Stephen Goldup, who mentored me through the trying times of my final year and who was never too busy to lend a friendly ear. Between them, these two are surely the best role-models that an aspiring chemist could have, and I am proud to consider them not only as colleagues, but also as friends.

Aside from these characters, I thank those with whom it has been my pleasure to work over the last three years (in no particular order): Vicki "V-Dawg" Ronaldson, Roy "Calamity" McBurney, Daniel D'Souza, Romen Carrillo, Barry Blight, Christiane Petzold, Michael Zengerle, Jhenyi Wu, Tao Long, Pepe Berná, Ai-Lan ("I know you!") Lee and Nick Gowans. Special thanks also to Diego Gonzalez-Cabrera (the man who taught me everything I know about fixing the NMR machine…), and to Max "Von Genius" von Delius and Paul "phenomenal" McGonigal for taking over the running of the machine from me and not telling anyone quite how badly I had maintained it. Thanks also to Bryan Koivisto and Paul Murray for all their help with the electrochemical studies in Chapter Five.

As far as collaborators at other universities are concerned, I would like to thank Alex Slawin at the University of St. Andrews for solving various X-ray crystal structures

and Francesco Zerbetto and Gilberto Teobaldi for the computational studies reported in Chapter Two.

Then there are those guys that I didn't get to work with, but that have helped to make the Group such a great place to work, in (roughly) chronological order: Euan, Barney, Drew, Anne-Marie, Julia, Smilja, Steve "The Mason?" Mason, Vince, Louise, Stewart, Laure, Weiquan, Chin-Fa, Andrea (thanks for putting out the fire), Marius, Aurélien, Mike, Max, Amaya, Satoshi, Monica, David, Phill, Adam, Katherine, Luciana, Kevin (that's the spirit that built America!), Takeshi, Anthony, Edzard-o, Dominik, Nathalie and all the others that I have surely forgotten…

Thanks also to all the support staff here at Edinburgh University: Amanda and Annette upstairs, Kenny, Tim, Derek and Raymond in stores, Alan Taylor, John Dalrymple and Paul "Casual" Angus in the mass spec. room and Juraj Bella and John Millar in the NMR suite (is there anything those guys *don't* know about NMR?).

And then there's the people that really matter: the people who (on the whole) don't work in the Chemistry Dept. Where would I have been without them? A huge thanks must go to my ever-patient house mates, for looking after me when I was too busy to do things for myself: Chris, Jen, Harry, Rob, Nat and especially John and Kirstie (although they knew what I was like before, so it's their own fault) and George (the same comment, but twice).

Thank you to Katherine, for all your understanding and love. I am a lucky man.

And finally, the family. Thank you to Richard (who first taught me to walk), Philip (for making me go to at least *some* of the festival each year) and my parents. Their counsel, love and support (financial, emotional, practical) have seen me through seven years of University education – this thesis is for you.

List of Abbreviations

δ	Chemical Shift
ATP	Adenosine triphosphate
Bipy	2,2'-Bipyridine
BOC	*tert*-Butyloxycarbonyl
Calc.	Calculated
CPK	Corey-Pauling-Koltun
CV	Cyclic Voltammetry
DBU	1,8-Diazabicyclo[5.4.0]undec-7-ene
dec.	Decomposes
DIAD	Diispropylazodicarboxylate
DMAP	4-Dimethylaminopyridine
DMEDA	*N,N'*-Dimethylethylenediamine
DMF	*N,N'*-Dimethylformamide
DMSO	Dimethylsulfoxide
DNA	Deoxyribonucleic acid
EDCI	1-(3-Dimethylaminopropyl)-3-ethylcarbodiimide hydrochloride
EDTA	Ethylenediaminetetraacetic acid
EI	Electron impact
equiv.	Equivalent(s)
ESI	Electrospray ionisation
Et_2O	Diethyl ether
EtOAc	Ethyl acetate
EtOH	Ethanol
FAB	Fast atom bombardment
H-bond	Hydrogen bond
HRMS	High resolution mass spectrometry
J	Coupling constant
LRMS	Low resolution mass spectrometry
Me	Methyl
MeOH	Methanol

MHz	Megahertz
min	minutes
m.p.	Melting Point
MS	Mass spectrometry
m/z	Mass-to-charge ratio
NMP	*N*-Methylpyrrolidone.
NMR	Nuclear magnetic resonance
3-NOBA	3-Nitrobenzyl alcohol
$Pd(dppf)Cl_2$	Dichloro[1,1'-bis(diphenylphosphino)ferrocene] palladium
$Pd(PPh_3)_4$	Tetrakis(triphenylphosphine)palladium(0)
$Pd(PPh_3)_2Cl_2$	Bis(triphenylphosphine)palladium dichlororide
Ph	Phenyl
phen	1,10-Phenanthroline
ppm	Part(s) per million
quant.	Quantitative
RT	Room temperature
SCE	Saturated calomel electrode
TBABF	Tetrabutylammonium tetrafluoroborate
terpy	2,2':6',2''-Terpyridine
TFA	Trifluoroacetic acid
THF	Tetrahydrofuran
THIOG	Thioglycerol
TLC	Thin layer chromatography
TsOH	4-*para*-Toluenesulfonic acid

Note: conventional abbreviations for units and physical quantities are not included.

General Remarks on Experimental Data

Unless stated otherwise, all reagents and anhydrous solvents were purchased from Aldrich Chemicals and used without further purification. Tetrahydrofuran, dichloromethane, chloroform, toluene, methanol, acetonitrile and *N*,*N*-dimethylformamide were dried using a solvent purification system manufactured by Innovative Technology, Newburyport, MA, USA. Unless stated otherwise, all reactions were carried out under an atmosphere of nitrogen. Column chromatography on silica was carried out using Silica 60A (particle size 35-70 μm, Fisher, UK) as the stationary phase, and TLC was performed on precoated silica gel plates (0.25 mm thick, 60 F_{254}, Merck, Germany) and observed under UV light. Microwave reactions were performed using a CEM Microwave Technology (Buckingham, UK) Discover apparatus, in Open Vessel mode and under one atmosphere of nitrogen. Unless otherwise stated, all ^{1}H and ^{13}C NMR spectra were recorded on a Bruker AV 400 instrument, at a constant temperature of 300 K. Chemical shifts are reported in parts per million from high to low field and referenced to residual solvent. Coupling constants (*J*) are reported in hertz (Hz). Standard abbreviations indicating multiplicity were used as follows: m = multiplet, br = broad, d = doublet, t = triplet, s = singlet. Melting points were determined using a Sanyo Gallenkamp apparatus and are reported uncorrected. FAB and EI mass spectrometry were carried out by the services at the University of Edinburgh and at the EPSRC National Mass Spectrometry Service, Swansea. Electrochemical studies were carried out using a DELL Optiplex GX110 PC with General Purpose Electrochemical System (GPES), version 4.8, software connected to an Autolab system containing a PGSTAT 20 potentiostat. The techniques used a three-electrode configuration, with a 0.5 mm diameter Pt disk working electrode, a Pt rod counter electrode, and an Ag/AgCl (saturated KCl) reference electrode against which the ferrocenium/ferrocene couple was measured to be +0.55 V. The supporting electrolyte was 0.1 M tetrabutylammonium tetrafluoroborate (TBABF). All solutions were purged with dry nitrogen prior to electrochemical study.

The Layout of this Thesis

Chapter One outlines some of the more pertinent examples of walking molecules (both natural and synthetic) along with a detailed discussion pertaining to the theory and design of synthetic walking systems. Chapters Two and Three are each presented in the form of articles that have already been published in peer-reviewed journals. No attempt has been made to re-write this work out of context, other than to insert cross-references to other Chapters (where appropriate) and to ensure consistency of presentation throughout this Thesis. These Chapters are both reproduced in the Appendix, in their published formats. Chapters Four and Five constitute the combined efforts of the Author and others towards synthetic walking systems. More specifically, Chapter Four gives an account of an (ultimately unsuccessful) initial design, and Chapter Five details the design and ongoing synthesis of an "improved" synthetic walking system (on which the Author is currently actively engaged).

CHAPTER ONE

Introduction

Acknowledgements

The Author thanks Dr. Euan Kay and Dr. Stephen Goldup for extremely useful discussions on ratchets and walkers, and Mark Witkin for his (very) patient explanation of Markov theory.

Synopsis

Controlling molecular-level motion is fundamental to all life processes. Without the ability to direct and regulate motion on the sub-nanometre scale, there would be no functioning enzymes; no self-replicating macromolecules. The Earth would be barren and sterile; the seas would be desolate voids. And yet it is only within the last half-century that a true appreciation of the molecular basis of life has been achieved. It is interesting and unsettling to note that whilst Nature uses controlled molecular motion to perform nearly all its key operations, the human race at the dawn of the 21st. century uses controlled molecular motion for nothing. This cannot remain the case indefinitely, however. The demands of technology and the very real dangers threatening our planet demand that we obtain the ability to manipulate matter on the smallest of scales. In this regard, chemistry is of vital importance. Synthetic molecular machines allow us to probe the most fundamental of the physical laws and to build imaginative and ingenious devices from the bottom up. Where Nature has shown possibilities, chemistry can deliver the practical and precise solutions required for our species' continued advancement.

This thesis aims to address one small area of this quest to control molecular-level motion. Biochemical assays have revealed a wealth of information on the natural motor proteins. Those motor proteins collectively known as Kinesins are known to "walk" along filaments within the cell, pulling molecular cargoes with them to defined destinations. However, despite the intense study these systems have received, very few attempts have been made to mimic their modes of action or to create synthetic systems able to move directionally. Those systems which have been created to date all rely on highly complex intercomponent interactions to achieve their goals and as a result further elaboration may prove very challenging. What is required is a set of principles laying out how such systems may be realised in minimalist, tuneable and robust systems. The design and synthesis of just such a fundamental, minimalist molecular walking system is the subject of this thesis.

1.1 Introduction

The challenges associated with the manipulation and control of objects on the sub-micrometre scale were first explicitly referred to by Richard Feynman in a landmark address to the American Physical Society fifty years ago.[1] Although a physicist, Feynman's inspiration came from biological systems; "At the atomic level, we have new kinds of forces and new kinds of possibilities, new kinds of effects. The problems of manufacture and reproduction of materials will be quite different. I am…inspired by the biological phenomena in which chemical forces are used in repetitious fashion to produce all kinds of weird effects…" The desire to know more about how cells use chemistry to achieve their multifarious ends has led to an explosion of understanding in the biological sciences since Feynman gave his lecture. Of particular relevance to the current discussion are studies aimed at elucidating the mode of action of motor proteins. Nature uses an array of motor proteins that are capable of controlled nano- and micrometre scale movements. These fall into two broad classes: rotary motors and linear motors.

1.2. Motor Proteins

1.2.1 Rotary Motor Proteins

One of the best studied, and certainly one of the most famous of all the motor proteins is the F_0F_1-ATPase (Figure 1.1a). The F_0 subunit of this enzyme sits in the mitochondrial inner membrane and exploits a transmembrane proton gradient to turn the camshaft unit γ and hence the F_1 subunit to which γ is attached. This facilitates the production of adenosine triphosphate (ATP) from adenosine diphosphate (ADP) and an inorganic phosphate molecule, by opening and closing the relevant active sites as the F_1 subunit rotates.[2,3] Rotary motor proteins are also capable of producing motion on the macroscopic level, with the bacterial flagellar motor being a pertinent example (Figure 1.1b). As in the F_0F_1-ATPase, the rotation of the bacterial flagellum is driven by a motor whose energy source is a proton gradient across a membrane (the cytoplasmic membrane in this case). Proton flux is tightly coupled to motor rotation and is directly proportional to motor speed.[4,5]

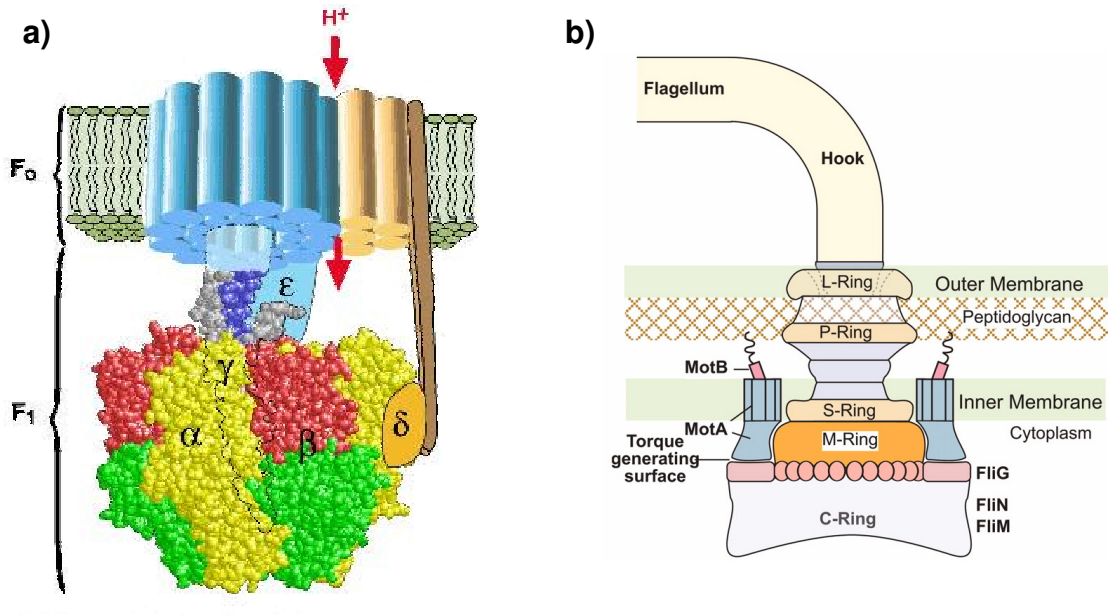

Figure 1.1 **(a)** A cartoon derived from the crystal structure of the F_0F_1-ATPase, adapted by permission from Macmillan Publishers Ltd: Nature, copyright 1998.[3] **(b)** A cartoon of the key torque-generating elements of the bacterial flagellar motor, adapted with permission from The National Academy of Sciences of the United States of America.[5]

On the macroscopic level, it is the conrotary motion of a bacterium's flagella that allows it to undertake ordered *chemotaxsis* towards (or away from) a particular stimulus. This transformation of nanometre-scale movements into macroscopic motion provides valuable insight into how synthetic molecular devices could be incorporated into the everyday world, at more human dimensions. In this regard, it is interesting to note that various filaments and beads have been successfully tethered to rotary motor proteins and these appendages used to observe the rotation of the motors directly under varying conditions.[6-9] It must be stated, however, that all rotary motor proteins are necessarily localised in the membranes that provide them with the ion gradients they need to function. Hence *linear* motor proteins provide greater scope for probing motion on the nanometre scale, as they are much less constrained with regards to their location within the cell.

1.2.2 Linear Motor Proteins

There are three general classes – or "superfamilies" – of linear motor proteins; myosins, dyenins and kinesins (Figure 1.2). The primary mode of locomotion

exhibited by all of these proteins differs fundamentally from that of the rotary motor proteins in that linear motors undertake *translation*, i.e. a net displacement of the motor itself from one part of the cell to another in a controlled fashion. The cytoplasm is an extremely crowded and viscous environment and as a consequence diffusion alone would be too slow to support the many competing reactions occurring within the cell. The controlled movement of specific cargoes to specific locations by linear motor proteins is thus essential to life.[2]

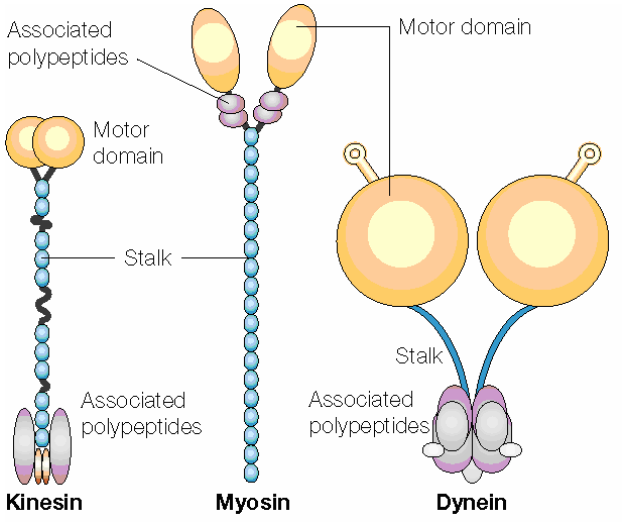

Figure 1.2 A comparative representation of the three main classes of linear motor protein. The yellowish "motor domains" contain the microtubule/actin binding sites, adapted by permission from Macmillan Publishers Ltd: Nature Reviews Molecular Cell Biology, copyright 2000.[10]

Part of this element of control is provided by the track to which individual motor proteins adhere and along which they can move, in much the same way as locomotives move on a railway. The myosins use actin filaments as tracks, whilst dyenins and kinesins both operate on microtubules. Kinesins as a family are generally well-suited to manipulation with the tools of molecular biology and the fundamental properties of these proteins have been established by the use of *in vitro* motility assays capable of measuring the physical and mechanical properties of single molecules.[11,12] Hence, although kinesins are the most recent of the three superfamilies of linear motor proteins to be discovered,[13] there is now a significant body of information concerning their behaviour, particularly kinesin-1 (also known as conventional kinesin) due to its ease of purification from the brain. The genome-sequencing project has revealed 45 different kinesins in humans alone, but only in

the motor domain is there any significant sequence homology.[14] The following more detailed description, therefore, will look specifically at the mode of action of conventional kinesin (hereafter referred to simply as "kinesin").

1.3 Kinesin

Kinesin is a homodimeric motor protein capable of directional walking with high *processivity* along microtubules, i.e. it is capable of walking large distances on the cellular scale in a defined direction without dissociation from its guiding rail. It consists of two motor heads (or "hands"), connected to a 70 nm long coiled-coil stalk (or "body") by a flexible neck linker region that enables motor stepping (Figure 1.3).[15] The stalk holds the two motor heads at an optimum separation (around 8.3 nm) and also connects the motor heads to the cargo-binding domain which can recognise various organelles and vesicles.[14,16]

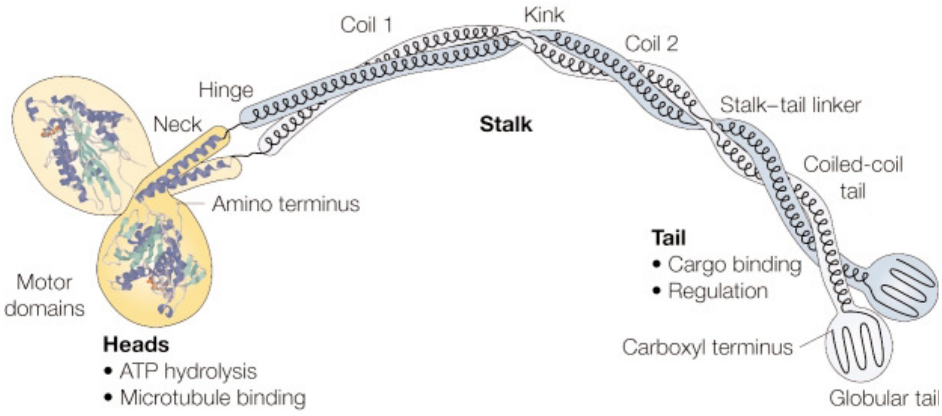

Figure 1.3 The domain organisation of conventional kinesin, based on the crystal structure of the catalytic domains and neck and electron-microscopy images of the stalk and tail regions, adapted by permission from Macmillan Publishers Ltd: Nature Reviews Molecular Cell Biology, copyright 2000.[10]

For the purposes of the current discussion, the mode of action of the head and neck regions will be of the most relevance. The two head units are identical and each consists of a catalytic core (the motor domain) that binds to tubulin subunits in the microtubule track with nucleotide-dependent affinity. When not bound to a nucleotide molecule, a head unit binds tubulin strongly. Nucleotide (normally ATP) binding then causes a conformational change in the head and neck regions of the motor domain, giving rise to a weakly-bound state. Hydrolysis of the bound ATP to

ADP and inorganic phosphate then occurs and the head dissociates completely from the microtubule track.[2] During this ATP binding and hydrolysis process, the other head of the kinesin dimer remains in the nucleotide-free and strongly bound conformation, preventing the complete dissociation of kinesin from the microtubule.[17-21] There then follows a "waiting period", during which the dissociated head may or may not be close in space to the strongly-bound head (Figure 1.4). However, the order of events that leads to ADP dissociation from the unbound head (causing it to then bind strongly to the microtubule track) and the subsequent binding of ATP to the previously strongly-bound head remains unclear, although recent evidence suggests that direct head-tail interactions play a key role.[22]

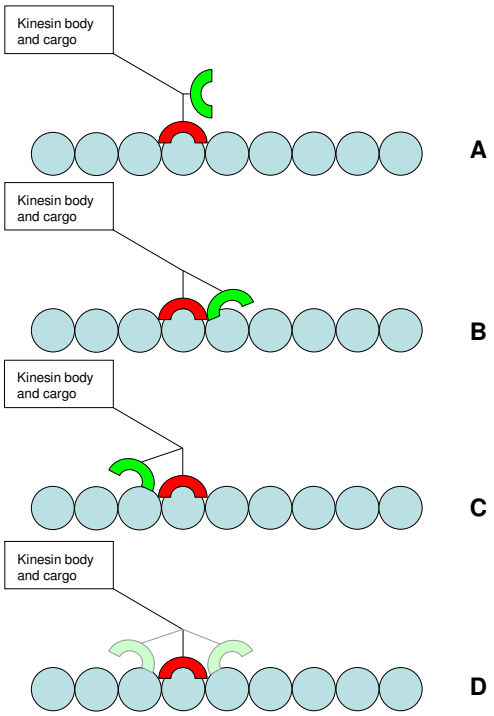

Figure 1.4 Possible locations for the dissociated head of kinesin (green) during the ATP waiting period: (A) completely detached from the track and "floating" somewhere near the strongly-bound head (red), (B) weakly bound to the "forward" binding site, (C) weakly bound to the last binding site, (D) diffusing between the forward and backward sites.

There is, however, no longer any significant debate regarding the mode of kinesin's walk. Previously, it was known that kinesin moved in 8.3 nm increments (corresponding to the typical distance between kinesin's heads as well as being roughly the spacing of the tubulin dimers in microtubules), with the hydrolysis of one molecule of ATP per step.[2] However, it was unclear whether kinesin conformed

to a "hand-over-hand" or an "inchworm" model of locomotion. In a hand-over-hand system, it is the trailing head that dissociates from the track and at some point during the ATP waiting period moves in front of the strongly bound head, eventually binding tightly to the rail at a distance of $2x$ from where it originally dissociated (where x is the observed step length – see Figure 1.5). The heads then swap roles, so for processive hand-over-hand motion both heads must hydrolyse ATP.

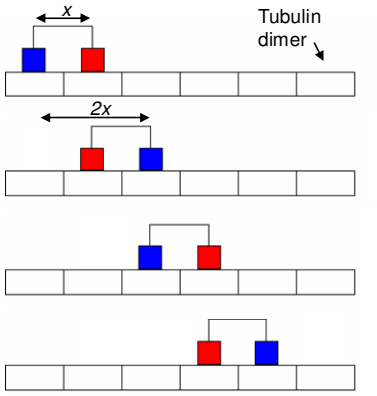

Figure 1.5 The hand-over-hand mechanism of walking, where the heads alternate roles as leading and trailing head. Heads have been coloured for clarity.

Alternatively, under an inchworm regime (Figure 1.6), one head always leads the other. This would imply that each head moves only in increments corresponding to the distance x. It would also imply that kinesin catalyses ATP hydrolysis in only one of its heads, as both its heads must move for a net displacement of x, but only one molecule of ATP is hydrolysed. To elucidate the mechanism of kinesin's walk, Kaseda *et al*[23] synthesised mutant kinesins where one head hydrolysed ATP 18 times slower than the other. Hence, depending on the position of the mutant head, an inchworm kinesin should either move at normal speed or be slowed by a factor of 18. Instead, a slowing of all the kinesins by a factor of 9 was observed. This indicates a hand-over-hand mechanism, where per net displacement of $2x$ there is one ATP hydrolysis at the usual rate (wild-type head) and one hydrolysis at a rate reduced by a factor of 18 (mutant head). Thus per step x, we see the averaged kinesin speed, reduced by a factor of 9. Yildiz *et al*[21] provided further evidence for a hand-over-hand mechanism using fluorescence labelling with one-nanometre accuracy (FIONA) to directly visualise a pre-labelled kinesin head moving only in steps of 16.6 nm ($2x$).

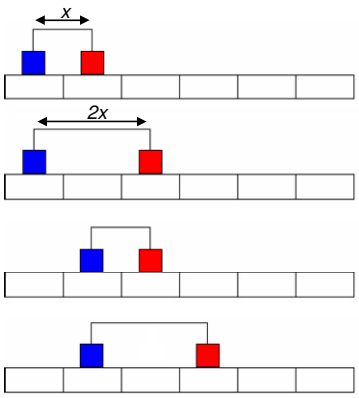

Figure 1.6 The inchworm mechanism of walking, where one head always trails the other on the microtubule. Heads have been coloured for clarity.

Another notable feature of kinesin's walk is its *unidirectionality* – i.e. kinesins tend to walk in only *one* direction along microtubules. The precise mechanism behind this still remains unclear,[18] but what is known is that microtubule tracks possess polarity.[24] Each tubulin dimer has a positive and a negative end, and these allow the self-assembly of many such dimers into long fibres which inherit the polarity of their constituents (Figure 1.7).

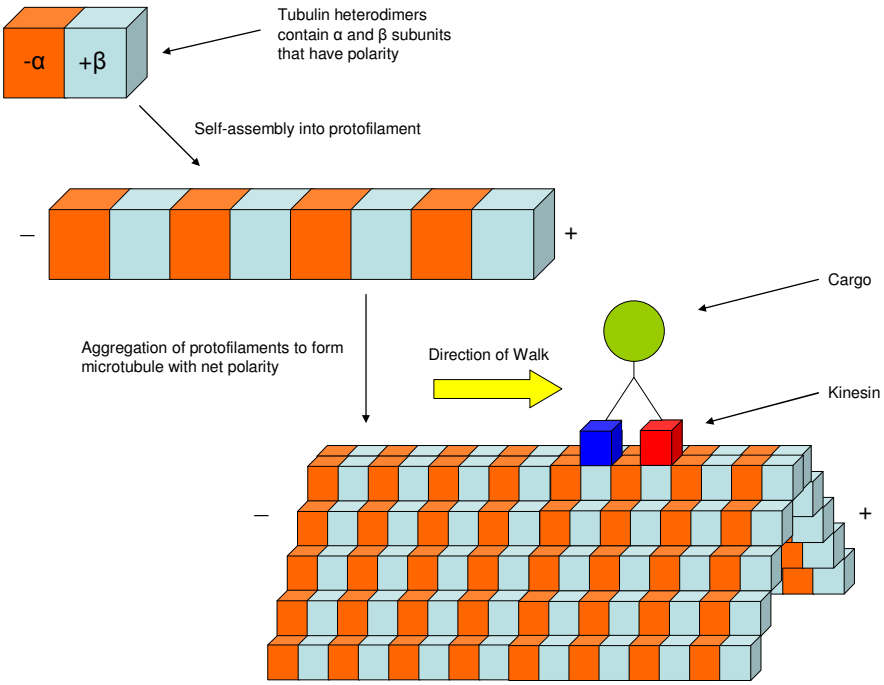

Figure 1.7 Cartoon outlining the self-assembly of tubulin into microtubules, along which conventional kinesin moves unidirectionally. Heads are coloured for clarity.

The vast majority of kinesins transport their cargoes away from the centre of the cell, towards the periphery – only three of the 45 human kinesins are known to walk towards the nucleus.[14] Furthermore, single-molecule studies in the 1990's revealed that kinesin is capable of completing around 100 ATP turnovers and hence walk up to 800 nm (in the same direction!) before dissociating from its rail.[11] By joining several kinesins to a particular cargo, cooperative binding effects can significantly increase the total distance travelled by a load before complete dissociation from the microtubule (the "run length") – theoretical calculations suggest that the run length scales as $5^{N-1}/N$, where N is the number of motors pulling a particular cargo.[25] Additionally, motility assays with kinesins attached to beads have shown that individual motors are capable of pulling against a load of up to 7 pN before stalling - i.e. an individual kinesin motor will continue to process unidirectionally towards the positive end of a microtubule, even against a retarding force of 7 pN (the stall force in this sense is the retarding force that gives an equal probability of a kinesin dimer either stepping forwards or of stepping backwards).[20]

1.4 Controlled Motion with Synthetic Molecular Machines

1.4.1 Switches

The discussion above shows that despite the dominance of viscous effects and Brownian motion at the molecular level,[26-28] controlled nanoscale motion *is* possible. Moreover, physical studies would suggest that the power output of a typical motor protein is around a billion times less than the random environmental buffeting experienced by molecules in solution at room temperature.[29,30] Thus the fact that motor proteins *can* do work has served as a great source of inspiration to synthetic chemists and has spawned a significant body of literature relating to systems where there is control of nanoscale motion.[31-35] The first example of a synthetic molecular machine capable of harnessing Brownian motion to produce well-defined movement of its constituent parts was described by Stoddart and Kaifer in 1994.[36] Their design, outlined in Scheme 1.1, uses a rotaxane architecture consisting of a thread (containing biphenol and benzidine units) and a tetra-cationic cyclophane

macrocycle. At 229 K, ^{1}H NMR and UV-visible absorption shows that the majority of the macrocycles are on the benzidine station at any one time. The system is very much in dynamic equilibrium, however, and a certain small percentage of the benzidine stations are unoccupied at all times. Upon addition of two equivalents of acid, any unoccupied benzidine units become protonated and the resulting unfavourable electrostatic interaction between the benzidine and the positively charged ring prevents the macrocycle from re-associating with the protonated benzidine station. This has the effect of steadily amplifying the amount of unoccupied benzidine in a sample, giving rise to a new statistical distribution of the macrocycle strongly in favour of the neutral biphenol station.

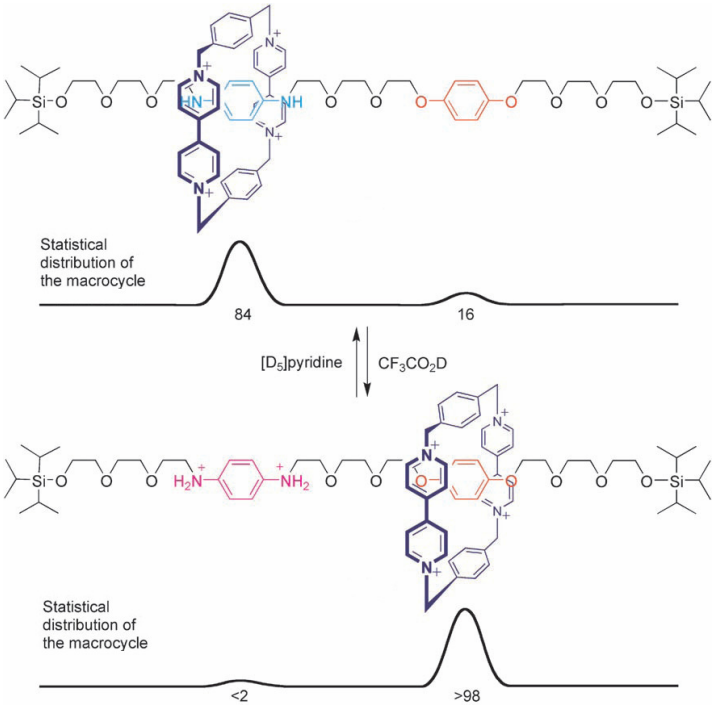

Scheme 1.1 The first switchable molecular shuttle.[36] Adapted by permission of WILEY-VCH Verlag GmbH & Co. KGaA, Weinheim, Germany.[35]

Since the Stoddart-Kaifer molecular shuttle was published, there has been increasing interest in designing systems where the motion of one component of a molecular machine relative to the other components can be accurately controlled. To this end, several groups have achieved unidirectional motion with synthetic molecular machines, the first example being that of Kelly in 1999.[37,38] In Kelly's system (Scheme 1.2), a triptycene subunit is essentially prevented from rotation relative to a helicene moiety by sterics – model studies show that the rate of rotation is extremely

slow and proceeds with equal probability in both senses. If the amino group is ignored, all three energy minima for the position of the helicene with respect to the triptycene are identical: the energy profile for 360° rotation would appear as three equal energy minima, separated by equal barriers. However, by adding phosgene (which reacts with the amino group to form the highly reactive isocyanate), the molecule becomes "primed" such that any small rotation that places the isocyanate near to an alcohol will lead to the formation of a more stable urethane linkage (the "ratcheting" step in Scheme 1.2). Although the direction of this rotation is random, the chiral nature of the molecule renders clockwise and anticlockwise rotations inequivalent. Hence, by judicious placement of the ratcheting alcohol group, it is possible to trap the molecule in an unfavourable geometry, from which the strain can only be released *via* a unidirectional 120˚ rotation ("relaxation"). Adding water to the system then destroys the urethane and reforms the original alcohol and amine functionalities, with the two subunits only capable of restricted rotation relative to each other as before.

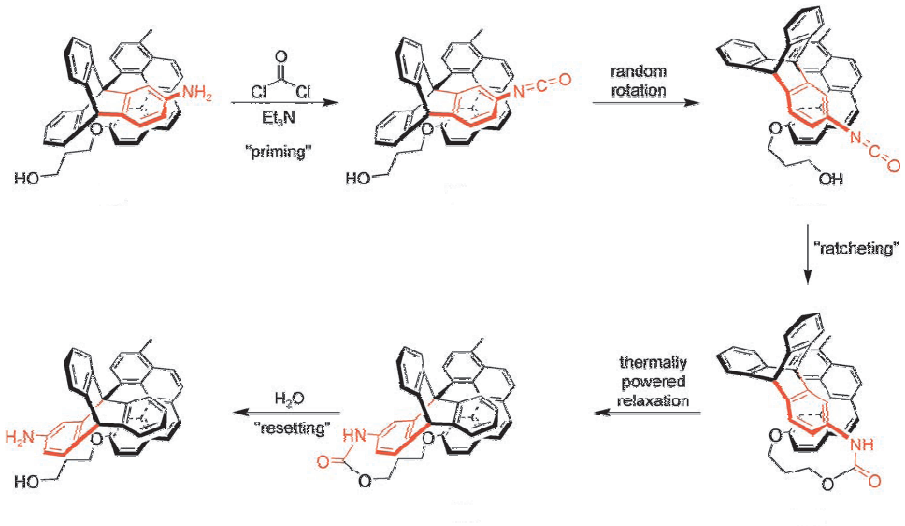

Scheme 1.2 Kelly's molecular rotor. One aromatic ring of the triptycene is coloured for clarity. Adapted by permission of WILEY-VCH Verlag GmbH & Co. KGaA, Weinheim, Germany.[35]

A limitation of Kelly's rotor is that it only performs unidirectional motion over 120˚. Feringa and co-workers, however, have devised systems capable of continuous unidirectional rotation, driven both chemically[39] and with light,[40] and have recently immobilised similar molecules on surfaces in order to study their properties.[41] In the basic light-driven system (Scheme 1.3), irradiation of isomers **A** and **C** at 280 nm

results in stereospecific isomerisation of the double bond, giving isomers **B** and **D** respectively. However, isomers **B** and **D** are both unstable and so undergo thermal relaxation to the more stable conformations. Hence, by sequential irradiation at the correct wavelengths continuous unidirectional rotation can be achieved.

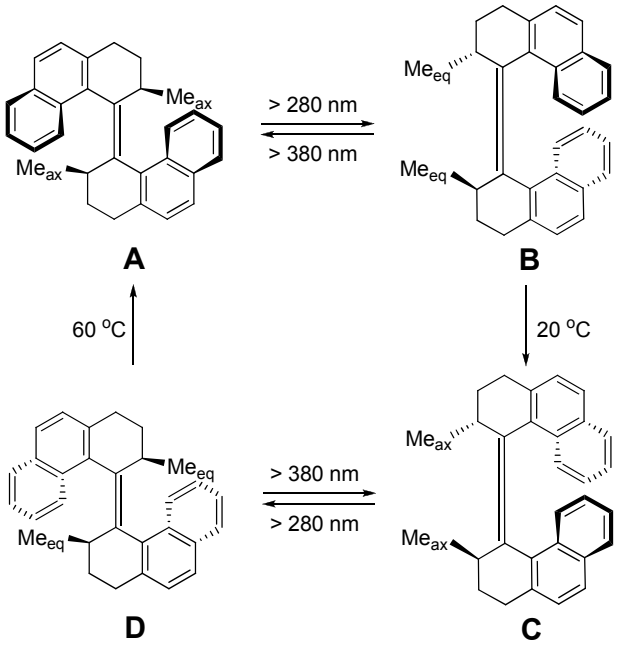

Scheme 1.3 Feringa's light-driven molecular rotor.[40]

1.4.2 Doing Work with Controlled Molecular Motion

An alternative approach to unidirectional rotation based on [2]- and [3]catenanes[42,43] has been pursued within the Leigh group, as an extension of their work with photo-responsive molecular shuttles.[44] The basic shuttle design (Scheme 1.4) consists of a thread containing both *trans*-fumaramide and succinamide binding sites.

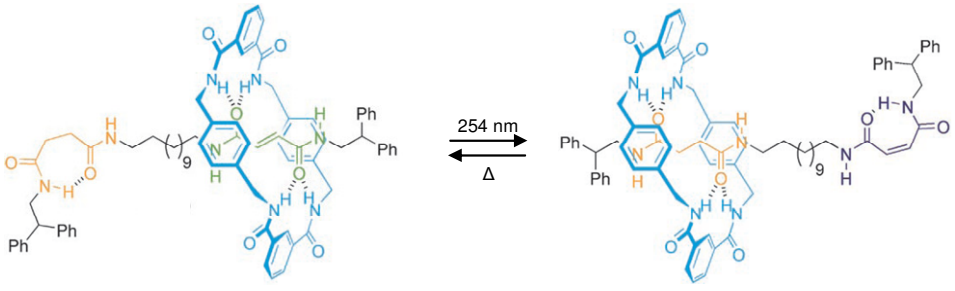

Scheme 1.4 Leigh's photo-responsive hydrogen-bonded molecular shuttle. The *trans*-fumaramide station is shown in green, the suucinamide station in orange and the *cis*-maleamide station in purple. Adapted by permission of WILEY-VCH Verlag GmbH & Co. KGaA, Weinheim, Germany.[44]

At room temperature, the macrocycle is free is explore both binding sites, but the statistical distribution lies in favour of the fumaramide station, on account of its greater pre-organisation for hydrogen-bonding to the amide hydrogens of the macrocycle. However, irradiation at 254 nm brings about the photoisomerisation of the *trans*-fumaramide station to its *cis*-maleamide isomer, resulting in the loss of a number of thread-ring hydrogen bonds. The statistical distribution of the macrocycle is now found to lie in favour of the saturated succinamide station, whilst the *cis*-maleamide station hydrogen-bonds to itself. This macrocycle-succinamide co-conformation is then dominant until the *cis*-maleamide station is converted back to the *trans*-fumaramide isomer by an appropriate stimulus, at which point the original equilibrium distribution is restored.

This shuttling mechanism has been used to produce unidirectional rotation in both [2]catenanes (Scheme 1.5)[42] and [3]catenanes.[43] In the case of [2]catenanes, combining sequential removal/reattachment of two different bulky groups (tBuSiMe$_2$ and CPh$_3$) with the isomerisation reactions shown in Scheme 1.4, causes the smaller ring to rotate unidirectionally around the larger ring. Scheme 1.5 shows this rotation to be dependent on the order of the removal/reattachment reactions; one order gives clockwise rotation, the other gives rise to anticlockwise rotation as drawn. Hence complete control over the direction of rotation is possible. The bulky groups are essential if the ensemble is to do work, as they allow the system to be "reset" to its initial isomerisation state without undoing the work done (i.e. without changing the distribution of the smaller macrocycle). Selective removal of one of the bulky groups then allows the system to return to equilibrium in a directional fashion.

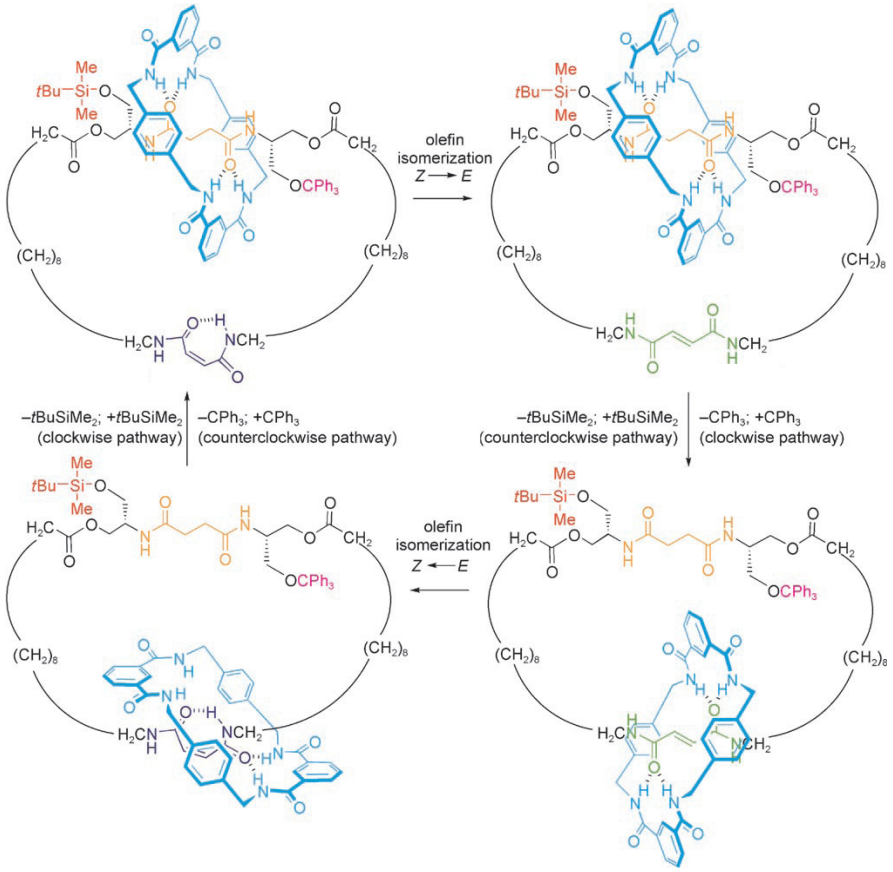

Scheme 1.5 Unidirectional rotation in a [2]catenane. Adapted by permission of WILEY-VCH Verlag GmbH & Co. KGaA, Weinheim, Germany. [35]

Systems such as this that are capable of transporting Brownian particles away from equilibrium are known as *Brownian ratchets* and fall into two general classes: *Energy ratchets*[45] and *Information ratchets*.[46,47] In an energy ratchet mechanism, the energy maxima and minima of the potential surface are varied irrespective of the Brownian particle's location – all identical binding sites within an ensemble are affected equally by an applied stimulus. In contrast, the potential energy surface in an information ratchet varies as a function of the position of the Brownian particle, allowing stimuli to be applied that only produce effects local to that particle (Figure 1.8). An information ratchet system is a much more efficient way of producing controlled motion on the molecular scale, as a given energy input can be directed to the locale of the particle undergoing that directed motion, rather than being applied globally to effect multiple identical changes, most of which have no bearing on the state of the Brownian particle.

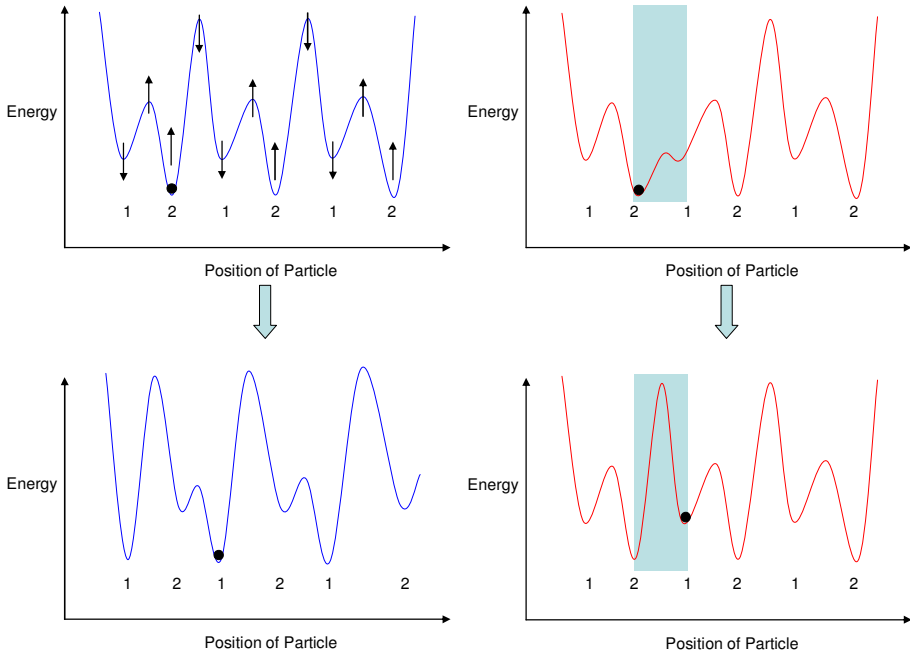

Figure 1.8 A particle (denoted ●) undertaking biased Brownian motion *via* an energy ratchet mechanism (left, shown in blue) and an information ratchet mechanism (right, shown in red). The black arrows show how the energy levels are varied in order to get motion of the Brownian particle from a site "2" to site "1". In an energy ratchet mechanism, the particle is passive and changes its position in response to what happens globally to the system – all equivalent parts of the energy profile change in the same way each time a particular stimulus is applied. Contrastingly, in an information ratchet mechanism, the potential energy surface changes *because of where the particle is* and so a given stimulus may produce effects only local to the Brownian particle – the rest of the surface remains unchanged. In this example, the particle sees a reduced kinetic barrier for passing from "2" to "1" (top, highlighted in blue), but the kinetic barrier for the reverse process is much higher (below, highlighted in blue). Hence the statistical distribution of the particle can be shifted in favour of the energetically uphill state by trading information for energy.

Despite the growing body of literature surrounding directional molecular motion within mechanically interlocked architectures such as those discussed above, examples of non-interlocked systems capable of controlled linear motions (e.g. molecular walkers) are still very rare. A 2005 review by Kelly[48] covers almost all the important examples of synthetic walking molecules to date, and even then identifies only four papers that could conceivably fall into that category (all of them based on DNA). However, before embarking on a detailed description as to how these walkers operate, the issue of what constitutes a walking molecule and the fundamental principles necessary for their design and operation must be undertaken.

1.5 Designing Walking Molecules

Firstly, we must define what a walking molecule is. The Collins English Dictionary defines walking as, "Moving along or travelling on foot…advancing in such a manner that at least one foot is always on the ground," whilst stepping is defined as, "The manner of walking or moving the feet; the act of raising the foot and setting it down again in coordination with the transference of the weight of the body." Hence any walking molecule must possess "feet" – at least two recognisable points of attachment to a track or surface, such that at least one foot is always in contact with the track or surface at any time, regardless of the state of the other foot/feet. Furthermore, the feet - whatever their precise nature and whatever other functions they may perform - must be the only points of attachment necessary for the molecule to walk; that is to say the feet must be well-defined species that are capable of mediating stepping. These distinctions are necessary in order to preclude *rolling* and *tumbling* from any discussion of walking molecules (see Section 1.5.3): it would indeed be an exaggeration to say that a man falling down a flight of stairs was walking on *n* different feet, where *n* could only be defined after the walk by tallying the injuries sustained. This does not mean to say that the steps taken by any given walker (molecular or otherwise) must be of regular interval in terms of time between steps or the distance travelled – hesitant limping is still walking. Nor does it mean that the feet must always move in a concerted (or predictable) manner, or even in any predictable order – stumbling using your right hand sometimes and your left hand occasionally still constitutes walking. You would, however, cease to be a walker and become either a roller or a slider at such a time as your centre of mass was translocated without the use of discrete steps – a slalom skier does not walk downhill any more than a cyclist walks the Tour de France (despite there being defined points of attachment always in contact with the relevant surface in both cases), as both can perform directed motion without the use of discrete steps. Given these *provisos*, there are two general classes of walker – those that use interactions between the feet and the surface alone to walk (walkers with passive linkers and tracks), and those that use some sort of active linker between the feet or the binding sites on the track (like a

spring, for example) to drive stepping. We shall address these in turn, starting with the simplest case: the walker with only two feet.[49]

1.5.1 Walkers with Passive Tracks and Linkers

Consider a track with two alternating stations *A* and *B* and a passing-leg (hand-over-hand) walker with two feet *1* and *2* that are not interlocked with that track. The feet are linked by a non-rigid but inelastic linker which allows the feet to be a maximum distance of *x* apart, where *x* is also the distance between adjacent stations. We shall specify that *1* and *2* will bind to both *A* and *B* to form stable complexes such that the generic complexes *1A, 1B, 2A* and *2B* can all be formed. We shall also state that foot *1* can switch its binding preference in response to a certain stimulus without affecting the status of foot *2* and *vice-versa*. Let us now consider what happens in a track of the form *ABABAB* (Figure 1.9).

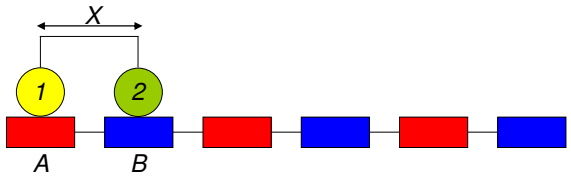

Figure 1.9 A generic two-footed walker on an *ABABAB* track in state [*1A, 2B*].

Let us take the initial position of the walker to be [*1A, 2B*], where the right entry in the brackets indicates the rightmost foot on the track as drawn. Foot *1* is shown in yellow, foot *2* in green and *A* and *B* are red and blue respectively. Now suppose that we apply some stimulus that makes complex *1A* labile whilst not affecting the status of *2B*. This generates the intermediate [*2B*]*1**, where foot *2* is still strongly bound to the track at *B* and *1** indicates that foot *1* is free to explore alternative binding sites. (For the purposes of this discussion, it will be assumed that the foot/foothold pairing not being stimulated is not labile.) If we allow rotation about the *2-B* bond, then remove or reverse the labilising stimulus such that foot *1* now favours association with *A*, the complex *1A* will re-form generating two spatial isomers in a statistical 1:1 ratio; [*1A, 2B*] and [*2B, 1A*'] (Figure 1.10), where *1A*' indicates that this complex is one *AB* unit away from the origin.

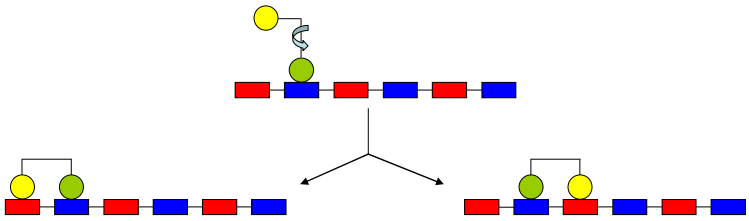

Figure 1.10 The mid-step co-conformation of [*2B*]*1** (top) gives rise to equal populations of the two states [*1A, 2B*] (left) and [*2B, 1A*'] (right) when a stimulus is applied favouring the formation of the generic complex *1A*.

Let us now apply a second stimulus that allows *2* to dissociate from *B* without affecting *1A* or *1A*', such that states of the type [*1A*]*2** are formed. Random rotation about the *1-A* bond followed by removal of the labilising stimulus then regenerates the complex *2B*, now with three statistically populated translational isomers; [*1A, 2B*], [*2B, 1A*'] and [*1A*', *2B*'] in the ratio 2:1:1 (Figure 1.11). This distribution comes about as all the walkers starting from state [*1A, 2B*] (half the total number) are prevented from any movement down the track to the next station by the inelastic linker to (non-labile) foot *1* on the first station *A*. Those walkers in state [*2B, 1A*'] when the stimulus is applied (the remaining half of the total number of walkers) are able to adopt one of two states upon stimulus-removal; they either perform the self-transformation to recover state [*2B, 1A*'] or they can advance to [*1A*', *2B*'], each with a probability of 0.5.

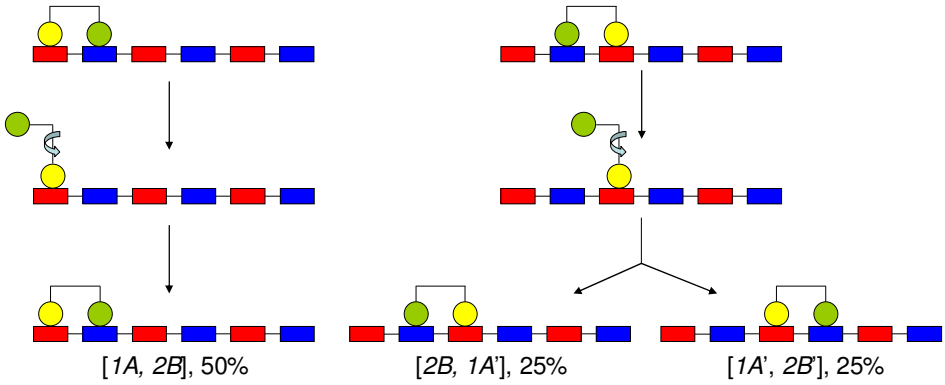

Figure 1.11 The three co-conformers possible after the second step of an *ABABAB* walker.

Reapplying the first stimulus (labilising the complexes *1A*) then generates various states [*2B*]*1**, which give rise to four different spatial isomers when that stimulus is removed or reversed in a 3:3:1:1 ratio (Figure 1.12).

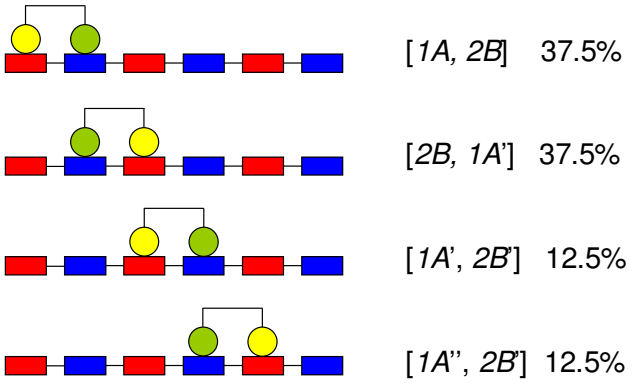

Figure 1.12 The distribution of walkers after the third cycle.

At first sight, it appears as if the ensemble is undergoing a net directed motion to the right. However, this is only because the walker started at one extreme of the chain. To explain what is happening, it is instructive to model the system as a *Markov Chain* - a sequence of random variables X_1, X_2, X_3, ... with the Markov property.[50] The Markov property means that given the present state of a system, any future states are completely independent of states in the past, i.e. a full description of the present state constitutes all the information necessary to predict a given future state of the system. More specifically, the Markov property asserts that the *conditional probability distribution* of the state in the future, given the state of the process currently and in the past, depends only on its current state and not on its state in the past. With regards to this simple *ABABAB* system, each step of the walker can be taken as a discrete stochastic process, with p = 0.5 for a forward or backward step from an intermediate state [*Nx*]*y** (the direction of the step is the random element). We shall assume that the probability of the walker dissociating from the track completely is zero. Such a Markov chain has a trivial transformation matrix and if run for an arbitrarily long time yields the probability distribution of the walkers as a normal distribution about the centre of the chain – i.e. the equilibrium distribution of walkers on the track is a normal distribution with the modal population class in the centre. Hence the apparent directed motion to the right is in fact just the system moving to equilibrium – had we started in the centre of the chain the averaged net displacement of the walkers would be zero (as might be expected from a system where there is nothing to bias the direction of stepping).

A more chemically intuitive way of interrogating such systems is to consider them as compartmentalised molecular machines operating through Brownian ratchet mechanisms (see Section 1.4.2). Thus, by treating the walker unit as a point particle on a potential surface, the qualitative energy diagram shown in Figure 1.13 can be obtained, where the point particle walker is denoted ●. When the walker is bound to the track in the state [*1A, 2B*], labilisation of *1A* leads to [*2B*]*1** at which point the walker is free to sample configurations [*1A, 2B*] and [*2B, 1A*']. These states represent minima of identical energy (as the binding sites available to the labile foot are the same) and conversion between the two forms is made possible by the low kinetic barrier between them (dotted arrows). Progression to states further down the track (e.g. [*1A', 2B*']) is not possible however, as *2B* is not labile, effectively giving all the other states infintite kinetic barriers in this simplified system (red arrows). Hence the walker is restricted to the two potential wells indicated by the dotted arrows and cannot access other states even though they have exactly the same energy. Applying a stimulus to cause the complex *1A* to become non-labile then generates the 1:1 ratio of [*1A, 2B*] and [*2B, 1A*'] derived before (Figure 1.10 and Figure 1.13, right hand side). If the complex *2B* is now allowed to become labile, those walkers in state [*1A, 2B*] are trapped in one minimum and cannot escape (as the complex *1A* is locked to the track) and so the green foot cannot access any binding sites other than the one it is already on (white circle). For walkers in state [*2B, 1A*'] (filled circle) two lowest-energy conformations are accessible [*2B, 1A*'] and [*1A', 2B*'], both of the same energy and with a relatively low kinetic barrier between them. Hence, the equilibrium distribution of 50:25:25 [*1A, 2B*]:[*2B, 1A*']:[*1A', 2B*'] (Figure 1.11) between the three possible conformations is obtained, with infinite kinetic barriers (provided by the non-labile complex *1A*) preventing the walker from sampling any other states.

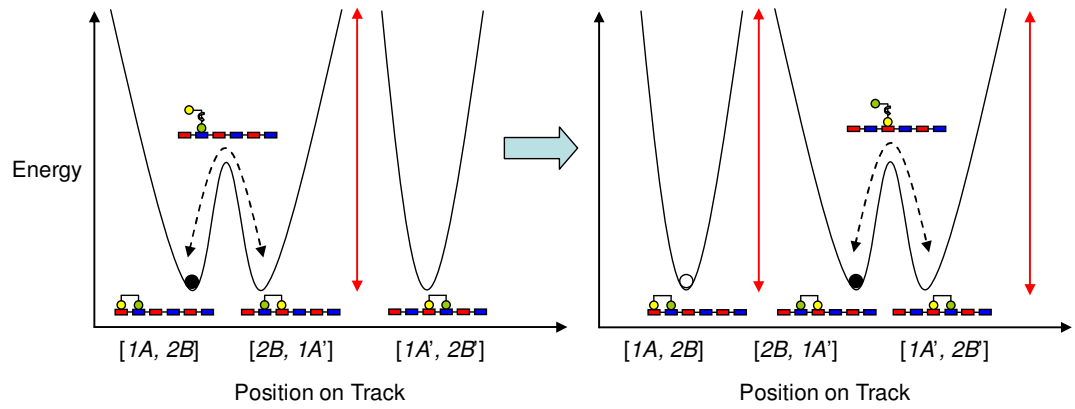

Figure 1.13 Left hand side: The potential energy surface as seen by a walker in state [*2B*]*1**, when *1A* is labile. Right hand side: The potential energy surface seen by walkers in states [*1A*]*2** (○) and [*1A*']*2** (●) when *2B* is labile.

Figure 1.13 suggests that if the potential energy surface available to the walker could be made *asymmetric* during the intermediate states [*Nx*]*y**, then directional motion should be possible. Interestingly, this can be achieved by simply re-ordering the stations of the track to give an *AABBAABB* arrangement (provided stations *A* and *B* are not energetically equivalent), as any stepping foot is now allowed to sample one red and one blue station instead of two stations of the same energy (Figure 1.14).

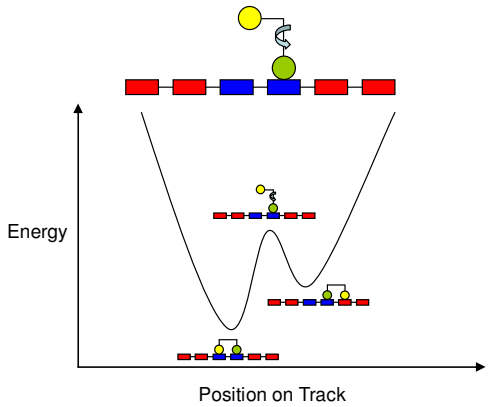

Figure 1.14 An asymmetric track presents the stepping foot (shown here in mid-step) with an asymmetric energy profile. Stepping will occur predominantly to the left as drawn. Stepping to alternative energetically equivalent sites (not shown) is again prevented by the kinetic barriers imposed by the non-labile foot/foothold complex which acts with the inelastic linker as a ratchet, effectively restricting the stepping foot to only two possible binding sites out of the many on the track.

This Brownian energy ratchet approach to molecular-scale walking systems shows that each foot of a walker acts very much like a *bis*-stable switch, with a certain set of stimuli required to bring about stepping. For processive, directed walking, each set of stimuli must comprise:

1. An impulse "breaking detailed balance", which could be a stimulus altering the relative energies of the binding sites available to a given foot (producing a thermodynamic driving force in favour of the desired step direction), or some sort of non-equilibrium chemical process coupled to stepping (see Section 1.5.2)
2. A second "linking" impulse allowing the selected foot to sample the available binding sites and thus to generate a new equilibrium as dictated by the balance breaking stimulus (this corresponds to lowering the kinetic barrier between neighbouring binding modes)
3. A third impulse to raise the kinetic barrier between the competing binding modes once the new equilibrium has been established, to give strongly-bound complexes that are incapable of further exchange ("fixing").[51]

Points 2 and 3 above relate to kinetics; the ability to switch a foot/binding site ensemble between being labile (to allow stepping) and non-labile (to allow that ensemble to act as the ratchet whilst the other foot is stepping). Point 1 is a thermodynamic consideration; the extent to which a stepping foot can be biased between one potential binding site and another determines the fidelity with which the walker processes – a strong thermodynamic bias in one direction will give rise to stepping predominantly in that direction, whilst little or no bias will result in little or no net directed motion of walkers when the linking stimulus is applied. It should be noted, however, that the orientation of the walker(s) on the *AABBAABB* track in Figure 1.14 is critical if there is to be directed motion in the bulk. This is because the walker can initially bind to the track in two energetically equivalent binding modes, giving rise to two spatial isomers in a 1:1 ratio (Figure 1.15). Application of the same order of stimuli to these populations would bring about unidirectional motion of half the walkers in one direction whilst the other half processed the other way, with no net unidirectional motion.

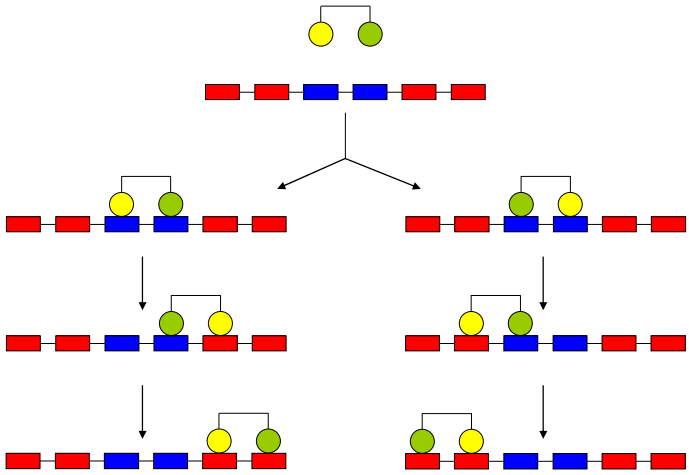

Figure 1.15 The same set of stimuli gives rise no net directed motion if the walker can bind to the track both ways round. Initially, a walker free in solution binds to two blue stations, in two energetically equivalent orientations. Applying a set of stimuli to make the yellow foot move to a red station, followed by a similar set making the green foot prefer a red station then produces two equal walker populations going in opposite directions.

This tells us that in order to perform directed motion in such a system, we need to know which way round the walkers are – we need information about their orientations in order to achieve unidirectional motion with a given set of stimuli. As chemists, this problem can be circumnavigated by using a more complicated track, so that the walkers can only bind to the track one way round under a given set of conditions (note that this does not mean that the walkers have ceased to behave like Markov chains as their orientation at any given point is still enough to tell us which way they will move). Some examples of how this can be achieved are given in Sections 1.5.2 and 1.5.4.

1.5.2 Walkers with Active Tracks and Linkers

All the walking systems covered in Section 1.5.1 had linker regions between the two feet of the walker that were essentially inert throughout the stepping process. Their only role was to act as a tether between the two feet, preventing the unbound foot from sampling more than one (or sometimes two) binding site(s) of the same energy. However, a linker capable of assuming two or more different, rigid extension states can bring about directional motion using an energy ratchet mechanism and operating on a very similar track to that seen in Figures 1.9-1.13.[52-54] This is because the

variable linker is now the agent supplying the balance-breaking impulse – the relative depths of the potential wells are given as a function of the linker length alone. As long as the various foot/binding site complexes are subject to orthogonal linking/fixing stimuli, directed motion along a track can be achieved simply by alternately elongating and contracting the linker (Figure 1.16). Thus applying a stimulus to labilise the complex of the yellow foot and red station followed by linker extension from length L_1 to L_2 gives rise to directed motion to the right upon addition of a fixing stimulus (as long as the linker is rigid and inflexible enough to prevent re-association with the original red station). Subsequent labilisation of the green foot/blue station complex and linker contraction back to L_1 then returns the system to its original state, one *AB* unit displaced to the right. The two feet need only form stable complexes with one type of station and as they will therefore only bind to the track one way round, we do not need any information regarding their orientation in order to achieve directed motion in the bulk.[55]

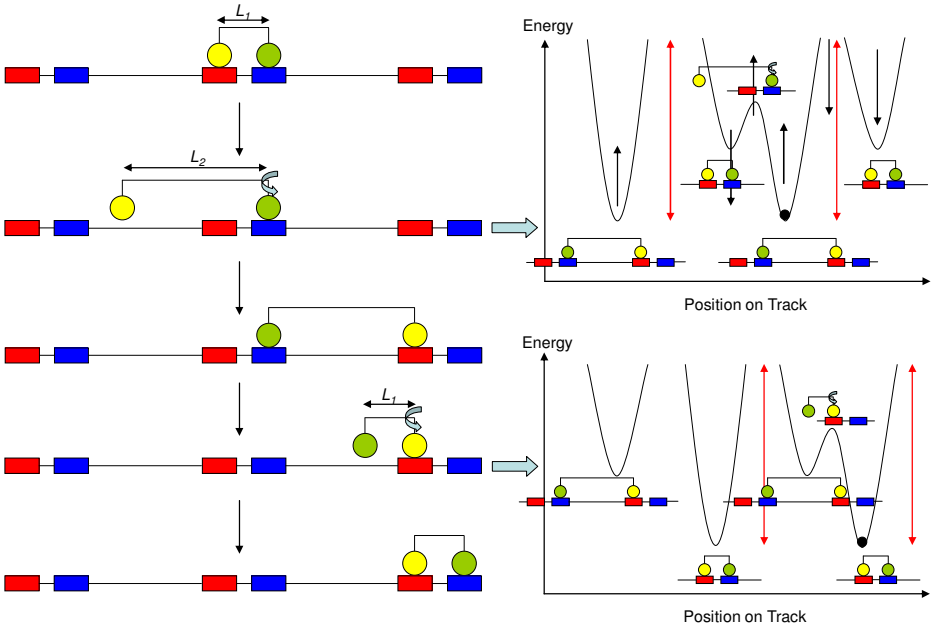

Figure 1.16 An active linker allows directed motion on an *ABABAB* track, without needing to know the orientation of the walker(s) by rendering otherwise identical binding sites energetically inequivalent. The energy diagrams on the right hand side show how the potential surface changes as the linker is elongated and contracted (black arrows, showing how the energy levels change in the following step). Note that the energies of all equivalent states are raised and lowered by the same amount as the linker expands and contracts, but that the walker is restricted to only two possible states by the ratcheting foot (giving the infinite kinetic barriers shown by the red arrows). A stepping foot is then biased towards its next foothold by thermodynamics alone (the lower of the accessible energy states being the one that puts the least strain on the walker/track ensemble), making this an energy ratchet walking mechanism.

Interestingly, if the orientation of the walkers on the track can be determined with certainty, then it can be shown that directed motion is possible with such a system even if all the stations are identical! Hence, as long as the complexes the two feet make with the track can be addressed separately, the appropriate order of stimuli will give rise to directed motion in the bulk (Figure 1.17).

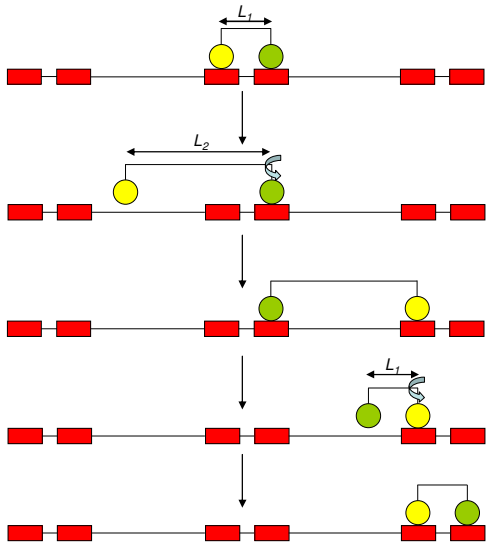

Figure 1.17 Directed motion on an *AAAAAA* track is possible, provided the orientation of the walker(s) is known.

Walking systems where the active component is in the track can also be envisaged (Figure 1.18), but as multiple elements are undergoing elongation/contraction (most of them not leading to productive stepping events of the walker) such a system would probably be much less efficient than the active linker walker systems outlined above.

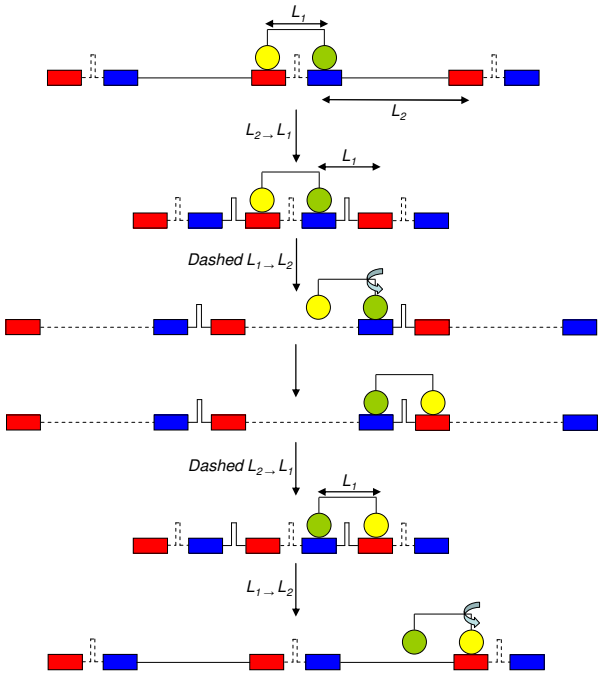

Figure 1.18 An active-track walking system. The track contains two active elements (solid lines and dashed lines), which can be switched orthogonally between contracted (L_1) and extended (L_2) forms. Hence by making the yellow foot/red station complex labile whilst simultaneously extending one set of these active elements, two otherwise energetically identical sites can be rendered inequivalent, allowing directional motion.

Active linker systems also provide a possible route to branched structures, in which a walking molecule may select one of several paths in response to appropriate stimuli. Consider the situation with a walker capable of three different (inelastic) states of linker extension; L_1, L_2 and L_3 and an *ABABAB* track incorporating these three lengths (Figure 1.19). As long as L_3 satisfies certain parameters (such as $L_3 \neq L_1 + L_2$), then application of the appropriate stimulus at the chain branching point should lead to a walker favouring either the "L_2" *or* "L_3" pathways. Indeed, judicious choice of stimulus should allow a walker on any pathway to select either of the other pathways at a junction.

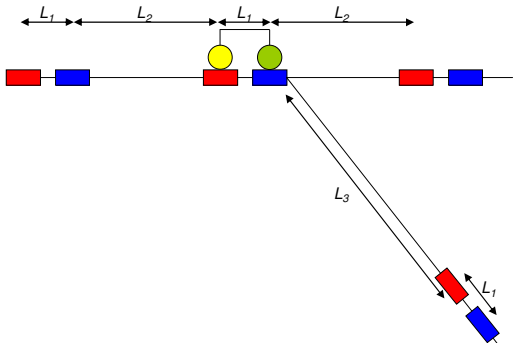

Figure 1.19 A branched active linker walker.

An alternative class of active linker walker uses well defined rotary motion to produce unidirectional translation along a chain. Consider a track consisting of repeating asymmetric footholds and a walker that has at least one foot that forms a diastereotopic ensemble with the track, such that that foot will only bind to the track in one orientation (Figure 1.20). This determines how the walker will associate with the track from solution. The other foot may be allowed to bind to the track regardless of orientation.

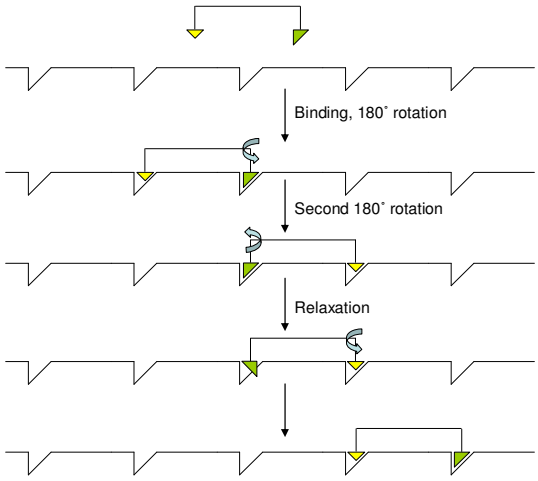

Figure 1.20 Turning rotary motion into linear motion using a highly constrained diastereotopic walker, where relaxation of a high energy state leads to directed motion as determined by the track's inherent polarity ("rectification").

The stepping mechanism relies on a highly rigid walker that is capable of two separate 180° rotations, but only when the appropriate stimuli are applied. Firstly, we supply the system with some stimulus that makes the yellow foot labile whilst a 180° rotation about the linker / green triangle bond takes place (note that rotation about this bond must only occur when the appropriate stimulus is applied if the walkers are

all to bind to the track in the same orientation at the start). This has the effect of swinging the yellow foot in front of the green foot. If the yellow foot is then made non-labile, a second 180° rotation about the rigid linker / green foot bond leads to a high energy state where the diastereotopic complementarity between the green foot and the track is broken - a situation that can be remedied by a further 180° rotation *via* Brownian motion ("relaxation").

So far, all the simple walking systems that have been considered have operated *via* energy ratchet mechanisms. Walkers based on information ratchets are also possible, however, and should operate highly efficiently as the energy input necessary for directed walking is always targeted at the walkers themselves, rather than applied to the system as a whole. An extreme example of such an information ratchet walker is the "burnt bridge" system, where a foot destroys the binding site to which it is currently bound before stepping to a new binding site.[56] An example of an information ratchet walker with more potential for repeated use of the same track is shown in Figure 1.21. In this case, the walker has two identical feet and the track has only one type of foothold, which is diastereotopic such that the walker can only bind to the track one way round. Both feet have sites on them to which an allosteric effector (the red triangle) can bind, but the binding site on the front foot is masked by the rear foot, such that the effector cannot bind to the front foot. When bound, the effector causes the foot to which it is attached to become labile, allowing that foot to sample alternative binding sites. At the same time, the binding of the effector to the rear foot causes a conformational change in the front foot (black triangle) preventing it from binding a second equivalent of effector (which would lead to complete dissociation of the walker from the track). In addition to this, the binding sites on each foot are capable of catalysing the transformation of the effector to a "waste" compound (white triangle), which diffuses rapidly from the binding site.

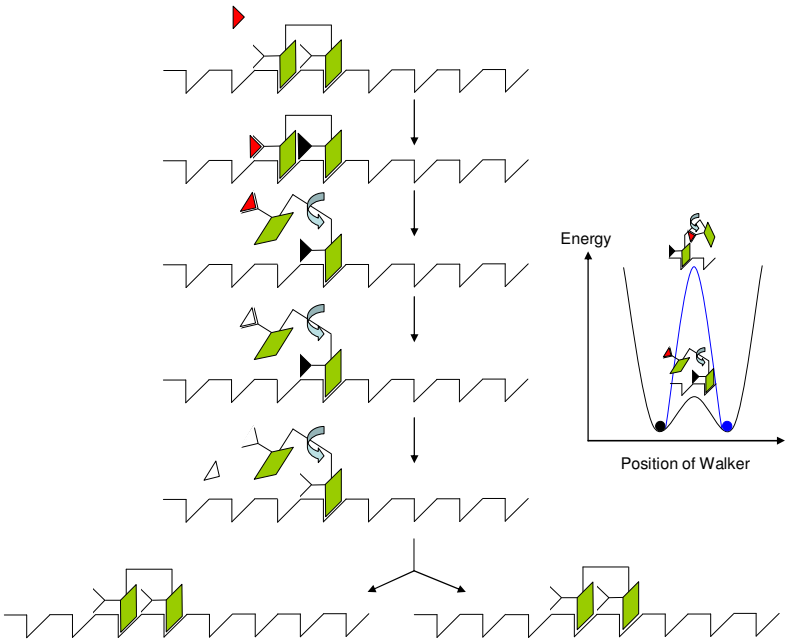

Figure 1.21 An information ratchet walking system that processes by virtue of the fact that only the rear foot can bind to an allosteric effector, which is itself consumed during stepping. The energy diagram on the right hand side highlights the information ratchet walking mechanism: a foot taking a forward step (denoted ●) sees only a small kinetic barrier to forming the effector-bound intermediate (black curve) but a foot stepping backwards (blue circle and curve) sees a large barrier to forming the analogous intermediate (as the walker/track ensemble would have to undergo considerable deformation to allow the effector to access the binding site on the front foot). Hence directional walking is possible, even though the various binding sites in the track all have the same affinity for both feet.

After binding a red triangle and catalysing its transformation to a white triangle, there are two possible fates for the stepping foot – it can re-associate with the track in its original position or it can swing in foot of the standing foot, at which point the standing foot becomes the rear foot (we shall assume that reassociation of the track and stepping foot after dissociation of the white triangle is fast compared to effector binding to improve efficiency and processivity). The fact that the effector "fuel" is destroyed during the stepping process is essential if the system is to walk directionally – the second law of thermodynamics states that energy must be expended if net directional motion of the walker is to be obtained. The thermodynamically favourable conversion of effector to white triangles can then be considered as being *coupled* to walking, just as Nature uses thermodynamically favourable reactions to drive otherwise unfavourable processes.

In this light, it is instructive to return to kinesin (Section 1.3). When a kinesin head is in the nucleotide-free state, it binds strongly to microtubules and operates as a ratchet for the other head. Upon binding and hydrolysing ATP, the head then becomes labile and it is able to dissociate from the track – in this sense ATP binding can be considered as the linking stimulus, just as effector binding is the linking stimulus in Figure 1.21. This situation continues until the ADP formed from ATP hydrolysis dissociates from the "unbound" head, at which point that head favours re-association with the microtubule in the strongly-bound (ratcheting) state. Hence ADP dissociation can be viewed as the fixing stimulus. The balance-breaking stimulus comes from the fact that the ATP hydrolysis reaction that allows kinesin to step is not at equilibrium in living cells[15] – ATP hydrolysis is coupled to directional stepping. The fact that the heads alternate their roles (i.e. the trailing head is the one that binds ATP and dissociates, not the leading head that has just completed a step) is highly reminiscent of the mode of action of the system in Figure 1.21 and suggests that kinesin operates *via* an information ratchet mechanism. As kinesin rarely takes idling steps (i.e. it rarely hydrolyses an ATP molecule without taking a forward step), it seems likely that some sort of conformational change takes place during the stepping process that swings the trailing foot in front of the standing foot – in this regard we can consider kinesin to possess some sort of active linker powered by ATP hydrolysis.[57,58]

1.5.3 Walking Systems as Functional Molecular Transport Devices

The fact that Nature uses walking molecules to achieve directed transport of cargoes in cells has significant implications in regard to synthetic attempts towards controlled, processive linear motions at the molecular scale. From an operational point of view, the inherent compartmentalisation of walking systems gives them substantial benefits over other potential approaches to such directional motion. For example, consider the putative molecular "roller" (essentially a one-headed walking system) depicted in Figure 1.22. The roller (green) can form stable interactions with both the red and blue stations and its affinity for one over the other can be accurately controlled. Furthermore, the roller is confined somehow (within a tube for example),

such that it is not able to detach from the track but must roll along it. In order to produce directional motion, the roller must be prevented from sampling other stations on the track of the same energy and this can be achieved by using blocking groups that are bulky enough to prevent the roller getting past (shown in yellow and grey). If these blocking groups can be selectively removed/reattached as the roller's binding preference is switched from red to blue and back to red, directional motion in either vector can be obtained. However, such a system presents more challenges to its realisation than a walker. The roller must be able to discriminate between the red and blue stations, which requires one switching mechanism. The stimuli needed for removal/reattachment of the two different blocking groups must be orthogonal not only to each other but also to the stimulus that switches the roller's binding preference (if the roller is to be capable of controlled rolling in both directions along the track). Hence the need for three orthogonal switching mechanisms for such a roller (based on an energy ratchet mechanism). Finally, the confinement of the roller (so that it does not drift off into solution or circumnavigate the blocking groups) necessitates the enclosure of the whole system, which could seriously impair any additional functions that the roller might be required to have, such as moving cargoes about in a controlled manner or being able to choose one pathway over another at a track-branching point.[59]

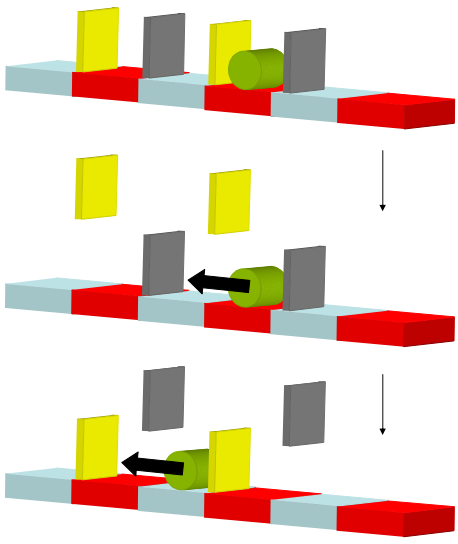

Figure 1.22 A molecular roller capable of controlled directed motion, operating through an energy-ratchet mechanism.

Conceivably, a molecular roller operating *via* an information ratchet mechanism would require only two orthogonal processes for directed motion along a track in both directions, but the efficiency of that directed motion would drop off substantially with increasing distance from the origin. Consider the system illustrated in Figure 1.23, where there is only one type of binding site for the roller, and blocking groups that can be addressed so that they only detach from the track (allowing the roller to pass) when the roller approaches from the right (stimulus 1) or the left (stimulus 2). As long as these two stimuli are truly orthogonal, the roller can be "pumped" from one end of the track to the other by repetitiously applying (for example) stimulus 1, and pumped in the reverse sense by application of stimulus 2. However, as there is nothing to bias the position of the roller when a particular bulky group is removed from the track, only half the rollers will progress to the next site per application of the stimulus, leading to an exponential drop-off in roller populations with increasing distance from the starting point. Obviously, the system could be made more efficient by using an *ABABAB*-type track (as in Figure 1.22), but that would require the additional complexity of the associated switching mechanism.

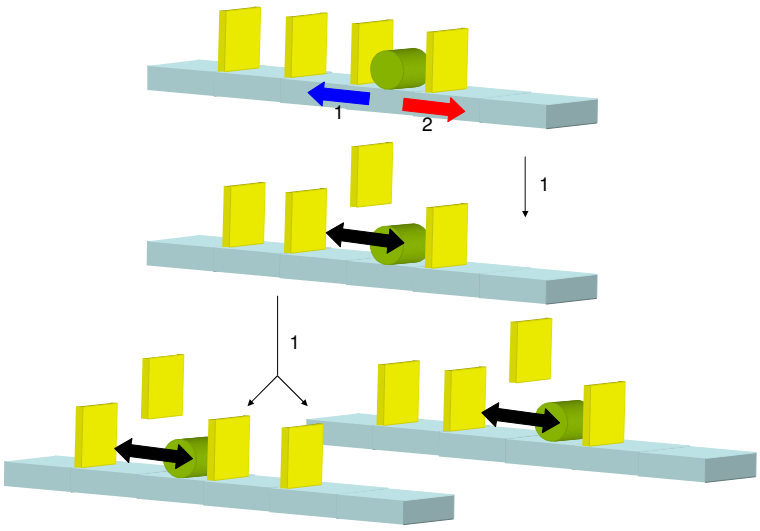

Figure 1.23 A molecular roller operating by an information ratchet mechanism, under action of a stimulus (1) causing the bulky groups to let the roller past only when the roller approaches the barrier from the right as drawn. Note that bulky groups not adjacent to the roller are not affected by the removal/reattachment stimuli.

In contrast to both these rollers, a walking system has at least two points of attachment to its track, and the foot that is not stepping acts as both an anchor to keep the ensemble connected to the track (ensuring processivity) and as a ratchet to restrict

the potential energy surface seen by the stepping foot. This allows controlled, efficient directed motion in either direction with the need for only two orthogonal switches (see Sections 1.5.1, 1.5.2 and 1.5.4) - i.e. walkers necessarily perform the roles of the blocking groups *and* confinement by virtue of the fact that one foot is always strongly bound to the track and that the two feet are physically joined to one another.

1.5.4 Rational Designs for Molecular Walkers

Sections 1.5.1 and 1.5.2 both dealt with walking systems whose design was minimalist from a theoretical point of view. All the examples given involved tracks with at most two different binding sites and walkers with at most two different feet. However, whilst it is relatively straightforward to draw such structures and show how they could lead to directional motion, actually designing real-world systems that would behave in the same way is much more challenging. In this regard, systems that at first might seem more complicated may, in fact, be easier to realise. As previously discussed, in order to ensure processive, directional translation it must be possible to address each foot/foothold complex independently of the other(s), using a set of balance-breaking/linking/fixing stimuli as outlined in Section 1.5.1. From a molecular machines perspective, this set of interactions constitutes a molecular switch, and so a possible compartmentalised approach to walking systems would be to use two such switches in tandem as shown in Figure 1.24. Here, the two orthogonally switchable interactions in question are that the green unit can bind to either the turquoise or red stations, whilst the yellow moiety forms stable complexes with either the blue or white stations. By combining these four different stations in a track with an alternating *ABCDABCD* pattern, a walker with green and yellow feet can be made to process unidirectionally along the track by alternately operating each switch, taking four switching events to complete a full cycle. In addition, the operator does not need to know the initial orientation of the walkers in order to perform directed motion in either vector – there should be only one way in which the walkers can bind to the track under a given set of conditions, and the walkers should all then process in the same direction under the action of a given set of stimuli

(although if the walkers were allowed to associate with the track at random from solution, then how far along the track they were would not be known).

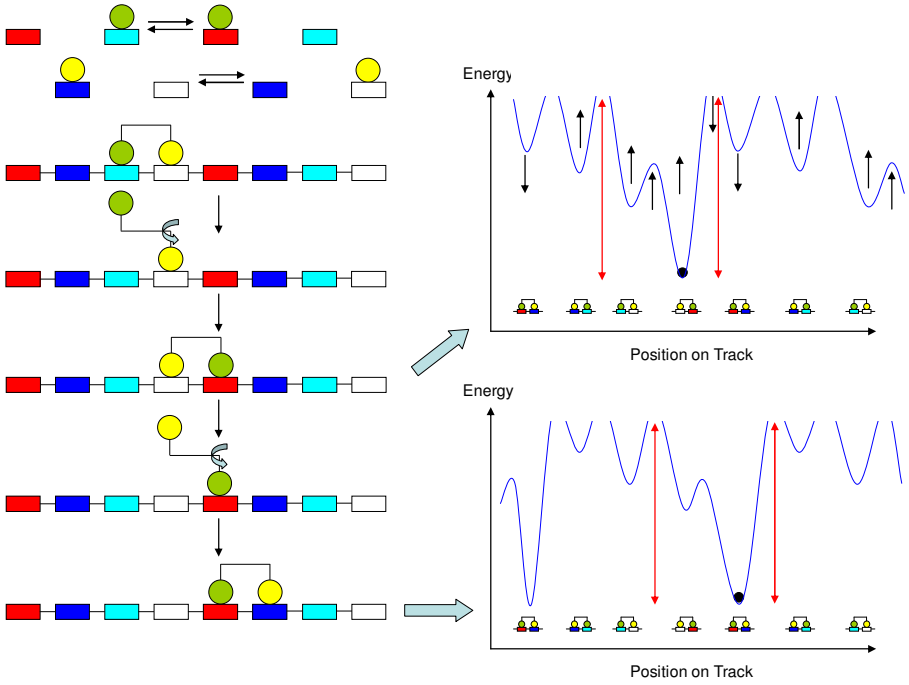

Figure 1.24 A walking system based on two orthogonal switches (green/red-green/turquoise and yellow/blue-yellow/white) with an *ABCDABCD* track. This operates *via* an energy ratchet mechanism, as shown by the potential energy curves on the right corresponding to the two steps drawn. The black arrows show how the energy surface of the entire track changes as the walker (considered here as a point particle, ●) is made to step. Note that although potential wells of the same energy exist elsewhere in the track, the walker is prevented from accessing them as this would require both feet to dissociate from the track (for which the kinetic energy barrier is very high: red arrows). Half of a complete cycle (two switching events) is shown.

Inspection of this system reveals that there is a level of redundancy in its design – the two feet could be the same provided that they formed independently addressable complexes with the track, which could potentially ease the synthesis of such ensembles.

A related idea to this, where the feet would have to bind to all the stations of the track, is walking systems based on an *ABCABC* track (Figure 1.25). In this design too, both feet can be the same and the orientation of the walkers need not be known for directed motion in either sense. However, although the track requires only three stations, implementation of such an *ABCABC* walking ensemble may prove more challenging than the system outlined in Figure 1.24, as the feet would have to form

stable and independently addressable complexes with all three different track stations, instead of just two as required by an *ABCDABCD* system.

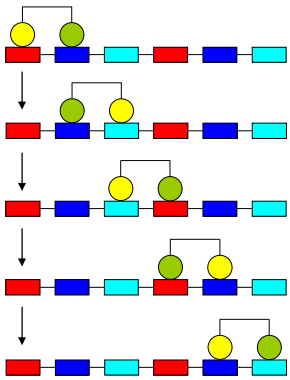

Figure 1.25 A walking system operating on an *ABCABC* track. Both feet must bind to all three stations.

These last two examples constitute just a few of the ways in which the basic principles expounded in Sections 1.5.1 and 1.5.2 can be applied to design a myriad of walking devices to suit the operator's requirements. Both are energy ratchet walkers: information ratchet walking systems can be envisaged (see Section 1.5.2), but such devices may well prove harder to design and synthesise. All the examples addressed so far have also had only two feet. However, systems with multiple feet allow simpler tracks to be utilised whilst simultaneously decreasing the chances of the walker and track dissociating. Consider the tripedal walking system depicted in Figure 1.26. As long as the three feet can form stable and independently addressable complexes with both stations of the track, directional (and highly processive) motion can be achieved. However, in this case, it would be necessary to have accurate information on the starting position of the walkers, as it is possible for the walker to associate with the track in two different isoenergetic orientations, the populations of which would process in opposite senses under the same set of stimuli.

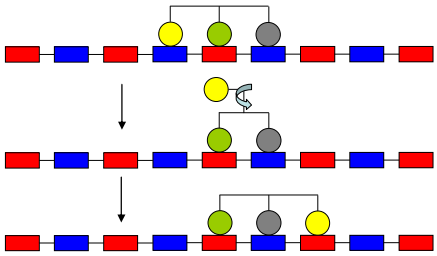

Figure 1.26 A three-legged walker can perform unidirectional motion on an *ABABAB* track using an energy ratchet mechanism. It is assumed that a stepping foot can only stretch to the binding sites on either side of the two feet that are anchored to the track and that there cannot be any vacant stations between the feet, such that the "middle" foot of the walker is effectively restricted to only one possible binding site.

Hence the range of walkers that can be designed seems limited only by the imagination. Equipped with these guidelines, definitions and mechanistic insights, it is now possible to review the current state of the art concerning molecular walkers in a constructive and rigorous fashion.

1.6 Synthetic "Walking" Molecules

Despite a not insubstantial body of literature dedicated to modelling the action of both natural[15,60-69] and artificial[52,70-73] walking systems, the practical complexities of synthesising such molecules mean that actual examples of synthetic walking machines are still very rare. Moreover, there exists some considerable confusion regarding walking terminology, which threatens to obscure some of the intricate science behind these devices. For example, Kwon *et al*[74] observed 9,10-dithioanthracene (DTA) undertaking 1D Brownian walks after deposition on a Cu(111) surface at 50-70 K (Figure 1.27). This phenomenon results from a mismatch between the periodicity of the copper surface and the distance between the sulfur atoms in a DTA molecule, which means that only one sulfur atom is able to assume its preferred geometry with regards to the surface at any one time. This sulfur atom then acts as an anchor for the other, which binds to the surface much less strongly making the whole molecule largely free to rotate. Stepping occurs when random rotation of the DTA molecule places the essentially unbound sulfur atom in a configuration where it can bind to the surface strongly, at which point there is a non-zero probability of that sulfur binding strongly to the surface and the previously

anchoring sulfur atom becoming "unbound". STM imaging was used to monitor the direction of motion of these molecules and it was found that they moved exclusively along only one axis.

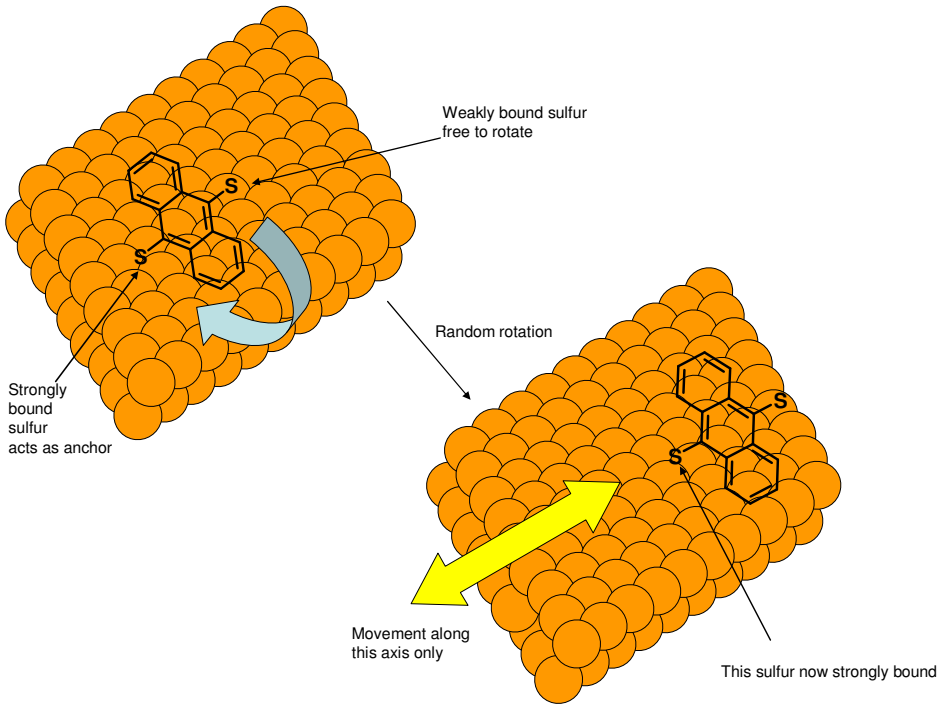

Figure 1.27 A DTA molecule undertakes a 1D random walk on a copper(111) surface at low temperatures.

Whilst this system does not fall foul of the definition of walking as outlined in Section 1.5, the authors' assertion that the motion is *unidirectional* appears inaccurate. Indeed, the authors themselves state that there is no bias in the system and so each walker is free to step in either direction at any time: the STM images show only *diffusion events* (albeit along a single axis). Hence we must consider this system as performing a 1D random walk and not directed motion.[75]

The remaining examples of synthetic walking machines in the literature are all based on DNA. The autonomous DNA transport device reported by Yin *et al*[76] (Figure 1.28) uses a walker module which moves along a DNA track in a fashion highly reminiscent of a crowd surfer being carried across a mosh pit. The concept uses DNA restriction and ligation enzymes to selectively join and then cut segments of DNA, with the net result that a six nucleotide fragment of DNA (the walker) is transported

from one end of the track to the other. Initially, this fragment (coloured red and denoted * in Figure 1.28) is attached to anchorage A on the track, giving A*.

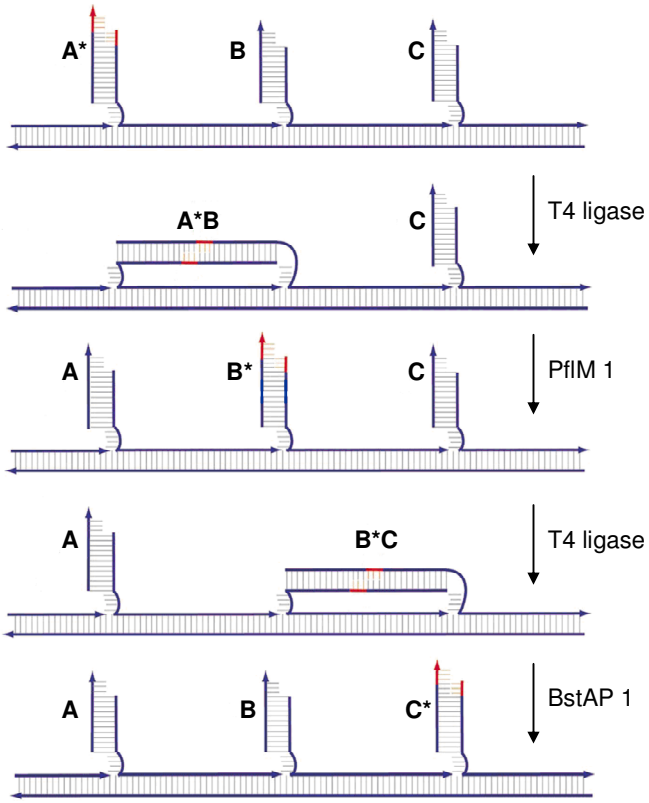

Figure 1.28 A molecular conveyor belt for the six nucleotide walker *, coloured red. Adapted by permission of WILEY-VCH Verlag GmbH & Co. KGaA, Weinheim, Germany.[76]

Action of T4 ligase then connects the anchorage A/walker hybrid to anchorage B *via* the three nucleotide sticky end on anchorage B, giving A*B. In so doing, a recognition site for the restriction enzyme PflM 1 is created, allowing this enzyme to cut the complex A*B in such a way that the six nucleotide fragment passes to anchorage B, giving B*. At this point T4 ligase can either re-ligate B* to A to give A*B again (an idling step), or it can join B* to C to give B*C (the forward step). However, whilst re-ligation of B* to A can be undone by the action of PflM 1 (regenerating B*), ligation of B* to C represents the point at which the walker cannot return to A, as B*C does not contain a restriction site for PflM 1. Instead, the final state C* must be generated by the action of a second restriction enzyme, BstAP 1, for which a restriction site is created when B* is ligated to C. As the walker cannot return to A after B*C has been formed, the authors rightly assert that the motion of * is unidirectional.[77] Yin *et al* were also unable to detect the linkage of two tracks by

one walker unit, suggesting that the motion undertaken is processive, and that scrambling of walkers and tracks does not occur. Furthermore, the unidirectional motion of the DNA fragment is *autonomous* under the conditions used by the authors – all that was necessary to complete the transport of * from one end of the track to the other was to mix all the components together and wait. Despite its rather unconventional gait, this system does constitute a walking system as defined in Section 1.5 – it has two feet (the two different ends of the six-nucleotide fragment), one of which is always in contact with the track, and it is able to step (by DNA restriction and subsequent ligation) in a reproducible (if not always reversible) manner.

The remaining examples of walking systems are more akin to the designs of Section 1.5.4. The first of these was reported by Sherman and Seeman[78] at around the same time as Yin *et al* published their autonomous transporter. Again based on DNA, the Sherman and Seeman design exploits the hybridisation of complementary strands of DNA to form double helices that anchor one foot to the track (also comprised of DNA), whilst allowing the other foot to dissociate from it. Both movement and standing still are achieved using single-stranded DNA oligomers known as "set strands" and "unset strands". Set strands hybridise both to a foothold on the track and to a foot of the walker module, forming stable double helices. At the top of each set strand, there is a short (8 nucleotide) "toehold" region that is not complementary to any of the feet or footholds (Figure 1.29). Unset strands complementary to a given set strand in its entirety (including the toehold) are then able to hybridise to the set strands preferentially and remove them as double helix "waste". This leaves the foot and foothold free to dissociate, and the addition of a set strand complementary to both the free foot and another foothold will cause the walker to step to that position. In this way, judicious choice of DNA sequences for the various set and unset strands and an appropriate order of addition leads to directed motion of the walker along the track (Figure 1.29).[79]

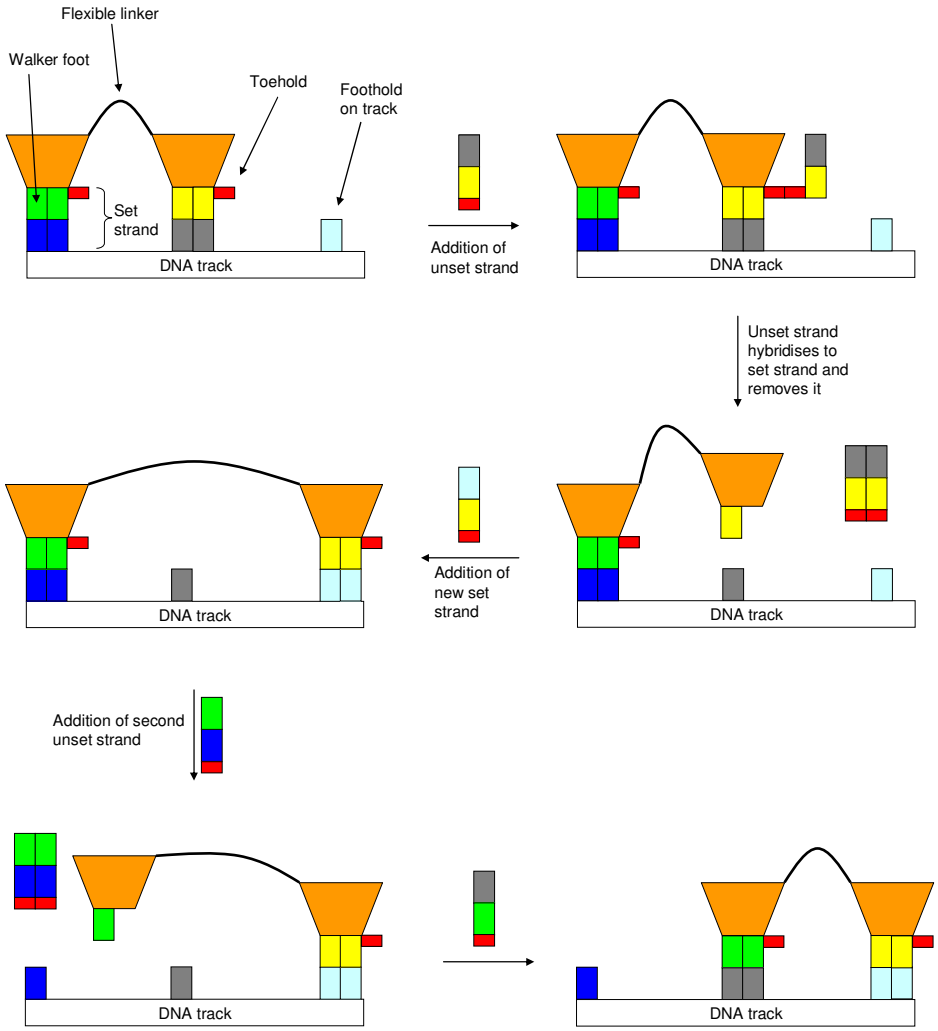

Figure 1.29 Pictorial representation of the Sherman-Seeman walker system.

Tian and Mao[80] have used a very similar idea to create a system of DNA-based "molecular gears", where two DNA "nanocircles" possessing single-stranded DNA "toeholds" are connected to one another by the addition of appropriate linking strands (Figure 1.30). These linking strands contain regions that are not complementary to any toeholds, such that addition of a removal strand with complementarity to the whole of the linker strand causes the removal of the linker strand as duplex waste. By careful ordering of the addition of linker and removal strands, the two nanocircles could be made to step around each other in a processive fashion.

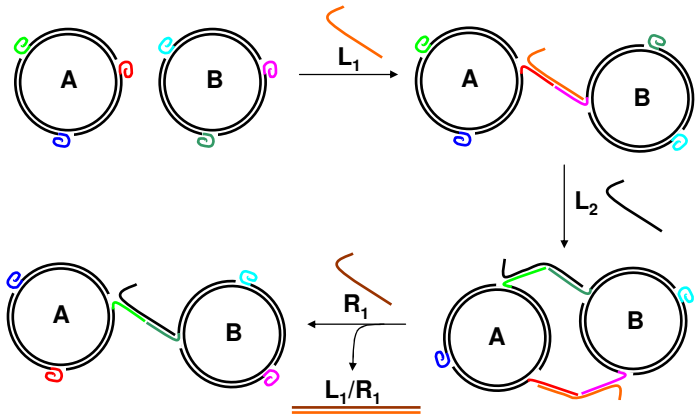

Figure 1.30 Pictorial representation of Mao's Molecular Gears. The linking strand L_1 causes the two nanocircles (A and B) to associate, whilst addition of a second linking strand (L_2) causes a second DNA duplex connection to be formed. Addition of a removal strand (R_1) which is complementary to all of L_1 (including the single stranded overhang) then breaks the original AL_1-BL_1 duplex. Subsequent addition of appropriate linking and removal strands then allows the circles to step processively around each other in a directional fashion.

Shin and Pierce[81] have expanded on these ideas, and have been able to create a walker/track system where the biped moves in a hand-over-hand fashion (the Sherman-Seeman walker/track ensemble operates under an inchworm regime). To do this, they designed a track consisting of four different footholds and a walker with two different feet. Set strands (A1, A2 – see Figure 1.31) are used to bind a given foot to a given foothold on the track, and unset strands (D1, etc.) can then be added which nucleate with the relevant (perfectly complementary) set strand *via* a 10-base toehold, removing the set strand as double helix waste and allowing the foot and foothold to dissociate. Again, the authors were able to demonstrate that the walking was both unidirectional (given a specific order of addition of set/unset strands) and processive.

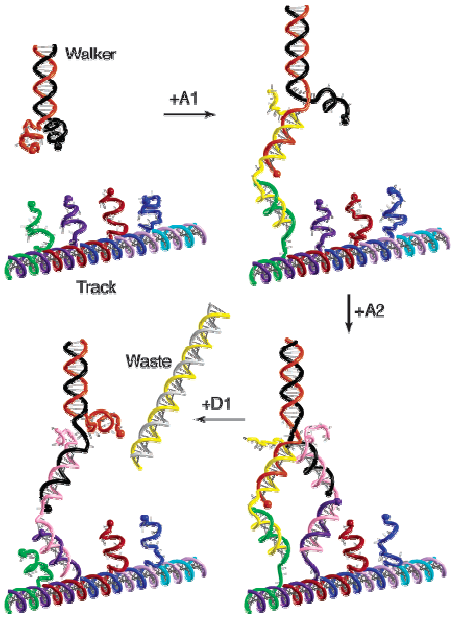

Figure 1.31 The Shin-Pierce hand-over-hand DNA walker[81] Adapted by permission of WILEY-VCH Verlag GmbH & Co. KGaA, Weinheim, Germany from Reference 48.

It is interesting to note that the Shin-Pierce system uses four different footholds (or binding sites) on the track, and two different feet. In this way, we can consider it to have an *ABCDABCD* track, where one foot of the walker hybridises only to footholds *A* and *C* and the other foot forms stable interactions only with footholds *B* and *D*. From a synthetic point of view, such a division or compartmentalisation of the interactions necessary for processive directed walking can be of immense assistance in simplifying a very complex problem down to a basic initial target: two orthogonally addressable switching mechanisms, each comprising a foot and its corresponding footholds.

1.7 Summary and Outlook

The success of the DNA-based molecular walkers shows that the synthesis of truly artificial walking molecules is possible. All of these designs rely on DNA base-pair recognition to promote stepping, with the dominant interactions (as in the association of kinesin with microtubules) being non-covalent interactions such as the hydrogen bond.[2] Although individual hydrogen bonds are relatively weak, multiple interactions can generate remarkably stable assemblies with a significant degree of specificity provided by the three-dimensional arrangement of the hydrogen bond donors and

acceptors within a given sequence. However, if *minimalist* walking molecular machines are to be realised, then an elaborate array of hydrogen bonding groups is not an appropriate basis for stepping or standing. Moreover, with the full range of interactions available to the synthetic chemist, there is no reason to suppose that highly robust, tuneable and addressable molecular walkers cannot be synthesised from wholly non-natural building blocks on a scale far smaller than that achieved by Nature. The design and synthesis of just such a fundamental synthetic molecular walking system will be addressed in the following Chapters.

1.8 References and Notes

(1) Feynman, R. P. *Annual Meeting of the American Physical Society,* Caltech **1959**.

(2) Stryer, L.; Berg, J. M.; Tymoczko, J. L. *Biochemistry.* 5th. ed. **2002**, W.H. Freeman: San Francisco.

(3) Wang, H.; Oster, G. *Nature* **1998**, *396,* 279-282.

(4) Meister, M.; Lowe, G.; Berg, H. C. *Cell* **1987**, *49,* 643-650.

(5) Xing, J.; Bai, F.; Berry, R.; Oster, G. *Proc. Nat. Acad. Sci.* **2006**, *103,* 1260-1265.

(6) Kinosita, K.; Yasuda, R.; Noji, H.; Ishiwata, S.; Yoshida, M. *Cell* **1998**, *93,* 21-24.

(7) Noji, H.; Yasuda, R.; Yoshida, M.; Kinosita, K. *Nature* **1997**, *386,* 299-302.

(8) Ueno, H.; Suzuki, T.; Kinosita, K.; Yoshida, M. *Proc. Nat. Acad. Sci.* **2005**, *102,* 1333-1338.

(9) Yasuda, R.; Noji, H.; Yoshida, M.; Kinosita, K.; Itoh, H. *Nature* **2001**, *410,* 898-904.

(10) Woehlke, G.; Schliwa, M. *Nat. Rev. Mol. Cell Biol.* **2000**, *1,* 50-58.

(11) Svoboda, K.; Schmidt, C. F.; Schnapp, B. J.; Block, S. M. *Nature* **1993**, *365,* 721-727.

(12) Howard, J. *Mechanics of motor proteins and the cytoskeleton.* **2001**, Sinauer Associates: Sunderland (MA).

(13) Vale, R. D.; Reese, T. S.; Sheetz, M. P. *Cell* **1985***, 42,* 39-50.

(14) Yildiz, A.; Selvin, P. R. *Trends Cell Biol.* **2005**, *15,* 112-120.

(15) The "anatomically-challenged" nature of the various kinesin nomenclatures has been noted by some of the more physically-minded investigators of the motor proteins, see: Astumian, R. D. *J. Phys.: Condens. Matter* **2005***, 17,* 3753-3766.

(16) Vale, R. D. *Cell* **2003**, *112,* 467-480.

(17) Carter, N. J.; Cross, R. A. *Nature* **2005**, *435,* 308-312.

(18) Carter, N. J.; Cross, R. A. *Curr. Opin. Struct. Biol.* **2006**, *18,* 61-67.

(19) Cross, R. A. *Trends Biochem. Sci.* **2004**, *29,* 301-309.

(20) Svoboda, K.; Block, S. M. *Cell* **1994**, *77,* 773-784.

(21) Yildiz, A.; Tomishige, M.; Vale, R. D.; Selvin, P. R. *Science* **2004**, *303,* 676-678.

(22) Dietrich, K. A.; Sindelar, C. V.; Brewer, P. D.; Downing, K. H.; Cremo, C. R.; Rice, S. E. *Proc. Nat. Acad. Sci.* **2008***, 105,* 8938-8943.

(23) Kaseda, K.; Higuchi, H.; Hirose, K. *Nat. Cell. Biol.* **2003***, 5,* 1079-1082.

(24) Wade, R. H.; Hyman, A. A. *Curr. Opin. Struct. Biol.* **1997***, 9,* 12-17.

(25) Klumpp, S.; Lipowsky, R. *Proc. Nat. Acad. Sci.* **2005**, *102,* 17284-17289.

(26) Brown, R. *The Miscellaneous Botanical Works of Robert Brown.* ed. Bennett, J. J. **1866**, Ray Society: London.

(27) Einstein, A. *Ann. Phys.* **1905***, 17,* 549-560.

(28) Haw, M. *Phys. World* **2005***, 18,* 19-22.

(29) *Molecular Motors.* ed. Schliwa, M. **2003**, Wiley-VCH: Weinheim.

(30) Reimann, P.; Hänggi, P. *Appl. Phys. A* **2002**, *75,* 169-178.

(31) Balzani, V.; Credi, A.; Raymo, Françisco M.; Stoddart, J. F. *Angew. Chem. Int. Ed.* **2000**, *39,* 3348-3391.

(32) Balzani, V.; Venturi, M.; Credi, A. *Molecular Devices and Machines - A Journey into the Nanoworld.* **2003**, Wiley-VCH: Weinheim.

(33) Pease, A. R.; Jeppesen, J. O.; Stoddart, J. F.; Luo, Y.; Collier, C. P.; Heath, J. R. *Acc. Chem. Res.* **2001**, *34,* 433-444.

(34) Raehm, L.; Sauvage, J.-P. *Struct. Bond.* **2001**, *99,* 55-78.

(35) Kay, E. R.; Leigh, D. A.; Zerbetto, F. *Angew. Chem. Int. Ed.* **2007**, *46,* 72-191.

(36) Bissell, R. A.; Cordova, E.; Kaifer, A. E.; Stoddart, J. F. *Nature* **1994**, *369,* 133-137.

(37) Kelly, T. R.; De Silva, H.; Silva, R. A. *Nature* **1999**, *401,* 150-152.

(38) Kelly, T. R.; Silva, R. A.; Silva, H. D.; Jasmin, S.; Zhao, Y. *J. Am. Chem. Soc.* **2000**, *122,* 6935-6949.

(39) Fletcher, S. P.; Dumur, F.; Pollard, M. M.; Feringa, B. L. *Science* **2005**, *310,* 80-82.

(40) Koumura, N.; Zijlstra, R. W. J.; van Delden, R. A.; Harada, N.; Feringa, B. L. *Nature* **1999**, *401,* 152-155.

(41) Pollard, M. M.; Lubomska, M.; Rudolf, P.; Feringa, B. L. *Angew. Chem. Int. Ed.* **2007***, 46,* 1278-1280.

(42) Hernandez, J. V.; Kay, E. R.; Leigh, D. A. *Science* **2004***, 306,* 1532-1537.

(43) Leigh, D. A.; Wong, J. K. Y.; Dehez, F.; Zerbetto, F. *Nature* **2003**, *424,* 174-179.

(44) Altieri, A.; Bottari, G.; Dehez, F.; Leigh, D. A.; Wong, J. K. Y.; Zerbetto, F. *Angew. Chem. Int. Ed.* **2003**, *42,* 2296-2300.

(45) Reimann, P. *Phys. Rep.* **2002**, *361,* 57-265.

(46) Alvarez-Perez, M.; Goldup, S. M.; Leigh, D. A.; Slawin, A. M. Z. *J. Am. Chem. Soc.* **2008**, *130,* 1836-1838.

(47) Serreli, V.; Lee, C.-F.; Kay, E. R.; Leigh, D. A. *Nature* **2007***, 445,* 523-527.

(48) Kelly, T. R. *Angew. Chem. Int. Ed.* **2005**, *44,* 4124-4127.

(49) In this discussion, we shall look only at passing-leg (hand-over-hand) modes of action, as these are the most pertinent to the case of synthetic kinesin analogues. However, the fundamental principles expounded in this section also hold true for walkers operating under inchworm regimes.

(50) Seneta, E. *Int. Stat. Rev.* **1996**, *64,* 255-263.

(51) Note that stimuli 2 and 3 could correspond to turning "on" and then turning "off" one particular interaction, for example stimulus 2 could make certain complexes labile and "stimulus 3" could then be simply to stop applying stimulus 2. It is also worth noting that the balance breaking stimulus could be the same for both foot/foothold complexes, as long as these complexes can be made labile or non-labile independently – a foot/foothold complex that is not labile cannot be affected by the balance-breaking stimulus until it is rendered labile by application of the appropriate linking stimulus.

(52) Li, D.; Fan, D.; Wang, Z. *J. Chem. Phys.* **2007**, *126,* 245105.

(53) Wang, Z. *Phys. Rev. E* **2004**, *70,* 031903.

(54) Li, D.; Fan, D.; Zheng, W.; Le, Y.; Wang, Z. *Chem. Phys.* **2008**, *352,* 235-240.

(55) Note that applying the stimuli in the reverse order (labilisation of the green foot from the blue station, linker elongation and subsequent fixing of the green foot back to the track, followed by yellow foot/red station labilisation, linker contraction and fixing) gives directed motion in the *other* direction.

(56) For an intriguing application of a diffusional burnt bridge walking system, leading to the controlled release of substrates from hydrogel matrices, see: (a) Pei, R.; Taylor, S. K.; Stefanovic, D.; Rudchenko, S.; Mitchell, T. E.; Stojanovic, M. N. *J. Am. Chem. Soc.* **2006**, *128*, 12693-12699. For articles expounding the physics of burnt bridge walkers, see: (b) Mai, J.; Sokolov, I. M.; Blumen, A. *Phys. Rev. E* **2001***, 64,* 011102. (c) Morozov, A. Y.; Kolomeisky, A. B. *J. Stat. Mech.* **2007**, *12*, 12008-12030. (d) Antal, T.; Krapivsky, P. L. *Phys. Rev. E* **2005**, *72,* 046104.

(57) It should be noted that in order to process directionally in the bulk, information ratchet walkers must have a preferred orientation on the track. In Figure 1.21, this was achieved by having a diastereotopic track to which the feet of the walker could only bind in one orientation. In the case of kinesin, this preferred orientation could be brought about as a result of the inherent polarity of the tubulin heterodimers of which microtubules are composed. Thus a kinesin dimer associating with a mictotubule at random from solution would have a preferred "front" and "back", such that it would process in one preferred direction in the presence of ATP.

(58) As kinesin processes in only one direction along microtubules, it is in fact essential that it takes only a limited number of steps (~100 on average) before dissociation from the track. Were it to be more

processive, then when it reached the end of a given microtubule the front foot would remain anchored to the track whilst the back foot performed a long series of abortive "forward" steps (consuming an ATP molecule for every "step"), always returning to the same position behind the anchored foot. Hence huge "traffic jams" of kinesins waiting to dissociate from their microtubules would build up, leading to a dearth of operational kinesins for carrying cargoes and wasting huge amounts of ATP. Thus it would seem that kinesin's ability to dissociate fully from microtubules after only a few tens of steps and diffuse at random back to the other end of the track is critical to its efficient transport of cargoes in the cell.

(59) A rotaxane-based architecture would be one way in which to achieve this confinement without the need to enclose the whole system in a tube.

(60) Wang, H. *J. Phys.: Condens. Matter* **2005***, 17,* 3997-4014.

(61) Mukherji, S. *Phys. Rev. E* **2008**, *77,* 051916.

(62) Jülicher, F.; Ajdari, A.; Prost, J. *Rev. Mod. Phys.* **1997**, *69,* 1269-1282.

(63) Derényi, I.; Vicsek, T. *Physica A* **1998***, 249,* 397-406.

(64) Derényi, I.; Vicsek, T. *Proc. Nat. Acad. Sci.* **1996**, *93,* 6775-6779.

(65) Lipowsky, R.; Klumpp, S.; Nieuwenhuizen, T. M. *Phys. Rev. Lett.* **2001**, *87,* 108101.

(66) Nieuwenhuizen, T. M.; Klumpp, S.; Lipowsky, R. *Phys. Rev. E* **2004**, *69,* 061911.

(67) Kolomeisky, A. B.; Fisher, M. E. *Biophys. J.* **2003**, *84,* 1642-1650.

(68) Saffarian, S.; Collier, I. E.; Marmer, B. L.; Elson, E. L.; Goldberg, G. *Science* **2004**, *306,* 108-111.

(69) Astumian, R. D. *Biosystems* **2008***, 93,* 8-15.

(70) Parmeggiani, A.; Franosch, T.; Frey, E. *Phys. Rev. Lett.* **2003**, *90,* 086601.

(71) Porto, M.; Urbakh, M.; Klafter, J. *Phys. Rev. Lett.* **2000***, 85,* 491-494.

(72) Oshanin, G.; Klafter, J.; Urbakh, M. *Europhys. Lett.* **2004**, *68,* 26-32.

(73) Dillmann, R.; Albiez, J.; Gaßmann, B.; Kerscher, T.; Zöllner, M. *Phil. Trans. R. Soc. A* **2007***, 365,* 133-151.

(74) Kwon, K.-Y.; Wong, K. L.; Pawin, G.; Bartels, L.; Stolbov, S.; Rahman, T. S. *Phys. Rev. Lett.* **2005**, *95,* 166101.

(75) This is not to detract from studies performed with the intention of modelling chemotaxis-type diffusions of molecules on surfaces, where the random walk of a molecule down a given concentration gradient mimics the motions of simple cells towards or away from stimuli, see for example: Chang, T.; Rozkiewicz, D. I.; Ravoo, B. J.; Meijer, E. W.; Reinhoudt, D. N. *Nano Lett.* **2007**, *7,* 978-980.

(76) Yin, P.; Yan, H.; Daniell, X. G.; Turberfield, A. J.; Reif, J. H. *Angew. Chem. Int. Ed.* **2004**, *43,* 4906-4911.

(77) In fact, as this system cannot return to its starting state after B*C has been formed, it constitutes a burnt bridge walker system and is therefore an information ratchet.

(78) Sherman, W. B.; Seeman, N. C. *Nano Lett.* **2004***, 4,* 1203-1207.

(79) The Sherman-Seeman, Tian-Mao and Shin-Pierce walking systems all operate *via* energy ratchet mechanisms: the stepping foot is biased towards a given binding site by thermodynamics alone. Hence addition of an unset strand can be considered as the linking stimulus and addition of an appropriate set strand is the fixing stimulus. Stepping occurs to the foothold with which the foot/set strand ensemble forms the most stable duplex (so the set strand also acts to break detailed balance in a stepping foot).

(80) Tian, Y.; Mao, C. *J. Am. Chem. Soc.* **2004**, *126,* 11410-11411.

(81) Shin, J. S.; Pierce, N. A. *J. Am. Chem. Soc.* **2004**, *126,* 10834-10835.

CHAPTER TWO

Cadiot-Chodkiewicz Active Template Synthesis of Rotaxanes and Switchable Molecular Shuttles with Weak Intercomponent Interactions

Published as *"Cadiot-Chodkiewicz Active Template Synthesis of Rotaxanes and Switchable Molecular Shuttles with Weak Intercomponent Interactions"* J. Berná, S. M. Goldup, A.-L. Lee, D. A. Leigh, M. D. Symes, G. Teobaldi, F. Zerbetto, *Angew. Chem. Int. Ed.* **2008**, *47*, 4392-4396.

Acknowledgements and Declaration

The following people are gratefully acknowledged for their contributions to this Chapter: Dr. Ai-Lan Lee and Dr. José Berná synthesised the model rotaxanes detailed in Tables 2.1 and 2.2, and investigated alternative reaction conditions (not described here); Dr. Gilberto Teobaldi performed the computation studies detailed in Section 2.7; the synthesis, characterisation and operation of molecular **12** represents a joint effort between Dr. Stephen Goldup and the Author.

Synopsis

The synthesis of rotaxanes has benefited greatly from the application of template-directed syntheses. However, the interactions between the thread and macrocycle which produce the template effect generally remain in the final rotaxane, thereby dictating the properties of the resulting molecule. Conversely, systems which lack significant intercomponent interactions, or have interactions that are too weak to lead to successful templates (e.g. single contact H-bonds) cannot be made to form interlocked architectures in useful yield. If mechanically interlocked molecules that contain only very weak intercomponent interactions are to be produced, a new templating method must be developed.

The Leigh group has introduced the active-metal template approach for the formation of rotaxanes. Active-template syntheses differ from classical template reactions in that a single species acts as both a template and a catalyst for covalent bond formation. Combining these two roles has several potential advantages over conventional "passive" template syntheses, including inherent efficiency and the possibility of traceless assembly.

This Chapter describes a traceless Cadiot-Chodkiewicz active-metal template pathway to heterocoupled [2]rotaxanes and its application to the synthesis of a molecular shuttle containing only a single thread-macrocycle H-bond, which would be extremely difficult to realise using traditional rotaxane-forming methods.

2.1 Introduction

The noncovalent binding motifs used to template the synthesis of mechanically interlocked architectures are generally retained in the final products.[1] This feature has been widely exploited to make molecular shuttles,[2] rotaxanes with two or more discrete binding sites or 'stations' on the thread between which the macrocycle shuttles incessantly through Brownian motion. However, the noncovalent interactions used to maximise the rotaxane yield and localise the position of the ring on the thread also provide the major contribution to the activation energy to shuttling.[3] To achieve faster moving rotaxane-based molecular machines, it will be necessary to make molecular shuttles with much weaker intercomponent interactions than are typically introduced with classical template methods.[4] Here we report on a new rotaxane-forming reaction that can produce rotaxanes with unsymmetrical threads (as required for switchable molecular shuttles) but does not leave strong intercomponent binding motifs in the rotaxane product. Instead the active template[5] Cadiot-Chodkiewicz[6] reaction is compatible with building blocks that can provide relatively modest macrocycle-thread binding motifs in the rotaxane, but which are still strong enough to afford good positional integrity of the ring. The methodology is exemplified through the synthesis of a 'weak interaction' molecular shuttle in which a single hydrogen bond between the components determines the predominant position of the macrocycle in each of two well-defined states, which can be switched between by reversible complexation with Li^+ or protonation.

Active template syntheses differ from classical 'passive-template' reactions in that a single species acts as both the template for the product architecture and as the catalyst for the formation of the covalent bond(s) that captures it.[5] Although combining these two roles has several potential advantages,[5a] controlling the positions of the metal-ligated building blocks during the reaction to template the product puts additional demands (which can themselves provide insight into the reaction pathway[5d]) on the mechanism of catalysis. Accordingly, successful combinations of ligands and metal-catalysed reactions for active template syntheses are still rare and the development of new systems remains challenging[5e].

2.2 Model Studies

The active metal template homodimerisation of acetylenes to form rotaxanes[5b, 5c] introduces a relatively rigid linear connector which inhibits folding—potentially desirable for fully exploiting the spatial separation of the ring between different states[7]—but can only be used to make [2]rotaxanes with symmetrical axles. The coupling of two different building blocks is necessary to produce bistable molecular shuttles in which the macrocycle can be switched between two different positions on the thread. The Cu(I)-mediated Cadiot-Chodkiewicz[6] heterocoupling of a terminal alkyne with an alkyne halide appeared a suitable candidate reaction for such studies (Table 2.1).

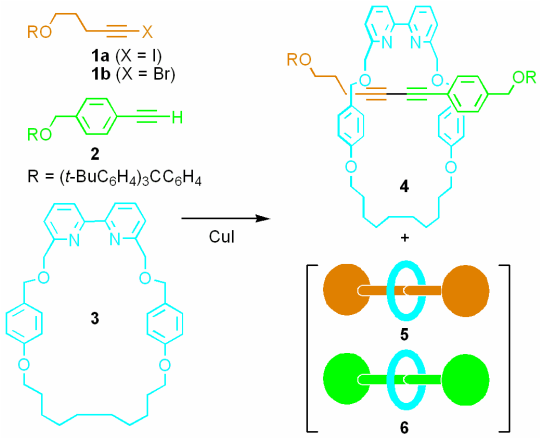

Entry	Alkyne halide	Solvent	Rotaxane yield **1+2+3→4+5+6**	Selectivity **4:5:6**
1	**1a**	$(i\text{-Pr})_2NH$	40%	10:9:1
2	**1a**	NEt_3	20%	2:15:1
3	**1a**	pyrrolidine	<2%	no rotaxane
4	**1a**	benzene[b]	35%	1.7:1:1
5	**1b**	$(i\text{-Pr})_2NH$	<5%	2:5:1

Table 2.1 Preliminary solvent screen for the bis-acetylene rotaxane forming active template Cadiot-Chodkiewicz reaction.[6] Conditions: [a] a solution of **1**, **2**, **3** and CuI (all one equivalent) was allowed to stir at 298 K under an atmosphere of N_2 for 18 hours. [b] Plus two equivalents of $(i\text{-Pr})_2NH$.

Promisingly, [2]rotaxane was produced (Table 2.1) using appropriately 'stoppered' alkyne-halide (**1a** or **1b**) and aryl-alkyne (**2**) derivatives and a bidentate macrocycle (**3**) under typical conditions[6] used for the Cadiot-Chodkiewicz reaction in non-aqueous solvents. However, in these initial studies poor selectivity for the heterocoupled rotaxane (**4**) versus the homocoupled rotaxanes (**5** and **6**) was observed, together with low overall conversion of the alkyne starting materials to bis-

acetylene products. In an attempt to improve both the reaction yield and the selectivity for the heterocoupled rotaxane, we investigated changing the traditional Cadiot-Chodkiewicz procedure of mixing the alkyne and alkyne-halide components with neutral amine bases, to pre-forming the copper acetylide by treatment of terminal alkyne **2** with *n*-BuLi, followed by transmetallation with CuI (Table 2.2).[8]

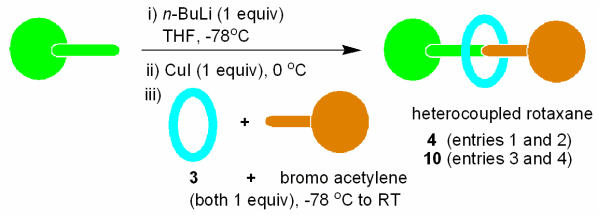

Entry	Terminal acetylene[a]	Bromo acetylene	Rotaxane yield [%]	Select-ivity
1	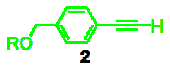 **2**	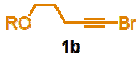 **1b**	84	>98%[b]
2	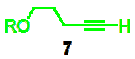 **7**	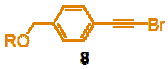 **8**	32	1.7:8:1 **4**:**5**:**6**
3	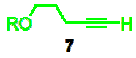 **7**	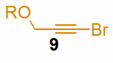 **9**	85	>98%[b]
4	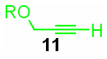 **11**	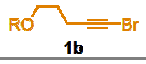 **1b**	74	>98%[b]

Table 2.2 Substrate scope of the Cadiot-Chodkiewicz active metal template synthesis of heterocoupled [2]rotaxanes. [a] R=(*t*-BuC_6H_4)$_3$CC_6H_4; [b] No homocoupled rotaxanes observed. Stacked plots of the ^{1}H NMR spectra for **4** and **10** (Figures 2.3 and 2.4, respectively) are given in Section 2.5.

Following this protocol, we were delighted to find that subsequent addition of bipyridine macrocycle **3** and bromoacetylene **1b** led to the desired [2]rotaxane **4** in high yield (84%) and with excellent selectivity (>98%) for the heterocoupled product (Table 2.2, entry 1).[9] Although the procedure did not prove compatible with reversing the reactive bromine/hydrogen functionalities of the alkyl and aryl-acetylene building blocks (**7** with **8**, Table 2.2, entry 2),[10] when coupling two different alkyl alkynes (**7** with **9** or **11** with **1b** to give **10**) either could be used successfully as the bromoacetylene partner whilst maintaining high yields and apparent exclusive selectivity for the heterocoupled rotaxane (Table 2.2, entries 3 and 4).

The Cadiot-Chodkiewicz reaction is thought to proceed via a different mechanism to the (also Cu(I)-catalysed) Glaser homocoupling of alkynes,[11] and the proposed pathway for the active-metal template rotaxane assembly of **4** is shown in Scheme 2.1. The pre-formed copper (I)-acetylide **I** is sequestered by bipyridine macrocycle **3**.[12] Oxidative addition across the C-Br bond of the bromoacetylene occurs from the opposite face of the macrocycle to produce the Cu(III) intermediate **II** and subsequent reductive elimination furnishes the heterocoupled [2]rotaxane.

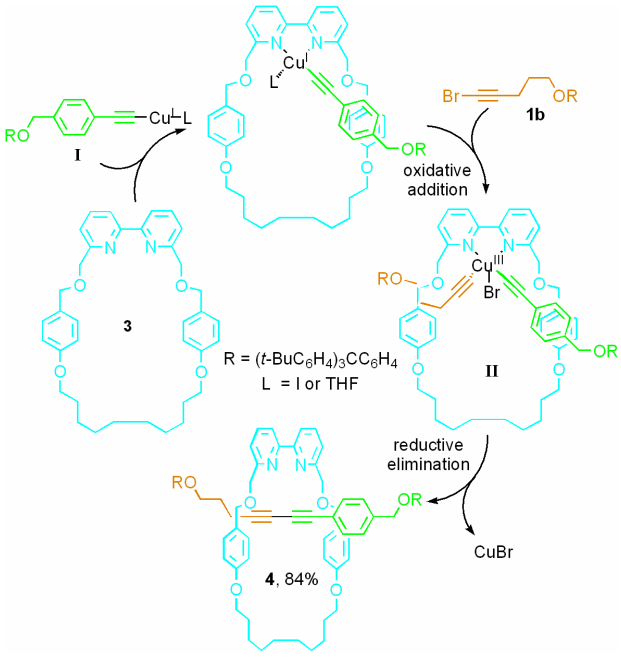

Scheme 2.1 Proposed mechanism for the Cadiot-Chodkiewicz active metal template formation of [2]rotaxane **4**.[11]

2.3 Design and Synthesis of a Switchable Molecular Shuttle with Weak Intercomponent Interactions

To demonstrate the utility of this new active template reaction, we synthesized a stimuli-switchable molecular shuttle, **12**, with modest strength intercomponent interactions of a type that would be difficult or impossible to access by traditional template methods. The single contact H-bond that molecular modelling (see Section 2.7 and Figure 2.2) indicates exists between the aniline unit of the thread and bipyridine group of the macrocycle in **12** is too weak to template rotaxane formation through 'stoppering' or 'clipping' strategies[1] and no passive metal templates which

utilize a 1+2 donor ligand set have been reported to date. However, the modified Cadiot-Chodkiewicz active metal template method readily produced molecular shuttle **12** in good yield (61%) from functionalized building blocks **13** and **14** with no homocoupled rotaxane products being detected (Scheme 2.2).

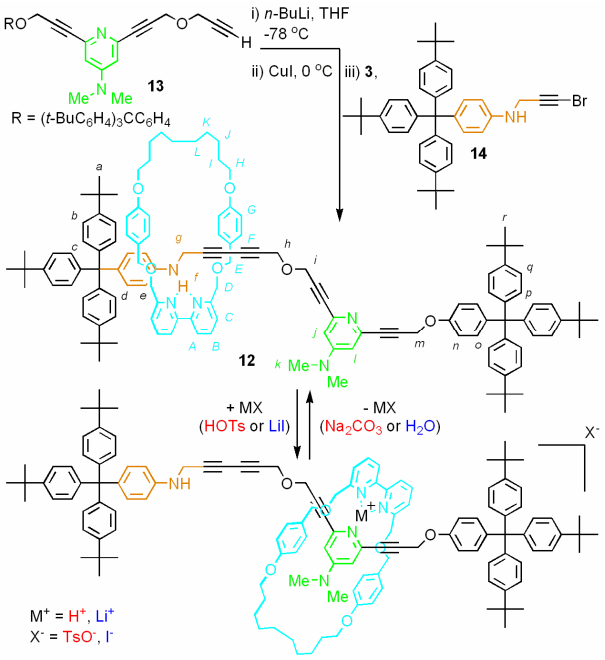

Scheme 2.2 Active template synthesis and stimulus-induced translocation of the macrocycle in molecular shuttle **12**. The stimulus applied is either protonation (MX = HOTs) or complexation with Li^+.

^{1}H NMR spectroscopy clearly shows the macrocycle to be predominantly held over the axle aniline unit in neutral molecular shuttle **12** at 300 K in CD_2Cl_2. The ^{1}H NMR spectrum of the rotaxane (Figure 2.1b) displays significant upfield shifts (H_d 0.2 ppm, H_e 0.4 ppm, H_g 0.6 ppm) of signals associated with the aniline station relative to those in the free thread (Figure 2.1a). Calculations on the macrocycle-station fragments for **12** in CH_2Cl_2 at *B3LYP/3-21G** level[13] (see Section 2.7) show that the minimum structure intercomponent binding energy, ΔG_{bind}, of -3.9 kcal mol^{-1} is largely attributable to a single contact H-bond of 2.1 Å between the N-*H* of the aniline and one nitrogen atom of the macrocycle bipyridine unit (Figure 2.2a). A review of the Cambridge Structural Database (CSD) reveals a range of 2.1-2.4 Å for similar aniline-to-pyridine contacts in the solid state.[14]

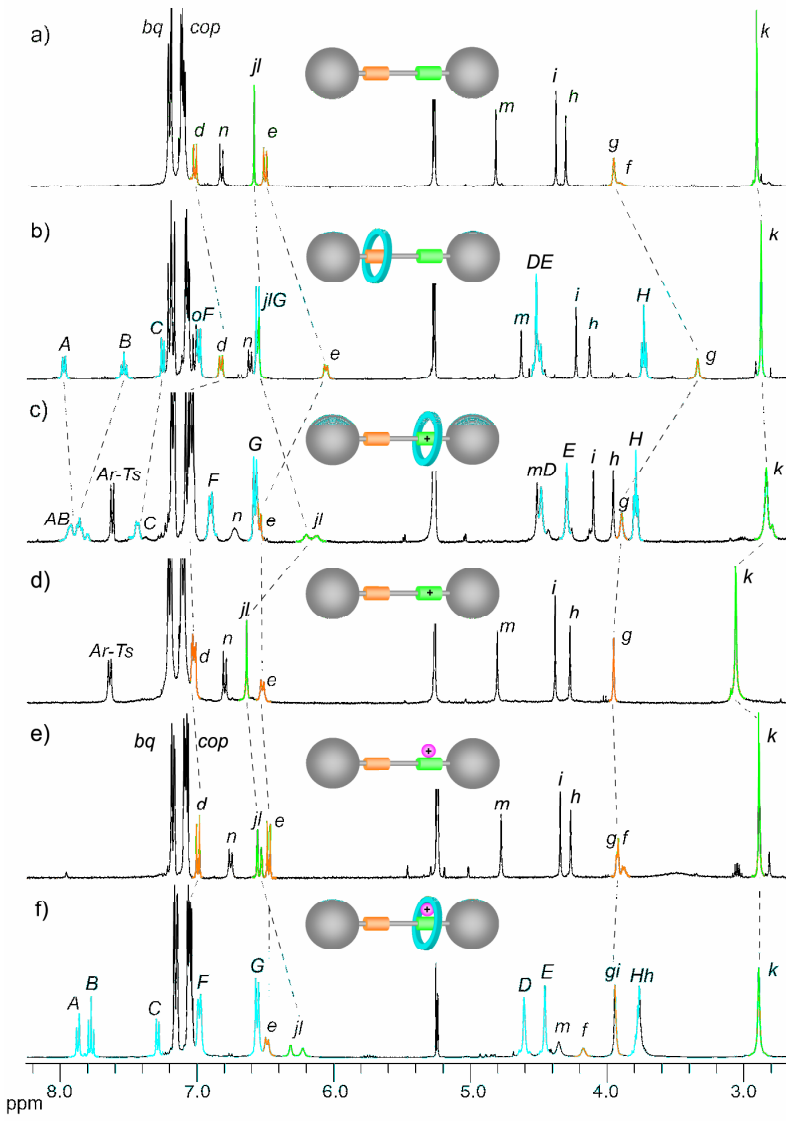

Figure 2.1 ^{1}H NMR spectra (400 MHz, CD_2Cl_2, 300 K) of (a) non-interlocked thread, (b) rotaxane **12**, (c) rotaxane **12** plus one equivalent TsOH, (d) non-interlocked thread plus one equivalent TsOH, (e) non-interlocked thread in the presence of excess LiI, (f) rotaxane **12** in the presence of excess LiI.

Addition of one equivalent of *p*-toluenesulfonic acid (TsOH) to a solution of rotaxane **12** in CD_2Cl_2 causes significant shifts in several of the axle signals in the ^{1}H NMR spectrum (Figure 2.1c).[15] Protons H_d, H_e and H_g associated with the aniline unit return to the position they occupy in the non-interlocked thread in the presence of TsOH (Figure 2.1d), while those of the 4-dimethylaminopyridine (DMAP) station (H_j and H_l each 0.5 ppm, H_k 0.2 ppm) shift to higher field. This is consistent with protonation of the DMAP nitrogen and translocation of the macrocycle along the thread so that the pyridinium N-H hydrogen bonds strongly with the bipyridine moiety of the macrocycle (Scheme 2.2, MX = HOTs). *B3LYP/3-21G** level

calculations (see Section 2.7) indicate that the protonated-DMAP-bound co-conformation is now favoured by ~0.9 kcal mol^{-1} (Figure 2.2b). A search of the CSD finds that the calculated H-bond contact distance of 1.8 Å is in the 1.4-1.9 Å range found for pyridinium-to-pyridine H-bonds in the solid state.[16] Treating a solution of rotaxane **12**-H^+ with solid Na_2CO_3 quantitatively regenerates the neutral molecular shuttle **12**, returning the macrocycle to its original position on the thread.

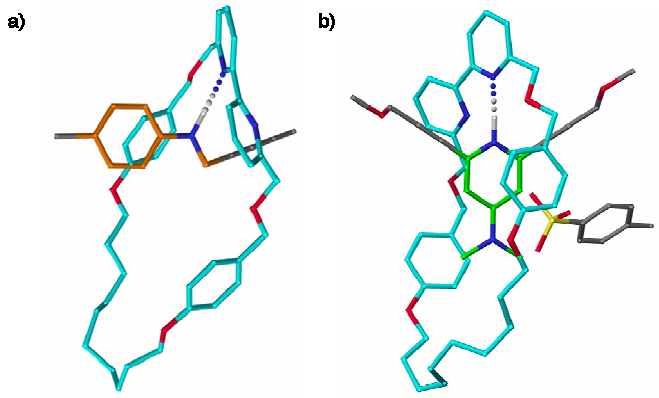

Figure 2.2 *B3LYP/3-21G** level quantum chemical calculated minimum energy macrocycle-station structures in CH_2Cl_2 at 298 K showing the single hydrogen bond interactions between the macrocycle and (a) aniline and (b) protonated-DMAP (tosylate counterion) stations present in molecular shuttle **12** and **12**-H^+.[13] Hydrogen atoms not attached to N atoms are not shown for clarity. Intercomponent N-H…N distances and angles: **12** 2.1 Å (153.6°); **12**-H^+ 1.8 Å (170.3°). Intercomponent binding energies (kcal mol^{-1}): Electronic, ΔE_{bind}, **12** -8.0 (±0.05), **12**-H^+ -14.1 (±0.05); enthalpic, ΔH_{bind}, **12** -6.7 (±0.04), **12**-H^+ -11.4 (±1); free energy, ΔG_{bind}, **12** -3.9 (±0.1), **12**-H^+ -4.8 (±1). The errors in the calculations were estimated by increasing the solvent cavity radius by 0.5 Å.

A similar change in co-conformation could be generated by shaking a solution of rotaxane **12** in CD_2Cl_2 with excess LiI (Scheme 2.2, MX = LiI). The ^1H NMR spectrum of the shuttle after treatment with LiI (Figure 2.1f) displays significant upfield shifts and broadening of the resonances of the pyridyl station (H_j, and H_l) compared with the corresponding protons in the non-interlocked thread in the presence of excess LiI (Figure 2.1e).[17] As was seen with protonation, the signals of the rotaxane aniline station H_d, H_e and H_g return to the position they occupy in the non-interlocked thread. These changes are consistent with the mechanically interlocked components of rotaxane **12** coordinating Li^+ though the bipyridine moiety of the macrocycle and the DMAP station of the axle. A simple aqueous wash removes the metal salt and regenerates rotaxane **12** in its original form.

2.4 Conclusions

The utility of the Cadiot-Chodkiewicz active template strategy has been exemplified through the construction and operation of a switchable molecular shuttle which features a single hydrogen bond between the mechanically interlocked components in each state, much less than half the intercomponent binding energy found in typical molecular shuttles yet still strong enough to ensure a high degree of positional integrity of the macrocycle in both forms. The methodology paves the way for faster moving, faster responding, mechanically interlocked molecular machines which can be designed to feature only the weakest noncovalent interactions necessary for their function.

2.5 Experimental Section

Terminal acetylenes **2**,[5d] **7**[5c] and **11**[5a] were prepared according to previously published procedures. Bromoacetylenes **1b**, **8** and **9** were prepared by treatment of the corresponding terminal acetylenes with NBS and AgNO3 in THF or acetone.[18] Macrocycle **3** was prepared according to a previously published procedure.[5c] Building blocks **S3, S4** and **S5** were prepared according to literature procedures.[19,15j,20]

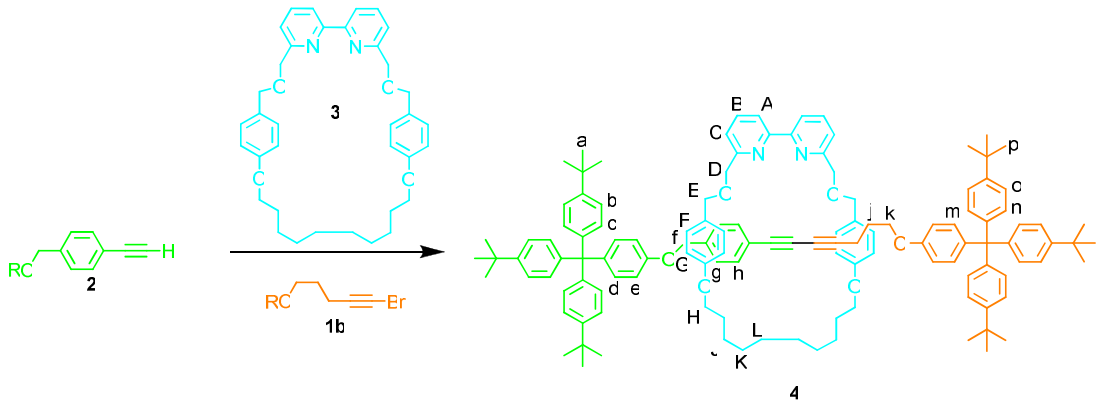

4

Scheme 2.3 Synthesis of rotaxane **4.** Reagents and conditions: *n*-BuLi, THF, -78 °C; ii) CuI, 0 °C → RT; iii) **3**, **1b**, -78 °C → RT, 20 h, 84%.

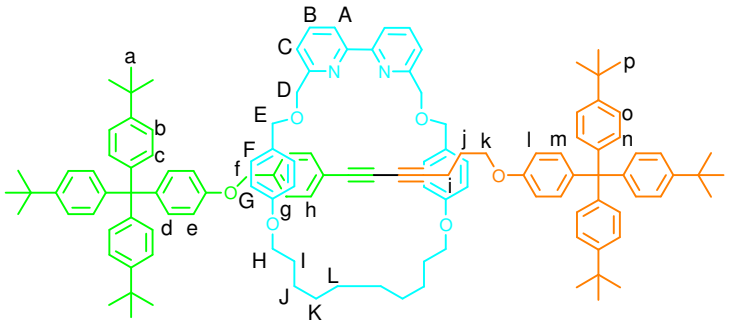

4

A solution of acetylene **2** (20 mg, 0.032 mmol) in THF (0.4 mL) was cooled to -78 °C. To this solution was added *n*-BuLi (0.32 mL, 0.1 M in THF) at -78 °C. The resulting solution was allowed to warm to 0 °C over 15 minutes. CuI (6.2 mg, 0.032 mmol) was added at 0 °C and the resulting yellow solution allowed to warm to RT over 15 minutes. The reaction mixture was returned to -78 °C and bipyridine macrocycle **3** (18 mg, 0.032 mmol) and bromoacetylene **1b** (22 mg, 0.032 mmol) were added as a solution in THF (0.6 mL). The resulting orange solution was allowed to stir at RT for 20 h before the reaction was quenched by addition of an aqueous solution of 17.5% NH_3 saturated with EDTA. The layers were allowed to stir in air for 40 minutes during which time the aqueous layer turned blue. The aqueous layer was extracted with CH_2Cl_2 (3 x 50 mL) and the combined organic layers washed with brine and dried over $MgSO_4$. Column chromatography on silica (7:2.5:0.5 hexane:CH_2Cl_2:MeCN) yielded [2]rotaxane **4** as a colourless film (47 mg, 84%): ^{1}H NMR (400 MHz, $CDCl_3$): δ 7.97 (d, J = 7.5, 2H, H_A), 7.50 (dd, J_1 = 7.6, J_2 = 7.5, 2H, H_B), 7.28 (d, J = 7.6, 2H, H_C), 7.26-7.22 (m, 12H, H_{b+o}) 7.12-7.05 (m, 18H, $H_{c+g+n+F}$), 7.02-6.97 (m, 4H, H_{d+m}), 6.85 (d, J = 8.3, 2H, H_h), 6.62 (d, J = 8.6, 4H, H_G), 6.52 (d, J = 8.9, 4H, H_{e+l}), 4.56 (s, 8H, H_{D+E}), 4.48 (s, 2H, H_f), 3.75 (t, J = 6.6, 4H, H_H), 3.69 (t, J = 6.0, 2H, H_k), 2.30 (t, J = 7.0, 2H, H_i), 1.73 (m, 2H, H_j), 1.58 (m, 4H, H_I), 1.31 (s, 54H, H_{a+p}), 1.26-1.05 (m, 12H, H_{J+K+L}). ^{13}C NMR (100 MHz, $CDCl_3$): δ 158.6, 158.2, 156.4, 155.4, 155.2, 148.3 (x 2), 144.2 (x 2), 139.7, 139.4, 137.9, 137.0, 132.3, 132.1, 130.7, 129.7 (x 2), 127.0, 124.1 (x 2), 124.0 (x 2), 121.2, 120.9, 119.6, 114.4, 113.2, 112.9, 83.6, 74.9 (x 2), 74.4, 72.4, 72.1, 69.0, 67.6, 65.6, 63.1, 63.0, 34.3, 31.4, 31.2, 29.7, 29.4, 29.0, 28.8, 28.0, 25.8, 15.3. LRFAB-MS (3-NOBA matrix): *m/z* = 1755 $[M+H]^+$. HRFAB-MS (3-NOBA matrix): *m/z* = 1755.0772 $[M+H]^+$ (calc. for $^{12}C_{122}{}^{13}C_2H_{140}N_2O_6$, 1755.0779 $[M+H]^+$).

Stacked plot of the ^{1}H-NMR spectra of **4** and **S1** in $CDCl_3$:

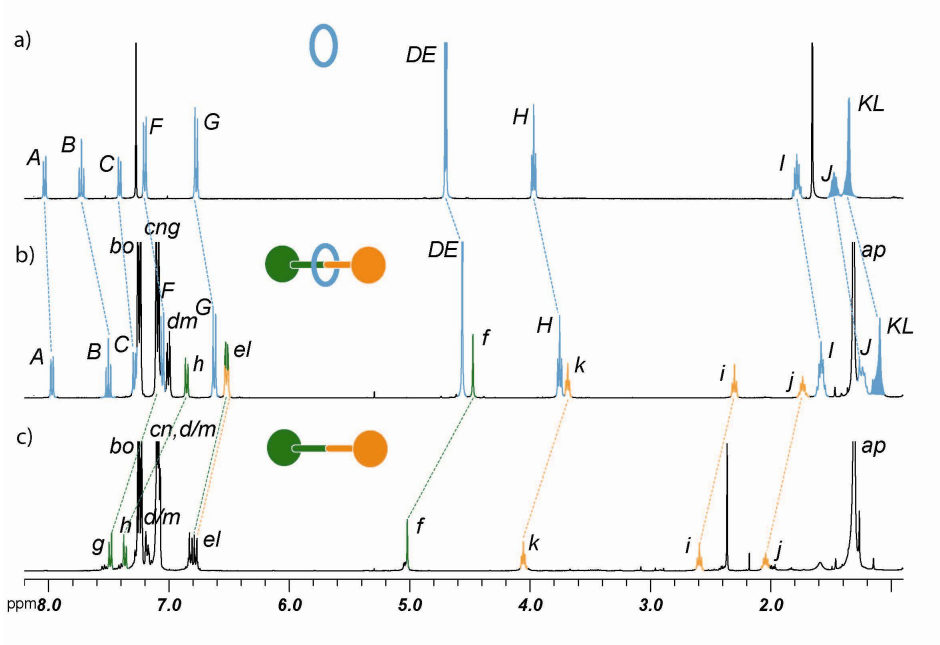

Figure 2.3 The ^{1}H NMR spectra (400 MHz, $CDCl_3$, 300 K) of a) macrocycle **3**, b) the [2]rotaxane **4**, c) the thread **S1**. The lettering corresponds to the ^{1}H NMR assignments given above.

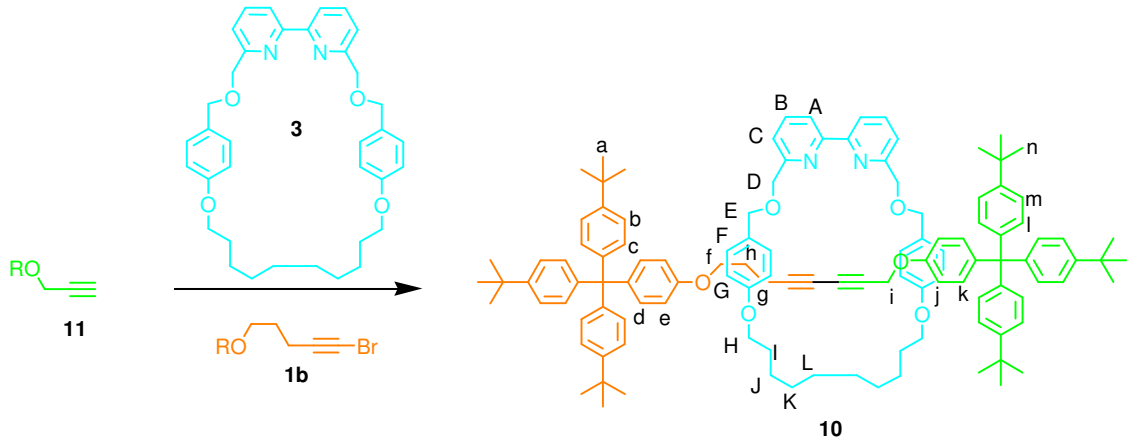

Scheme 2.4 Synthesis of rotaxane **10.** Reagents and conditions: *n*-BuLi, THF, -78 °C; ii) CuI, 0 °C → RT; iii) **3**, **1b**, -78 °C → RT, 20 h, 74%.

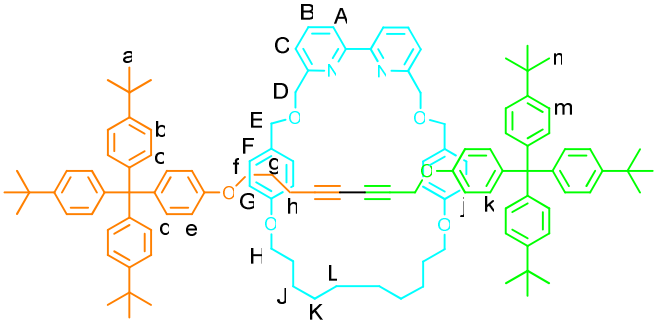

10

A solution of acetylene **11** (18 mg, 0.032 mmol) in THF (0.4 mL) was cooled to -78 °C. To this solution was added *n*-BuLi (0.32 mL, 0.1 M in THF) at -78 °C. The resulting solution was allowed to warm to 0 °C over 15 minutes. CuI (6.2 mg, 0.032 mmol) was added at 0 °C and the resulting yellow solution allowed to warm to RT over 15 minutes. The reaction mixture was returned to -78 °C and bipyridine macrocycle **3** (18 mg, 0.032 mmol) and bromoacetylene **1b** (22 mg, 0.032 mmol) were added as a solution in THF (0.6 mL). The resulting orange solution was allowed to stir at RT for 20 h before the reaction was quenched by addition of an aqueous solution of 17.5% NH_3 saturated with EDTA. The layers were allowed to stir in air for 40 minutes during which time the aqueous layer turned blue. The aqueous layer was extracted with CH_2Cl_2 (3 x 50 mL) and the combined organic layers washed with brine and dried over $MgSO_4$. Column chromatography (SiO_2, 7:2.5:0.5 hexane:CH_2Cl_2:MeCN) yielded [2]rotaxane **10** as a white foam (40 mg, 74%). ^{1}H NMR (400 MHz, $CDCl_3$): δ 8.02 (d, J = 7.6, 2H, H_A), 7.51 (dd, J_1 = 7.8, J_2 = 7.6, 2H, H_B), 7.27 (d, J = 7.8, 2H, H_C), 7.26.7.20 (m, 12H, H_{b+m}), 7.10-7.02 (m, 16H, H_{c+l+F}), 6.98 (d, J = 8.9, 2H, H_k), 6.93 (d, J = 8.9, 2H, H_d), 6.61 (d, J = 8.6, 4H, H_G), 6.54 (d, J = 8.9, 2H, H_j), 6.33 (d, J = 8.9, 2H, H_e), 4.58 (s, 4H, $H_{D\ or\ E}$), 4.56 (s, 4H, $H_{D\ or\ E}$), 4.38 (s, 2H, H_i), 3.79-3.73 (m, 4H, H_H), 3.36 (t, J = 5.9, 2H, H_f), 1.97 (t, J = 7.1, 2H, H_h), 1.63-1.59 (m, 4H, H_I), 1.47-1.40 (m, 2H, H_g), 1.31-1.20 (m, 66H, $H_{a+n+J+K+L}$). ^{13}C NMR (100 MHz, $CDCl_3$): δ 158.6, 158.2, 156.3, 155.4, 155.3, 148.3, 148.2, 144.2, 144.1, 140.2, 139.3, 137.1, 132.1, 132.0, 130.7, 129.7, 129.6, 124.1 (×4), 119.7, 114.4, 113.0, 112.8, 80.9, 72.4 72.2, 71.9 (×2), 70.7, 67.6, 65.4, 64.8, 63.0, 56.0, 34.3 (×2), 31.4 (×2), 29.4, 28.9, 28.8, 27.7, 25.7, 15.8. LRFAB-MS (3-NOBA matrix): *m/z* = 1679 $[M+H]^+$. HRFAB-MS (3-NOBA matrix): *m/z* = 1678.0542 $[M]^+$ (calc. for $C_{118}H_{136}N_2O_6$, 1678.0477 $[M]^+$).

Stacked plot of the ^{1}H-NMR spectra of **10** and **S2** in $CDCl_3$:

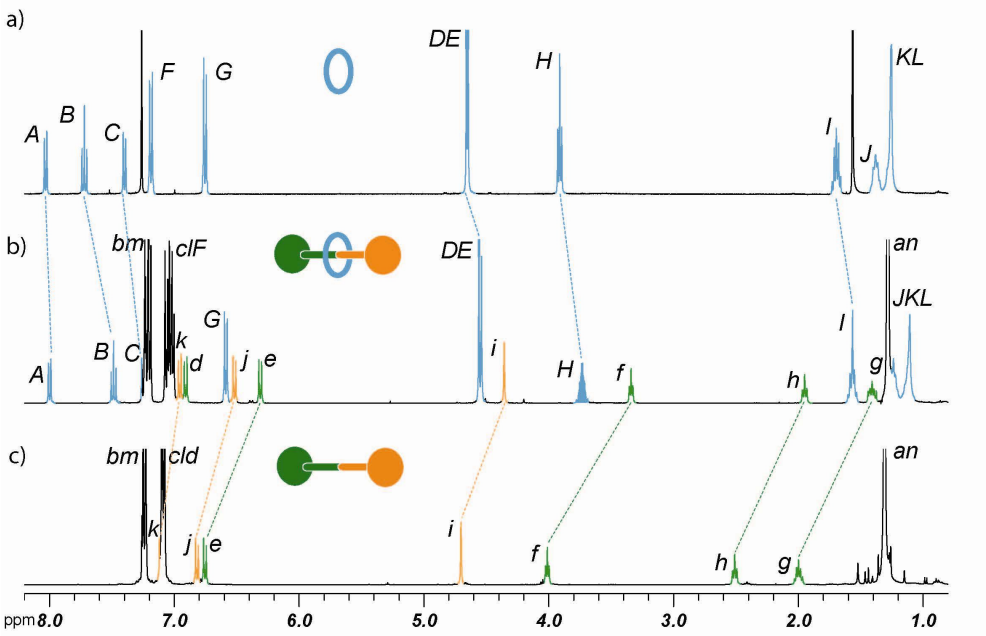

Figure 2.4 The ^{1}H NMR spectra (400 MHz, $CDCl_3$, 300 K) of a) macrocycle **3**, b) the [2]rotaxane **10**, c) the thread **S2**.

The non-interlocked threads **S1** and **S2** were prepared following standard Cadiot-Chodkiewicz type coupling procedure[6c] in 94% and 76% yield respectively and characterised for comparison with rotaxanes **4** and **10**:

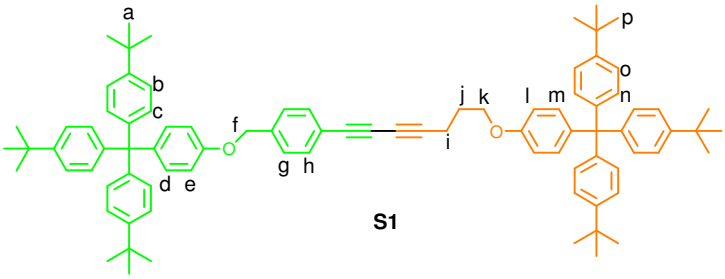

S1

Mp 235-238 °C; ^{1}H NMR (400 MHz, $CDCl_3$): δ 7.49 (d, J = 8.3, 2H, H_g), 7.37 (d, J = 8.3, 2H, H_h), 7.24 (d, J = 8.5, 12H, H_{b+o}), 7.18 (d, J = 7.4, 2H, $H_{d\ or\ m}$), 7.11-7.07 (m, 14H, H_{c+n} + $H_{d\ or\ m}$), 6.82-6.78 (m, 4H, H_{e+l}), 5.02 (s, 2H, H_f), 4.06 (t, J = 5.5, 2H, H_k), 2.59 (t, J = 6.9, 2H, H_i), 2.04 (m, 2H, H_j), 1.31 (s, 54H, H_{a+p}). ^{13}C NMR (100 MHz, $CDCl_3$): δ 156.5, 156.4, 148.3 (x 2), 144.1, 144.0, 140.1, 139.7, 138.1, 132.7, 132.3, 132.2, 130.7 (x 2), 127.3, 124.0 (x 2), 121.4, 113.2, 112.9, 83.7, 74.7,

74.4, 69.4, 65.9, 65.8, 65.6, 63.0, 34.3 (x 2), 31.4 (x 2), 28.1, 16.5. LRFAB-MS (3-NOBA matrix): *m/z* = 1187 $[M]^+$. HRFAB-MS (3-NOBA): *m/z* = 1187.7701 $[M+H]^+$ (calc. for $C_{88}H_{99}O_2$, 1187.7645 $[M+H]^+$).

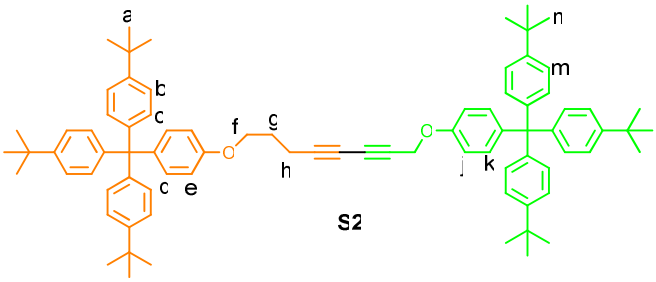

Mp 255-258 °C; ^{1}H NMR (400 MHz, $CDCl_3$): δ 7.24 (d, *J* = 8.3, 12H, H_{b+m}), 7.12-7.07 (m, 16H, $H_{c+d+k+l}$), 6.82 (d, *J* = 8.9, 2H, H_j), 6.75 (d, *J* = 8.9, 2H, H_e), 4.70 (s, 2H, H_i), 4.01 (t, *J* = 5.9, 2H, H_f), 2.51 (t, *J* = 6.9, 2H, H_h), 2.00 (m, 2H, H_g), 1.31 (s, 54H, H_{a+n}). ^{13}C NMR (100 MHz, $CDCl_3$): δ 156.5, 155.4, 148.3, 148.2, 144.1, 144.0, 140.5, 139.7, 132.3, 132.2, 130.7 (×2), 124.0 (×2), 113.2, 112.9, 80.9, 71.9, 70.8, 65.8, 65.0, 63.0 (×2), 56.3, 34.3 (×2), 31.4 (×2), 28.0, 16.2. LRFAB-MS (3-NOBA matrix): *m/z* = 1111 $[M]^+$. HRFAB-MS (3-NOBA): *m/z* = 1110.7191 $[M]^+$ (calc. for $C_{82}H_{94}O_2$, 1110.7254 $[M]^+$).

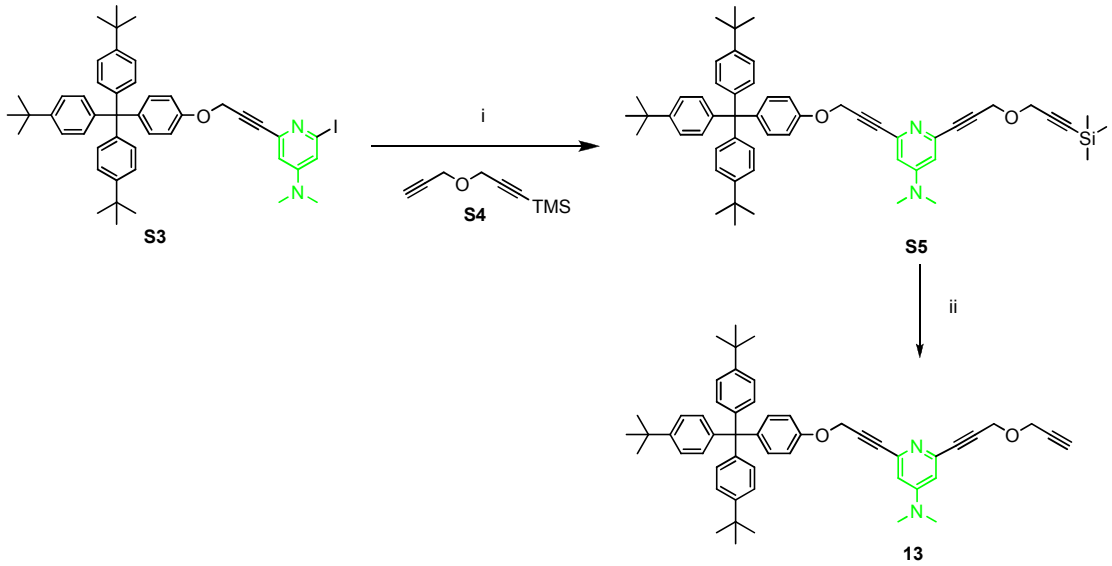

Scheme 2.5 Synthesis of half-thread **13**. Reagents and conditions: i) $Pd(PPh_3)_2Cl_2$, CuI, THF, Et_3N, RT, 36 h, 98%; ii) KF, MeOH, THF, RT, 24 h, 89%.

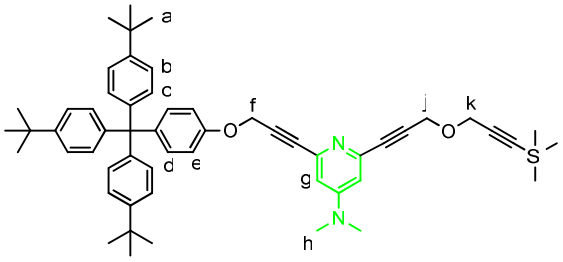

S5

To a solution of iodide **S3**[15j] (200 mg, 0.25 mmol) in THF (20 mL) and Et_3N (10 mL) was added $Pd(PPh_3)_2Cl_2$ (9.0 mg, 0.013 mmol), CuI (5.0 mg, 0.025 mmol) and acetylene **S4**[20] (63 mg, 0.38 mmol) and the reaction stirred at RT for 36 h. After this time, the reaction was quenched with aqueous saturated NH_4Cl (25 mL), the layers separated and the aqueous layer was extracted with dichloromethane (2 x 50 mL). The combined organic extracts were then washed with brine and dried over Na_2SO_4. Removal of the solvents under reduced pressure followed by column chromatography on silica (eluting first with 1:4 Et_2O:hexane and then 1:1 Et_2O:hexane) gave acetylene **S5** as a white solid, m.p. 113-114 °C (210 mg, 98%). ^{1}H NMR (400 MHz, $CDCl_3$): δ 7.25-7.21 (m, 6H, H_b), 7.11-7.06 (m, 8H, H_{c+d}), 6.90-6.86 (m, 2H, H_e), 6.63 (s, 2H, H_{g+i}), 4.87 (s, 2H, H_f), 4.46 (s, 2H, H_j), 4.31 (s, 2H, H_k), 2.98 (s, 6H, H_h), 1.30 (s, 27H, H_a), 0.19 (s, 9H, H_l). ^{13}C NMR (100 MHz, $CDCl_3$): δ 155.7, 154.2, 148.3, 144.0, 142.6, 142.5, 140.3, 132.3, 130.7, 124.0, 113.3, 109.7, 109.6, 100.5, 92.2, 86.6, 86.4. 82.8, 82.6, 63.0, 57.5, 57.0, 56.4, 39.2, 34.3, 31.3, -0.2. LRFAB-MS (3-NOBA matrix): *m/z* = 826 $[M]^+$. HRFAB-MS (3-NOBA matrix): *m/z* = 827.4966 $[M+H]^+$ (calc. for $C_{56}H_{67}N_2O_2Si$, 827.4972 $[M+H]^+$).

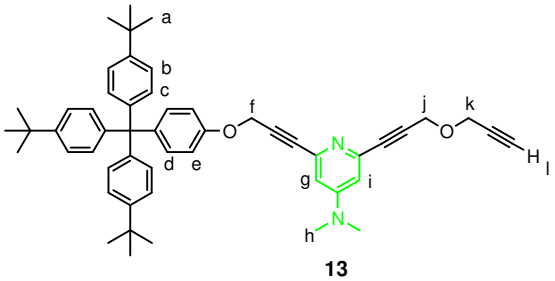

13

KF (290 mg, 4.98 mmol) in MeOH (7 mL) was added to a solution of **S5** (206 mg, 0.249 mmol) in THF (25 mL) and the reaction mixture was allowed to stir at RT for

24 h. The solvents were then removed *in vacuo* and the crude residue was purified by column chromatography on silica (1:1 hexane:Et_2O) to yield terminal acetylene **13** as a white solid, m.p. 104-106 °C (168 mg, 89%). ^{1}H NMR (400 MHz, $CDCl_3$): δ 7.24-7.21 (m, 6H, H_b), 7.11-7.06 (m, 8H, H_{c+d}), 6.89-6.86 (m, 2H, H_e), 6.65-6.63 (m, 2H, H_{g+i}), 4.87 (s, 2H, H_f), 4.47 (s, 2H, H_j), 4.32 (d, J = 2.4, 2H, H_k), 2.99 (s, 6H, H_h), 2.46 (t, J = 2.4, 1H, H_l), 1.30 (s, 27H, H_a). ^{13}C NMR (100 MHz, $CDCl_3$): δ 155.7, 154.3, 148.3, 144.0, 142.5 (x 2), 140.4, 132.3, 130.7, 124.1, 113.3, 109.8, 109.7, 85.6 (x 2), 82.7 (x 2), 78.9, 75.1, 60.2, 57.1, 56.7, 56.4, 39.3, 34.3, 31.4. LRFAB-MS (3-NOBA matrix): *m/z* = 755 $[M+H]^+$. HRFAB-MS (3-NOBA): *m/z* = 755.4544 $[M+H]^+$ (calc. for $C_{53}H_{59}N_2O_2$, 755.4577 $[M+H]^+$).

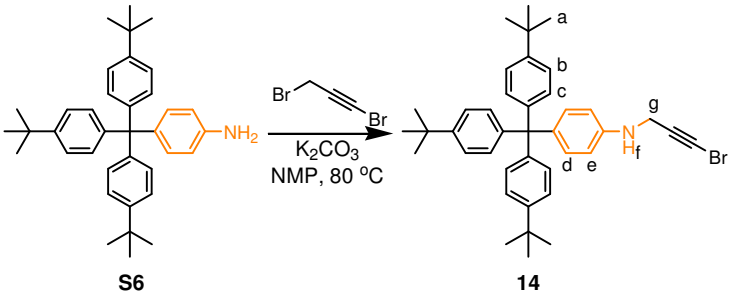

Scheme 2.6 Synthesis of half-thread **14**. Reagents and conditions: K_2CO_3, 1,3-dibromopropyne, NMP, 80 °C, 16 h, 50%.

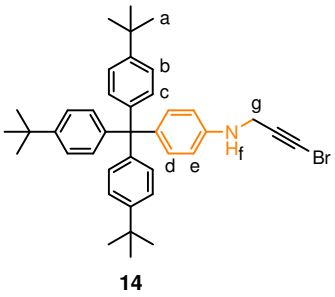

A suspension of aniline **S6**[19] (0.504 g, 1.00 mmol, 1.0 equiv.) and K_2CO_3 (0.550 g, 4.00 mmol, 1.0 equiv.) in NMP (2 mL) was stirred at 80 °C for 1 h at which time a solution of 1,3-dibromopropyne[21] (2.0 M in NMP 0.500 mL, 1.00 mmol, 1.0 equiv.) was added and the mixture stirred for 16 h at 80 °C. The reaction mixture was partitioned between Et_2O (200 mL) and water (200 mL) and the layers separated. The organic phase was washed with water (2 x 200 mL), dried ($MgSO_4$) and the

solvent removed under reduced pressure. Column chromatography on silica (10:3 hexane:CH_2Cl_2) gave bromoacetylene **14** as a pale yellow foam, m.p. 113-115 °C (310 mg, 50%). ^{1}H NMR (400 MHz, $CDCl_3$): δ 7.24-7.22 (m, 6H, H_b), 7.10-7.08 (m, 6H, H_c), 7.03-7.00 (m, 2H, H_d), 6.57-6.54 (m, 2H, H_e), 3.93 (s, 2H, H_g), 3.87-3.77 (br, 1H, H_f), 1.31 (s, 27H, H_a). ^{13}C NMR (100 MHz, $CDCl_3$): δ 156.4, 156.1, 148.3, 144.0, 132.3, 132.2, 130.7, 127.3, 124.0, 113.2, 69.4, 34.3 (x 2), 31.4. LRFAB-MS (3-NOBA matrix): *m/z* = 620 $[M^{79}Br+H]^+$, 622 $[M^{81}Br+H]^+$. HRFAB-MS (3-NOBA): *m/z* = 620.2896 $[M^{79}Br+H]^+$ (calc. for $C_{40}H_{47}N^{79}Br$, 620.2886 $[M^{79}Br+H]^+$).

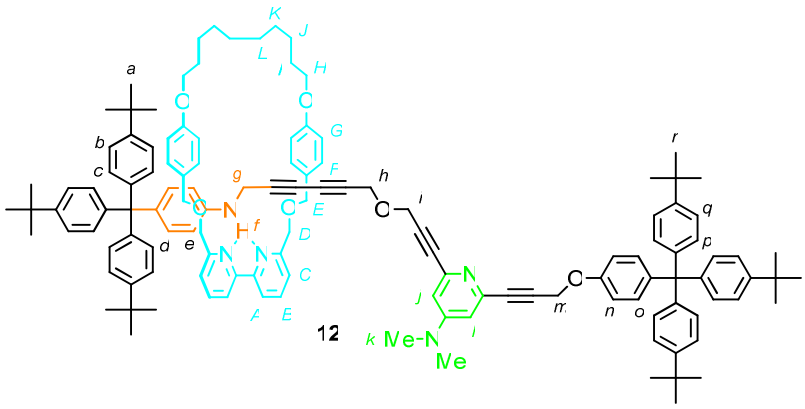

A solution of acetylene **13** (48 mg, 0.064 mmol, 1.0 equiv.) in THF (0.4 mL) was cooled to -78 °C. To this solution was added *n*-BuLi (0.1 M in THF, 0.64 mL, 0.064 mmol, 1.0 equiv.) at -78 °C. The resulting solution was allowed to warm to 0 °C over 15 minutes. CuI (12 mg, 0.064 mmol, 1.0 equiv.) was added at 0 °C. The resulting yellow solution was allowed to warm to RT over 15 minutes. Bipy macrocycle **3** (36 mg, 0.064 mmol, 1.0 equiv.) and bromo acetylene **14** (40 mg, 0.064 mmol, 1.0 equiv.) were added as a solution in THF (1.2 mL) at -78 °C. The resulting orange solution was allowed to stir at RT for 20 h before the reaction was quenched by addition of an aqueous solution of 17.5% NH_3 saturated with EDTA (50 mL). The layers were allowed to stir in air for 40 minutes after which the aqueous layer turned blue. The aqueous layer was extracted with CH_2Cl_2 (3 x 50 mL) and the combined organic layers washed with brine and dried ($MgSO_4$). Purification by column chromatography on silica (gradient elution from 1% to 5% acetone in CH_2Cl_2) yielded the title product **12** as a white foam (73 mg, 61%). ^{1}H NMR (400 MHz, CD_2Cl_2): δ 8.04 (d, *J* = 7.8, 2H, H_A), 7.62-7.56 (m, 2H, H_B), 7.31 (d, *J* = 7.7, 2H,

H_C), 7.29-7.21 (m, 12H, H_{b+q}), 7.18-7.02 (m, 18H, $H_{c+o+p+F}$), 6.88 (d, J = 8.4, 2H, H_d), 6.67 (d, J = 8.8, 2H, H_n), 6.65-6.59 (m, 6H, H_{j+l+G}), 6.11 (d, J = 8.4, 2H, H_e), 4.69 (s, 2H, H_m), 4.61-4.52 (m, 8H, H_{D+E}), 4.29 (s, 2H, H_i), 4.19 (s, 2H, H_h), 3.96-3.86 (br, 1H, H_f), 3.79 (t, J = 6.6, 4H, H_H), 3.40 (s, 2H, H_g), 2.93 (s, 6H, H_k), 1.65-1.50 (m, 4H, H_I), 1.36-1.09 (m, 66H, $H_{a+r+J+K+L}$). ^{13}C NMR (100 MHz, CD_2Cl_2): δ 158.6, 158.5, 155.6, 155.4, 154.3, 148.4, 148.2, 144.8, 144.5 (x 2), 142.5, 142.4, 140.4, 137.2, 136.8, 131.9, 131.4, 130.5, 130.4, 129.9, 129.8, 124.3, 124.2, 121.6, 119.7, 114.3, 113.3, 111.8, 109.7 (x 2), 86.7, 86.6, 82.2 (x 2), 77.5, 73.1, 72.4 (x 2), 71.1, 67.7, 66.4, 63.0, 57.2, 57.1, 56.3, 39.1, 34.2 (x 2), 33.5, 31.1 (x 2), 29.7, 29.4, 28.9, 28.8, 25.8; LRFAB-MS (3-NOBA matrix): *m/z* = 1862 $[M+H]^+$. HRFAB-MS (3-NOBA): *m/z* = 1862.1265 $[M+H]^+$ (calc. for $C_{129}H_{146}N_5O_6$, 1862.1307 $[M+H]^+$).

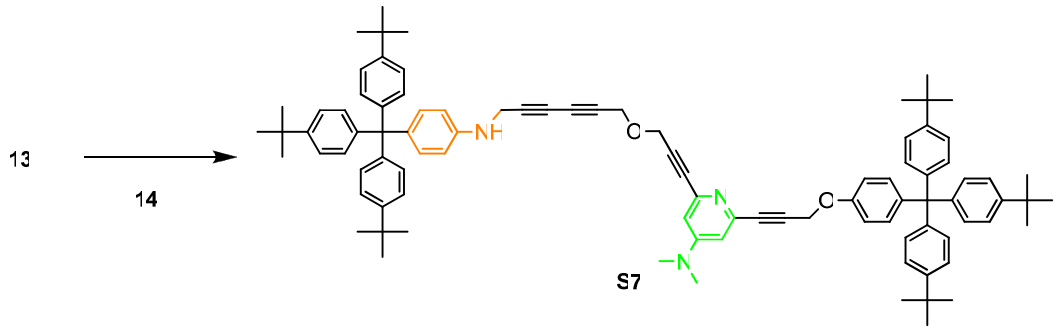

Scheme 2.7 Synthesis of thread **S7**. Reagents and conditions: *n*-BuLi, CuI, 2,2'-dimethylbipyridine, THF, -78 °C → RT, 20 h, 29%.

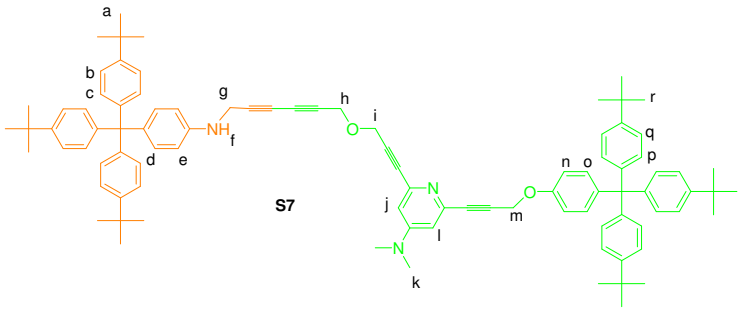

To a solution of acetylene **13** (37 mg, 0.049 mmol, 1.0 equiv.) in THF (1 mL) at -78 °C was added *n*-BuLi (0.16 M in THF, 0.31 mL, 0.049 mmol, 1.0 equiv.) and the solution stirred at -78 °C for 20 minutes. This solution was then transferred *via* cannula to a mixture of CuI (9.3 mg, 0.049 mmol, 1.0 equiv.) and 2,2'-dimethylbipyridine (9.0 mg, 0.049 mmol, 1.0 equiv.) in THF (2 mL) at -78 °C and the resulting solution allowed to stir at 0 °C for 15 minutes. The solution was then re-

cooled to -78 °C and a solution of bromoacetylene **14** (30 mg, 0.049 mmol, 1.0 equiv.) in THF (2 mL) was added. The orange reaction mixture was then allowed to warm to RT and stirred overnight. The reaction was quenched by addition of an aqueous solution of 17.5% NH_3 saturated with EDTA (10 mL). The layers were allowed to stir in air for 40 minutes after which the aqueous layer turned blue. The aqueous layer was extracted with EtOAc (2 x 50 mL) and the combined organic layers washed with brine and dried (Na_2SO_4). Purification by column chromatography on silica (5:1 hexane:EtOAc with 1% Et_3N) yielded thread **S7** as an off-white foam (18 mg, 29%). ^{1}H NMR (400 MHz, $CDCl_3$): δ 7.24-7.19 (m, 12H, H_{b+q}), 7.11-7.06 (m, 14H, H_{c+o+p}), 7.03-6.99 (m, 2H, H_d), 6.89-6.85 (m, 2H, H_n), 6.65-6.62 (m, 2H, H_{j+l}), 6.56-6.53 (m, 2H, H_e), 4.86 (s, 2H, H_m), 4.45 (s, 2H, H_i), 4.37 (s, 2H, H_h), 4.00 (s, 2H, H_g), 3.90-3.73 (br, 1H, H_f), 2.98 (s, 6H, H_k), 1.29 (s, 54H, H_{a+r}). LRFAB-MS (3-NOBA matrix): *m/z* = 1295 $[M+H]^+$. HRFAB-MS (3-NOBA): *m/z* = 1294.8171 $[M+H]^+$ (calc. for $C_{93}H_{104}N_3O_2$, 1294.8129 $[M+H]^+$).

2.6 Shuttling Experiments

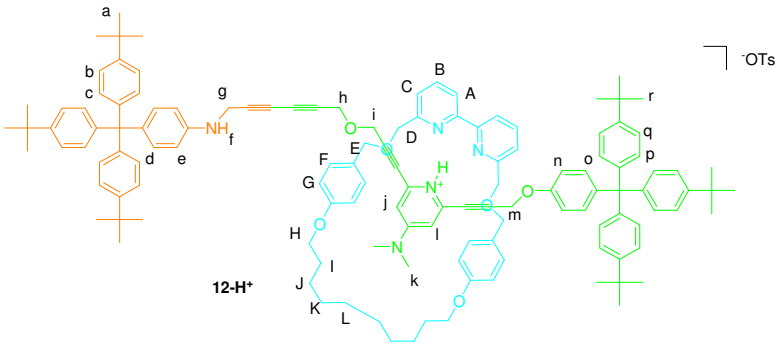

A solution of rotaxane **12** (9.8 mg, 0.0053 mmol, 1.0 equiv.) in CD_2Cl_2 was charged with *p*-TsOH (1.0 mg, 0.0053 mmol, 1.0 equiv.) and the mixture sonicated gently at RT for 10 minutes. After this time, ^{1}H NMR analysis indictated the formation of pyridinium **12**-H^+. ^{1}H NMR (400 MHz, CD_2Cl_2): δ 8.08-7.83 (m, 4H, H_{A+B}), 7.68 (d, *J* = 8.1, 2H, $H_{TsOAr-H}$), 7.57-7.41 (m, 2H, H_C), 7.31-7.19 (m, 12H, H_{b+q}), 7.17-7.09 (m, 18H, $H_{c+d+o+p+TsOAr-H}$), 7.01-6.88 (m, 4H, H_F), 6.86-6.74 (br, 2H, H_n), 6.67-6.54 (m, 6H, H_{e+G}), 6.34-6.02 (br, 2H, H_{j+l}), 4.58-4.43 (m, 6H, H_{m+D}), 4.43-4.37 (m, 4H, H_E), 4.16 (s, 2H, H_i), 4.04-3.93 (m, 4H, H_{g+h}), 3.87-3.80 (m, 4H, H_H), 2.94-2.78 (br,

6H, H_k), 2.30 (s, 3H, $H_{TsOAlk\text{-}H}$), 1.77-1.67 (m, 4H, H_l), 1.34-1.20 (m, 66H, $H_{a+r+J+K+L}$).

H_f and the pyridinium H^+ are too broad to identify.

Passing pyridinium **12**-H^+ through a plug of Na_2CO_3 (eluting in CH_2Cl_2) then regenerated rotaxane **12** as previously characterised.

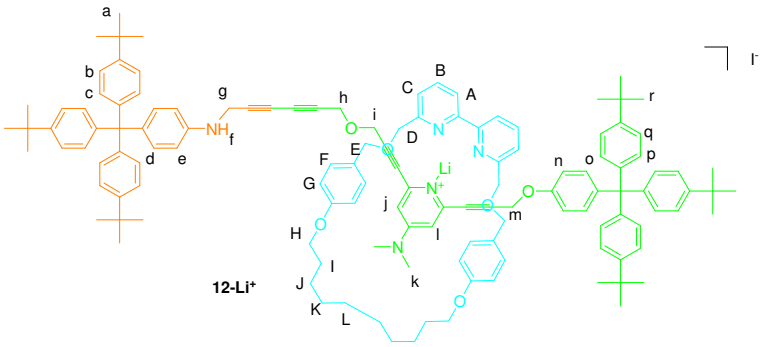

A solution of rotaxane **12** (7.0 mg, 0.0038 mmol) in CD_2Cl_2 was charged with excess anhydrous LiI and the mixture sonicated gently at RT for 10 minutes. After this time, ^{1}H NMR analysis indictated the formation of metal complex **12**-Li^+. ^{1}H NMR (400 MHz, CD_2Cl_2): δ 7.95 (d, *J* = 7.8, 2H, H_A), 7.86 (t, *J* = 7.8, 2H, H_B), 7.37 (d, *J* = 7.8, 2H, H_C), 7.27-7.22 (m, 12H, H_{b+q}), 7.17-7.11 (m, 14H, H_{c+o+p}), 7.08-7.04 (m, 6H, H_{d+F}), 6.66-6.62 (m, 6H, H_{n+G}), 6.57 (d, *J* = 8.2, 2H, H_e), 6.40 (s, 1H, $H_{j\ or\ l}$), 6.31 (s, 1H, $H_{j\ or\ l}$), 4.72-4.65 (m, 4H, H_D), 4.57-4.50 (m, 4H, H_E), 4.43 (s, 2H, H_m), 4.25 (s, 1H, H_f), 4.02 (s, 4H, H_{g+i}), 3.90-3.80 (m, 6H, H_{h+H}), 2.97 (s, 6H, H_k), 1.73-1.66 (m, 4H, H_l), 1.39-1.23 (m, 66H, $H_{a+r+J+K+L}$).

Washing the NMR sample of metal complex **12**-Li^+ with water for 10 minutes, followed by separation of the organic phase and drying over Na_2SO_4 regenerated rotaxane **12** as previously characterised.

Threads **S7**-H^+ and **S7**-Li^+ were prepared from thread **S7** in an analogous fashion to the rotaxanes.

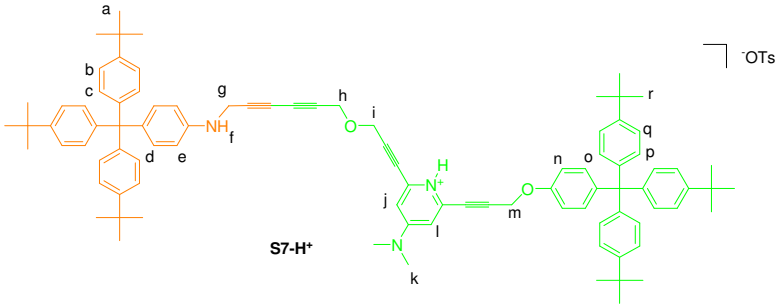

S7-H+

^{1}H NMR (400 MHz, CD_2Cl_2): δ 7.70 (d, *J* = 7.8, 2H, $H_{TsOAr\text{-}H}$), 7.29-7.22 (m, 12H, H_{b+q}), 7.20-7.13 (m, 14H, H_{c+o+p}), 7.10-7.07 (m, 4H, $H_{d+TsOAr\text{-}H}$), 6.88-6.84 (m, 2H, H_n), 6.70 (s, 2H, H_{j+l}), 6.58 (d, *J* = 7.9, 2H, H_e), 4.86 (s, 2H, H_m), 4.44 (s, 2H, H_i), 4.33 (s, 2H, H_h), 4.01 (s, 2H, H_g), 3.12 (s, 6H, H_k), 2.25 (s, 3H, $H_{TsOAlk\text{-}H}$), 1.30-1.26 (m, 54H, H_{a+r}).

H_f and the pyridinium H^+ are too broad to identify.

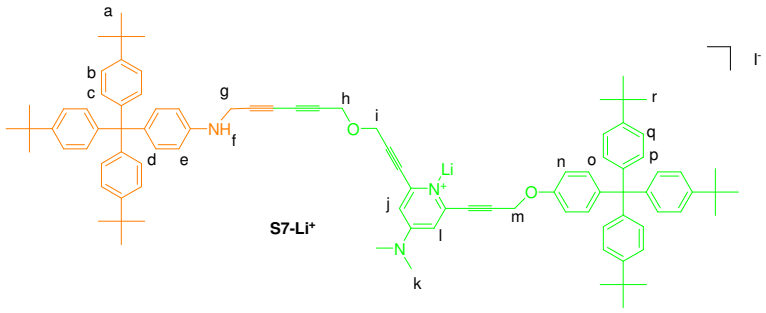

S7-Li+

^{1}H NMR (400 MHz, CD_2Cl_2): δ 7.27-7.24 (m, 12H, H_{b+q}), 7.18-7.14 (m, 14H, H_{c+o+p}), 7.08-7.06 (m, 2H, H_d), 6.83 (d, *J* = 8.7, 2H, H_n), 6.64-6.60 (m, 2H, H_{j+l}), 6.57-6.54 (m, 2H, H_e), 4.85 (s, 2H, H_m), 4.42 (s, 2H, H_i), 4.35 (s, 2H, H_h), 4.01-3.94 (m, 3H, H_{f+g}), 2.97 (s, 6H, H_k), 1.29 (s, 54H, H_{a+r}).

2.7 Computational Studies

Geometry optimisations and frequency calculations were carried out at *B3LYP/3-21G** level with the Gaussian03 program.[13a] The hybrid exchange-correlation B3LYP[13b] functional was adopted on the basis of its reported suitability to describe both hydrogen-bonding interactions and aromatic stacking interactions,[13c]

particularly in the presence of *N*-based π-electron systems such as those here considered.[13d] Specifically, it has been shown to properly account for geometry, proton and hydrogen bonding affinity of both aniline[13e,f] and pyridinium based systems in the gas-phase.[13g] Solvent phase CH_2Cl_2 calculations were performed with the self-consistent reaction field method (SCRF)[13h] as implemented in the Gaussian program.[13a] Within the SCRF approach, the solvent is modelled as a uniform dielectric around a spherical cavity of radius a_0, occupied by the solute. The dielectric constant used in the calculations for CH_2Cl_2 was the experimental one (8.93). Cavity radii were determined on the basis of the recommended 0.001 *e bohr*$^{-}$ [13a] constant density contours/envelops and the dependence of the results on the isocontour value checked by arbitrarily increasing the cavity radius by 0.5 Å.

In order to further reduce the computational cost, both **12** and **12**-H^+ were modelled considering only the corresponding fragment of the global thread. This was accomplished by cutting the global thread at the etheric junctions (see Figure 2.5).

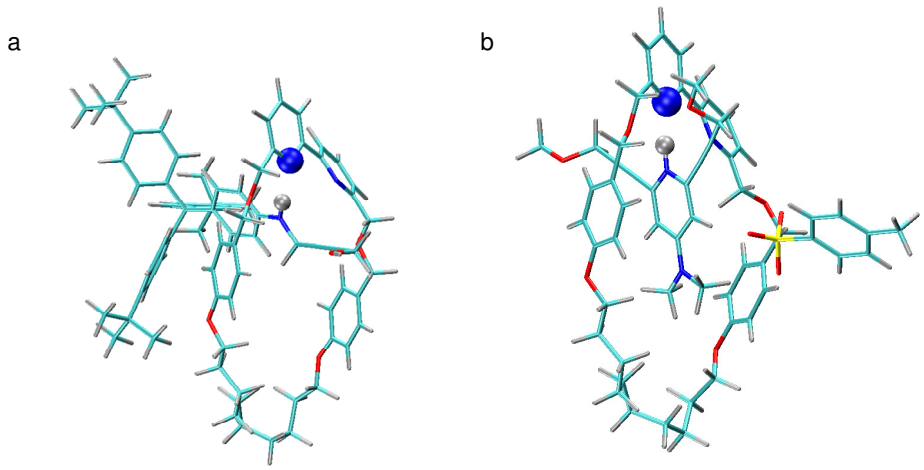

Figure 2.5 Optimised structures of a) **12**, b) **12**-H^+.

The terminal oxygen atom was eventually saturated with one hydrogen atom and one methyl group for **12** and **12**-H^+, respectively. By changing the terminal hydroxyl group for a terminal methyl group, the binding (electronic) energy of **12** was found to be converged within 0.04 kcal mol^{-1}. In line with previous results which have thoroughly shown the suitability of B3LYP to properly account for the H-bonding affinities of aniline, anilinium and anilide complexes,[13g] the calculated binding

enthalpy of -5.76 kcal mol^{-1} for **12** (see Table 2.3) is found to be reasonably smaller (i.e. larger in absolute value) than for the ammonia dimer in vacuum (experimental value: -4.30 kcal mol^{-1})[13d] and, at the same time, the larger extent of the modelled association enthalpy for **12**-H$^+$ (-19.12 kcal mol^{-1}) finds a robust correspondence in the experimentally reported values of -24.6 kcal mol^{-1} and -17.21 kcal mol^{-1} for pyridnium-pyridine and pyridinium-ammonia complexes, respectively.[13d]

	N····H	ΔE_{bind}	ΔH_{bind}	ΔG_{bind}
12 (vacuum)	2.07 (153.5°)	-7.70	-5.76	-5.29
12 (CH_2Cl_2)	2.07 (153.6°)	-8.03 (±0.05)	-6.65 (±0.04)	-3.89 (±0.09)
12-H$^+$ (vacuum)	1.79 (171.3°)	-22.36	-19.12	-9.01
12-H$^+$ (CH_2Cl_2)	1.77 (170.3°)	-14.10	11.43(±1.03)	-4.78(±1.02)

Table 2.3 Selected quantum chemical results for **12** and **12**-H$^+$: N···H distances are given in Å, with the hydrogen bond angles given in brackets; the electronic binding energy, ΔE_{bind}, enthalpy, ΔH_{bind} and free energy, ΔG_{bind}, are given in kcal mol^{-1}. The error bars of the CH_2Cl_2 calculations have been estimated by changing (+0.5 Å) the cavity radius, a_0.

The calculated binding free energies (Table 2.3) can be considered in semi-quantitative agreement with the experimental one, although likely overestimated due to the neglect of the configurational contributions and ensuing dissipative effects on the calculated binding free energies. Specifically for the **12**-H$^+$ fragment, the reported values can be considered as two limiting cases of the actual complex stability. The reduced effects of the solvent with respect to the binding free energies (with deviations smaller than 1.5 kcal mol^{-1} between gas-phase and solvent phase binding free energies) can be understood by considering that the solvent is weakly polar, while the donor-acceptor systems have larger dipole moments. The energy of solvation, G_{solv}, is proportional to the product of the dipoles and therefore is small for all systems (both when they are complexed and when they are not). Complexation reduces partly the surface of the solutes accessible to the dipoles of each solvent molecule, but the variation of G_{solv} is only by a modest amount of an already small contribution to the total free energy.

2.8 References and Notes

(1) a) D. B. Amabilino, J. F. Stoddart, *Chem. Rev*. **1995**, *95*, 2725–2828; b) *Molecular Catenanes, Rotaxanes and Knots: A Journey Through the World of Molecular Topology* (Eds.: J.-P. Sauvage, C. Dietrich-Buchecker), Wiley-VCH, Weinheim, 1999.

(2) a) For the first molecular shuttle with degenerate stations, see: P. L. Anelli, N. Spencer, J. F. Stoddart, *J. Am. Chem. Soc.* **1991**, *113*, 5131–5133. b) For the first switchable molecular shuttle, see: R. A. Bissell, E. Córdova, A. E. Kaifer, J. F. Stoddart, *Nature* **1994**, *369*, 133–136. c) For a recent review on molecular shuttles, see: H. Tian, Q.-C. Wang, *Chem. Soc. Rev*. **2006**, *35*, 361–374.

(3) The intercomponent binding interactions employed in classical template reactions—typically 12-30 kcal mol^{-1} or more[1]—are much stronger than is necessary to give good positional discrimination of the ring on the thread in a rotaxane. For an unsymmetrical thread featuring two different stations, a 2 kcal mol^{-1} difference in binding affinity is sufficient to ensure 95% occupancy of the preferred binding site at room temperature [a) A. Altieri, G. Bottari, F. Dehez, D. A. Leigh, J. K. Y. Wong, F. Zerbetto, *Angew. Chem*. **2003**, *115*, 2398–2402; *Angew. Chem. Int. Ed*. **2003**, *42*, 2296–2300]. The length of the thread only accounts for ~1 kcal mol^{-1} of the activation energy in a typical 1.5 nm molecular shuttle [b) A. S. Lane, D. A. Leigh, A. Murphy, *J. Am. Chem. Soc*. **1997**, *119*, 11092–11093].

(4) E. R. Kay, D. A. Leigh, F. Zerbetto, *Angew. Chem*. **2007**, *119*, 72–196; *Angew. Chem. Int. Ed*. **2007**, *46*, 72–191.

(5) a) V. Aucagne, K. D. Hänni, D. A. Leigh, P. J. Lusby, D. B. Walker, *J. Am. Chem. Soc.* **2006**, *128*, 2186–2187; b) S. Saito, E. Takahashi, K. Nakazono, *Org. Lett*. **2006**, *8*, 5133–5136; c) J. Berná, J. D. Crowley, S. M. Goldup, K. D. Hänni, A.-L. Lee, D. A. Leigh, *Angew. Chem*. **2007**, *119*, 5811–5815; *Angew. Chem. Int. Ed*. **2007**, *46*, 5709–5713; d) V. Aucagne, J. Berná, J. D. Crowley, S. M. Goldup, K. D. Hänni, D. A. Leigh, P. J. Lusby, V. E. Ronaldson, A. M. Z. Slawin, A. Viterisi, D. B. Walker, *J. Am. Chem. Soc.* **2007**, *129*, 11950–11963; e) J. D. Crowley, K. D. Hänni, A.-L. Lee, D. A. Leigh, *J. Am. Chem. Soc*. **2007**, *129*, 12092–12093; f) S. M. Goldup, D. A. Leigh, P. J. Lusby, R. T. McBurney, A. M. Z. Slawin, *Angew. Chem*. **2008**, *120*, 3429–3432; *Angew. Chem. Int. Ed*. **2008**, *47*, 3381–3384.

(6) a) W. Chodkiewicz, *Ann. Chim. Paris* **1957**, *2*, 819–869; b) P. Cadiot, W. Chodkiewicz in *Chemistry of Acetylenes*, (Ed: H. G. Viehe), Marcel Dekker, Inc., New York, 1969, pp. 597–647; c) M. Alami, F. Ferri, *Tetrahedron Lett*. **1996**, *37*, 2763-2766; d) J. M. Montierth, D. R. DeMario, M. J. Kurth, N. E. Schore, *Tetrahedron* **1998**, *54*, 11741–11748.

(7) S. Nygaard, B. W. Laursen, T. S. Hansen, A. D. Bond, A. H. Flood, J. O. Jeppesen, *Angew. Chem*. **2007**, *119*, 6205–6209; *Angew. Chem. Int. Ed*. **2007**,

46, 6093–6097.

(8) a) R. F. Curtis, J. A. Taylor, *J. Chem. Soc. C* **1971**, 186–188; b) U. Niedballa, in *Methoden der Organischen Chemie. Houben Weyl,* Vol. V/2a (Ed.: E. Müller), Thieme, Stuttgart, 1977, pp. 925–937; c) C. Hartbaum, H. Fisher, *Chem. Ber.* **1997**, *130*, 1063–1067.

(9) Employing an iodoacetylene in place of the bromoacetylene led to poor selectivity (8:2:5 of 4:5:6) and reduced (78%) conversion.

(10) As well as producing only 32% rotaxane (the majority arising from homodimerization of the bromoacetylene; Table 2.2, entry 2), 8 is prone to decomposition. To ensure high yields and selectivity of the heterocoupled rotaxane, it appears that aryl acetylenes should only be employed as the terminal acetylene coupling partner in such reactions.

(11) The mechanism of the Cadiot-Chodkiewicz coupling is generally held to proceed in an analogous fashion to the Castro-Stephens reaction [a) R. D. Stephens, C. E. Castro, *J. Org. Chem.* **1963**, *28*, 3313–3315; b) P Siemens, R. C. Livingston, F. Diederich, *Angew. Chem.* **2000**, *112*, 2740–2767; *Angew. Chem. Int. Ed.* **2000**, *39*, 2632–2657; c) R. Bruckner, in *Advanced Organic Chemistry: Reaction Mechanisms*, Harcourt/Academic Press, San Diego, 2002, pp. 538]. This differs markedly from the accepted mechanism of the Glaser Cu(I)-catalysed homocoupling of alkynes in that i) the key intermediate is mono-metallic and ii) the oxidation state of copper formally changes from Cu(I) to Cu(III) during the key step of the Cadiot-Chodkiewicz and Castro-Stephens reactions, whereas in the Glaser homocoupling it switches between Cu(I) and Cu(II).

(12) The heterocoupling does not proceed in the absence of the bipyridine macrocycle ligand **3** under these conditions. A control reaction repeating this procedure in the absence of **3** resulted in no heterocoupled thread (by ^{1}H NMR analysis). The high yields of the active template rotaxane forming reaction without the need for excess reactants can be attributed to the absence of background reactivity.

(13) Geometry optimizations and frequency calculations for the macrocycle-station fragments of **12** and **12**.HOTs were carried out at *B3LYP/3-21G** level with the Gaussian03 program [a) M. J. Frisch, et al. Gaussian 03, revision C.02; Gaussian, Inc., Wallingford CT, 2004]. The hybrid exchange-correlation *B3LYP* [b) A. D. J. Becke, *J. Chem. Phys*. **1993**, *98*, 5648–5652] functional was adopted on the basis of its reported suitability in describing both hydrogen bonding interactions and aromatic stacking interactions [c) Y. Zhao, D.G. Truhlar*, J. Chem. Theory Comput*. **2005**, *1*, 415–432], particularly in the presence of *N*-based π-electron systems such as those considered here [d) G. Bouchoux, *Mass Spec. Rev*. **2007**, *26*, 775–835]. Specifically, it has been shown to properly account for the geometry and proton and hydrogen bonding affinity of both aniline [e) N. Russo, M. Toscano, A. Grand, T. Mineva, *J. Phys. Chem. A* **2000**, *104*, 4017–4021; f) V. Q. Nguyen, F.

Tureček, *J. Mass Spectrom*. **1997**, *32*, 55–63] and pyridinium based systems [g) H. Szatyłowicz, T. M. Krygowski, J. E. Zachara-Horeglad, *J. Chem. Inf. Model.* **2007**, *47*, 875–886]. Solvent phase (CH_2Cl_2) calculations were performed with the self-consistent reaction field method (SCRF) [h) M. W. Wong, K. B. Wiberg, M. J. Frisch*, J. Am. Chem. Soc.* **1992**, *114*, 1645–1652 and references therein] implemented in the Gaussian program.

(14) a) N. Haider, K. Mereiter, R. Wanko, *Heterocycles* **1995**, *41*, 1445–1459; b) Q. Ye, X. S. Wang, H. Zhao, R. G. Xiong, *Tetrahedron: Asymmetry* **2005**, *16*, 1595–1602; c) C. D. Hopkins, H. C. Malinakova, *Org. Lett.* **2006**, *8*, 5971–5974.

(15) For examples of molecular shuttles that are reversibly switchable by protonation, see reference 2b and: a) M.-V. Martínez-Díaz, N. Spencer, J. F. Stoddart, *Angew. Chem.* **1997**, *109*, 1991–1994; *Angew. Chem. Int. Ed.* **1997**, *36*, 1904–1907; b) P. R. Ashton, R. Ballardini, V. Balzani, I. Baxter, A. Credi, M. C. T. Fyfe, M. T. Gandolfi, M. Gómez-López, M.-V. Martínez-Díaz, A. Piersanti, N. Spencer, J. F. Stoddart, M. Venturi, A. J. P. White, D. J. Williams, *J. Am. Chem. Soc*. **1998**, *120*, 11932–11942; c) A. M. Elizarov, S.-H. Chiu, J. F. Stoddart, *J. Org. Chem*. **2002**, *67*, 9175–9181; d) J. D. Badjić, V. Balzani, A. Credi, S. Silvi, J. F. Stoddart, *Science* **2004**, *303*, 1845–1849; e) C. M. Keaveney, D. A. Leigh, *Angew. Chem.* **2004**, *116*, 1242–1244; *Angew. Chem. Int. Ed*. **2004**, *43*, 1222–1224; f) S. Garaudée, S. Silvi, M. Venturi, A. Credi, A. H. Flood, J. F. Stoddart, *ChemPhysChem*. **2005**, *6*, 2145–2152; g) J. D. Badjić, C. M. Ronconi, J. F. Stoddart, V. Balzani, S. Silvi, A. Credi, *J. Am. Chem. Soc*. **2006**, *128*, 1489–1499; h) Y. Tokunaga, T. Nakamura, M. Yoshioka, Y. Shimomura, *Tetrahedron Lett.* **2006**, *47*, 5901–5904; i) D. A. Leigh, A. R. Thomson, *Org. Lett*. **2006**, *8*, 5377–5379; j) J. D. Crowley, D. A. Leigh, P. J. Lusby, R. T. McBurney, L.-E. Perret-Aebi, C. Petzold, A. M. Z. Slawin, M. D. Symes, *J. Am. Chem. Soc.* **2007**, *129*, 15085–15090.

(16) a) K. Biradha, R. E. Edwards, G. J. Foulds, W. T. Robinson, G. R. Desiraju, *Chem. Commun.* **1995**, 1705–1707; b) D. Braga, S. L. Giaffreda, M. Polito, F. Grepioni, *Eur. J. Inorg. Chem.* **2005**, 2737–2746; c) A. R. Kennedy, M. Kittner, *Acta Crystallogr. Sect. E: Struct. Rep. Online* **2005**, *61*, o333–o334.

(17) For molecular shuttles that are reversibly switchable by complexation with Li^+, see reference 15h and: a) S. A. Vignon, T. Jarrosson, T. Iijima, H.-R Tseng, J. K. M. Sanders, J. F. Stoddart, *J. Am. Chem. Soc.* **2004**, *126*, 9884–9885; b) Y. Nagawa, J.-I. Suga, K. Hiratani, E. Koyama, M. Kanesato, *Chem. Commun.* **2005**, 749–751; c) N.-C. Chen, P.-Y. Huang, C.-C. Lai, Y.-H. Liu, Y. Wang, S.-M. Peng, S.-H. Chiu, *Chem. Commun.* **2007**, 4122–4124.

(18) C. D. J. Boden, G. Pattenden, T. Ye, *J. Chem. Soc., Perkin Trans. 1* **1996,** *20*, 2417-2419.

(19) H. W. Gibson, S. H. Lee, P. T. Engen, P. Lecavalier, J. Sze, Y. X. Shen, M. Bheda, *J. Org. Chem.* **1993**, *58*, 3748-3756.

(20) S.-I. Ikeda, H. Watanabe, Y. Sato, *J. Org. Chem.* **1998**, *63,* 7026-7029.

(21) W.-J. Yoo, A. Allen, K. Villeneuve, W. Tam, *Org. Lett.* **2005**, *7*, 5853-5856.

CHAPTER THREE

A Switchable Palladium-Complexed Molecular Shuttle and Its Metastable Positional Isomers

Published as *"A Switchable Palladium-Complexed Molecular Shuttle and Its Metastable Positional Isomers"* J. D. Crowley, D. A. Leigh, P. J. Lusby, R. T. McBurney, L.-E. Perret-Aebi, C. Petzold, A. M. Z. Slawin, and M. D. Symes, *J. Am. Chem. Soc.*, **2007**, *129*, 15085–15090.

Acknowledgements and Declaration

The following people are gratefully acknowledged for their contributions to this Chapter: Dr. Paul Lusby synthesised rotaxane *Py*-**L2**Pd for the first time; Dr. James Crowley developed synthetic routes to compounds **1**, **S1**, and **2**; Dr. Christiane Petzold undertook the synthesis and model studies detailed in Section 3.10; Prof. Alexandra Slawin solved the X-ray crystal structures of compounds **L1**Pd(2,6-dipropylDMAP) and **L1**Pd(2,6-dipropylPy); Dr. Steve Mason and Marius Kroll provided the Author with samples of compound **S2**; Dr. Laure-Emmanuelle Perret-Aebi and Roy McBurney investigated alternative synthetic strategies that are not described here.

Synopsis

This Chapter reports the design, synthesis, characterisation, and operation of a [2]rotaxane in which a palladium-complexed macrocycle can be translocated between 4-dimethylaminopyridine (DMAP) and pyridine monodentate ligand sites via *reversible protonation, the metal remaining coordinated to the macrocycle throughout. The substitution pattern of the ligands and the kinetic stability of the Pd-N bond mean that changing the chemical state of the thread does not automatically cause a change in the macrocycle's position in the absence of additional inputs (heat and coordinating solvent/anion). Accordingly, under ambient conditions all of the four possible states of the rotaxane (neutral and protonated with the macrocycle on DMAP, and neutral and protonated with the macrocycle on pyridine) can be isolated, manipulated and characterised.*

3.1 Introduction

Despite the success and influence of the redox-responsive Cu(I)/Cu(II) catenane and rotaxane systems developed in Strasbourg,[1,2] there are no other examples of stimuli-switchable molecular shuttles[3] based on the manipulation of metal-ligand interactions between the components.[4,5] This lack of switchable metal coordination motifs for interlocked molecules may be set to change, however, following the recognition of the need to vary the kinetics of binding events and transportation pathways (e.g., ratcheting and escapement[6]) in any mechanical molecular machine more sophisticated than a switch,[7] and the crucial role played by metastability in the functioning of rotaxanes currently being investigated for molecular electronics.[8] Here we describe a simple-to-assemble-and-operate [2]rotaxane in which a palladium-complexed macrocycle can be translocated between 4-dimethylaminopyridine (DMAP) and pyridine (Py) ligand sites *via* reversible protonation (the metal remaining coordinated to the macrocycle throughout). The substitution pattern of the ligands and the kinetic stability of the Pd-N bond mean that changing the chemical state of the thread (adding or removing protons) does not automatically cause a change in the macrocycle's position in the absence of heat and a coordinating solvent or anion. Accordingly, under ambient conditions all four of the possible co-conformers of the [2]rotaxane can be selected, manipulated, isolated, and characterised.

3.2 Basis of the Design: Protonation/Deprotonation-Driven Ligand Exchange Experiments

The shuttle is based on a recognition motif previously used to assemble rotaxanes and catenanes by organizing tridentate pyridine 2,6-dicarboxamide and appropriately derivatised monodentate pyridine ligands about a square planar Pd(II) template.[9] In a simple exchange experiment with non-interlocked versions of these ligands (Scheme 3.1a), we found that the pyridine group of **L1**PdPy was rapidly[10] and quantitatively substituted for DMAP.[11] By adding an equivalent of *p*-toluenesulfonic acid (TsOH), the process could be reversed (Scheme 3.1b).[12]

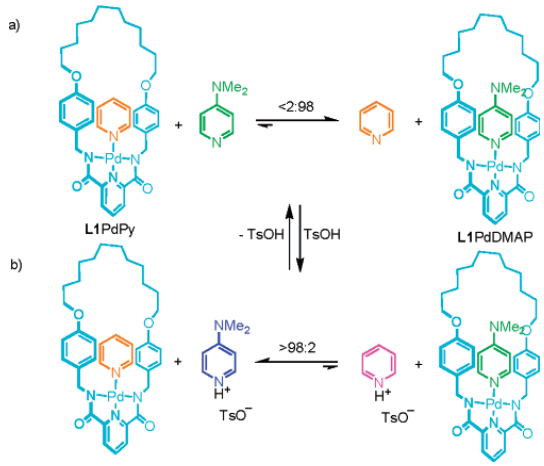

Scheme 3.1 Reversible substitution of pyridine and DMAP ligands in macrocycle-Pd complex **L1**PdPy/DMAP in d_7-DMF at 298 K. Upon mixing the substrates, equilibrium is reached within the time taken to acquire a ^{1}H NMR spectrum. (a) Neutral conditions; (b) in the presence of TsOH (one equivalent).

The reasons for the selectivity in Scheme 3.1b are quite subtle: although both heterocycles are "coordinated" (one to Pd(II) and one to H^+) on both sides of the equation (Scheme 3.1b), protonation of the more basic heterocycle determines the position of equilibrium because the N-H bond is significantly stronger than the Pd-N bond.[13] In other words, a proton differentiates DMAP and Py more effectively than does Pd(II). The results suggested that a palladium-complexed [2]rotaxane incorporating both DMAP and Py binding sites in the thread could operate as a proton-switchable molecular shuttle.

3.3 Synthesis and Characterisation of Palladium-Coordinated Molecular Shuttle L2Pd

A candidate [2]rotaxane, **L2**Pd, was synthesized in nine steps using a "threading-followed-by-stoppering" strategy[14] (Scheme 3.2). 2,6-Diiodo-4-dimethylaminopyridine, **1**, was prepared via a modified literature procedure[15] (Scheme 3.2, step a) and subjected to consecutive Sonogashira cross-coupling reactions,[16] first with propargyl alcohol (one equivalent) and then with decadiyne (five equivalents), to afford the unsymmetrical *DMAP*-station[17] intermediate **3** (Scheme 3.2, step c). The synthesis of the *Py*-station fragment was achieved by desymmetrisation of commercially available 2,6-dibromopyridine through a Sonogashira cross-coupling with one equivalent of propargyl alcohol to give **2**

(Scheme 3.2, step b), followed by hydrogenation (over PtO_2) and Mitsunobu reaction[18] with bulky phenol **4**[19] to give **5** (Scheme 3.2, step d). The coupling of **3** and **5** *via* another Pd-catalysed Sonogashira reaction and subsequent hydrogenation over $Pd(OH)_2/C$, afforded the saturated monostoppered thread, **6** (Scheme 3.2, step e). Coordination of the macrocycle-palladium complex to the *DMAP* site of **6** occurred upon simple stirring with **L1**Pd(CH_3CN)[9c] in dichloromethane (298 K, one hour). The resulting threaded pseudo-rotaxane complex was captured covalently with **4** (DIAD, PPh_3, THF) to give the [2]rotaxane, **L2**Pd, in 26% yield[20] after column chromatography (Scheme 3.2, step f).

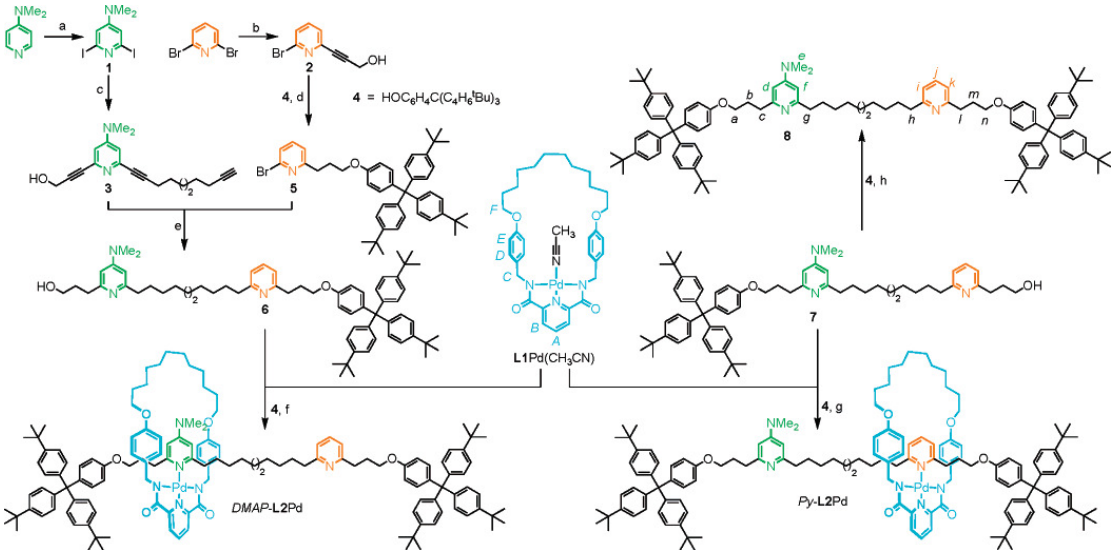

Scheme 3.2 Synthesis of Palladium-Complexed Molecular Shuttle **L2**Pd. Reagents and conditions: (a) $BF_3{\cdot}OEt_2$, LDA, I_2, THF, 40%; (b) propargyl alcohol, $Pd(PPh_3)_4$, CuI, Et_3N/THF, 66%; (c) (i) propargyl alcohol, $Pd(PPh_3)_4$, CuI, Et_3N/THF, 75%, (ii) 1,9-decadiyne (5 equiv), $Pd(PPh_3)_4$, CuI, Et_3N/THF, 77%; (d) (i) H_2, PtO_2, EtOH/Et_3N, 94%, (ii) 4, DIAD, PPh_3, THF, 61%; (e) (i) $Pd(PPh_3)_4$, CuI, Et_3N/THF, 66%, (ii) H_2, $Pd(OH)_2/C$, THF, 88%; (f) (i) L1Pd(CH_3CN), CH_2Cl_2, 90%, (ii) 4, DIAD, PPh_3, THF, 25% (from 6); (g) (i) L1Pd(CH_3CN), CH_2Cl_2, 67%, (ii) 4, DIAD, PPh_3, THF, 21% (from 7); (h) 4, DIAD, PPh_3, THF, 26%.

Mass spectrometry confirmed the constitution of the product as **L2**Pd, and ^{1}H NMR spectroscopy (Figure 3.1b) showed the co-conformation formed to be exclusively *DMAP*-**L2**Pd;[17] i.e., the Pd-macrocycle fragment, **L1**Pd, was solely coordinated to the *DMAP* binding site. A comparison of the spectra of free thread **8** (Figure 3.1a) and *DMAP*-**L2**Pd in $CDCl_3$ (Figure 3.1b) shows significant differences between the signals of the *DMAP* station ($H_{d\text{-}f}$) for the rotaxane and thread, while the *Py* station signals ($H_{i\text{-}k}$) of the rotaxane occur at very similar values to those of the free thread.

Interestingly, attempting the threading protocol with **7**, a close analogue of **6** in which the positions of the two stations were reversed (i.e., the *Py* binding site was closest to the unstoppered end of the thread; Scheme 3.2, step g), led mainly to the formation of *Py*-**L2**Pd. The outcomes of the two threading reactions indicate that the pyridine and DMAP binding sites are both very efficient at capturing the Pd-macrocycle component from **L1**Pd(CH_3CN) on its initial pass over the heterocycle at the open end of the thread, irrespective of relative orientation, solvation, or other factors.

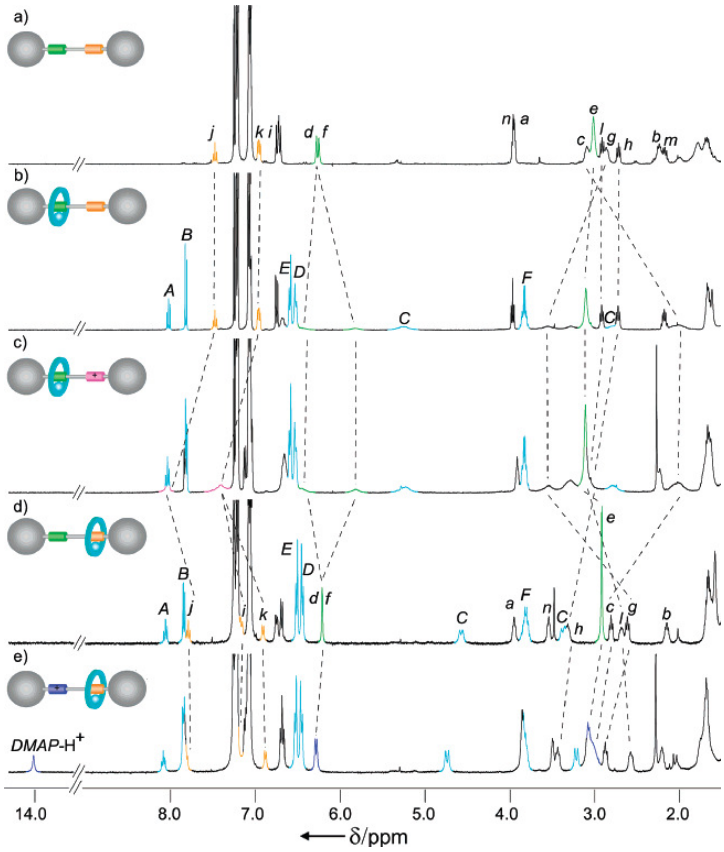

Figure 3.1 ^{1}H NMR spectra (400 MHz, $CDCl_3$, 300 K) of palladium rotaxane **L2**Pd in its four different protonated and co-conformational states, and for comparison the free thread: (a) Thread **8**; (b) *DMAP*-**L2**Pd; (c) *DMAP*-[**L2**HPd]OTs; (d) *Py*-**L2**Pd; (e) *Py*-[**L2**HPd]OTs. The lettering in the figure refers to the assignments in Scheme 3.2.

3.4 Macrocycle-to-Py-Station Protonation-Driven Shuttling Experiments

Switching of the macrocycle position in *DMAP*-**L2**Pd was attempted by the addition of one equivalent of TsOH in $CDCl_3$ (Scheme 3.3). The ^{1}H NMR spectrum of the resulting adduct (Figure 3.1c) showed significant changes in the *Py* resonances, $H_{i\text{-}k}$,

but no discernible shift of the *DMAP* signals, $H_{d\text{-}f}$, indicating that protonation of the *Py* station had occurred but the position of the macrocycle had not changed; i.e., the chemical structure was now *DMAP*-[**L2**HPd]OTs (Scheme 3.3). No changes to the ^{1}H NMR spectrum of the sample were observed over several days, indicating that this co-conformer is effectively stable at room temperature in $CDCl_3$. Somewhat surprisingly, however, given the results of the exchange experiments reported in Scheme 1,[10] even in neat coordinating solvents (d_6-DMSO or d_7-DMF) no evidence of translocation of the ring in *DMAP*-[**L2**HPd]OTs was observed at room temperature. Translocation of the palladium macrocycle subcomponent (**L1**Pd) only takes place at elevated temperatures (383 K), in both coordinating (d_7-DMF) and non-coordinating solvents ($C_2D_2Cl_4$), in both cases reaching an equilibrium 89:11 ratio of *Py*:*DMAP*-[**L2**HPd]OTs (Scheme 3.3) after 16 hours (d_7-DMF) or 36 hours ($C_2D_2Cl_4$).

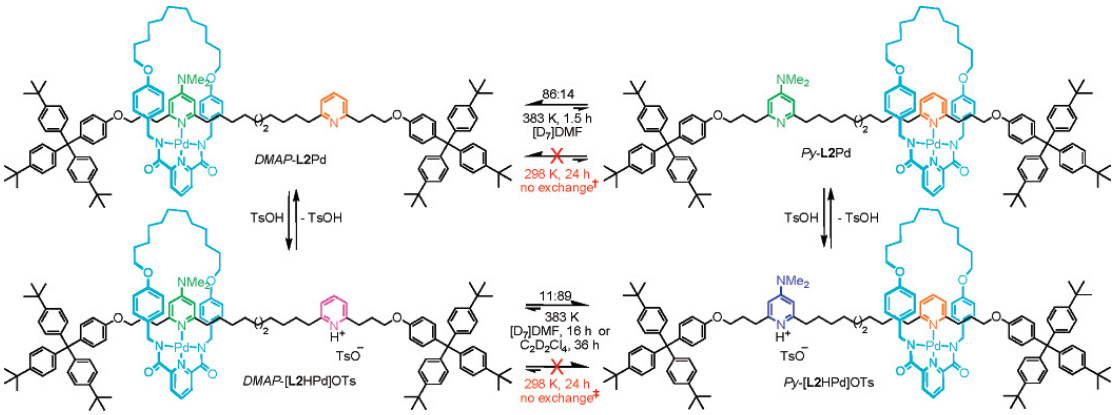

Scheme 3.3 Operation of the palladium-complexed molecular shuttle **L2**Pd. †No macrocycle translocation observed over 24 hours in d_7-DMF at 298 K or in $C_2D_2Cl_4$ over 24 hours at 383 K; ‡No macrocycle translocation observed in either d_7-DMF or $C_2D_2Cl_4$ at 298 K over 24 hours.

3.5 Ligand Exchange Experiments and X-ray Crystallography Using 2,6-Dialkyl-Substituted Heterocycles

The dramatic kinetic stability of the *DMAP*-Pd bond in the protonated [2]rotaxane led us to re-examine the kinetics of non-interlocked ligand exchange, this time using 2,6-dialkyl-substituted heterocycles (Scheme 3.4). Indeed, using 2,6-dipropylPy and 2,6-dipropylDMAP as the monodentate components of the **L1**Pd-heterocycle complex (Scheme 3.4) produced the same extremely slow exchange of ligands as observed in the [2]rotaxane.

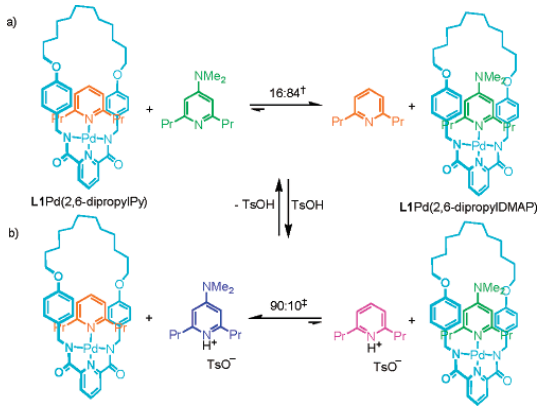

Scheme 3.4 Reversible substitution of 2,6-dipropylpyridine and 2,6-dipropylDMAP ligands in macrocycle-Pd complex **L1**Pd(2,6-dipropylPy)/(2,6-dipropylDMAP) in d_7–DMF. (a) Neutral conditions; (b) in the presence of TsOH (one equivalent). Time required to reach equilibrium:[10] †60 minutes at 358 K; ‡130 minutes at 358 K. No exchange of the 2,6-dipropylheterocycle ligands was observed in $CDCl_3$, under either neutral conditions or in the presence of TsOH, even under heating at reflux over seven days.

Single crystals of both **L1**Pd(2,6-dipropylPy) and **L1**Pd(2,6-dipropylDMAP) were subsequently grown by vapour diffusion of diethyl ether into saturated solutions of the complexes in dichloromethane. The X-ray crystal structures of these two complexes (Figures 3.2a and 3.2b) are indicative of the likely coordination mode and geometry of the macrocycle at the two different binding sites in the [2]rotaxane. The crystal structures suggest that the reason for the enhanced kinetic stability of the Pd-coordinated 2,6-dialkylheterocycle units is that the α-hydrogen atoms of the alkyl substituents block the pathway of incoming nucleophiles to the Pd(II) centre.[21]

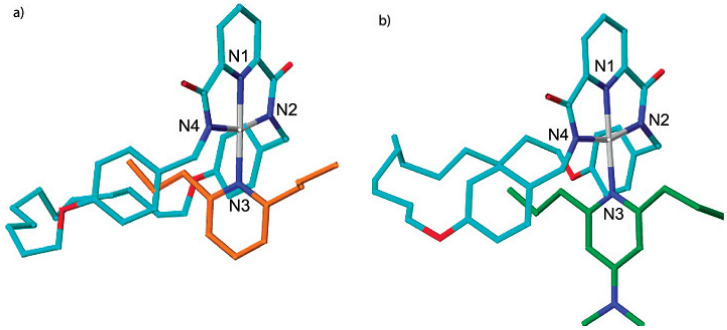

Figure 3.2 X-ray crystal structures of (a) **L1**Pd(2,6-dipropylPy) and (b) **L1**Pd(2,6-dipropylDMAP). Carbon atoms of the macrocycle are shown in light blue, and those of the monodentate ligands, in orange and green, respectively; oxygen atoms are red; nitrogen, dark blue; and palladium, gray. Selected bond lengths [Å] and angles [deg]: (a) N1-Pd 1.94, N2-Pd 2.03, N3-Pd 2.06, N4-Pd 2.03, N2-Pd-N4 161.6; (b) N1-Pd 1.93, N2-Pd 2.03, N3-Pd 2.06, N4-Pd 2.02, N2-Pd-N4 161.4.

3.6 Macrocycle-to-DMAP-Station Deprotonation-Driven Shuttling Experiments

Deprotonation of the 89:11 *Py*:*DMAP* equilibrium mixture of [**L2**HPd]OTs (Na_2CO_3, CH_2Cl_2, 30 minutes) generated the neutral co-conformers which were readily separated by column chromatography to give pure, kinetically stable samples of both *DMAP*-**L2**Pd (minor product) and *Py*-**L2**Pd (major product). Their ^{1}H NMR spectra are shown in Figure 3.1b and 3.1d, respectively. As before, the relative shifts of the resonances of the *DMAP* and *Py* stations unambiguously confirmed the position of the macrocycle in the *Py*-**L2**Pd isomer. Reprotonation of *Py*-**L2**Pd (one equivalent of TsOH in $CDCl_3$) quantitatively generated *Py*-[**L2**HPd]OTs (^{1}H NMR spectrum, Figure 3.1e), as another kinetically stable, out-of-equilibrium co-conformer.

To complete the cycle of operations on **L2**Pd, pure *Py*-**L2**Pd and the non-equilibrium, 11:89, mixture of *DMAP*/*Py*-**L2**Pd were each heated at 383 K in d_7-DMF. After 90 minutes both had reached identical 86:14 ratios of *DMAP*/*Py*-**L2**Pd which did not change upon further heating (Scheme 3.3). Unlike the proton-driven translocation, no macrocycle translational isomerisation was observed when *Py*-**L2**Pd was heated in $C_2D_2Cl_4$. Similarly, 2,6-dipropylDMAP did not undergo a substitution reaction with **L1**Pd(2,6-dipropylPy) in non-coordinating solvents (Scheme 3.4).

3.7 Conclusions

The practical realisation and mechanistic investigation of molecular-level systems in which both the kinetics and thermodynamics of binding events can be varied and controlled is profoundly important for the development of sophisticated molecular machine systems.[7b] Although nature is clearly able to achieve this through the rapid manipulation of hydrogen bonding and electrostatic interactions, the transient nature of such weak binding events makes it hard to see how to emulate this in synthetic systems given current levels of understanding and expertise. We anticipate that metal-ligand coordination (and dynamic covalent) chemistry will play a prominent role in the early development of synthetic molecular machine systems.

3.8 Experimental Section

General

Propargyl ether, 1,9-decadiyne and 2,6-dibromopyridine were purchased from the Aldrich Co. 4-Hydroxybenzylamine,[22] *trans*-dichloro(1,3-bis-(2,6-diisopropylphenyl)imidazolylidinium)(3-chloropyridine)palladium (PEPPSI)[23-27] and 4-[tris-(4-*tert*-butylphenyl)methyl]phenol[19] (**4**) were prepared according to literature procedures.

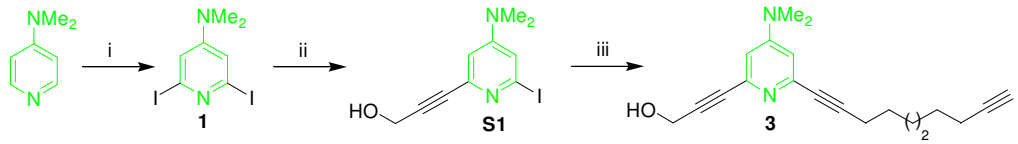

Scheme 3.5 (i) a) $BF_3{\cdot}Et_2O$, THF, 0.5 h, 0 ˚C; b) LDA, THF, 1 h, -78 ˚C; c) I_2, THF, 20 h, -78 ˚C → RT, 40%, (ii) propargyl alcohol, $Pd(PPh_3)_4$, CuI, THF, Et_3N, 36 h, RT, 75%; (iii) 1,9-decadiyne, $Pd(PPh_3)_4$, CuI, THF, Et_3N, 16 h, RT, 77%.

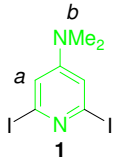

1

To solution of DMAP (7.50 g, 61.0 mmol, 1.0 equiv.) in THF (400 mL) at 0 °C was added boron trifluoride diethyl etherate (8.55 mL, 67.0 mmol, 1.1 equiv) *via* syringe. The resulting suspension was stirred at 0 °C for 30 minutes and then cooled to -78 °C. In a separate flask, *n*-butyllithium (1.6 M in hexanes, 100 mL, 153 mmol, 2.5 equiv.) was added *via* cannula to a 0 °C solution of diisopropyl amine (22.0 mL, 153 mmol, 2.5 equiv.) in THF (100 mL) and was stirred for 30 minutes. The solution of lithium diisopropyl amide was then transferred *via* cannula to the –78 °C solution of the DMAP-boron trifluoride complex. The resulting mixture was stirred for 30 minutes at –78 °C. Iodine (40.0 g, 159 mmol, 2.6 equiv.) was dissolved in THF (150 mL) and transferred *via* cannula to the –78 °C solution. After the addition was complete the reaction mixture was warmed to RT and stirred overnight. Saturated aqueous $Na_2S_2O_3$ (200 mL) was added and the layers were separated. The aqueous phase was extracted with EtOAc (3 x 200 mL) and the combined organic layers were washed with brine (200 mL) and dried (Na_2SO_4). After removing the solvents under reduced pressure, the residue was purified by column chromatography on silica (hexane:EtOAc 2:1) followed by recrystallisation (hexane/CH_2Cl_2) to provide 2,6-diiodo-4-(dimethylamino)-pyridine (2,6-diiodoDMAP, **1**) as a white solid, m.p. 142-145 °C (9.18 g, 40%). ^{1}H NMR (400 MHz, $CDCl_3$): δ 2.93 (s, 6H, H_b), 6.86 (s, 2H, H_a). ^{13}C NMR (100 MHz, $CDCl_3$): δ 39.3, 116.0, 116.6, 155.0. LRESI-MS (MeOH/TFA): *m/z* = 375 $[M+H]^+$. HRFAB-MS (THIOG matrix): *m/z* = 374.8854 (calc. for $C_7H_9N_2I_2$, 374.8855 $[M+H]^+$).

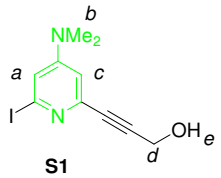

S1

To a solution of 2,6-diiodoDMAP **1** (5.00 g, 13.4 mmol, 1.0 equiv.) in THF (40 mL) and Et_3N (20 mL), was added CuI (0.153 g, 0.804 mmol, 0.06 equiv.) and $Pd(PPh_3)_4$ (0.465 g, 0.402 mmol, 0.03 equiv.). Propargyl alcohol (0.750 g, 0.780 mL, 13.4

mmol, 1.0 equiv.) was then added to the reaction and the mixture was stirred in the absence of light for 20 h at RT. After this time the solvent was removed under reduced pressure. The resulting residue was dissolved in EtOAc (100 mL) and washed with saturated aqueous NH_4Cl (3 x 50 mL). The aqueous phase was extracted with EtOAc (3 x 50 mL) and the combined organic extracts were washed with brine (50 mL) and dried (Na_2SO_4). The solvent was removed under reduced pressure and the resulting residue purified by column chromatography on silica (CH_2Cl_2:acetone 19:1), providing **S1** as a white solid, m.p. 150 °C (dec.) (3.01 g, 75%). ^{1}H NMR (400 MHz, $CDCl_3$): δ 2.51 (br, 1H, H_e), 2.97 (s, 6H, H_b), 4.49 (s, 2H, H_d), 6.63 (d, J = 2.4, 1H, H_c), 6.83 (d, J = 2.4, 1H, H_a). ^{13}C NMR (100 MHz, $CDCl_3$): δ 39.3, 51.4, 84.5, 87.1, 109.9, 116.2, 118.1, 154.5, 157.7. LRESI-MS (MeOH/TFA): m/z = 303 $[M+H]^+$. HRFAB-MS (3-NOBA matrix): m/z = 302.9984 (calc. for $C_{10}H_{12}N_2OI$, 302.9994 $[M+H]^+$).

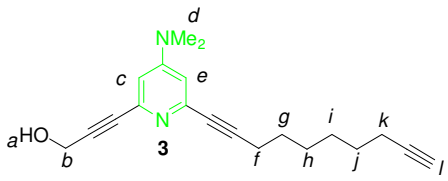

To a solution of **S1** (0.855 g, 2.83 mmol, 1.0 equiv.) in THF (40 mL) and Et_3N (20 mL), was added CuI (0.108 g, 0.566 mmol, 0.2 equiv.) and $Pd(PPh_3)_4$ (0.327 g, 0.283 mmol, 0.1 equiv.). Subsequently 1,9-decadiyne (1.90 g, 14.2 mmol, 5.0 equiv.) was added and the mixture was stirred in the absence of light at RT for 12 h. After this time, the solvent was removed under reduced pressure and the resulting residue was redissolved in CH_2Cl_2 (100 mL) and washed with a saturated aqueous solution of NH_4Cl (50 mL). The aqueous phase was extracted with CH_2Cl_2 (3 x 100 mL), and the combined organic extracts washed with brine (100 mL) and dried (Na_2SO_4). The solvent was removed under reduced pressure and the resulting residue purified by column chromatography on silica (Et_2O:hexane 1:1 then Et_2O), to give **3** as a white solid, m.p. 85-86 °C (0.688 g, 77%). ^{1}H NMR (400 MHz, $CDCl_3$): δ 1.38-1.64 (m, 8H, $H_{g+h+i+j}$), 1.94 (t, J = 2.6, 1H, H_l), 2.19 (td, J = 2.6, 7.0, 2H, H_k), 2.27 (br, 1H, H_a), 2.39 (t, J = 7.1, 2H, H_f), 2.98 (s, 6H, H_d), 4.48 (s, 2H, H_b), 6.55 (d, J = 2.5, 1H, H_e), 6.59 (d, J = 2.5, 1H, H_c). ^{13}C NMR (100 MHz, $CDCl_3$): δ 18.3, 19.2, 28.2, 28.2,

28.3, 28.4, 39.2, 51.3 68.2, 80.6, 84.6, 85.2, 86.1, 89.4, 108.8, 109.0, 142.4, 143.6, 154.4. LRESI-MS (MeOH/TFA): *m/z* = 309 $[M+H]^+$. HRFAB-MS (3-NOBA matrix): *m/z* = 309.1957 (calc. for $C_{20}H_{25}ON_2$, 309.1967 $[M+H]^+$).

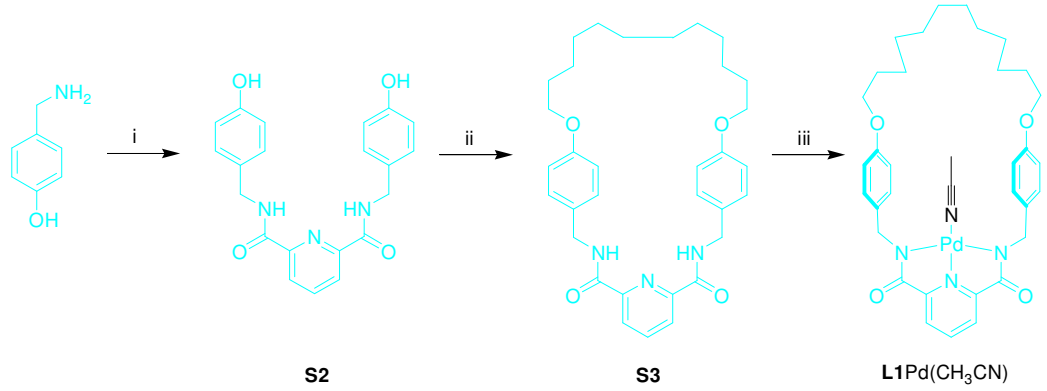

Scheme 3.6 (i) 2,6-pyridinedicarbonyl dichloride, Et_3N, THF, 12 h, 78 ˚C → RT, 99%, (ii) 1,12-dibromododecane, K_2CO_3, butanone, 48 h, reflux, 46%, (iii) $Pd(OAc)_2$, CH_3CN, 6 h, RT, 89%.

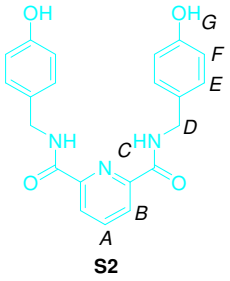

A solution of 4-hydroxybenzylamine[22] (3.15 g, 25.6 mmol, 2.0 equiv.) in THF (100 mL) and Et_3N (3.24 g, 4.46 mL, 32.0 mmol, 2.5 equiv.) was cooled to –78 °C and 2,6-pyridinedicarbonyl dichloride (2.61 g, 12.8 mmol, 1.0 equiv.) in THF (50 mL) added to the reaction mixture dropwise over 2 h whilst maintaining the temperature at –78 °C. When the addition was complete, the reaction was allowed to warm to RT and stirred overnight. The resulting precipitate was collected *via* vacuum filtration and washed with $CHCl_3$ to afford **S2** as an off-white solid, m.p. 200 °C (dec.) (4.80 g, 99%). ^{1}H NMR (400 MHz, d_6-DMSO): δ 4.48 (d, *J* = 6.4, 4H, H_D), 6.69-6.73 (m, 4H, H_F), 7.10-7.14 (m, 4H, H_E), 8.16-8.25 (m, 3H, H_{A+B}), 9.23-9.33 (br, 2H, H_G), 9.79 (t, *J* = 6.4, 2H, H_C). ^{13}C NMR (100 MHz, d_6-DMSO): δ 41.6, 115.0, 124.3, 128.1, 129.4, 139.4, 148.7, 156.2, 163.1. LR-FABMS (3-NOBA matrix): *m/z* = 378 $[M+H]^+$. HR-

FABMS (3-NOBA matrix): *m/z* = 395.1717 $[M+NH_4]^+$ (calc. for $C_{21}H_{23}N_4O_4$, 395.1714 $[M+NH_4]^+$).

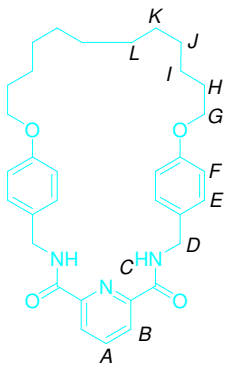

S3

A mixture of **S2** (1.00 g, 2.65 mmol, 1.0 equiv.), 1,12-dibromododecane (0.869 g, 2.65 mmol, 1.0 equiv.), K_2CO_3 (3.66 g, 26.5 mmol, 10.0 equiv.) and butanone (1 L) was heated at reflux for 48 h. After this time, the reaction mixture was filtered through celite and the filtrate concentrated under reduced pressure. The resulting crude residue was purified by column chromatography on silica (EtOAc:CH_2Cl_2 1:4) to give **S3** as a white solid, m.p. 230-232 °C (0.661 g, 46%). ^{1}H NMR (400 MHz, $CDCl_3$): δ 1.24-1.33 (m, 12H, H_{J+K+L}), 1.41-1.47 (m, 4H, H_I), 1.73-1.80 (m, 4H, H_H), 3.95 (t, *J* = 6.4, 4H, H_G), 4.63 (d, *J* = 6.2, 4H, H_D), 6.82-6.86 (m, 4H, H_F), 7.21-7.25 (m, 4H, H_E), 7.85-7.88 (m, 2H, H_C), 8.05 (t, *J* = 7.8, 1H, H_A), 8.41 (d, *J* = 7.8, 2H, H_B). ^{13}C NMR (100 MHz, $CDCl_3$): δ 25.4, 28.2, 28.4, 28.7, 28.9, 42.8, 67.6, 114.6, 125.3, 129.1, 129.8, 138.9, 148.8, 158.6, 163.3. LR-FABMS (3-NOBA matrix): *m/z* = 544 $[M+H]^+$. HR-FABMS (3-NOBA matrix): *m/z* = 544.3164 (calc. for $C_{33}H_{42}N_3O_4$, 544.3175 $[M+H]^+$).

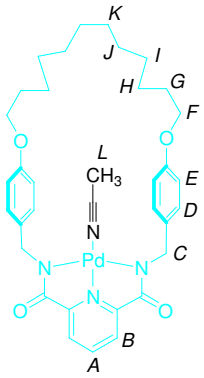

L1Pd(CH_3CN)

To a solution of **S3** (0.918 g, 1.69 mmol, 1.0 equiv.) in CH_3CN (150 mL) was added a solution of $Pd(OAc)_2$ (0.455 g, 2.03 mmol, 1.2 equiv.) in CH_3CN (30 mL) and the solution stirred at RT. The reaction mixture turned black almost immediately and subsequently a yellow precipitate formed. The extent of the reaction was monitored by ^1H NMR and was found to be complete after 6 h, at which point the suspension was gently heated until all the yellow precipitate had dissolved. Filtration through celite whilst hot afforded a yellow solution, which was concentrated under reduced pressure to yield an off-yellow solid. Recrystallisation from hot CH_3CN gave **L1**Pd(CH_3CN) as a yellow crystalline solid, m.p. 250 °C (dec.) (1.04 g, 89%). ^1H NMR (400 MHz, $CDCl_3$:CD_3CN 98:2): δ 1.21-1.49 (m, 16H, $H_{H+I+J+K}$), 1.70-1.82 (m, 4H, H_G), 1.99 (s, 3H, H_L), 3.91 (t, J = 6.5, 4H, H_F), 4.45 (s, 4H, H_C), 6.75-6.80 (m, 4H, H_E), 7.14-7.21 (m, 4H, H_D), 7.74 (d, J = 7.8, 2H, H_B), 8.06 (t, J = 7.8, 1H, H_A). ^{13}C NMR (100 MHz, $CDCl_3$:CD_3CN 98:2): δ 1.8, 25.4, 28.3, 28.4, 28.9 (x 2), 49.5, 67.6, 114.1, 116.4, 124.7, 128.4, 133.3, 140.9, 153.0, 157.6, 170.4. LRESI-MS (MeOH/TFA): m/z = 689 $[M+H]^+$; HR-FABMS (3-NOBA matrix): m/z = 689.2313 (calc. for $C_{35}H_{43}N_4O_4{}^{106}Pd$, 689.2316 $[M+H]^+$).

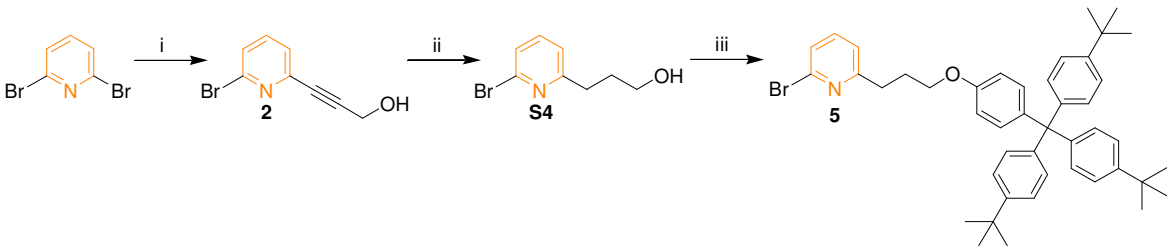

Scheme 3.7 (i) propargyl alcohol, $Pd(PPh_3)_4$, CuI, THF, Et_3N, 20 h, RT, 66%, (ii) PtO_2, H_2, EtOH, Et_3N, 2 h, RT, 94%, (iii) **4**, PPh_3, DIAD, THF, 72 h, 0 °C → RT, 61%.

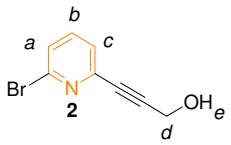

To a solution of 2,6-dibromopyridine (3.00 g, 12.7 mmol, 1.0 equiv.) in THF (20 mL) and Et_3N (10 mL) was added propargyl alcohol (0.710 g, 0.740 mL, 12.7 mmol, 1.0 equiv.), $Pd(PPh_3)_4$ (0.761 g, 0.658 mmol, 0.05 equiv.) and CuI (0.241 g, 1.27 mmol, 0.1 equiv.). The resulting mixture was stirred at RT for 20 h. The solvent was removed under reduced pressure and the residue was redissolved in CH_2Cl_2 (100 mL) and washed with a saturated aqueous solution of NH_4Cl (3 x 50 mL) and brine (100 mL). The organic layer was dried (Na_2SO_4), the solvent removed under reduced pressure and the crude residue purified by column chromatography on silica (CH_2Cl_2:acetone 85:15) to give **2** as a white solid, m.p. 87-88 °C (1.77 g, 66%). ^{1}H NMR (400 MHz, $CDCl_3$): δ 2.15 (br, 1H, H_e), 4.52 (s, 2H, H_d), 7.38 (dd, J_1 = 7.5, J_2 = 0.9, 1H, H_c), 7.44 (dd, J_1 = 8.0, J_2 = 0.9, 1H, H_a), 7.50-7.54 (m, 1H, H_b). ^{13}C NMR (100 MHz, $CDCl_3$): δ 51.2, 83.5, 88.3, 125.8, 127.8, 138.5, 141.6, 143.1. LRESI-MS (MeOH/TFA): *m/z* = 212 $[M^{79}Br+H]^+$, 214 $[M^{81}Br+H]^+$. HR-FABMS (3-NOBA matrix): *m/z* = 213.9592 (calc. for $C_8H_7NO^{81}Br$, 213.9692 $[M^{81}Br+H]^+$).

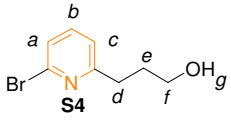

To a solution of **2** (2.89 g, 13.6 mmol, 1.0 equiv.) in degassed EtOH (70 mL) and Et_3N (3.5 mL) was added PtO_2 (0.309 g, 1.36 mmol, 0.1 equiv.), and the mixture was stirred at RT under a hydrogen atmosphere for 2 h. After this time, the solvents were removed under reduced pressure and the residue purified by column chromatography on silica (Et_2O:hexane 1:1 then Et_2O) to give **S4** as a pale yellow oil (2.77 g, 94%). ^{1}H NMR (400 MHz, $CDCl_3$): δ 1.95-2.01 (m, 2H, H_e), 2.35 (br, 1H, H_g), 2.98 (t, *J* = 7.3, 2H, H_d), 3.70 (t, *J* = 6.1, 2H, H_f), 7.13 (d, *J* = 7.5, 1H, H_c), 7.31 (d, *J* = 7.8, 1H, H_a), 7.44-7.48 (m, 1H, H_b). ^{13}C NMR (100 MHz, $CDCl_3$): δ 31.9, 34.5, 62.1, 121.8, 125.4, 138.9, 141.4, 163.2. LRESI-MS (MeOH/TFA): *m/z* = 216 $[M^{79}Br+H]^+$, 218 $[M^{81}Br+H]^+$. HRESI-MS: *m/z* = 216.9923 $[M^{81}Br]^+$ (calc. for $C_8H_{10}NO^{81}Br$, 216.9920 $[M^{79}Br]^+$).

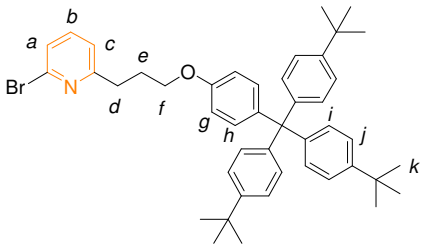

5

To a solution of **4** (0.752 g, 1.49 mmol, 1.0 equiv.) and PPh_3 (0.469 g, 1.79 mmol, 1.2 equiv.) in THF (20 mL) was added a solution of **S4** (0.355 g, 1.64 mmol, 1.1 equiv.) in THF (10 mL). The resulting mixture was cooled to 0 ºC and a solution of DIAD (0.412 mL, 2.09 mmol, 1.4 equiv.) in THF (15 mL) was added to the reaction mixture dropwise over 2 h at 0 ºC. When the addition was complete, the resulting orange solution was allowed to warm to RT and stirred for 72 h. After this time, the solvent was removed under reduced pressure and the residue purified by column chromatography on silica (EtOAc:hexane 1:19) to give **5** as a white solid, m.p. 200 ºC (dec.) (0.639 g, 61%). ^{1}H NMR (400 MHz, $CDCl_3$): δ 1.30 (s, 27H, H_k), 2.17-2.24 (m, 2H, H_e), 2.94-2.98 (m, 2H, H_d), 3.97 (t, J = 6.1, 2H, H_f), 6.73-6.76 (m, 2H, H_g), 7.05-7.10 (m, 8H, H_{h+i}), 7.14 (d, J = 7.3, 1H, H_c), 7.21-7.25 (m, 6H, H_j), 7.31 (d, J = 7.7, 1H, H_a), 7.43-7.46 (m, 1H, H_b). ^{13}C NMR (100 MHz, $CDCl_3$): δ 29.1, 31.4, 34.3, 34.4, 63.0, 66.7, 112.9, 121.8, 124.0, 125.5, 130.7, 132.2, 138.6, 139.5, 141.6, 144.1, 148.3, 156.7, 163.1. LR-FABMS (3-NOBA matrix): *m/z* = 702 $[M^{79}Br+H]^+$, 704 $[M^{81}Br+H]^+$. HR-FABMS (3-NOBA matrix): *m/z* = 704.3301 (calc. for $C_{45}H_{53}NO^{81}Br$, 704.3290 $[M^{81}Br+H]^+$).

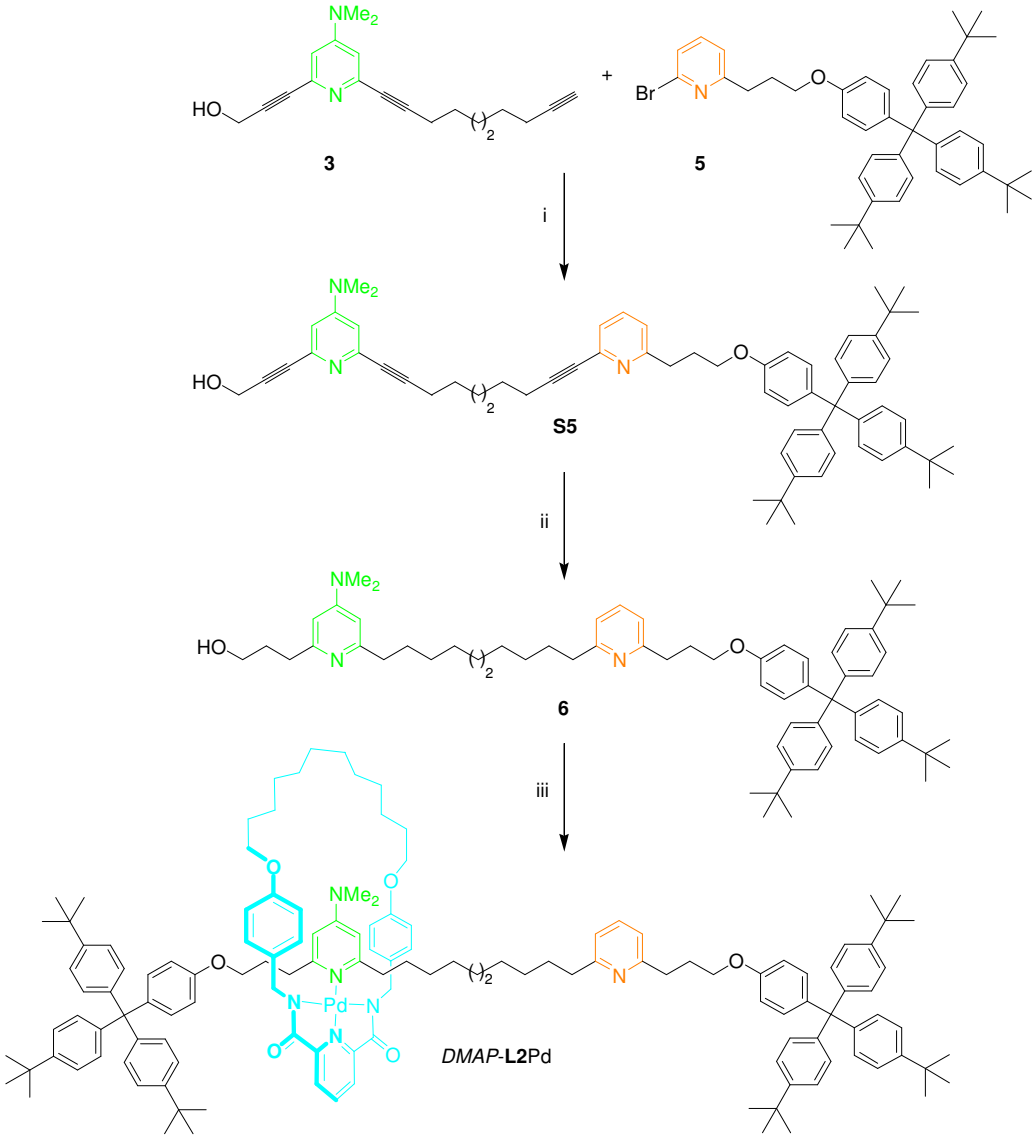

Scheme 3.8 (i) $Pd(PPh_3)_4$, CuI, THF, Et_3N, 48 h, RT, 66%, (ii) $Pd(OH)_2/C$, H_2, THF, 4h, RT, 88%, (iii) a) **L1**Pd(CH_3CN), CH_2Cl_2, 1 h, RT, 90%; b) **4**, PPh_3, DIAD, THF, 36 h, RT, 29% (26% from **6**).

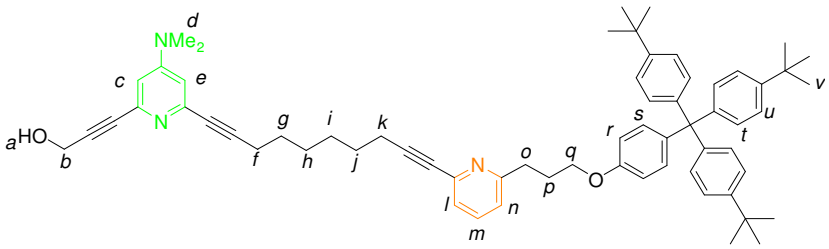

S5

To a solution of **5** (1.52 g, 2.17 mmol, 1.0 equiv.) in THF (80 mL) and Et_3N (40 mL), was added CuI (82.0 mg, 0.433 mmol, 0.2 equiv.) and $Pd(PPh_3)_4$ (0.250 g, 0.217 mmol, 0.1 equiv.). Subsequently **3** (0.668 g, 2.17 mmol, 1.0 equiv.) was added and the mixture stirred at RT in the absence of light for 48 h. After this time, the solvent was removed under reduced pressure and the resulting residue was redissolved in EtOAc and washed with saturated aqueous NH_4Cl (3 x 50 mL). The aqueous phase was then extracted with EtOAc (3 x 100 mL), and the combined organic extracts washed with brine (100 mL) and dried (Na_2SO_4). The solvent was removed under reduced pressure and the resulting residue purified by column chromatography on silica (EtOAc), followed by recrystallisation from CH_2Cl_2/CH_3CN to give **S5** as a cream solid, m.p. 113-115 °C (1.32 g, 66%). ^{1}H NMR (400 MHz, $CDCl_3$): δ 1.30 (s, 27H, H_v), 1.45-1.51 (m, 4H, H_{h+i}), 1.59-1.68 (m, 4H, H_{g+j}), 1.95 (br, 1H, H_a), 2.16-2.23 (m, 2H, H_p), 2.39-2.46 (m, 4H, H_{f+k}), 2.93-3.00 (m, 8H, H_{d+o}), 3.96 (t, J = 6.2, 2H, H_q), 4.47 (s, 2H, H_b), 6.56-6.59 (m, 2H, H_{c+e}), 6.73-6.76 (m, 2H, H_r), 7.05-7.09 (m, 9H, H_{n+s+t}), 7.21-7.24 (m, 7H, H_{l+u}), 7.49- 7.53 (m, 1H, H_m). ^{13}C NMR (100 MHz, $CDCl_3$): δ 19.2, 19.3, 28.1 (x 2), 28.4, 28.5, 29.4, 31.3, 34.2, 34.8, 39.1, 51.3, 62.9, 66.8, 80.5, 80.7, 85.5, 85.7, 89.3, 90.6, 108.8, 109.0, 112.9, 121.6, 123.9, 124.4, 130.6, 132.1, 136.3, 139.4, 142.4, 143.3, 143.7, 144.1, 148.2, 154.3, 156.7, 161.6. LR-FABMS (3-NOBA matrix): m/z = 931 $[M+H]^+$. HR-FABMS (3-NOBA matrix): m/z = 930.5943 (calc. for $C_{65}H_{76}N_3O_2$, 930.5938 $[M+H]^+$).

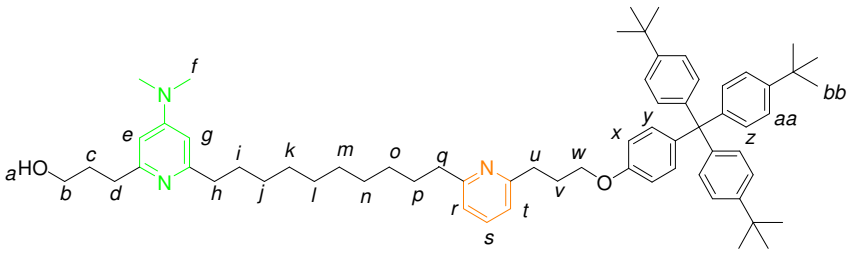

6

To a solution of **S5** (1.22 g, 1.31 mmol, 1.0 equiv.) in THF (40 mL) was added 10% $Pd(OH)_2/C$ (0.280 g, 20% b/w) and the mixture stirred at RT under a hydrogen atmosphere for 4 h. After this time, the reaction mixture was filtered through celite, concentrated under reduced pressure and purified by column chromatography on silica (MeOH:acetone 1:5) to give **6** as a cream solid, m.p. 159-161 °C (1.09 g, 88%). ^{1}H NMR (400 MHz, $CDCl_3$): δ 1.21-1.39 (m, 40H, $H_{a+j+k+l+m+n+o+bb}$), 1.63-1.73 (m, 4H, H_{i+p}), 1.91-1.98 (m, 2H, H_c), 2.16-2.23 (m, 2H, H_v), 2.65-2.75 (m, 4H, H_{h+q}), 2.90-2.95 (m, 4H, H_{d+u}), 3.01 (s, 6H, H_f), 3.71-3.73 (m, 2H, H_b), 3.97 (t, J = 6.3, 2H, H_w), 6.21-6.25 (m, 2H, H_{e+g}), 6.72-6.77 (m, 2H, H_x), 6.95-6.98 (m, 2H, H_{r+t}), 7.05-7.09 (m, 8H, H_{y+z}), 7.21-7.23 (m, 6H, H_{aa}), 7.46-7.50 (m, 1H, H_s). ^{13}C NMR (100 MHz, $CDCl_3$): δ 29.4 (x4), 29.5 (x3), 29.8, 30.1, 31.3, 31.4, 34.2, 34.7, 35.5, 37.5, 38.4, 39.3, 62.2, 62.9, 67.0, 102.9, 103.2, 112.9, 119.8, 119.8, 123.9, 130.6, 132.1, 136.5, 139.3, 144.1, 148.1, 155.8, 156.7, 159.5, 160.3, 160.5, 162.0. LR-FABMS (3-NOBA matrix): *m/z* = 943 $[M+H]^+$. HR-FABMS (3-NOBA matrix): *m/z* = 942.6866 (calc. for $C_{65}H_{88}N_3O_2$, 942.6877 $[M+H]^+$).

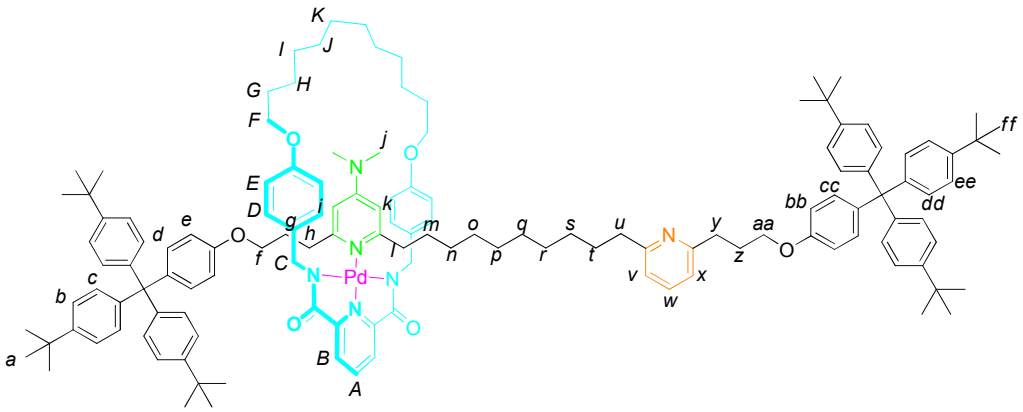

DMAP-**L2**Pd

To a solution of **6** (0.043 g, 0.046 mmol, 1.0 equiv.) in CH_2Cl_2 (30 mL) was added **L1**Pd(CH_3CN) (0.032 g, 0.046 mmol, 1.0 equiv.) and the solution stirred at RT for 1 h. The solvent was removed under reduced pressure and the crude residue was purified by column chromatography (MeOH:CH_2Cl_2, 4:96) to give the threaded pre-rotaxane (0.066 g, 90%). LRESI-MS (MeOH/TFA): *m/z* = 1590 $[M^{106}Pd]^+$. To a solution of this pre-rotaxane (0.054 g, 0.030 mmol, 1.0 equiv.), PPh_3 (0.013 g, 0.051 mmol, 1.5 equiv.) and **4** (0.026 g, 0.051 mmol, 1.5 equiv.) in THF (10 mL) was added DIAD (0.010 mL, 0.051 mmol, 1.5 equiv.) *via* microsyringe, and the resulting solution was stirred at RT for 36 h. After removal of the solvent under reduced pressure, the crude residue was purified by column chromatography on silica (EtOAc:CH_2Cl_2 2:3) and washed with ice-cold CH_3CN to yield *DMAP*-**L2**Pd as a yellow solid, m.p. 170-172 °C (0.025 g, 29% from the pre-rotaxane, 26% from **6**). ^{1}H NMR (400 MHz, $CDCl_3$): δ 1.01- 1.43 (m, 84H, $H_{a+g+n+o+p+q+r+s+ff+H+I+J+K}$), 1.61-1.79 (m, 6H, H_{t+G}), 1.90-2.13 (m, 4H, H_{h+m}), 2.15-2.25 (m, 2H, H_z), 2.65-3.38 (m, 14H, $H_{j+l+u+y+C'}$), 3.43-3.67 (m, 2H, H_f), 3.80-3.89 (m, 4H, H_F), 3.98 (t, *J* = 6.3, 2H, H_{aa}), 5.10-5.41 (br, 2H, H_C), 5.68-5.97 (br, 1H, $H_{(i \text{ or } k)}$), 6.40-6.80 (m, 13H, $H_{e+bb+D+E+(i \text{ or } k)}$), 6.93-7.02 (m, 2H, H_{v+x}), 7.05-7.11 (m, 16H, $H_{c+d+cc+dd}$), 7.19-7.25 (m, 12H, H_{b+ee}), 7.45-7.53 (m, 1H, H_w), 7.83 (d, *J* = 7.8, 2H, H_B), 8.04 (t, *J* = 7.8, 1H, H_A). LRESI-MS (MeOH/TFA): *m/z* = 2076 $[M^{106}Pd+H]^+$. HR-FABMS (3-NOBA matrix): *m/z* = 2075.2072 $[M]^+$ (calc. for $C_{135}H_{168}N_6O_6{}^{106}Pd$ 2075.2060 $[M]^+$).

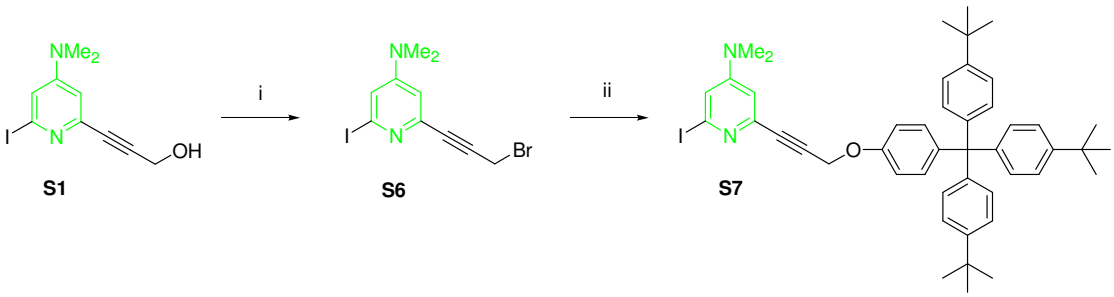

Scheme 3.9 (i) CBr_4, PPh_3, CH_2Cl_2, 12 h, 0 ˚C → RT, 86%, (ii) **4**, K_2CO_3, butanone, 36 h, reflux, 95%.

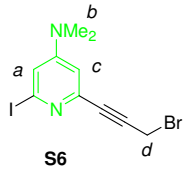

To a solution of **S1** (1.17 g, 3.87 mmol, 1.0 equiv.) and CBr_4 (1.41 g, 4.26 mmol, 1.1 equiv.) in CH_2Cl_2 (100 mL) at 0 °C was added PPh_3 (1.12 g, 4.26 mmol, 1.1 equiv.), and the solution was stirred at RT overnight. The solvent was removed under reduced pressure and the crude residue purified by column chromatography on silica (CH_2Cl_2) to give **S6** as an off-white solid, m.p. 120 °C (dec.) (1.21 g, 86%). ^{1}H NMR (400 MHz, $CDCl_3$): δ 2.96 (s, 6H, H_b), 4.09 (s, 2H, H_d), 6.62 (d, J = 2.3, 1H, H_c), 6.83 (d, J = 2.3, 1H, H_a). ^{13}C NMR ($CDCl_3$, 100 MHz): δ 14.3, 39.2, 83.4, 85.2, 110.3, 116.4, 118.2, 141.7, 154.3. LRESI-MS (MeOH/TFA): m/z = 365 $[M^{79}Br+H]^+$, 367 $[M^{81}Br+H]^+$. HRFAB-MS (THIOG matrix): m/z = 366.9124 (calc. for $C_{10}H_{11}{}^{81}Br^{127}IN_2$, 366.9131 $[M^{81}Br+H]^+$).

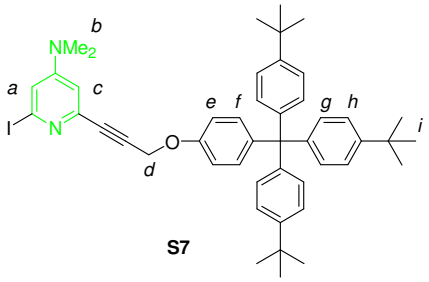

To a solution of **S6** (0.179 g, 0.490 mmol, 1.0 equiv.) and **4** (0.247 g, 0.490 mmol, 1.0 equiv.) in butanone (50 mL) was added K_2CO_3 (0.677 g, 4.90 mmol, 10 equiv.) and the resulting mixture was heated at reflux for 36 h. After this time, the reaction

was filtered through celite, and the resultant solution concentrated under reduced pressure and the crude residue purified by column chromatography on silica (CH_2Cl_2), to give **S7** as a white solid, m.p. 250 °C (dec.) (0.368 g, 95%). ^{1}H NMR (400 MHz, $CDCl_3$): δ 1.30 (s, 27H, H_i), 2.96 (s, 6H, H_b), 4.85 (s, 2H, H_d), 6.65 (d, *J* = 2.4, 1H, H_c), 6.83-6.89 (m, 3H, H_{a+e}), 7.05-7.13 (m, 8H, H_{f+g}), 7.20-7.25 (m, 6H, H_h). ^{13}C NMR ($CDCl_3$, 100 MHz): δ 31.4, 34.3, 39.2, 56.4, 63.1, 83.6, 85.8, 110.3, 113.4, 116.3, 118.3, 124.0, 130.7, 132.3, 140.5, 142.0, 144.0, 148.3, 154.4, 155.5. LRESI-MS (MeOH/TFA): *m/z* = 789 $[M+H]^+$. HRFAB-MS (THIOG matrix): *m/z* = 789.3280 (calc. for $C_{47}H_{54}IN_2O$, 789.3281 $[M+H]^+$).

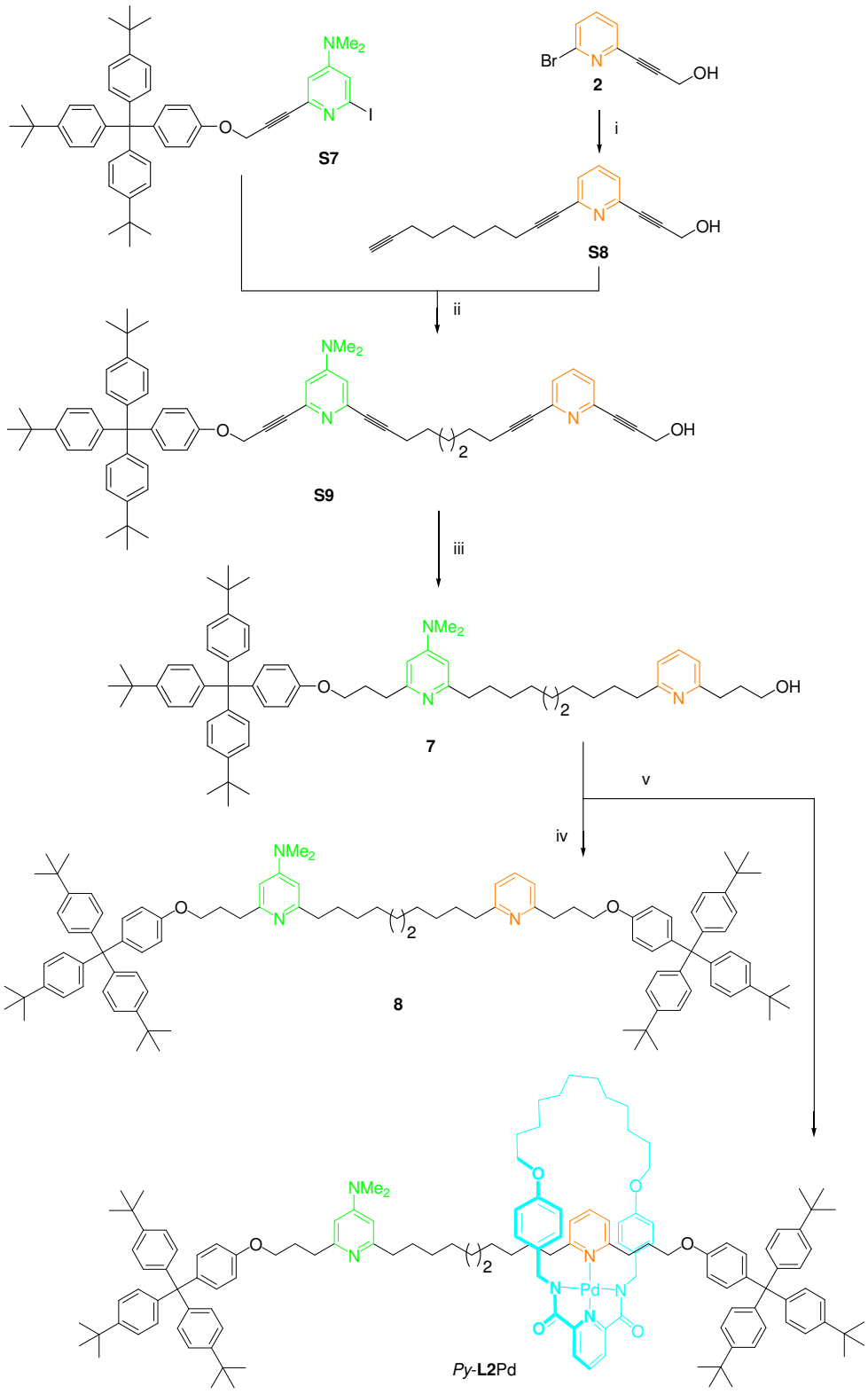

Scheme 3.10 (i) 1,9-decadiyne, $Pd(PPh_3)_4$, CuI, THF, NEt_3, 48 h, RT, 90%, (ii) $Pd(PPh_3)_2Cl_2$, CuI, THF, NEt_3, 48 h, RT, 72%, (iii) $Pd(OH)_2/C$, H_2, THF, 2h, RT, 67%, (iv) **4**, PPh_3, DIAD, THF, 24 h, RT, 25%, (v) **L1**Pd(CH_3CN), CH_2Cl_2, 1 h, RT, 67%; b) **4**, PPh_3, DIAD, THF, 12 h, 0 ˚C → RT, 21% (from **7**).

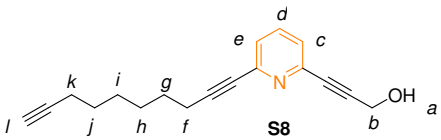

S8

To a solution of **2** (1.74 g, 8.21 mmol, 1.0 equiv.) in THF (20 mL) and Et_3N (10 mL), was added CuI (0.156 g, 0.821 mmol, 0.10 equiv.) and $Pd(PPh_3)_4$ (0.474 g, 0.410 mmol, 0.05 equiv.). Subsequently 1,9-decadiyne (5.51 g, 41.0 mmol, 5.0 equiv.) was added and the mixture was stirred in the absence of light for 48 h at RT. After this time, the solvents were removed under reduced pressure and the resulting residue was redissolved in CH_2Cl_2 (50 mL) and washed with saturated aqueous NH_4Cl (50 mL). The aqueous phase was extracted with CH_2Cl_2 (3 x 100 mL), the combined organic layers were then washed with brine (100 mL) and dried (Na_2SO_4). The solvent was removed under reduced pressure and the crude residue was purified by column chromatography on silica (Et_2O:hexane 1:1) to give **S8** as a cream solid, m.p. 57-59 °C (1.96 g, 90%). ^{1}H NMR (400 MHz, $CDCl_3$): δ 1.40-1.66 (m, 8H, $H_{g+h+i+j}$), 1.94 (t, J = 2.6, 1H, H_l), 2.10-2.23 (m, 3H, H_{a+k}), 2.43 (t, J = 7.1, 2H, H_f), 4.50 (s, 2H, H_b), 7.29-7.32 (m, 2H, H_{c+e}), 7.57 (t, J = 7.8, 1H, H_d). ^{13}C NMR (100 MHz, $CDCl_3$): δ 18.3, 19.3, 28.1, 28.2, 28.3, 28.4, 51.4, 68.2, 79.9, 84.5, 84.6, 87.7, 91.7, 125.5, 126.2, 136.4, 142.7, 144.2. LRESI-MS (MeOH/TFA): *m/z* = 266 $[M+H]^+$. HRFAB-MS (THIOG matrix): *m/z* = 266.1542 (calc. for $C_{18}H_{20}NO$, 266.1545 $[M+H]^+$).

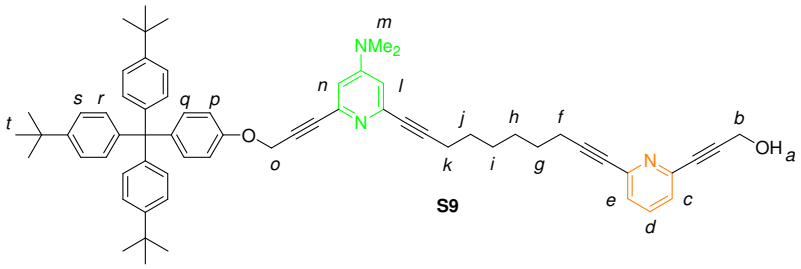

S9

To a solution of **S7** (1.24 g, 1.57 mmol, 1.0 equiv.) in THF (100 mL) and Et_3N (50 mL) was added CuI (60.0 mg, 0.314 mmol, 0.2 equiv.) and $Pd(PPh_3)_2Cl_2$ (0.110 g, 0.157 mmol, 0.1 equiv.). A solution of **S8** (0.416 g, 1.57 mmol, 1.0 equiv.) in THF (15 mL) was added to the reaction *via* cannula and the mixture was stirred in the absence of light at RT for 48 h. After this time, the solvents were removed under reduced pressure and the resulting residue was redissolved in EtOAc (100 mL) and

washed with saturated aqueous NH_4Cl (100 mL). The aqueous phase was extracted with EtOAc (3 x 200 mL), the combined organic layers were washed with brine (100 mL) and dried (Na_2SO_4). The solvent was removed under reduced pressure and the crude residue purified by column chromatography on silica (EtOAc:CH_2Cl_2 1:9) to give **S9** as a cream solid, m.p. 180 °C (dec.) (1.04 g, 72%). ^{1}H NMR (400 MHz, $CDCl_3$): δ 1.29 (s, 27H, H_t), 1.45-1.51 (m, 4H, H_{h+i}), 1.57-1.66 (m, 4H, H_{g+j}), 2.00 (br, 1H, H_a), 2.39-2.44 (m, 4H, H_{f+k}), 2.97 (s, 6H, H_m), 4.49 (s, 2H, H_b), 4.86 (s, 2H, H_o), 6.56 (d, J = 2.5, 1H, H_l), 6.60 (d, J = 2.5, 1H, H_n), 6.85-6.89 (m, 2H, H_p), 7.05-7.11 (m, 8H, H_{q+r}), 7.20-7.24 (m, 6H, H_s), 7.27-7.32 (m, 2H, H_{c+e}), 7.56 (t, J = 7.8, 1H, H_d). ^{13}C NMR ($CDCl_3$, 100 MHz): δ 19.2, 19.3, 28.0, 29.2, 28.4, 28.5, 31.4, 34.3, 39.2, 51.4, 56.5, 63.1, 80.0, 80.8, 82.3, 84.7, 86.8, 87.4, 89.3, 91.7, 109.2, 109.2, 113.4, 124.0, 125.4, 126.2, 130.7, 132.3, 136.4, 140.3, 142.3, 142.7, 143.9, 144.0, 144.2, 148.3, 154.3, 155.7. LRESI-MS (MeOH/TFA): *m/z* = 927 $[M+H]^+$. HRFAB-MS (THIOG matrix): *m/z* = 926.5629 (calc. for 926.5625, $C_{65}H_{72}N_3O_2$ $[M+H]^+$).

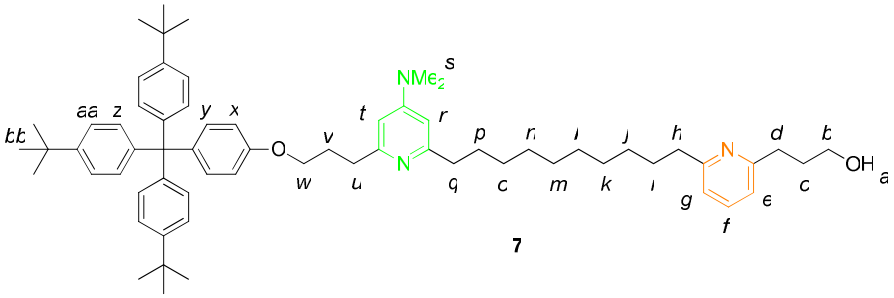

7

To a solution of **S9** (0.441 g, 0.476 mmol, 1.0 equiv.) in degassed THF (25 mL) was added 10% $Pd(OH)_2/C$ (88.0 mg, 20% b/w) and the reaction was stirred under a hydrogen atmosphere at RT for 2 h. After this time the reaction was filtered through celite, the solvent was removed under reduced pressure and the resulting crude residue purified by column chromatography on silica (CH_2Cl_2:CH_3CN:NH_3 79.5:20:0.5) to give **7** as a cream solid, m.p. 129-131 °C (0.302 g, 67%). ^{1}H NMR (400 MHz, $CDCl_3$): δ 1.22-1.37 (m, 40H, $H_{a+j+k+l+m+n+o+bb}$), 1.64-1.72 (m, 4H, H_{i+p}), 1.93-1.99 (m, 2H, H_c), 2.15-2.22 (m, 2H, H_v), 2.63-2.67 (m, 2H, H_q), 2.72-2.76 (m, 2H, H_h), 2.82-2.86 (m, 2H, H_u), 2.91-2.97 (m, 8H, H_{d+s}), 3.72 (t, J = 5.7, 2H, H_b), 3.95-3.99 (m, 2H, H_w), 6.21-6.24 (m, 2H, H_{r+t}), 6.75-6.78 (m, 2H, H_x), 6.94-6.97 (m,

2H, H_{e+g}), 7.07-7.11 (m, 8H, H_{y+z}), 7.21-7.24 (m, 6H, H_{aa}), 7.48 (t, J = 7.6, 1H, H_f). ^{13}C NMR (100 MHz, $CDCl_3$): δ 29.2, 29.3, 29.4 (x3), 29.5, 29.6, 29.8, 30.4, 31.2, 31.3, 34.2, 34.9, 35.7, 38.0, 38.8, 39.1, 62.3, 62.9, 67.0, 102.8, 103.1, 112.9, 112.0, 120.2, 123.9, 130.6, 132.1, 137.0, 139.2, 144.1, 148.1, 155.2, 156.8, 160.3, 160.5, 161.4, 161.9. LRESI-MS (MeOH/TFA): m/z = 943 $[M+H]^+$, 472 $[M+2H]^{2+}$.

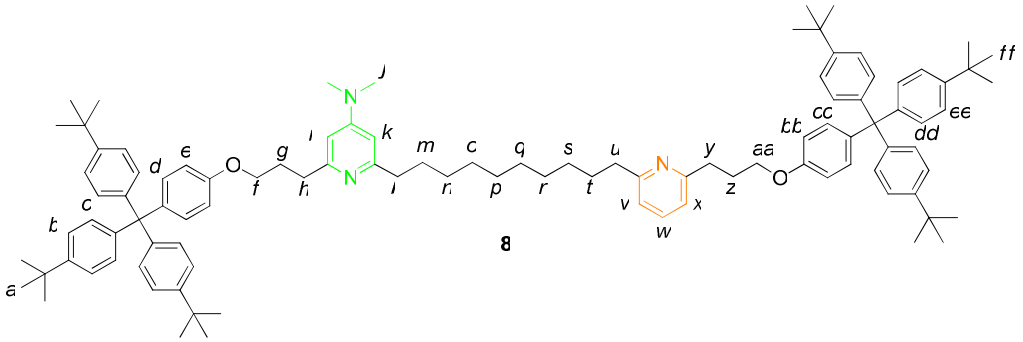

To a solution of **7** (0.039 g, 0.041 mmol, 1.0 equiv.), **4** (0.21 g, 0.41 mmol, 10 equiv.) and PPh_3 (0.022 g, 0.83 mmol, 2.0 equiv.) in THF (10 mL) was added DIAD (0.016 mL, 0.83 mmol, 2.0 equiv.) and the solution was stirred at RT for 24 h. After this time, the solvent was removed under reduced pressure and the crude residue purified by column chromatography on silica (MeOH:CH_2Cl_2 3:97) to give **8** as an off-white solid, m.p. 250 °C (dec.) (0.015 g, 25%). ^{1}H NMR (400 MHz, $CDCl_3$, 298 K): δ 1.25-1.34 (m, 58H, $H_{a+p+q+ff}$), 1.57-1.91 (m, 12H, $H_{m+n+o+r+s+t}$), 2.13-2.30 (m, 4H, H_{g+z}), 2.69-2.78 (m, 2H, H_u), 2.83-3.17 (m, 12H, $H_{h+j+l+y}$), 3.92-4.01 (m, 4H, H_{f+aa}), 6.25-6.30 (m, 2H, H_{i+k}), 6.70-6.78 (m, 4H, H_{e+bb}), 6.95-6.99 (m, 2H, H_{v+x}), 7.05-7.10 (m, 16H, $H_{c+d+cc+dd}$), 7.19-7.25 (m, 12H, H_{b+ee}), 7.48 (t, J = 6.7, 1H, H_w). LR-FABMS (3-NOBA matrix): m/z = 1430 $[M+H]^+$. HR-FABMS (3-NOBA matrix): m/z = 1430.0153 (calc. for $C_{102}H_{130}N_3O_2$, 1430.0197 $[M+H]^+$).

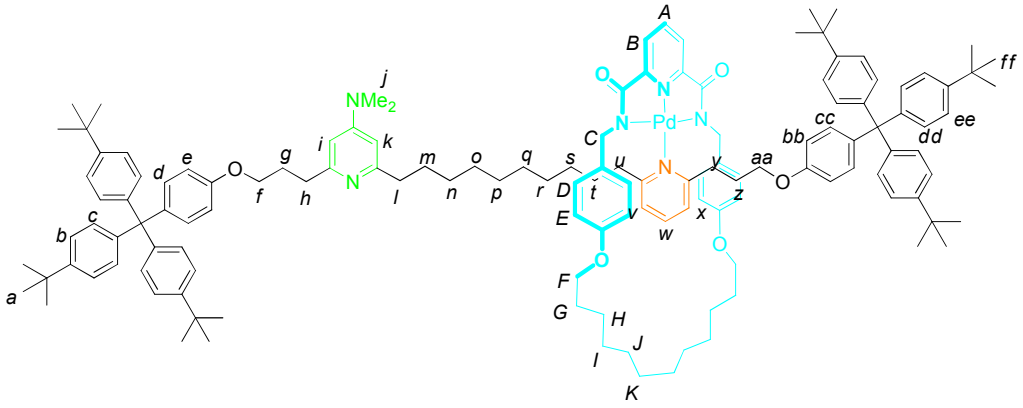

Py-**L2**Pd

To a solution of **7** (0.105 g, 0.118 mmol, 1.0 equiv.) in CH_2Cl_2 (30 mL) was added **L1**Pd(CH_3CN) (82.0 mg, 0.118 mmol, 1.0 equiv.) and the solution stirred at RT for 1 h. After this time, the solvent was removed under reduced pressure to give the threaded pre-rotaxane, which was isolated in 67% yield using column chromatography (MeOH:CH_2Cl_2 1:19), and used without further purification. LRESI-MS (MeOH/TFA): *m/z* = 1590 $[M^{106}Pd]^+$. This complex was dissolved in THF (50 mL) together with PPh_3 (93.0 mg, 0.354 mmol, 3.0 equiv.) and **4** (0.179 g, 0.354 mmol, 3.0 equiv.). Subsequently DIAD (70.0 mL, 0.354 mmol, 3.0 equiv.) was added to the solution dropwise over 15 minutes at 0 °C. When the addition was complete, the reaction was allowed to warm to RT and stirred for 18 h. The solvent was removed under reduced pressure and the crude residue purified by column chromatography on silica (MeOH:CH_2Cl_2 1:19) to give *Py*-**L2**Pd as a yellow solid (0.051 g, 30% from pre-rotaxane, 21% from **7**). ^{1}H NMR (400 MHz, $CDCl_3$): δ 1.07-1.43 (m, 82H, $H_{a+n+o+p+q+r+s+ff+H+I+J+K}$), 1.47-1.72 (m, 10H, $H_{m+t+z+G}$), 2.14-2.23 (m, 2H, H_g), 2.57-3.00 (m, 12H, $H_{h+j+l+y}$), 3.29-3.43 (m, 4H, H_{u+C}), 3.52-3.59 (m, 2H, H_{aa}), 3.78-3.88 (m, 4H, H_F), 3.93-4.00 (m, 2H, H_f), 4.59 (d, *J* = 12.5, 2H, $H_{C'}$), 6.21-6.23 (m, 2H, H_{i+k}), 6.44-6.47 (m, 4H, H_D), 6.49-6.56 (m, 4H, H_E), 6.68-6.79 (m, 4H, H_{e+bb}), 6.92 (d, *J* = 7.6, 1H, H_x), 7.05-7.11 (m, 16H, $H_{c+d+cc+dd}$), 7.17-7.24 (m, 13H, H_{b+v+ee}), 7.79-7.82 (m, 1H, H_w), 7.84-7.87 (m, 2H, H_B), 8.05-8.09 (m, 1H, H_A). LRESI-MS (MeOH/TFA): *m/z* = 2075 $[M^{106}Pd]^+$.

3.9 Protonation of *DMAP*-L2HPd and *Py*-L2Pd and Rotaxane Shuttling Experiments

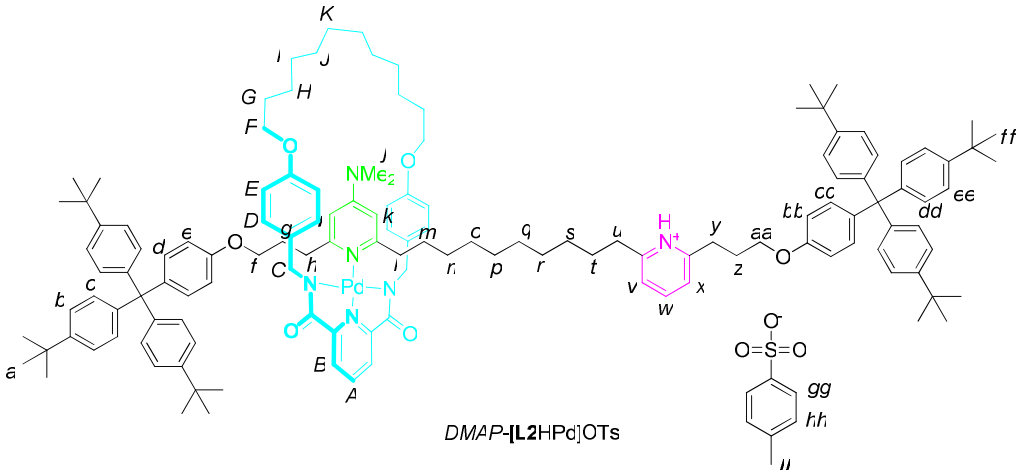

To a solution of *DMAP*-**L2**Pd (29.5 mg, 0.0142 mmol, 1.0 equiv.) in $CDCl_3$ (2 mL) was added TsOH (2.70 mg, 0.0142 mmol, 1.0 equiv.) and the reaction stirred at RT until all TsOH had dissolved (5 minutes). Analysis by ^{1}H NMR revealed quantitative formation of *DMAP*-[**L2**HPd]OTs had occurred. ^{1}H NMR (400 MHz, $CDCl_3$): δ 1.00-1.40 (m, 82H, $H_{a+n+o+p+q+r+s+ff+H+I+J+K}$), 1.59-1.77 (m, 10H, H $H_{g+m+t+G}$), 2.03 (br, 2H, H_h), 2.19-2.31 (m, 5H, H_{z+ii}), 2.69-3.42 (m, 14H, $H_{f+j+u+y+C}$), 3.56 (br, 2H, H_l), 3.79-3.94 (m, 6H, H_{aa+F}), 5.23 (br, 2H, $H_{C'}$), 5.82 (br, 1H, $H_{(i\ or\ k)}$), 6.39-6.71 (m, 13H, $H_{e+(i\ or\ k)+bb+D+E}$), 7.05-7.14 (m, 18H, $H_{c+d+cc+dd+hh}$), 7.21-7.24 (m, 12H, H_{b+ee}), 7.44 (br, 2H, H_{v+x}), 7.82-7.85 (m, 4H, H_{gg+B}), 8.02-8.14 (m, 2H, H_{w+A}).

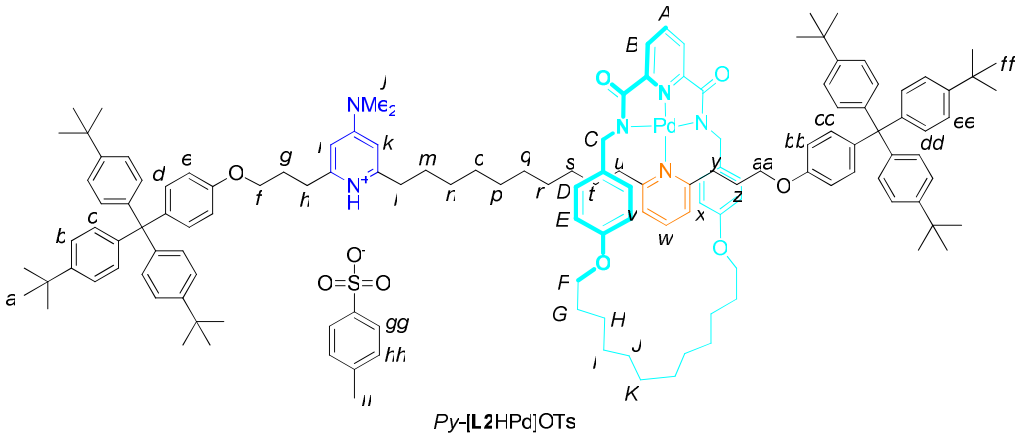

To a solution of *Py*-**L2**Pd (22.1 mg, 0.0106 mmol, 1.0 equiv.) in $CDCl_3$ (2 mL) was added TsOH (2.02 mg, 0.0106 mmol, 1.0 equiv.) and the reaction stirred at RT until all TsOH had dissolved (5 minutes). Analysis by ^{1}H NMR revealed quantitative formation of *Py*-[**L2**HPd]OTs had occurred. ^{1}H NMR (400 MHz, $CDCl_3$): δ 1.47-1.66 (m, 82H, $H_{a+n+o+p+q+r+s+ff+H+I+J+K}$), 1.58-1.81 (m, 10H, $H_{m+t+z+G}$), 2.16-2.32 (m, 5H, H_{g+ii}), 2.53-2.63 (m, 2H, H_y), 2.83-3.26 (m, 12H, $H_{h,j,l,C}$), 3.40-3.53 (m, 4H, H_{u+aa}), 3.79-3.90 (m, 6H, H_{f+F}), 4.74 (d, J = 13.9, 2H, $H_{C'}$), 6.28 (d, J = 7.6, 2H, H_{i+k}), 6.42-6.57 (m, 8H, H_{D+E}), 6.66-6.71 (m, 4H, H_{e+bb}), 6.88 (d, J = 7.3, 1H, H_x), 7.02-7.15 (m, 19H, $H_{c+d+v+cc+dd+hh}$), 7.18-7.26 (m, 12H, H_{b+ee}), 7.80-7.86 (m, 5H, H_{w+gg+B}), 8.06-8.10 (m, 1H, H_A), 14.00 (br, 1H, *DMAP*-H^+).

Representative shuttling experiments

DMAP-[**L2**HPd]OTs (32.2 mg, 0.0142 mmol) was dissolved in DMF-d_7 (1 g) and a control ^{1}H NMR spectrum acquired. The sample was then heated to 110 °C and monitored regularly by ^{1}H NMR. Analysis of the ^{1}H NMR showed that an equilibrium of 89:11 *Py*:*DMAP* -[**L2**HPd]OTs had been reached after 16 h, and this ratio remained unchanged upon further heating. (Similarly, heating *DMAP*-[**L2**HPd]OTs at 110 °C in $C_2D_2Cl_4$ for 36 h also gave the above ratio of isomers and subsequent heating did not alter the product distribution.) After removal of d_7-DMF under reduced pressure, the reaction mixture was redissolved in CH_2Cl_2 (10 mL) and stirred with a large excess of Na_2CO_3 (5 g) for 30 minutes. Filtration through celite followed by removal of the solvent under reduced pressure gave a yellow solid. ^{1}H

NMR (400 MHz, $CDCl_3$) analysis revealed that the crude residue was comprised of a mixture of *Py*:*DMAP*-**L2**Pd in an unchanged ratio of 89:11. These two compounds were separated by column chromatography on silica (MeOH:CH_2Cl_2 1:19) to give pure samples of both *Py*-**L2**Pd and *DMAP*-**L2**Pd as previously characterised. The *Py*-**L2**Pd thus obtained was subsequently heated to 110 °C in d_7-DMF (1 g) and monitored *via* ^{1}H NMR at regular intervals. A ratio of 86:14 *DMAP*:*Py*-**L2**Pd had been established after 1.5 h and further heating did not alter this ratio. Upon heating *Py*-**L2**Pd to 110 °C in $C_2D_2Cl_4$, no isomerisation was observed, even after 7 days heating at 110 °C.

3.10 Synthesis of Model Compounds and Representative Shuttling Experiments

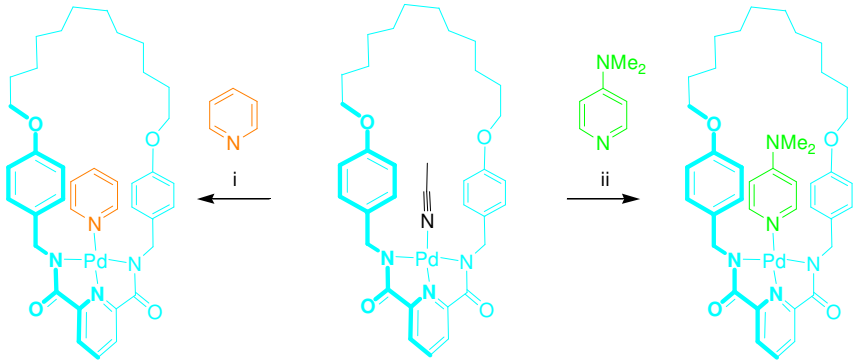

Scheme 3.11 (i) CH_2Cl_2, 1 h, RT, 90%; (ii) CH_2Cl_2, 1 h, RT, 95%.

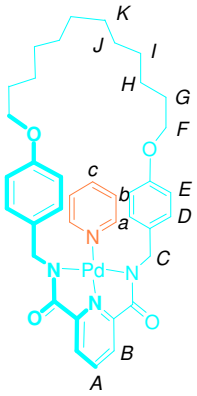

L1Pd(Py)

A solution of **L1**Pd(CH_3CN) (0.050 g, 0.070 mmol, 1.0 equiv.) and pyridine (7.1 mg, 0.090 mmol, 1.25 equiv.) was stirred in CH_2Cl_2 (5 mL) at RT for 1 h. After evaporation of the solvent the greenish-yellow solid was purified by column chromatography on silica (CH_2Cl_2 then CH_2Cl_2:acetone 3:2) yielding **L1**Pd(Py) as a yellow solid, m.p. 188 ˚C (dec.) (0.047 g, 90%). ^{1}H NMR (400 MHz, $CDCl_3$): δ 1.27-1.34 (m, 12H, H_{I+J+K}), 1.42-1.47 (m, 4H, H_H), 1.72-1.78 (m, 4H, H_G), 3.87 (t, J = 6.5, 4H, H_F), 4.13 (s, 4H, H_C), 6.59 (d, J = 8.8, 4H, H_E), 6.65 (d, J = 8.8, 4H, H_D), 7.08 (m, 2H, H_b), 7.72 (m, 1H, H_c), 7.82 (d, J = 7.8, 2H, H_B), 8.05 (t, J = 7.8, 1H, H_A), 8.09 (d, J = 5.0, 2H, H_a). ^{13}C NMR (100 MHz, $CDCl_3$): δ 25.5, 28.4, 28.5, 28.9, 28.9, 48.6, 67.6, 114.0, 124.7, 125.0, 128.0, 132.9, 138.1, 140.6, 151.7, 152.9, 157.6, 170.9. LR-FABMS (3-NOBA matrix): m/z = 727 [M^{106}Pd+H]$^+$.

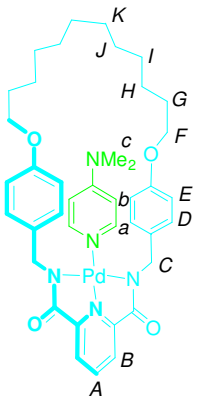

L1Pd(DMAP)

A solution of **L1**Pd(CH_3CN) (0.050 g, 0.070 mmol, 1.0 equiv.) and DMAP (9.8 mg, 0.080 mmol, 1.1 equiv.) was stirred in CH_2Cl_2 (5 mL) at RT for 1 h. After evaporation of the solvent the greenish-yellow solid was purified by column

chromatography on silica (CH_2Cl_2 then CH_2Cl_2:acetone 3:1) yielding **L1**Pd(DMAP) as a yellow solid, m.p. 180 °C (dec.) (0.051 g, 95%). ^{1}H NMR (400 MHz, d_7-DMF): δ 1.26-1.44 (m, 12H, H_{I+J+K}), 1.66-1.74 (m, 8H, H_{G+H}), 3.11 (s, 6H, H_c), 3.89-3.93 (m, 8H, H_{F+C}), 6.40 (br, 2H, H_b), 6.69 (d, J = 8.4, 4H, H_E), 6.79 (d, J = 8.5, 1H, H_a), 6.83 (d, J = 8.4, 4H, H_D), 7.03 (d, J = 8.5, 1H, $H_{a'}$), 7.79 (d, J = 7.8, 2H, H_B), 8.34 (t, J = 7.8, 1H, H_A). ^{13}C NMR (100 MHz, $CDCl_3$): δ 25.6, 28.4, 28.7, 29.0, 29.2, 38.8, 47.6, 67.3, 114.1, 124.4, 128.5, 130.5, 133.9, 141.7, 152.8, 153.1, 155.0, 157.9, 170.7. LR-FABMS (3-NOBA matrix): m/z = 770 $[M^{106}Pd+H]^+$.

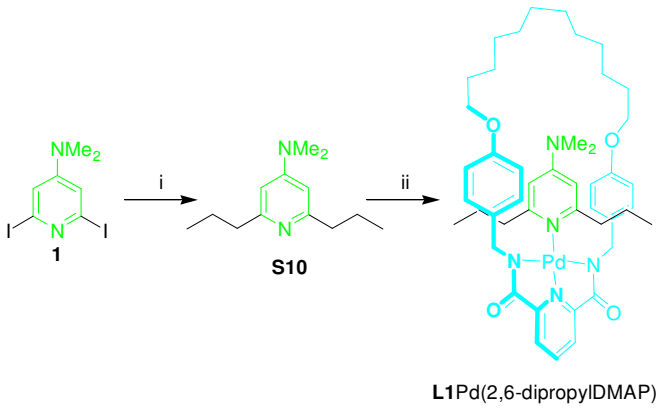

Scheme 3.12 (i) PrZnBr,[28] PEPPSI, NMP, THF, 5h, RT, 96%, (ii) **L1**Pd(CH_3CN), CH_2Cl_2, 16 h, RT, 92%.

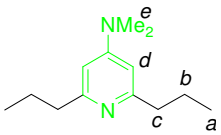

S10

According to Huo's protocol,[28] iodine (0.136 g, 0.540 mmol, 0.3 equiv.) was added to a suspension of *n*-propylbromide (0.976 mL, 10.7 mmol, 6.0 equiv.) and activated zinc dust (1.05 g, 16.1 mmol, 9.0 equiv.) in NMP (4 mL), and the suspension was heated for 4 h at 85 °C. The reaction mixture was transferred *via* cannula to a solution of LiBr (1.87 g, 21.5 mmol, 12 equiv.), PEPPSI (60.8 mg, 0.090 mmol, 0.05 equiv.) and 2,6-diiodo-DMAP **1** (0.669 g, 1.79 mmol, 1.0 equiv.) in NMP (4 mL) and THF (4 mL). After stirring for 5 h at RT the reaction was diluted with Et_2O (20 mL) and washed successively with an aqueous solution of Na_3EDTA (1 M, 20 mL), water (20 mL) and brine (20 mL). After drying ($MgSO_4$) the solvent was concentrated under reduced pressure and the residue purified by column

chromatography on silica (hexane:EtOAc 2:1 then hexane:EtOAc:Et_3N 65:30:5) to give **S10** as colourless oil (0.357 g, 96%). ^{1}H NMR (400 MHz, $CDCl_3$): δ 0.96 (t, *J* = 7.2, 6H, H_a), 1.70-1.72 (m, 4H, H_b), 2.61-2.65 (m, 4H, H_c), 3.00 (s, 6H, H_e), 6.22 (s, 2H, H_d). ^{13}C NMR (100 MHz, $CDCl_3$): δ 14.0, 23.6, 39.2, 41.1, 102.9, 155.3, 161.8. LR-FABMS (3-NOBA matrix): *m/z* = 207 $[M+H]^+$. HR-FABMS (3-NOBA matrix): *m/z* = 207.1859 (calc. for $C_{13}H_{23}N_2$, 207.1861 $[M+H]^+$).

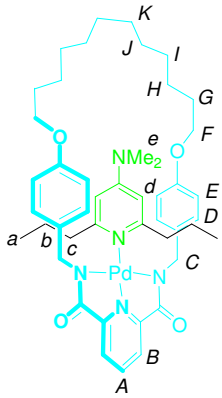

L1Pd(2,6-dipropylDMAP)

To a solution of **S10** (0.016 g, 0.080 mmol, 1.1 equiv.) in CH_2Cl_2 (8 mL) was added **L1**Pd(CH_3CN) (0.050 g, 0.070 mmol, 1.0 equiv.) and the solution was stirred at RT overnight. The solvent was then removed under reduced pressure to give the crude complex which was purified by column chromatography on silica (CH_2Cl_2 then CH_2Cl_2:acetone 3:1) to yield **L1**Pd(2,6-dipropylDMAP) as a yellow solid, m.p. 220 ˚C (dec.) (0.055 g, 92%). Crystals suitable for X-ray analysis were obtained by slow diffusion of Et_2O into a solution of the complex in CH_2Cl_2. ^{1}H NMR (400 MHz, DMF-d_7): δ 0.34 (br, 3H, H_a), 0.84 (br, 3H, $H_{a'}$), 1.10-1.30 (m, 16H, $H_{H+L+J+K}$), 1.40-1.49 (m, 4H, H_G), 1.65-1.72 (m, 4H, H_b), 1.72 (br, 2H, H_c), 2.13 (br, 2H, $H_{c'}$), 3.18 (s, 6H, H_e), 3.60 (br, 2H, H_C), 3.90 (t, *J* = 6.0, 4H, H_F), 5.13 (br, 2H, $H_{C'}$), 5.70 (br, 1H, H_d), 6.40 (br, 1H, $H_{d'}$), 6.63 (d, *J* = 9.2, 4H, H_E), 6.67 (d, *J* = 8.8, 4H, H_D), 7.82 (d, *J* = 7.7, 2H, H_B), 8.36 (t, *J* = 7.7, 1H, H_A). LR-FABMS (3-NOBA matrix): *m/z* = 854 $[M^{106}Pd+H]^+$. HR-FABMS (3-NOBA matrix): *m/z* = 854.3855 (calc. for $C_{46}H_{62}N_5O_4{}^{106}Pd$, 854.3837 $[M^{106}Pd+H]^+$).

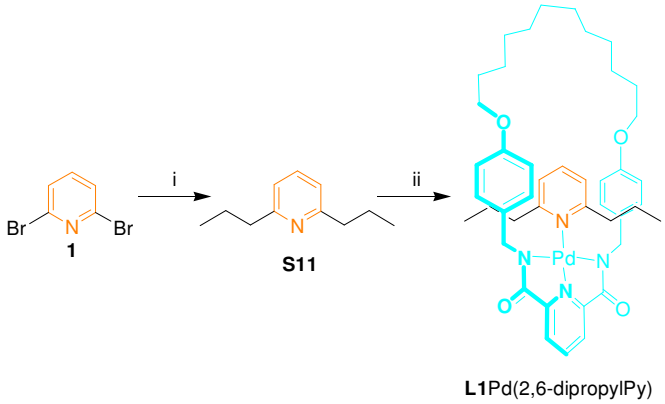

Scheme 3.13 (i) PrZnBr, $Pd(PPh_3)_4$, DMF, 20 h, RT, 43%, (ii) **L1**$Pd(CH_3CN)$, CH_2Cl_2, 16 h, RT, 90%.

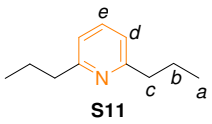

According to Huo's procedure,[28] iodine (0.596 g, 2.30 mmol, 0.1 equiv.) was added to a suspension of *n*-propylbromide (4.27 mL, 47.0 mmol, 2.5 equiv.) and activated zinc dust (4.60 g, 70.0 mmol, 3.0 equiv.) in DMF (24 mL), and the suspension was heated for 5 h at 85 ˚C. After the reaction cooled to RT, 2,6-dibromopyridine (4.40 g, 18.6 mmol, 1 equiv.) and $Pd(PPh_3)_4$ (0.600 g, 0.500 mmol, 0.03 equiv.) in DMF (7 mL) were added and the reaction mixture was stirred overnight at RT. The reaction was monitored by TLC (silica, hexane:EtOAc 1:1). Once complete, the reaction mixture was quenched with a 1:1 mixture of conc. aqueous NH_3 solution (200 mL) and an aqueous solution of Na_3EDTA (1 M, 200 mL) and extracted with EtOAc (2 x 200 mL). The organic layer was washed with water (400 mL) and brine (400 mL). Drying ($MgSO_4$) and removal of the solvent yielded a pale brown oil. Hexane was added to induce precipitation of unreacted starting material, which was removed by filtration, and the remaining oil was purified first by column chromatography on silica (hexane then hexane:EtOAc 1:1) and then by Kugelrohr (120 ˚C, approx. 100 mbar) to yield 2,6-di-*n*-propylpyridine **S11** as a colourless oil (1.30 g, 43%). ^{1}H NMR and ^{13}C NMR data were consistent with the published data.[29]

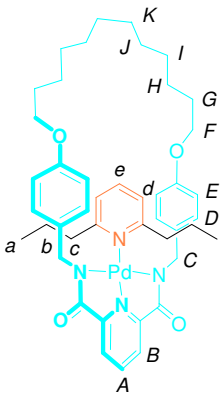

L1Pd(2,6-dipropylPy)

A solution of **L1**Pd(CH_3CN) (0.050 g, 0.070 mmol, 1.0 equiv.) and **S11** (0.017 g, 0.080 mmol, 1.1 equiv.) were stirred at RT overnight in CH_2Cl_2 (10 mL). The solvent was removed under reduced pressure and the crude greenish-yellow solid was purified by column chromatography on silica (CH_2Cl_2 then CH_2Cl_2:acetone 3:1) yielding **L1**Pd(2,6-dipropylPy) as a yellow solid, m.p. 225 ˚C (dec.) (0.051 g, 90%). Crystals suitable for X-ray analysis were obtained by slow diffusion of Et_2O into a solution of the complex in CH_2Cl_2. ^{1}H NMR (400 MHz, $CDCl_3$): δ 0.80 (t, J = 7.2, 6H, H_a), 1.25-1.47 (m, 20H, $H_{G+H+I+J+K}$), 1.69-1.75 (m, 4H, H_b), 2.82 (t, J = 8.0, 4H, H_c), 3.84 (t, J = 6.0, 4H, H_F), 3.96 (s, 4H, H_C), 6.49 (d, J = 8.8, 4H, H_E), 6.54 (d, J = 8.8, 4H, H_D), 7.03 (d, J = 7.6, 2H, H_d), 7.78 (t, J = 7.6, 1H, H_e), 7.88 (d, J = 7.8, 2H, H_B), 8.11 (t, J = 7.8, 1H, H_A). ^{13}C NMR (100 MHz, $CDCl_3$): δ 13.8, 20.9, 25.6, 28.4, 28.8, 29.0, 29.3, 40.6, 49.3, 67.1, 113.7, 120.9, 124.7, 128.4, 133.1, 138.7, 140.3, 152.9, 157.7, 163.9, 171.3. LR-FABMS (3-NOBA matrix): m/z = 811 [M^{106}Pd+H]$^+$. HR-FABMS (3-NOBA matrix): m/z = 811.3398 (calc. for $C_{44}H_{57}N_4O_4{}^{106}$Pd, 811.3415 [$M^{106}$Pd+H]$^+$).

Exchange Experiments

The exchange of unsubstituted Py and DMAP ligands.

L1Pd(DMAP) (0.013 g, 0.015 mmol, 1.0 equiv.) was dissolved in DMF-d_7 (0.75 mL), to which pyridinium *p*-toluenesulfonate (2.5 mg, 0.015 mmol, 1.0 equiv.) was added at RT and the ^{1}H NMR spectrum acquired immediately. The ^{1}H NMR spectrum

showed the presence of only protonated DMAP and **L1**Pd(Py) in a ratio of **L1**Pd(Py)**:L1**Pd(DMAP) >98:2 (limit measurable by ^{1}H NMR).

The DMF-d_7 solution of the complexes was filtered through a Pasteur pipette packed with cotton wool and Na_2CO_3 and the ^{1}H NMR spectrum of the elute acquired immediately. This ^{1}H NMR spectrum showed a product ratio of **L1**Pd(DMAP)**:L1**Pd(Py) of >98:2, which remained unchanged over time.

The exchange of 2,6-dipropylDMAP and 2,6-dipropylPy ligands.

L1Pd(2,6-dipropylDMAP) (0.013 g, 0.015 mmol, 1.0 equiv.) was dissolved in DMF-d_7 (0.75 mL), and **S11** (2.4 mg, 0.015 mmol, 1.0 equiv.) was added. The ^{1}H NMR spectrum was acquired as a control. After addition of *p*-toluensulfonic acid monohydrate (2.8 mg, 0.015 mmol, 1.0 equiv.) the subsequent ^{1}H NMR spectrum showed the presence of protonated **S11** and **L1**Pd(2,6-dipropylDMAP); no ligand exchange had occurred at RT. Heating the reaction for 130 minutes at 85 ˚C yielded **L1**Pd(2,6-dipropylPy):**L1**Pd(2,6-dipropylDMAP in a ratio of 90:10. Continued heating of the sample resulted in no further change in the ratio of isomers.

The above DMF-d_7 solution of complexes was filtered through a Pasteur pipette packed with cotton wool and Na_2CO_3, which gave an unaltered 90:10 ratio of **L1**Pd(2,6-dipropylPy):**L1**Pd(2,6-dipropylDMAP by ^{1}H NMR. The sample was then heated to 85 ˚C, and after 60 minutes a 86:14 ratio of **L1**Pd(2,6-dipropylDMAP):**L1**Pd(2,6-dipropylPy) was observed by ^{1}H NMR spectroscopy. No further change in the ratio of isomers was observed upon prolonged heating.

3.11 General crystal data and structure refinement for L1Pd(2,6-dipropylDMAP) and L1Pd(2,6-dipropylPy)

Structural data for both **L1**Pd(2,6-dipropylDMAP) and **L1**Pd(2,6-dipropylPy) were collected at 93 K using a Rigaku Mercury diffractometer (MM007 high-flux RA/MoKa radiation, confocal optic). All data collections employed narrow frames

(0.3–1.0) to obtain at least a full hemisphere of data. Intensities were corrected for Lorentz polarization and absorption effects (multiple equivalent reflections). The structures were solved by direct methods, non-hydrogen atoms were refined anisotropically with CH protons being refined in riding geometries (SHELXTL) against F^2.

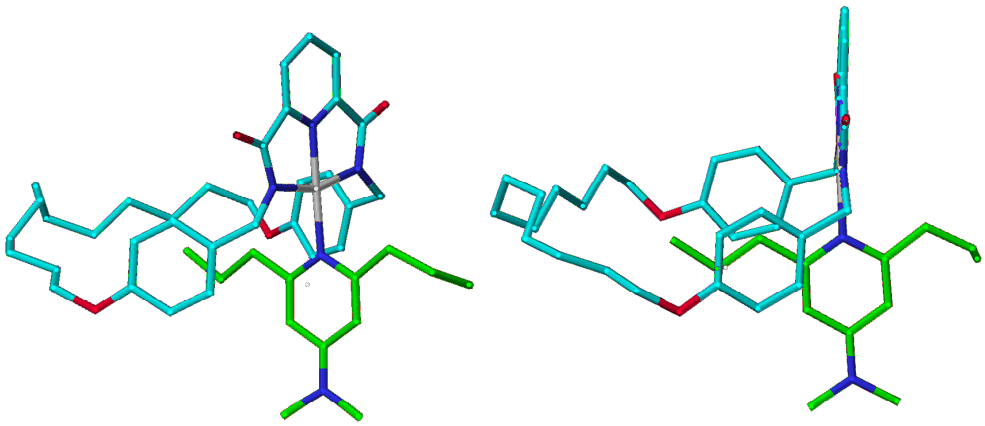

Figure 3.3 A staggered (left) and side (right) view of the X-ray crystal structure of **L1**Pd(2,6-dipropylDMAP)**.**

Table 3.1 Crystal data and structure refinement for **L1**Pd(2,6-dipropylDMAP)**.**

Identification code	**L1**Pd(2,6-dipropylDMAP)	
Empirical formula	$C_{46}H_{61}N_5O_4Pd$	
Formula weight	854.40	
Temperature	93(2) K	
Wavelength	0.71073 Å	
Crystal system	Monoclinic	
Space group	P2(1)/c	
Unit cell dimensions	a = 18.098(2) Å	a= 90°.
	b = 18.151(2) Å	b= 91.62(3)°.
	c = 12.7405(14) Å	g = 90°.
Volume	4183.6(8) $Å^3$	
Z	4	
Density (calculated)	1.357 Mg/m^3	
Absorption coefficient	0.493 mm^{-1}	
F(000)	1800	
Crystal size	0.0800 x 0.0800 x 0.0800 mm^3	
Theta range for data collection	1.59 to 25.36°.	
Index ranges	-21<=h<=18, -21<=k<=19, -15<=l<=14	
Reflections collected	27337	
Independent reflections	7572 [R(int) = 0.0510]	
Completeness to theta = 25.00°	99.1 %	

Absorption correction	Multiscan
Max. and min. transmission	1.0000 and 0.6966
Refinement method	Full-matrix least-squares on F^2
Data / restraints / parameters	7572 / 0 / 506
Goodness-of-fit on F^2	1.125
Final R indices [I>2sigma(I)]	R1 = 0.0512, wR2 = 0.1178
R indices (all data)	R1 = 0.0642, wR2 = 0.1268
Largest diff. peak and hole	1.273 and -1.090 e.Å^{-3}

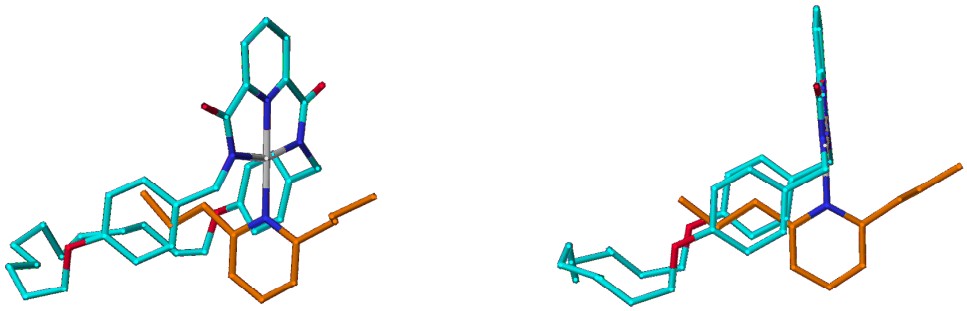

Figure 3.4 A staggered (left) and side (right) view of the x-ray crystal structure of **L1**Pd(2,6-dipropylPy).

Table 3.2 Crystal data and structure refinement for **L1**Pd(2,6-dipropylPy).

Identification code	**L1**Pd(2,6-dipropylPy)
Empirical formula	$C_{44}H_{56}N_4O_4Pd$
Formula weight	811.33
Temperature	93(2) K
Wavelength	0.71073 Å
Crystal system	Monoclinic
Space group	P2(1)/c
Unit cell dimensions	
a = 14.437(6) Å	a= 90°.
b = 18.314(6) Å	b= 12.170(9)°.
c = 16.522(6) Å	g = 90°.
Volume	4045(3) Å^3
Z	4
Density (calculated)	1.332 Mg/m^3
Absorption coefficient	0.505 mm^{-1}
F(000)	1704
Crystal size	0.0500 x 0.0300 x 0.0300 mm^3
Theta range for data collection	1.52 to 25.36°.
Index ranges	-11<=h<=17, -22<=k<=22, -19<=l<=19
Reflections collected	26021
Independent reflections	7361 [R(int) = 0.2872]
Completeness to theta = 25.00°	99.5 %
Absorption correction	Multiscan

Max. and min. transmission	1.0000 and 0.7249
Refinement method	Full-matrix least-squares on F^2
Data / restraints / parameters	7361 / 34 / 479
Goodness-of-fit on F^2	0.953
Final R indices [I>2sigma(I)]	R1 = 0.0937, wR2 = 0.1565
R indices (all data)	R1 = 0.2561, wR2 = 0.1982
Largest diff. peak and hole	1.263 and -0.812 e.$Å^{-3}$

3.12 References and Notes

(1) For macrocycle translocation in Cu(I)/Cu(II)-coordinated rotaxanes, see: (a) Gaviña, P.; Sauvage, J.-P. *Tetrahedron Lett.* **1997**, *38*, 3521-3524. (b) Armaroli, N.; Balzani, V.; Collin, J.-P.; Gaviña, P.; Sauvage, J.-P.; Ventura, B. *J. Am. Chem. Soc.* **1999**, *121*, 4397-4408. (c) Durola, F.; Sauvage, J.-P. *Angew. Chem., Int. Ed.* **2007**, *46*, 3537-3540. For macrocycle translocation in Cu(I)/Cu(II)-coordinated catenanes, see: (d) Livoreil, A.; Dietrich-Buchecker, C. O.; Sauvage, J.-P. *J. Am. Chem. Soc.* **1994**, *116*, 9399-9400. (e) Cárdenas, D. J.; Livoreil, A.; Sauvage, J.-P. *J. Am. Chem. Soc.* **1996**, *118*, 11980-11981. (f) Livoreil, A.; Sauvage, J.-P.; Armaroli, N.; Balzani, V.; Flamigni, L.; Ventura, B. *J. Am. Chem. Soc.* **1997**, *119*, 12114-12124. For macrocycle rotation in Cu(I)/Cu(II)-coordinated rotaxanes, see: (g) Raehm, L.; Kern, J.-M.; Sauvage, J.-P. *Chem. Eur. J.* **1999**, *5*, 3310-3317. (h) Weber, N.; Hamann, C.; Kern, J.-M.; Sauvage, J.-P. *Inorg. Chem.* **2003**, *42*, 6780-6792. (i) Poleschak, I.; Kern, J.-M.; Sauvage, J.-P. *Chem. Commun.* **2004**, 474-476. (j) Létinois-Halbes, U.; Hanss, D.; Beierle, J. M.; Collin, J.-P.; Sauvage, J.-P. *Org. Lett.* **2005**, *7*, 5753-5756. For a recent review of transition metal complexed molecular machines, see: (k) Bonnet, S.; Collin, J.-P.; Koizumi, M.; Mobian, P.; Sauvage, J.-P. *Adv. Mater.* **2006**, *18*, 1239-1250.

(2) ` For contraction/stretching in a rotaxane dimer through Cu(I)-Zn(II) exchange, see: (a) Jiménez, M. C.; Dietrich-Buchecker, C.; Sauvage, J.-P. *Angew. Chem., Int. Ed.* **2000**, *39*, 3284-3287. (b) Jiménez-Molero, M. C.; Dietrich-Buchecker, C.; Sauvage, J.-P. *Chem. Eur. J.* **2002**, *8*, 1456-1466.

(3) (a) Bissell, R. A.; Córdova, E.; Kaifer, A. E.; Stoddart, J. F. *Nature* **1994**, *369*, 133-136. For other examples of pH-responsive molecular shuttles see: (b) Martínez-Díaz, M.-V.; Spencer, N.; Stoddart, J. F. *Angew. Chem., Int. Ed. Engl.* **1997**, *36*, 1904-1907. (c) Ashton, P. R.; Ballardini, R.; Balzani, V.; Baxter, I.; Credi, A.; Fyfe, M. C. T.; Gandolfi, M. T.; Gómez-López, M.; Martínez-Díaz, M.-V.; Piersanti, A.; Spencer, N.; Stoddart, J. F.; Venturi, M.; White, A. J. P.; Williams, D. J. *J. Am. Chem. Soc.* **1998**, *120*, 11932-11942. (d) Elizarov, A. M.; Chiu, S.-H.; Stoddart, J. F. *J. Org. Chem.* **2002**, *67*, 9175-9181. (e) Badjić, J. D.; Balzani, V.; Credi, A.; Silvi, S.; Stoddart, J. F. *Science* **2004**, *303*, 1845-1849. (f) Keaveney, C. M.; Leigh, D. A. *Angew. Chem., Int. Ed.* **2004**, *43*, 1222-1224. (g) Garaudée, S.; Silvi, S.; Venturi, M.; Credi, A.; Flood, A. H.; Stoddart, J. F. *ChemPhysChem.* **2005**, *6*, 2145-2152.

(h) Badjić, J. D.; Ronconi, C. M.; Stoddart, J. F.; Balzani, V.; Silvi, S.; Credi, A. *J. Am. Chem. Soc*. **2006**, *128*, 1489-1499. (i) Tokunaga, Y.; Nakamura, T.; Yoshioka, M.; Shimomura, Y. *Tetrahedron Lett.* **2006**, *47*, 5901-5904. (j) Leigh, D. A.; Thomson, A. R. *Org. Lett*. **2006**, *8*, 5377-5379.

(4) For ruthenium-coordinated catenanes and rotaxanes which undergo photoinduced decomplexation of the components, see: (a) Mobian, P.; Kern, J.-M.; Sauvage, J.-P. *Angew. Chem., Int. Ed.* **2004**, *43*, 2392-2395. (b) Collin, J.-P.; Jouvenot, D.; Koizumi, M.; Sauvage, J.-P. *Eur. J. Inorg. Chem.* **2005**, 1850-1855. For other types of rotaxanes and catenanes which feature intercomponent metal-ligand coordination, see: (c) Hutin, M.; Schalley, C. A.; Bernardinelli, G.; Nitschke, J. R. *Chem. Eur. J.* **2006**, *12*, 4069-4076. (d) Blight, B. A.; Wisner, J. A.; Jennings, M. C. *Chem. Commun*. **2006**, 4593-4595. (e) Blight, B. A.; Wisner, J. A.; Jennings, M. C. *Angew. Chem., Int. Ed*. **2007**, *46*, 2835-2838.

(5) For examples of rotaxanes and catenanes which utilise transition metal ions to switch on/off other types of intercomponent interaction, see: (a) Korybut-Daszkiewicz, B.; Więckowska, A.; Bilewicz, R.; Domagaã, S.; Woźniak, K. *Angew. Chem., Int. Ed.* **2004**, *43*, 1668-1672. (b) Jiang, L.; Okano, J.; Orita, A.; Otera, J. *Angew. Chem., Int. Ed.* **2004**, *43*, 2121-2124. (c) Leigh, D. A.; Lusby, P. J.; Slawin, A. M. Z.; Walker, D. B. *Angew. Chem., Int. Ed.* **2005**, *44*, 4557-4564. (d) Leigh, D. A.; Lusby, P. J.; Slawin, A. M. Z.; Walker, D. B. *Chem. Commun.* **2005**, 4919-4921. (e) Marlin, D. S.; González Cabrera, D.; Leigh, D. A.; Slawin, A. M. Z. *Angew. Chem., Int. Ed.* **2006**, *45*, 77-83. (f) Marlin, D. S.; González Cabrera, D.; Leigh, D. A.; Slawin, A. M. Z. *Angew. Chem., Int. Ed.* **2006**, *45*, 1385-1390.

(6) Chatterjee, M. N.; Kay, E. R.; Leigh, D. A. *J. Am. Chem. Soc.* **2006**, *128*, 4058-4073.

(7) (a) Kay, E. R.; Leigh, D. A. *Nature* **2006**, *440*, 286-287. (b) Kay, E. R.; Leigh, D. A.; Zerbetto, F. *Angew. Chem., Int. Ed*. **2007**, *46*, 72-191.

(8) (a) Tseng, H.-R.; Wu, D.; Fang, N. X.; Zhang, X.; Stoddart, J. F. *ChemPhysChem* **2004**, *5*, 111-116. (b) Steuerman, D. W.; Tseng, H.-R.; Peters, A. J.; Flood, A. H.; Jeppesen, J. O.; Nielsen, K. A.; Stoddart, J. F.; Health, J. R. *Angew. Chem., Int. Ed.* **2004**, *43*, 6486-6491. (c) Flood, A. H.; Peters, A. J.; Vignon, S. A.; Steuerman, D. W.; Tseng, H.-R.; Kang, S.; Heath, J. R.; Stoddart, J. F. *Chem. Eur. J*. **2004**, *10*, 6558-6564. (d) Flood, A. H.; Stoddart, J. F.; Steuerman, D. W.; Heath, J. R. *Science* **2004**, *306*, 2055-2056. (e) Choi, J. W.; Flood, A. H.; Steuerman, D. W.; Nygaard, S.; Braunschweig, A. B.; Moonen, N. N. P.; Laursen, B. W.; Luo, Y.; Delonno, E.; Peters, A. J.; Jeppesen, J. O.; Xu, K.; Stoddart, J. F.; Heath, J. R. *Chem. Eur. J*. **2006**, *12*, 261-279.

(9) (a) Fuller, A.-M.; Leigh, D. A.; Lusby, P. J.; Oswald, I. D. H.; Parsons, S.; Walker, D. B. *Angew. Chem., Int. Ed.* **2004**, *43*, 3914-3918. (b) Furusho, Y.;

Matsuyama, T.; Takata, T.; Moriuchi, T.; Hirao, T. *Tetrahedron Lett.* **2004**, *45*, 9593-9597. (c) Fuller, A.-M. L.; Leigh, D. A.; Lusby, P. J.; Slawin, A. M. Z.; Walker, D. B. *J. Am. Chem. Soc*. **2005**, *127*, 12612-12619. (d) Fuller, A.-M. L.; Leigh, D. A.; Lusby, P. J. *Angew. Chem., Int. Ed.* **2007**, *46*, 5015-5019.

(10) Exchange of the unsubstituted heterocycles in $CDCl_3$, $C_2D_2Cl_4$, or DMF-d_7 was complete within the time frame of mixing the **L1**PdPy complex with DMAP and acquiring a ^{1}H NMR spectrum, as was the reverse proton-driven exchange upon adding TsOH. However, the 2,6-dipropyl substituted heterocycles did not exchange in $CDCl_3$ even over extended periods (seven days) or upon heating at reflux. In d_7-DMF at 358 K equilibrium was reached after 60 minutes (neutral conditions) or 130 minutes (in the presence of TsOH). For full details of the exchange experiments, see the Section 3.10.

(11) For the exchange of various 4-substituted pyridine ligands at the fourth coordination site of Pd-pincer complexes, see: (a) van Manen, H.-J.; Nakashima, K.; Shinkai, S.; Kooijman, H.; Spek, A. L.; van Veggel, F. C. J. M.; Reinhoudt, D. N. *Eur. J. Inorg. Chem*. **2000**, 2533-2540. The exchange of DMAP for poly(4-vinylpyridine) at the fourth coordination site of bimetallic Pd- and Pt-pincer complexes has been exploited in the chemoresponsive viscosity switching of a metallo-supramolecular network; see: (b) Loveless, D. M.; Jeon, S. L.; Craig, S. L. *J. Mater. Chem.* **2007**, *17*, 56-61.

(12) A proton-driven ligand exchange of diethylamine and lutidine coordinated to Pd(II) has previously been reported; see: (a) Hamann, C.; Kern, J.-M.; Sauvage, J.-P. *Dalton Trans.* **2003**, 3770-3775. For the proton-driven exchange of one amine for another within copper-coordinated imine ligands, see: (b) Nitschke, J. R. *Angew. Chem., Int. Ed*. **2004**, *43*, 3073-3075. (c) Nitschke, J. R.; Schultz, D.; Bernardinelli, G.; Gérard, D. *J. Am. Chem. Soc*. **2004**, *126*, 16538-16543. (d) Schultz, D.; Nitschke, J. R. *Proc. Natl. Acad. Sci. U.S.A*. **2005**, *102*, 11191-11195. (e) Nitschke, J. R. *Acc. Chem. Res*. **2007**, *40*, 103-112.

(13) (a) Sanderson, R. T. *Chemical Bonds & Bond Energy*; Academic Press: New York, 1976. (b) Cotton, F. A.; Wilkinson, G.; Murillo, C.; Bochmann, M.; Grimes, R.; Murillo, C. A.; Bochmann M. *Advanced Inorganic Chemistry: A Comprehensive Text*, 6th ed.; John Wiley & Sons: New York, 1999. A contributing reason as to why the proton discriminates DMAP and pyridine better than the Pd-macrocycle complex may be because the proton is charged while the Pd-macrocycle is not. However, since this is not the situation in reference 12a, where proton-driven ligand exchange at Pd(II) also occurs, it is presumably not a major factor in the present system either.

(14) Amabilino, D. B.; Stoddart, J. F. *Chem. Rev*. **1995**, *95*, 2725-2828.

(15) Wayman, K. A.; Sammakia, T. *Org. Lett.* **2003**, *5*, 4105-4108.

(16) Sonogashira, K.; Tohda, Y.; Hagihara, N. *Tetrahedron Lett.* **1975**, *16*, 4467-4470.

(17) The italicised prefixes *DMAP*- and *Py*- denote the position of the macrocycle on the thread in the rotaxane.

(18) Mitsunobu, O.; Yamada, Y. *Bull. Chem. Soc. Jpn.* **1967**, *40*, 2380-2382.

(19) Gibson, H. W.; Lee, S. H.; Engen, P. T.; Lecavalier, P.; Sze, J.; Shen, Y. X.; Bheda, M. *J. Org. Chem.* **1993**, *58*, 3748-3756.

(20) The modest yield of rotaxane in the stoppering step is probably a consequence of using a triphenylphosphine-mediated reaction with a Pd-complexed pseudo-rotaxane. Alternative methodologies are currently being investigated.

(21) Similar effects have been observed upon increasing the steric bulk about the coordination sphere in other Pd and Pt complexes. For examples, see: (a) Atwood, J. D. *Inorganic and Organometallic Reaction Mechanisms*, 2nd ed.; Wiley-VCH: New York, 1997. (b) Yount, W. C.; Loveless, D. M.; Craig, S. L. *J. Am. Chem. Soc*. **2005**, *127*, 14488-14496.

(22) Selva, M.; Tundo, P.; Perosa, A.; Dall'Acqua, F. *J. Org. Chem.* **2005**, *70*, 2771-2777.

(23) Kantchev, E. A. B.; O'Brien, C. J.; Organ, M. G. *Aldrichimica Acta* **2006**, *39*, 97-111.

(24) Kantchev, E. A. B.; O'Brien, C. J.; Organ, M. G. *Angew. Chem. Int. Ed.* **2007**, *46*, 2768-2813.

(25) O'Brien, C. J.; Kantchev, E. A. B.; Valente, C.; Hadei, N.; Chass, G. A.; Lough, A.; Hopkinson, A. C.; Organ, M. G. *Chem. Eur. J.* **2006**, *12*, 4743-4748.

(26) Organ, M. G.; Abdel-Hadi, M.; Avola, S.; Hadei, N.; Nasielski, J.; O'Brien, C. J.; Valente, C. *Chem. Eur. J.* **2006**, *13*, 150-157.

(27) Organ, M. G.; Avola, S.; Dubovyk, I.; Hadei, N.; Kantchev, E. A. B.; O'Brien, C. J.; Valente, C. *Chem. Eur. J.* **2007**, *12*, 4749-4755.

(28) Huo, S. *Org. Lett.* **2003**, *5*, 423-425.

(29) Xi, Z.; Sato, K.; Gao, Y.; Lu, J.; Takahashi, T. *J. Am. Chem. Soc.* **2003**, *125*, 9568-9569.

CHAPTER FOUR

A First Generation Molecular Walker

Acknowledgements and Declaration

Dr. Christiane Petzold undertook the synthesis of Compounds **31**-**41**. The remaining synthesis detailed in this Chapter represents a joint and equal effort by Dr. James Crowley and the Author.

Synopsis

The Introduction laid down the basic requirements for the directional procession of a walker along a track. Central amongst these were the requirements that the standing foot acts as a ratchet whilst the stepping foot is labile and that both feet are capable of switching between standing and stepping modes in response to orthogonal stimuli. It was then shown that two chemically different feet, where the labilisation of each foot was independently controlled would be one way in which to achieve this alternating standing/stepping regime for each foot.

In the previous Chapter, a dynamic system based on ligand exchange at a Pd(II) centre was discussed. In this system, the labilising stimulus for the monodentate ligand is the presence of coordinating solvent/anion and elevated temperatures, whilst the fixing stimulus is simply to allow the system to cool to room temperature. The system can be biased in favour of one monodentate ligand in the thread over the other (when in the labile state) by the addition or removal of protons. However, regardless of the protonation state of the thread, translocation of the macrocycle is only observed when the labilising stimulus is applied. Hence it was reasoned that a walker foot based on a similar Pd(II) motif would display the required switchable kinetic stability required for a processive "hand-over-hand" walker. For the other foot, an orthogonal switching mechanism to protonation/deprotonation was sought, and redox-driven exchange at a Cu(I)/Cu(II) centre was chosen, based on the pioneering work of Jean-Pierre Sauvage. This Chapter outlines the design and synthesis of a walker/track system based on these two switching mechanisms.

4.1 Introduction

The Pd(II)-based molecular shuttle detailed in Chapter Three displays remarkable kinetic stability when at room temperature or at elevated temperatures in non-coordinating solvents.[1] Model studies with the non-interlocked system shown in Scheme 4.1 indicated that the Pd(II)-monodentate ligand bond was only labile in coordinating solvent (d_7-DMF) at 85 ˚C, suggesting that in DMF temperature could be used as a labilising/fixing stimulus for such complexes. Furthermore, it was found that it was possible to bias the thermodynamic equilibrium from strongly in favour of **L1**Pd(2,6-dipropylDMAP) under neutral conditions to strongly in favour of **L1**Pd(2,6-dipropylPy) in the presence of one equivalent of *p*-toluenesulfonic acid (TsOH).

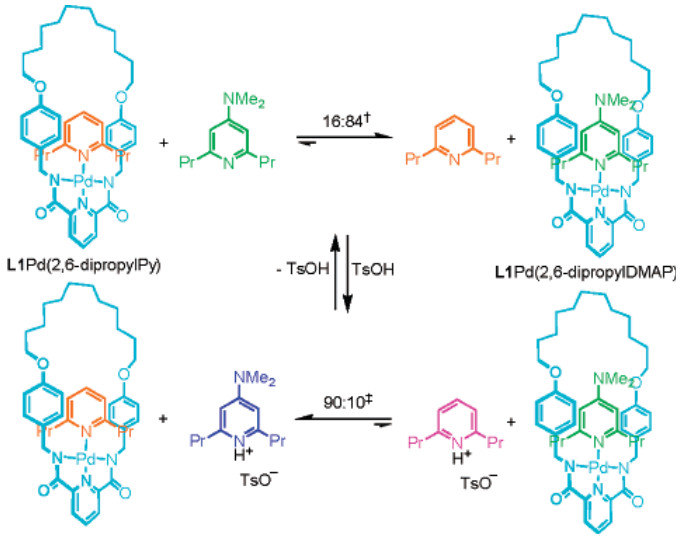

Scheme 4.1 The switchable kinetics and thermodynamics of the Pd(II)-based tridentate pyridine 2,6-dicarboxamide binding motif described in Chapter Three. Conditions: † 60 min at 358 K; ‡ 130 min at 358 K in d_7-DMF. Reproduced with permission from The Journal of the American Chemical Society, Copyright 2007, American Chemical Society.[1]

The switchable kinetics and thermodynamics displayed by this system seemed well-suited to the requirements for a processive, hand-over-hand walking molecule on an *ABCDABCD* track (see Sections 1.5.1-1.5.4), and it was reasoned that this system could operate as one foot/binding site combination (Figure 4.1).

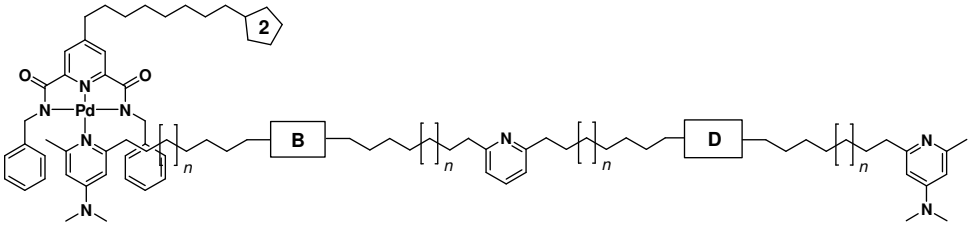

Figure 4.1 The Pd(II) chemistry from Chapter Three could be used as part of an *ABCDABCD* walking system.

The compartmentalised approach to *ABCDABCD* walkers outlined in Chapter One calls for two orthogonally addressable switching mechanisms. Hence a second switch (corresponding to the states **2B** and **2D** in Figure 4.1) that could be operated independently of the palladium-based chemistry of Chapter Three was sought. Among the most prominent examples of stimuli-switchable molecular machines in the literature are the Cu(I)/Cu(II) redox-responsive catenanes[2-4] and rotaxanes[5-12] developed by Jean-Pierre Sauvage and co-workers. These systems exploit the different preferred coordination geometries of copper when in its first (preferring tetrahedral environments) and second oxidation states (preferring pentavalent or hexavalent coordination environments). The archetypal molecular shuttle of this sort is shown in Scheme 4.2.[5,7]

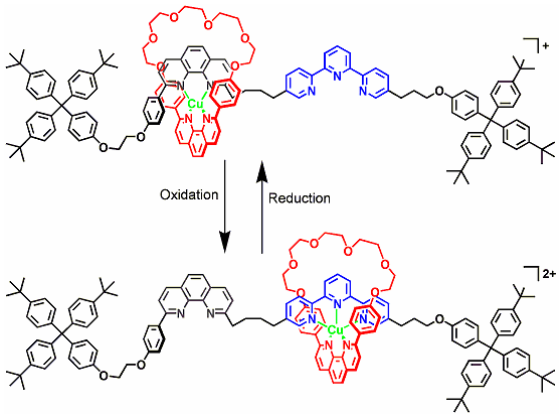

Scheme 4.2 Jean-Pierre Sauvage's Cu(I)/Cu(II) redox-switchable molecular shuttle. Anions have been omitted for clarity.

Shuttling of the macrocycle between the binding sites of the thread was achieved through both electrochemical and photochemical methods. Under the photochemical regime, light excitation at 464 nm in the presence of a suitable electron acceptor (*para*-nitrobenzylbromide in this case) caused oxidation of Cu(I) to Cu(II), with subsequent shuttling of the macrocycle from the phenanthroline station of the thread

to the terpyridine station, in accordance with the change in the metal's preferred coordination number from four to five. Adding excess ascorbic acid to the rotaxane solution then gave reduction of Cu(II) back to Cu(I), and concomitant shuttling of the macrocycle to the phenanthroline station restored the original rotaxane co-conformer. Electrochemical switching was achieved by passing one Faraday per mole of rotaxane through a solution of the molecular shuttle in degassed acetonitrile at +1.0 V (*vs*. SCE). This gave oxidation of Cu(I) to Cu(II), and shuttling of the macrocycle from the phenanthroline site to terpyridine site then took place over the course of several hours. A second electrolysis at –0.3 V then reduced Cu(II) to Cu(I), with shuttling of the macrocycle back to the phenanthroline station, to regenerate the original rotaxane solution. The highly reversible nature of this redox-driven exchange, along with the comparatively high kinetic stability of these and similar copper complexes[13] implied that this system would be ideal as the second foot/foothold switch.

4.2 The Design of a First Generation Synthetic Molecular Walker

Combining the Pd(II) and Cu(I)/Cu(II) systems described in Section 4.1 gives the generic structure outlined in Figure 4.2, with walking from the left hand end of the track to the right (as drawn) occurring in response to an appropriate order of stimuli.

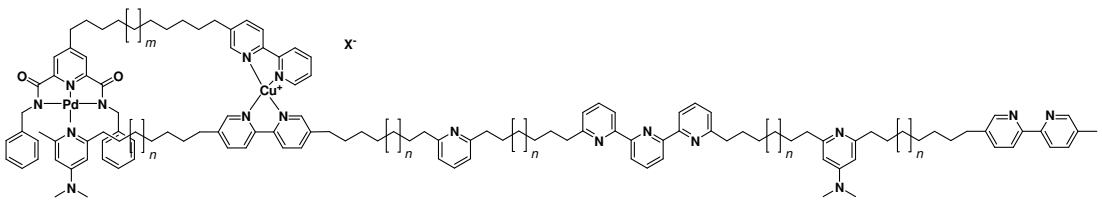

Figure 4.2 The proposed generic structure of the walking system. X = PF_6 or some other non-coordinating anion.

Scheme 4.3 shows the proposed operation of the system, leading to processive directional motion. In the first instance, the ensemble was to be synthesised so that the walker was initially bound on the first set of DMAP and bipyridine stations of the six station track, yielding complex **A**. The point of this strategy was to ensure that all the walkers started from the same end of the track – in a system where the track is

only long enough for the walker to perform one complete cycle and there are two energetically identical sets of binding sites at either end, it is essential that the walkers all start from the same end of the track so that one complete cycle of directed motion can be demonstrated unambiguously. Treatment of this initial complex with two equivalents of TsOH, followed by heating in coordinating solvent would then result in protonation of both DMAP stations of the thread, with concomitant coordination of the tridentate Pd(II)-containing foot to the available pyridine station giving **B**. During this process, the walker unit would still be attached to the track *via* the copper-bound foot. Oxidation of copper(I) to copper(II) would then cause this "copper foot" to form a complex with the now more thermodynamically favoured terpyridine station, while the palladium-containing foot maintained structural integrity between the walker and the track, giving **C**. Removal of the protons from the DMAP pyridinium species and heating in coordinating solvent would then generate the third stepping movement, but unlike the first two steps the palladium-containing foot would now have a choice of two DMAP sites with which to bind – the more remote starting position or the closer internal DMAP station. Provided that the distances between the stations on the track and the length of the walker linker are complementary, then the lower energy state at thermodynamic equilibrium (when the linking stimulus of heat is in operation) is the structure in which the palladium-containing foot associates with the internal (nearest) DMAP station.[14] Removal of this linking stimulus would then lead predominantly to state **D**, giving self-ratcheted directional motion. Finally, the reduction of Cu(II) back to Cu(I) would result in the formation of a tetrahedral copper complex between the walker and the neighbouring terminal bipyridine site, forming **E**. Overall the motion of the walker in response to these stimuli would be unidirectional from left-to-right along the track in Scheme 4.3, with the walker proceeding through a full cycle (i.e. back to a state isoenergetic with its starting state) in the process.

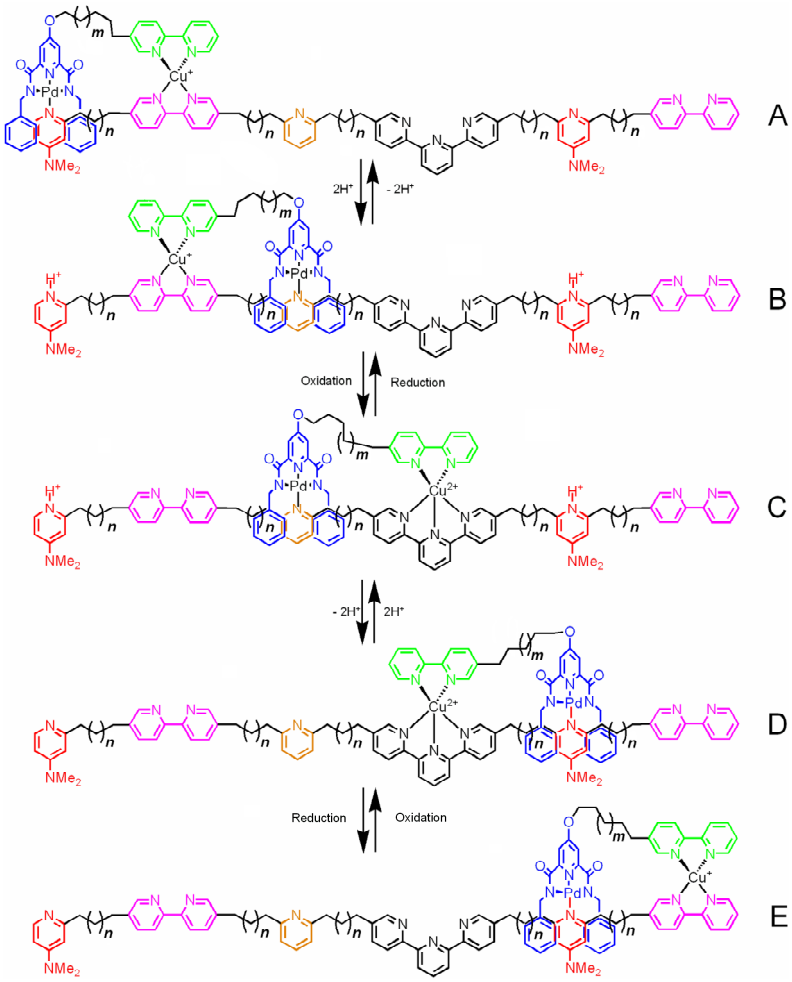

Scheme 4.3 The proposed operation of the walker. Counterions have been omitted for clarity.

It was hoped to be able to follow the progress of the walker along the track by monitoring the characteristic changes in various ^{1}H NMR shifts. However, when paramagnetic Cu(II) was present, ^{1}H NMR would probably not yield much useful information in this regard, and in those cases it was hoped to infer the position of the walker through UV-Visible analysis and/or cyclic voltammtery. Such studies would allow the position of the walker on the track to be ascertained, but they would not give any information on the processivity of the walk. In order to probe the processivity, it was proposed to synthesise two different versions of the track-walker ensemble. In one version, the track would have a 4-*tert*-butylphenol substituent at one end and the walker would similarly be labelled with two *tert*-butyl groups. In the other version, the track would have only a 4-methylphenol substituent and the walker would be unlabelled. These two walker systems should operate identically, as CPK

modelling suggested that the additional bulk of the *tert*-butyl groups would not affect the coordination of any of the track/walker metal complexes. Hence, if the two systems were then to be combined and the mixture subjected to the sequence of stimuli outlined in Scheme 4.3, ESI-MS of the reaction mixtures obtained at each step should allow the masses of all the species present to be seen and should highlight any scrambling between the two types of walker and the two types of track (which would indicate a lack of processivity).

4.3 Retrosynthesis

The proposed retrosynthesis of the walker units is shown in Scheme 4.4. The two mass-labelled tridentate binding sites were to be synthesised from chelidamic acid and appropriate commercial benzylamine derivatives. The bidentate metal binding site was to be prepared *via* a Sonogashira coupling[15] between 5-hexyn-1-ol and 6-bromo-2,2'-bipyridinyl.[16] The alcohol of this unit would then be converted to the tosylate and coupled to one of the tridentate units *via* a Williamson ether coupling to give the two metal-free walker ligands. Subsequently, it was hoped to insert the palladium into the tridentate binding sites before coordinating the walkers to the appropriate first two stations of the track. The Cu(I) complex between the bipyridines of the walker and the track would then be made once the Pd(II)-containing foot had been coordinated to the track in this fashion (Scheme 4.5).

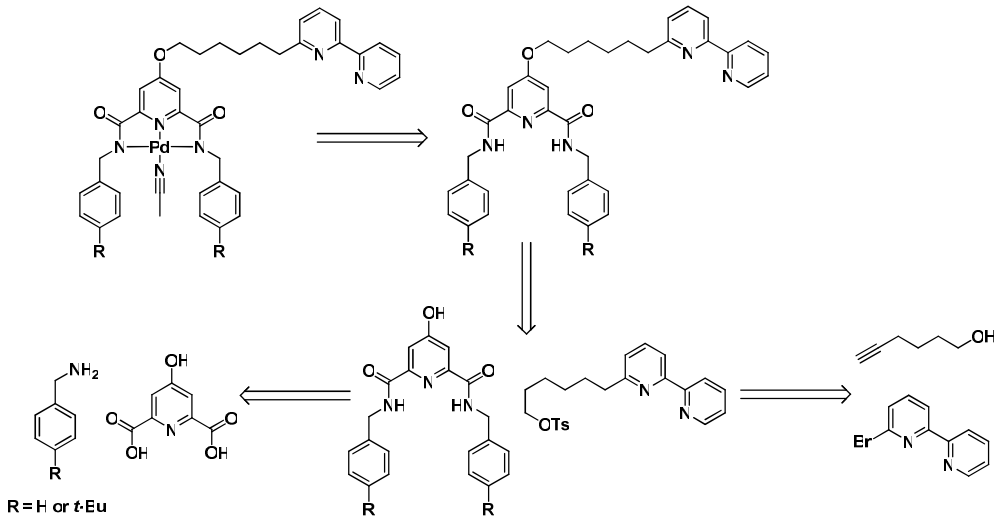

Scheme 4.4 Retrosynthesis of the proposed walker units.

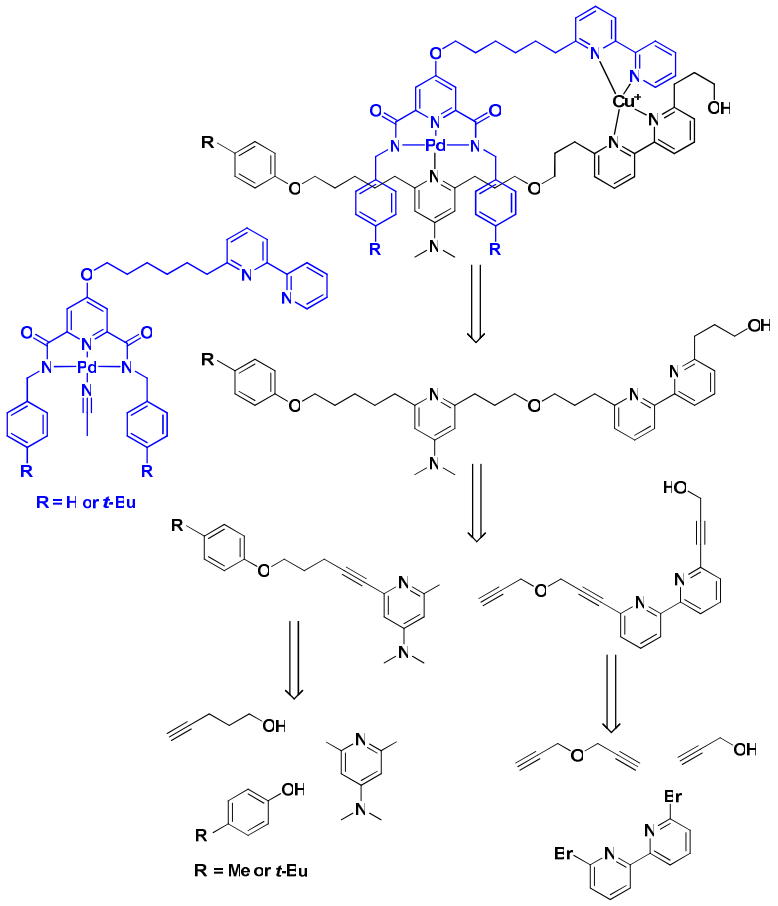

Scheme 4.5 Retrosynthesis of the walker on the first two stations of the track. Strategic choices such as the nature of the spacers on the track and the substitution patterns on the polypyridyl ligands will be discussed in Section 4.4. Counterions have been omitted and the walker unit coloured for clarity.

The retrosynthesis of the walker on the first two stations of the track is shown in Scheme 4.5. The proposed strategy was repeated Sonogashira couplings between the relevant bromo- or iodo-(poly)pyridyls and various commercial acetylenes. To this end, it was proposed to synthesise an unsymmetrical bipyridyl moiety (by sequential reactions with propargyl alcohol and then propargyl ether) bearing a terminal alkyne, to which the mass-labelled first station of the track could be attached, again *via* a Sonogashira coupling. After hydrogenation of the acetylenes, it was proposed to coordinate the walker to the DMAP-derived station through its Pd(II)-containing foot, before then adding Cu(I) to give the mono cationic complex, ready for attachment to the rest of the track.

Scheme 4.6 shows the retrosynthesis of the proposed final two-station block of the track. This was to be prepared in an analogous fashion to the first two stations of the

track, initially by reacting 6-bromo-2,2'-bipyridinyl with propargyl ether under Sonogashira coupling conditions. The terminal acetylene thus produced would then be coupled with 2,6-diiodoDMAP[1] to give the mono-substituted DMAP-derivative, for connection to the middle two stations of the track *via* another Sonogashira coupling.

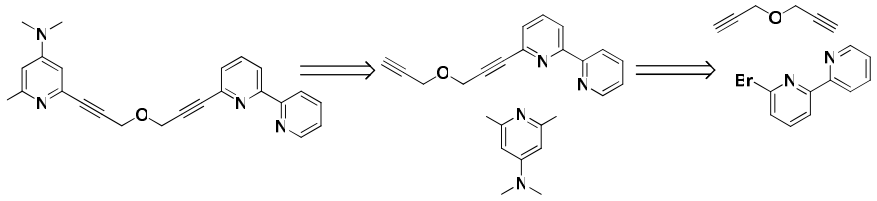

Scheme 4.6 Retrosynthesis of the final two stations of the track.

The retrosynthesis of the proposed middle two stations of the track is shown in Scheme 4.7. It was proposed to synthesise the terpyridyl station of the track *via* Sonogashira coupling of 6,6''-dibromo-2,2':6',2''-terpyridine[17] and propargyl ether, to give a di-substituted moiety which would then be desymmetrised by a further Sonogashira coupling with the pyridine-derived station. This pyridine-derived station was be to prepared from 2-bromo-6-(hydroxymethyl)-pyridine[18] and phthalimide.

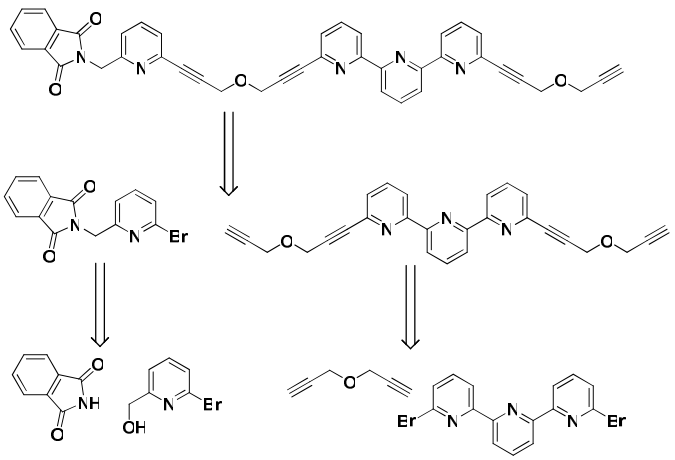

Scheme 4.7 Retrosynthesis of the middle two stations of the track.

Sonogashira coupling of the middle two-station block with the final two-station block would then provide (after hydrogenation of the acetylenes and removal of the phthalimide protecting group) the completed four-station unit for attachment to the walker/first two station unit shown in Scheme 4.5. It was proposed to perform the

final coupling reaction by converting the amine of the four station block to the isocyanate, which would then be reacted with the free alcohol of the walker/first two station units to give the completed walker/track ensembles connected by a urethane linkage as shown in Scheme 4.8.

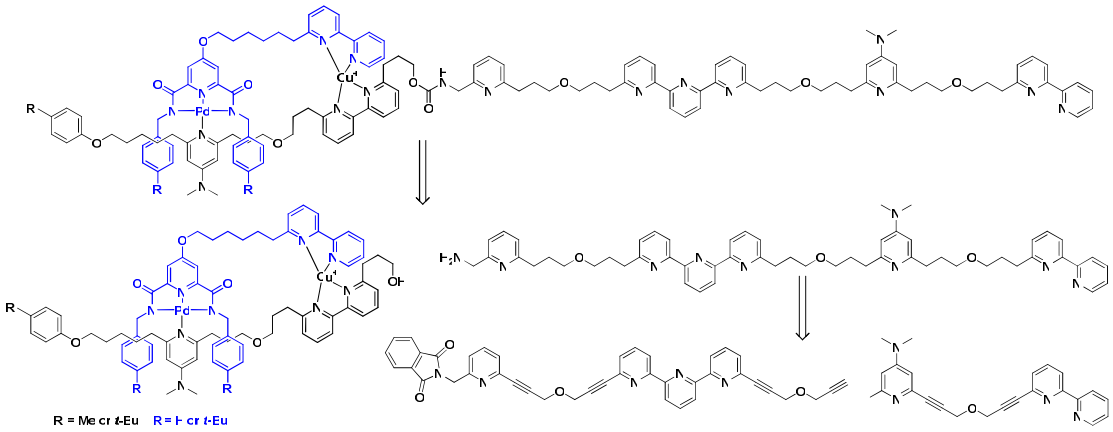

Scheme 4.8 Retrosynthesis of the completed walker/track ensemble. Counterions have been omitted and the walker coloured for clarity.

4.4 Synthesis

The synthesis of the proposed walker unit shown in Scheme 4.4 is outlined in Scheme 4.9. For the copper-binding foot, 6-bromo-2,2'-bipyridinyl (**1**) was synthesised *via* a literature procedure[16] and derivatised with 5-hexyn-1-ol under Sonogashira coupling conditions to give alcohol **2** in good yield. Subsequent hydrogenation over Pd/C followed by activation of primary alcohol **3** with *para*-toluenesulfonyl chloride generated bipyridine **4**. The two mass-labelled palladium-binding feet were synthesised using pentaflourophenol (PFP) promoted amide couplings[19] of chelidamic acid monohydrate with either benzylamine (furnishing ligand **5a**) or 4-(*t*-butyl)benzylamine (giving ligand **5b**). Ligand **5a** was then connected to bipyridine **4** by a Williamson phenol ether synthesis to give the free (unmetallated) walker unit **6**.

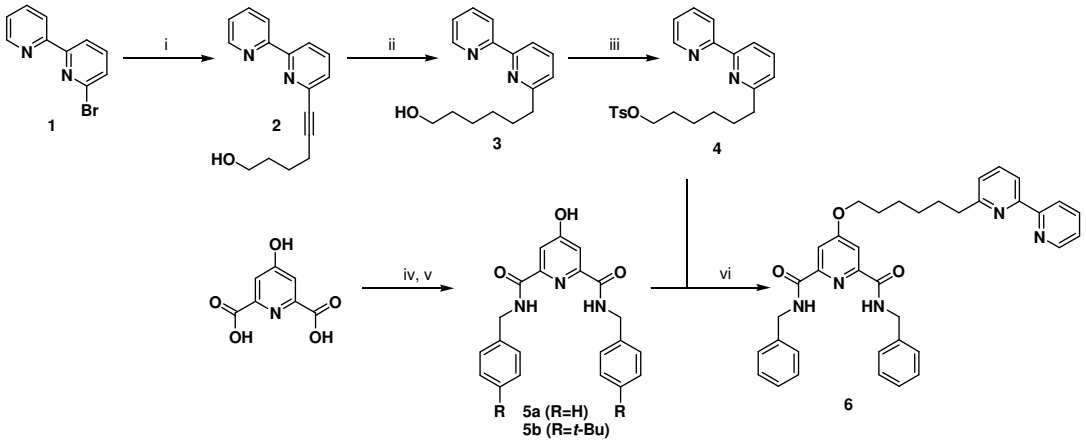

Scheme 4.9 The synthesis of free walker unit **6**. Reagents and conditions: (i) 5-hexyn-1-ol, $Pd(dppf)Cl_2$, CuI, THF/Et_3N, 16 h, RT, 88%, (ii) Pd/C, H_2, THF, 12 h, RT, 81%, (iii) *p*-TsCl, Et_3N, CH_2Cl_2, 18 h, RT, 75%, (iv) (a) EDCI, PFP, CH_2Cl_2, 20 h, RT, 90%, (iv) (b) EDCI, PFP, CH_2Cl_2, 20 h, RT, 90%, (v) (a) benzylamine, Et_3N, CH_2Cl_2, 2 h, RT, 75%, (v) (b) 4-(*t*-butyl)benzylamine, Et_3N, CH_2Cl_2, 2 h, RT, 88%, (vi) K_2CO_3, butanone, 24 h, reflux, 56%.

It was then proposed to insert Pd(II) into the tridentate pyridine 2,6-dicarboxamide binding site by refluxing ligand **6** with $Pd(OAc)_2$ in acetonitrile, as had proved efficacious for inserting palladium into similar tridentate ligands in the past.[20,21] However, none of the desired product (i.e. with Pd(II) bound in the tridentate binding site) could be isolated, either under these conditions or the more aggressive approach of treating ligand **6** with three equivalents of NaH in DMF and then refluxing overnight in the presence of $PdCl_2(CH_3CN)_2$.[22] The model studies outlined in Scheme 4.10 give the reason for this. The simple pyridine 2,6-dicarboxamide ligand **7**[23] was treated with one equivalent of $Pd(OAc)_2$ in acetonitrile in the presence of one equivalent of 2,2'-bipyridine. When the reaction was monitored by ^1H NMR, no change was observed in the signals corresponding to ligand **7** but there were significant changes in the signals attributed to 2,2'-bipyridine, indicating that Pd(II) was coordinated to the bidentate ligand in a manner which is known from the literature.[24] The spectrum remained unchanged after heating at reflux for 12 hours, indicating that the Pd(II) complex with 2,2'-bipyridine is remarkably stable, and that there was little prospect of introducing Pd(II) selectively into the tridentate site.[25]

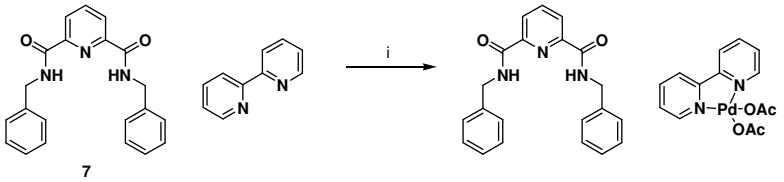

Scheme 4.10 Pd(II) shows a strong preference for 2,2'-bipyridine over the tridentate binding site. Reagents and conditions: (i) $Pd(OAc)_2$, CH_3CN, 12 h, reflux.

In an attempt to "block" the bipyridine on the walker unit, such that addition of Pd(II) would give palladation of the tridentate site, ligand **6** was stirred in acetonitrile at room temperature with half an equivalent of $[Cu(CH_3CN)_4](PF_6)$, giving the deep red complex **8** in quantitative yield (Scheme 4.11). However, all subsequent efforts to insert palladium into the tridentate site resulted in displacement of Cu(I) from the bipyridines (as evinced by the rapid loss of the deep red colour from solutions of complex **8** when treated with various Pd(II) salts) and gave very complicated mixtures of products as identified by ^{1}H NMR and ESI-MS.

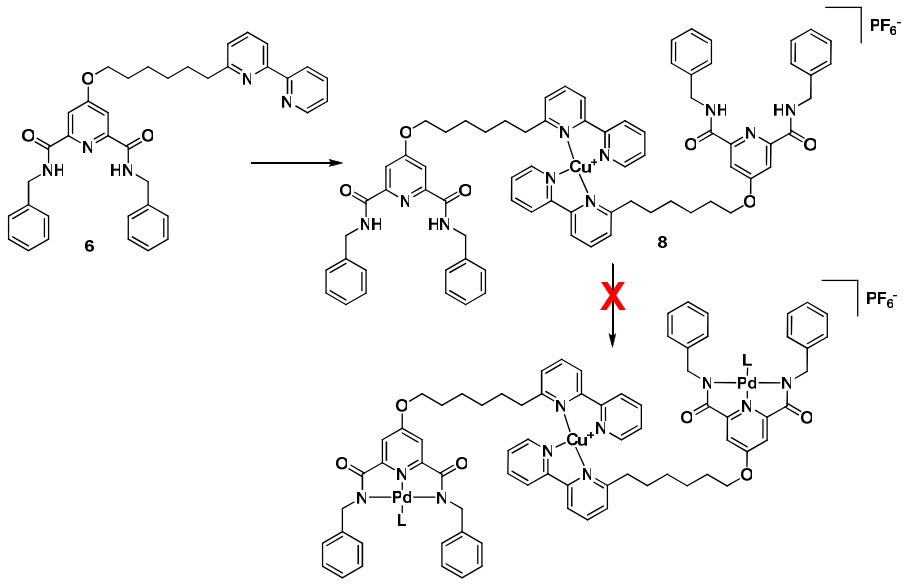

Scheme 4.11 Addition of Cu(I) to ligand **6** in an attempt to prevent the Pd(II) binding to the bipyridine of the walker. Reagents and conditions: (i) $[Cu(CH_3CN)_4](PF_6)$, CH_3CN, 0.5 h, RT, 99%, (ii) $Pd(OAc)_2$, CH_3CN, 12 h, RT *or* $Pd(OAc)_2$, CH_3CN, 12 h, reflux *or* $PdCl_2(CH_3CN)_2$, NaH, DMF, 12 h, RT *or* $PdCl_2(CH_3CN)_2$, NaH, DMF, 12 h, reflux. L = CH_3CN.

Failure to introduce the palladium into the tridentate site under any conditions when 2,2'-bipyridine was present implied that a synthetic route where Pd(II) was inserted into the pyridine 2,6-dicarboxamide motif before the bidentate binding site was added to the molecule would be expedient. However, attempts to metallate ligand **5a** gave no palladium-containing products, possibly as a result of tautomerisation of the

ligand to the less reactive keto-form. Hence it was decided to alkylate the phenolic oxygen of ligands **5a** and **5b** before inserting Pd(II) (Scheme 4.12). This was achieved by Williamson ether couplings of ligands **5a** and **5b** with commercially available ethyl 7-bromoheptanoate, followed by hydrolysis of the crude reaction mixtures with lithium hydroxide to furnish acids **9a** and **9b** in 92% and 65% yield respectively over two steps. It was envisaged that the carboxylic acid functionality thus introduced would be amenable to a range of coupling reactions with which to attach the bipyridine foot to the walker. This coupling reaction would have to be mild enough to prevent demetallation of the palladium-containing foot and also not involve any reagents that might coordinate irreversibly to the Pd(II) centre. In light of this, it was decided to convert acids **9a** and **9b** to the activated esters **10a** and **10b** *via* EDCI-mediated conjunctions with N-hydroxysuccinimide. Metallation of these ligands was then performed by stirring esters **10a** and **10b** at room temperature overnight with $Pd(OAc)_2$ in acetonitrile to give complexes **11a** and **11b** respectively. Complex **11a** was then protected as the Pd(II)-DMAP adduct **12** and subsequent addition of 5-(aminomethyl)-2,2'-bipyridine[26] in CH_2Cl_2 at room temperature gave the model palladium-containing walker unit **13** in good yield.[27]

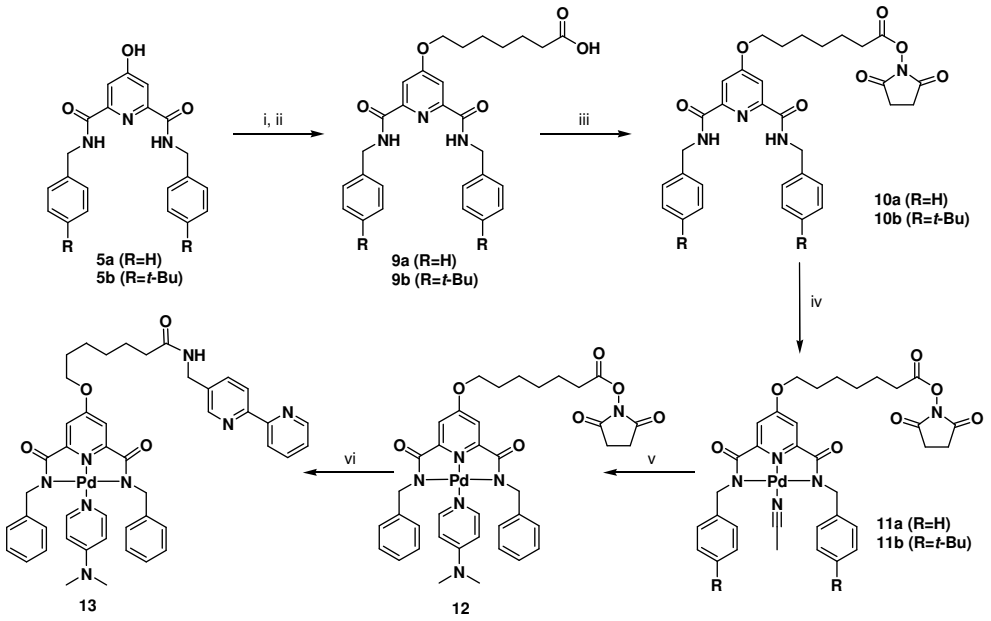

Scheme 4.12 Synthesis of model walker unit **13**. Reagents and conditions: (i) (a) ethyl 7-bromoheptanoate, K_2CO_3, butanone, 20 h, reflux, (i) (b) ethyl 7-bromoheptanoate, K_2CO_3, butanone, 20 h, reflux, (ii) (a) LiOH, THF/H_2O, 36 h, RT, 92% (over two steps), (ii) (b) LiOH, THF/H_2O, 36 h, RT, 65% (over two steps), (iii) (a) N-hydroxysuccinimide, EDCI, DMAP, CH_2Cl_2, 20 h, RT, 92%, (iii) (b) N-hydroxysuccinimide, EDCI, DMAP, CH_2Cl_2, 20 h, RT, 63%, (iv) (a) $Pd(OAc)_2$, CH_3CN, 20 h, RT, 83%, (iv) (b) $Pd(OAc)_2$, CH_3CN, 20 h, RT, 81%, (v) DMAP, CH_2Cl_2, 15 mins, RT, 75%, (vi) 5-(aminomethyl)-2,2'-bipyridine, CH_2Cl_2, 16 h, RT, 64%.

With a general strategy for the synthesis of the walker unit now in place, synthetic efforts were directed towards the track. Following on from the successful synthesis of the Pd(II)-containing molecular shuttle reported in Chapter Three,[1] it was decided to construct the track *via* repeated Sonogashira couplings between a terminal acetylene-bearing spacer precursor and the relevant *ortho*-bromo or iodo (poly)pyridines. The spacer precursor chosen was propargyl ether, due to its commercial availability. Once incorporated into the track, hydrogenation of the acetylenes from this spacer would leave $-(CH_2)_3-O-(CH_2)_3-$ units, which would give a spacing of seven atoms between each station. This distance was found by CPK modelling to be complementary to a range of walker linker lengths from 6-10 atoms, allowing significant synthetic freedom should further alterations to the walker be necessary. Furthermore, the central oxygen atom of this spacer would act to simplify ^{1}H NMR spectra of the hydrogenated track and track/walker ensembles.

The substitution pattern of the track stations was chosen to be *ortho* to the pyridyl nitrogen(s) both for synthetic ease and in order to mimic the favourable kinetics around the metal centre seen with the Pd(II)-containing shuttle from Chapter Three. It was decided to synthesise the track in three blocks of two stations, two of which would be joined to give a four station unit while the third block would be coordinated to the walker unit before attachment to the rest of the track (see Schemes 4.5-4.8). For this final coupling step, a mild, high yielding and robust reaction was sought, and it was decided that the reaction of an isocyanate and an alcohol to form a urethane would meet these requirements. Scheme 4.13 summarises the synthesis of the first two stations of the track, incorporating the alcohol for this proposed urethane formation.

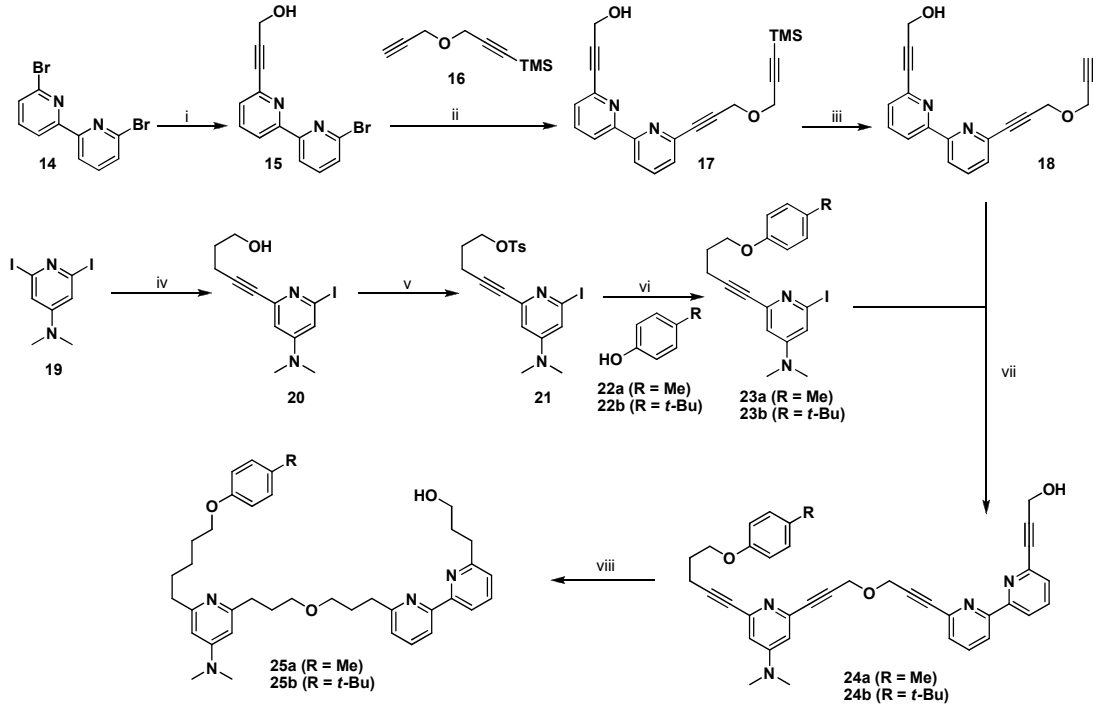

Scheme 4.13 Synthesis of the first two stations of the track. Reagents and conditions: (i) propargyl alcohol, $Pd(dppf)Cl_2$, CuI, toluene/Et_3N, 36 h, reflux, 40%, (ii) $Pd(dppf)Cl_2$, CuI, toluene/Et_3N, 20 mins (microwave), 100 ºC, 82%, (iii) K_2CO_3, MeOH/THF, 0 °C, 1 h, 98%, (iv) 4-Pentyn-1-ol, $Pd(PPh_3)_2Cl_2$, CuI, THF/Et_3N, 20 h, RT, 80%, (v) *p*-TsCl, Et_3N, CH_2Cl_2, 18 h, RT, 84%, (vi) (a) K_2CO_3, butanone, 20 h, reflux, 56%, (vi) (b) K_2CO_3, butanone, 24 h, reflux, 80%, (vii) (a) $Pd(dppf)Cl_2$, CuI, toluene/Et_3N, 20 mins (microwave), 100 ºC, 74%, (vii) (b) $Pd(dppf)Cl_2$, CuI, toluene/Et_3N, 40 mins (microwave), 100 ºC, 60%, (viii) (a) $Pd(OH)_2/C$, H_2, THF, 5 h, RT, 97%, (b) $Pd(OH)_2/C$, H_2, THF, 5 h, RT, 99%.

The bidentate binding site of this two-station block was prepared by desymmetrising 6,6'-dibromo-2,2'-bipyridine (**14**)[28] with propargyl alcohol under Sonogashira coupling conditions to give the monosubstituted bipyridine derivative **15**. A second (microwave-promoted) Sonogashira coupling with excess trimethyl-(3-prop-2-ynyloxy-prop-1-ynyl)-silane (**16**)[29] then gave bipyridine **17**, which was deprotected cleanly to give the terminal acetylene-bearing bipyridine **18** in good yield. The first monodentate station of the track was then prepared from 2,6-diiodoDMAP (**19**). A high-yielding desymmetrisation with 4-pentyn-1-ol, followed by activation of the alcohol with *para*-toluenesulfonyl chloride furnished tosylate **21**, upon which Williamson ether syntheses were carried out with either commercially available 4-methylphenol (**22a**) or 4-*tert*-butylphenol (**22b**) to give DMAP stations **23a** and **23b** respectively. Microwave-assisted Sonogashira coupling of bipyridine **18** with either DMAP stations **23a** or **23b** then gave the rigid two-station blocks **24a** and **24b** respectively, both of which were then hydrogenated over $Pd(OH)_2/C$ to give track

blocks **25a** and **25b** in excellent yield, ready for complexation to the appropriate walker units.[30]

The synthesis of the final two-station block of the track is shown in Scheme 4.14. 2-Bromo-6-iodopyridine (**26**)[31,32] was reacted under Sonogashira coupling conditions with the mono-protected propargyl ether derivative **16** to give pyridine **27** in excellent yield. Subsequent Negishi coupling[33] of pyridine **27** with commercially available 2-pyridylzinc bromide (**28**) produced bipyridyl **29**, which was subjected to *in situ* deprotection with DBU/water followed by Sonogashira coupling with 2,6-diiodoDMAP (**19**) to furnish the two-station block **30** in good yield.

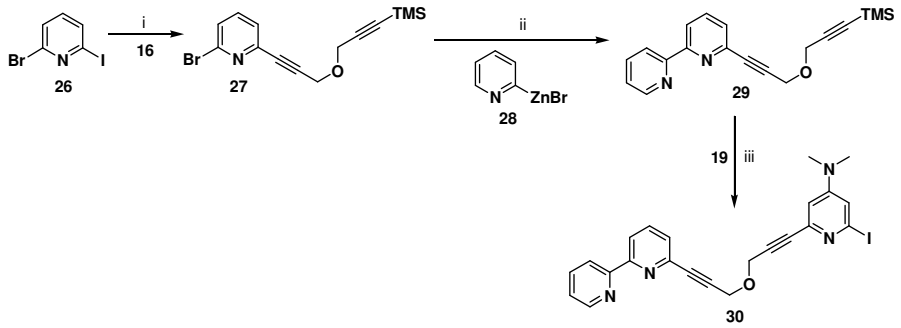

Scheme 4.14 Synthesis of the final two stations of the track. Reagents and conditions: (i) $Pd(PPh_3)_2Cl_2$, CuI, THF/Et_3N, 16 h, RT, 90%, (ii) $Pd(PPh_3)_4$, THF, 20 h, reflux, 65%, (iii) $Pd(PPh_3)_2Cl_2$, CuI, DBU, water, benzene, 36 h, RT, 65%.

The central two station block was synthesised as shown in Scheme 4.15. 6,6''-Dibromo-2,2':6',2''-terpyridine (**31**) was coupled to mono-protected propargyl ether **16** under Sonogashira conditions to give terpyridine **32**, which was mono-deprotected by stirring with one equivalent of potassium carbonate at 0 ˚C in a methanol/tetrahydrofuran solvent system, yielding terpyridine **33** in 45% yield. Another 45% of unreacted **32** could be recovered from the reaction mixture and recycled.

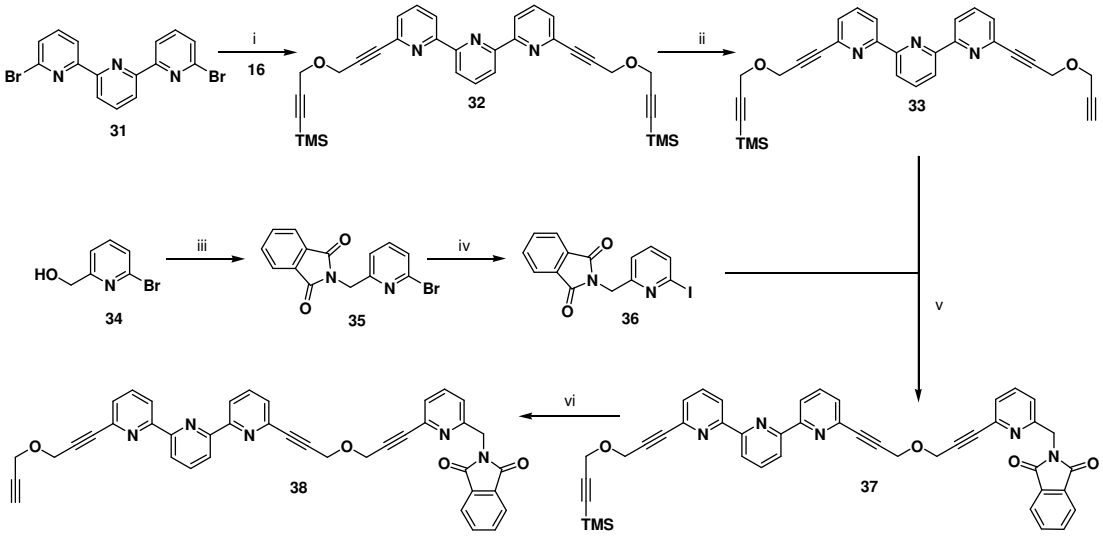

Scheme 4.15 Synthesis of the middle two stations of the track. Reagents and conditions: (i) $Pd(dppf)Cl_2$, CuI, toluene/Et_3N, 6 h, reflux, 93%, (ii) K_2CO_3, MeOH/THF, 30 mins, 0 ˚C, 45%, (iii) phthalimide, PPh_3, DIAD, THF, 16 h, 0 ºC → RT, 85%, (iv) DMEDA, CuI, NaI, dioxane, 105 ˚C, 48 h, 90%, (v) $Pd(PPh_3)_4$, CuI, THF/Et_3N, 5 days, 35 ˚C, 85%, (vi) K_2CO_3, MeOH/THF, 3 h, 0 ˚C, 95%.

Meanwhile, 2-bromo-6-(hydroxymethyl)-pyridine (**34**) was coupled to phthalimide in a Mitsunobu reaction[34] to give the protected amine **35**. Attempts to couple **35** with terpyridine **33** under Sonogashira conditions gave only trace amounts of the desired product **37**, and so it was decided to convert **35** to the more reactive iodo compound (**36**) *via* an aromatic Finkelstein reaction[35] prior to reaction with terpyridine **33**. This furnished two-station block **37** in excellent yield after prolonged stirring with mild heating. A final deprotection with potassium carbonate in methanol/tetrahydrofuran gave two-station block **38**, ready for coupling to block **30**, as outlined in Scheme 4.16.

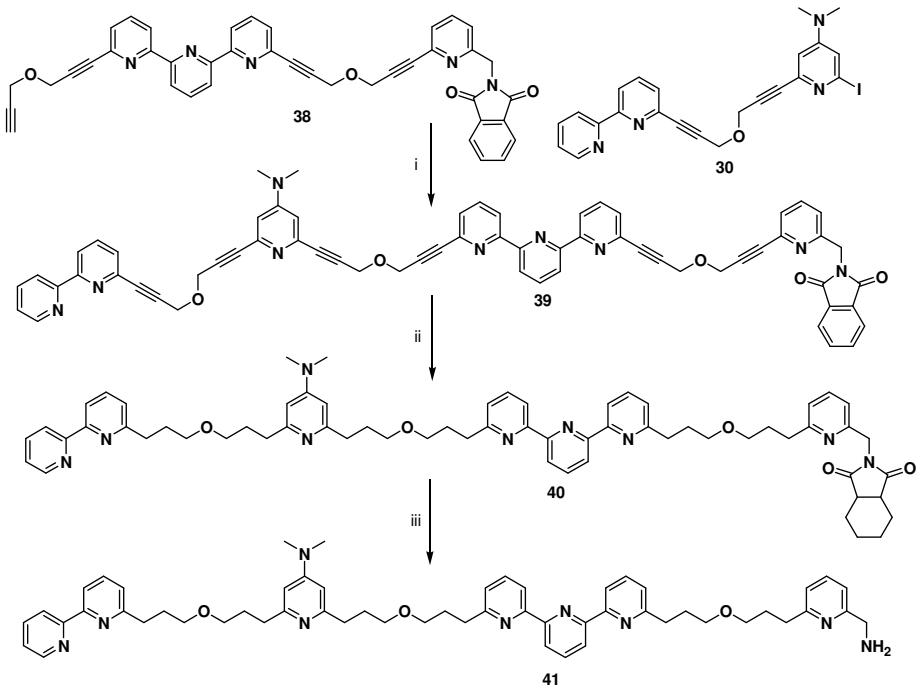

Scheme 4.16 Synthesis of the four station block **41**. Reagents and conditions: (i) $Pd(PPh_3)_4$, CuI, THF/Et_3N, 5 days, 35 ˚C, 65%, (ii) PtO_2, H_2, THF/EtOH, 16 h, RT, 63%, (iii) $N_2H_4.H_2O$, EtOH, 6 days, reflux, 18%.

Sonogashira coupling of two station blocks **38** and **30** proceeded smoothly with gentle warming for five days to give the relatively rigid hexa-acetylene four-station unit **39** in 65% yield. However, hydrogenation of the acetylenes of molecule **39** could only be accomplished by using platinum(IV) oxide in a protic solvent mixture, which also led to full hydrogenation of the phthalimide unit, giving track element **40**. All attempts to deprotect the amine to render the desired four-station block **41** (for conversion to the isocyanate and subsequent coupling to the first two stations of the track) gave only very low yields, perhaps as a consequence of the unexpected over-hydrogenation encountered in the previous step.

However, more serious problems were encountered during preparation of the walker unit on the first two stations of the track (Scheme 4.17). The initial complexation of walker module **11a** to 4-methylphenol-labelled track unit **25a** proceeded in excellent yield, and coupling of the resulting complex **42** with 5-(aminomethyl)-2,2'-bipyridine to give walker/track complex **43** gave similarly satisfactory results. The copper-containing completed walker/two station moiety **44** was then prepared by suspending complex **43** in acetonitrile and adding $[Cu(CH_3CN)_4](PF_6)$, the desired product being

characterised by ESI-MS and showing only one main peak, corresponding to the molecular ion $[M\text{-}PF_6]^+$.

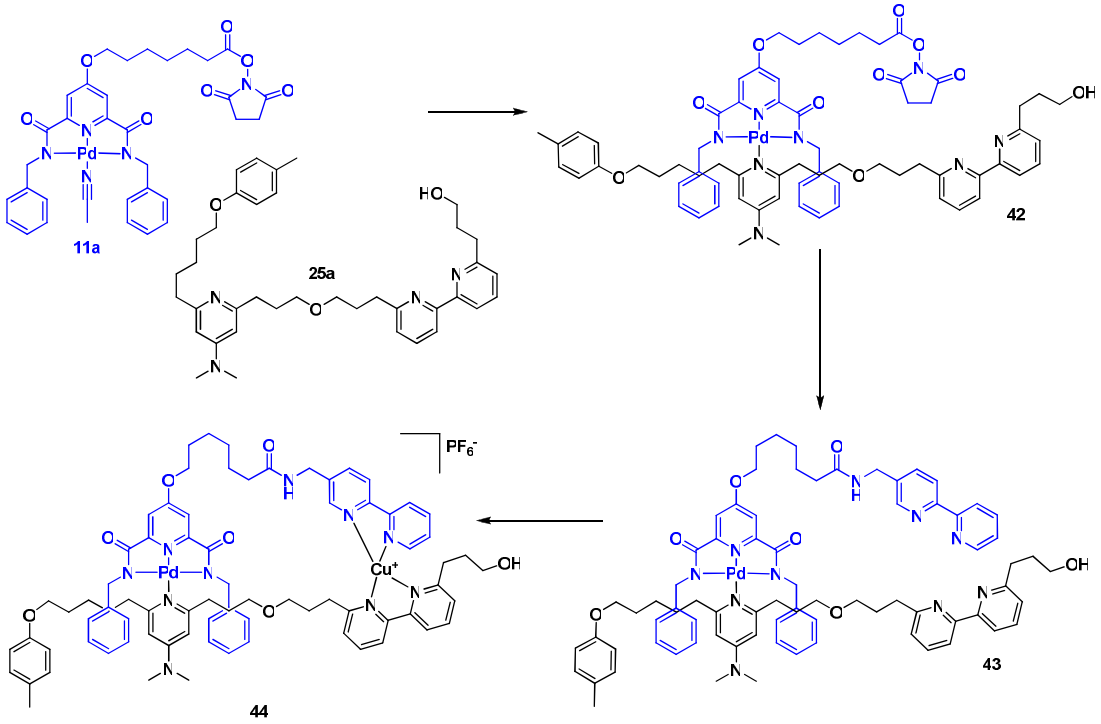

Scheme 4.17 Coordination of the walker to the first two stations of the track. Reagents and conditions: (i) d_7-DMF, 1 h, RT, 89%, (ii) 5-(aminomethyl)-2,2'-bipyridine, CH_2Cl_2, 16 h, RT, 71%, (iii) $[Cu(CH_3CN)_4](PF_6)$, CH_3CN, 30 mins, RT. The walker unit has been coloured for clarity.

However, ^{1}H NMR spectra of complex **44** at room temperature (in both $CDCl_3$ and CD_3CN) showed only broad peaks, making assignments impossible. After standing at room temperature overnight, the intensity of both samples relative to background noise had decreased markedly. Continued monitoring of the ^{1}H NMR spectra showed that the signal intensity got progressively lower and lower over the course of several days, and after about a week an amorphous red precipitate had formed in both samples. These data all seemed to suggest that whilst complex **44** had formed initially, it was unstable in solution with respect to oligomerisation, the products of which became less soluble as they got bigger and hence precipitated from solution, with a concomitant reduction in the ^{1}H NMR signal strength. This result was very disappointing, as it implied that the Cu(I) complex formed was labile (and hence able to scramble and oligomerise) even in a non-coordinating solvent (chloroform) at room temperature. Hence the stability of such complexes under the conditions required to labilise the Pd(II)-containing foot (heating in coordinating solvent) would

almost certainly be insufficient to prevent the complete dissociation of the walker from the track.

Further evidence of the highly labile nature of the copper walker/track complex **44** was obtained by treating complex **43** with only a quarter of an equivalent of $[Cu(CH_3CN)_4](PF_6)$, added as a solution in acetonitrile dropwise over the course of two hours to a solution of the ligand (in 6:1 acetonitrile:dichloromethane). The ^1H NMR spectrum of the resulting red solution did not show a 3:1 ratio of ligand **43** to copper complex **44**, but instead gave a spectrum looking qualitatively very much like that obtained when the ratios of complex **43** and $[Cu(CH_3CN)_4](PF_6)$ were equal, implying that there was ready exchange of ligands around the Cu(I) centre. Furthermore, low temperature ^1H NMR experiments with this mixture evinced dynamic behaviour as low as 230 K in a 1:1 mix of $CDCl_3$ and CD_3CN. Removal of the copper (but not the Pd(II)) proved possible, by simply shaking a dichloromethane solution of complex **44** with an aqueous EDTA/K_2CO_3 solution for 15 minutes, cleanly regenerating complex **43** in quantitative yield.

4.5 Summary and Outlook

The unexpected lability of the copper track/walker complex **44** precludes its use as one of the foot/foothold pairings in an *ABCDABCD* walker system akin to that envisaged in Figure 4.1. The dynamic exchange shown by this system even at very low temperatures is convincing evidence that it would not act as an effective ratchet for the Pd(II)-containing foot and that opportunities for processive walking using such complexes would therefore be very limited with the proposed design. Additionally, it was noted that a new protection strategy was necessary for the amine of the four-station unit, as yields for the late-stage removal of the phthalimide protecting group were unacceptably low. However, we were encouraged by other elements of the synthesis of both the walker and track, notably the creation of a walker unit able to bind two different metals in specific locations and the overall success of the Sonogashira coupling strategy for synthesising extended polypyridyl

chains. A revised target walking system incorporating these strengths and addressing the weaknesses of this initial approach is expounded in Chapter Five.

4.6 Experimental Section

General

Chelidamic acid monohydrate, 2,6-dibromopyridine, 2-pyridylzinc bromide (**28**), 4-methylphenol (**22a**), 4-*tert*-butylphenol (**22b**), ethyl 7-bromoheptanoate, propargyl ether and propargyl alcohol were purchased from the Aldrich Co. 6-Bromo-2,2'-bipyridinyl (**1**),[16] pyridine-2,6-dicarboxylic acid bis-benzylamine (**7**),[23] 2,6-diiodo-4-(dimethylamino)pyridine (**19**),[1] 2-bromo-6-iodopyridine (**26**),[31,32] 6,6'-dibromo-2,2'-bipyridine (**14**),[28] 6,6''-dibromo-2,2':6',2''-terpyridine (**31**),[17] 2-bromo-6-(hydroxymethyl)-pyridine (**34**),[18] trimethyl-(3-prop-2-ynyloxy-prop-1-ynyl)-silane (**16**)[29] and 5-(aminomethyl)-2,2'-bipyridine[26] were prepared according to literature procedures.

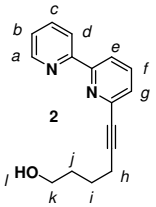

To a solution of 6-bromo-2,2'-bipyridinyl (**1**) (0.500 g, 2.13 mmol, 1.0 equiv.) in THF (20 mL)/Et_3N (10 mL) was added CuI (41.0 mg, 0.213 mmol, 0.1 equiv.) and Pd(dppf)Cl_2 (87.0 mg, 0.106 mmol, 0.05 equiv.). 5-Hexyn-1-ol (0.523 g, 0.594 mL, 5.33 mmol, 2.5 equiv.) was then added and the reaction stirred at RT overnight. After this time, the solvents were removed under reduced pressure and the resulting residue redissolved in EtOAc and washed with an aqueous saturated NH_4Cl solution (2 x 50 mL), and brine (2 x 50 mL). The combined organic fractions were dried (Na_2SO_4), filtered, concentrated under reduced pressure, and then subjected to column chromatography on silica (eluting in 1:1 hexane:EtOAc), giving crude **2** as a brown oil. This was redissolved in CH_2Cl_2 and acidified to pH 2-3 (0.6 *N* HCl in Et_2O), extracted into water (3 x 20 mL) and the combined aqueous extracts neutralised with aqueous NaOH (1 M). This aqueous suspension was then extracted with CH_2Cl_2 (3 x

100 mL) and the organic fractions concentrated *in vacuo* to give **2** as a yellow oil (0.470 g, 88%). ^{1}H NMR ($CDCl_3$, 400 MHz): δ 1.44 (t, *J* = 5.4, 1H, H_l), 1.74-1.81 (m, 4H, $H_{i,j}$), 2.53 (t, *J* = 6.6, 2H, H_h), 3.72-3.76 (m, 2H, H_k), 7.28-7.33 (m, 1H, H_b), 7.39 (d, *J* = 7.6, 1H, H_g), 7.72-7.82 (m, 2H, $H_{c,f}$), 8.30 (d, *J* = 7.9, 1H, H_e), 8.43 (d, *J* = 8.0, 1H, H_d), 8.65 (d, *J* = 4.3, 1H, H_a). ^{13}C NMR ($CDCl_3$, 100 MHz): δ 18.9, 24.5, 24.6, 62.2, 80.9, 90.4, 119.9, 121.5, 123.9, 126.9, 136.9, 137.0, 143.1, 149.0, 155.4, 156.2. LRESI-MS (MeOH): *m/z* = 253 $[M+H]^+$. HRESI-MS: *m/z* = 253.1336 $[M+H]^+$ (calc. for $C_{16}H_{17}N_2O_1$, 253.1335).

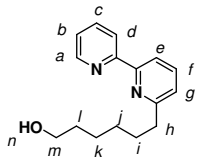

3

A solution of **2** (0.530 g, 2.10 mmol) in THF (15 mL) was charged with 10% Pd/C (10% by weight, 53.0 mg) and degassed first with nitrogen and then with hydrogen. The mixture was stirred under a hydrogen atmosphere at RT for 12 h, after which the reaction mixture was filtered through a plug of celite. Concentration of the filtrate *in vacuo* gave the title compound as a yellow oil (0.437 g, 81%). ^{1}H NMR ($CDCl_3$, 400 MHz): δ 1.30 (t, *J* = 5.3, 1H, H_n), 1.40-1.47 (m, 4H, $H_{j,k}$), 1.54-1.62 (m, 2H, H_i), 1.79-1.86 (m, 2H, H_l), 2.87 (t, *J* = 7.7, 2H, H_h), 3.62-3.67 (m, 2H, H_m), 7.15 (d, *J* = 7.6, 1H, H_g), 7.28-7.32 (m, 1H, H_b), 7.69-7.73 (m, 1H, H_f), 7.79-7.83 (m, 1H, H_c), 8.17 (d, *J* = 7.8, 1H, H_e), 8.42-8.44 (m, 1H, H_d), 8.65-8.69 (m, 1H, H_a). ^{13}C NMR ($CDCl_3$, 100 MHz): δ 25.3, 29.5, 32.5 (x 2), 38.0, 62.5, 118.1, 121.2, 122.6, 123.3, 136.8, 136.9, 148.8, 155.2, 156.4, 161.7. LRESI-MS (MeOH/TFA): *m/z* = 257 $[M+H]^+$. HRESI-MS: *m/z* = 257.1641 $[M+H]^+$ (calc. for $C_{16}H_{21}N_2O_1$, 257.1648).

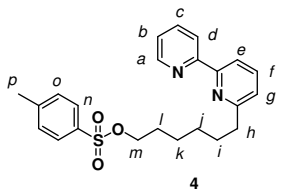

4

To a solution of **3** (0.437 g, 1.70 mmol, 1.0 equiv.) and *p*-toluenesulfonyl chloride (0.390 g, 2.05 mmol, 1.2 equiv.) in dry CH_2Cl_2 was added Et_3N (0.290 mL, 2.05 mmol, 1.2 equiv.) and the mixture stirred at RT for 18 h. After this time, the reaction

mixture was mixed directly with an aqueous saturated NH_4Cl solution (50 mL), the layers separated and the aqueous phase extracted with CH_2Cl_2 (3 x 50 mL). The combined organic extracts were then washed with brine (2 x 50 mL), dried (Na_2SO_4) and concentrated *in vacuo*. The resulting residue was then purified by column chromatography on silica (5:1 hexanes:EtOAc), giving **4** as a brown oil (0.524 g, 75%). ^{1}H NMR ($CDCl_3$, 400 MHz): δ 1.30-1.42 (m, 4H, $H_{j,k}$), 1.62-1.69 (m, 2H, H_i), 1.72-1.80 (m, 2H, H_l), 2.43 (s, 3H, H_p), 2.81 (t, *J* = 7.6, 2H, H_h), 4.02 (t, *J* = 6.5, 2H, H_m), 7.13 (d, *J* = 7.6, 1H, H_g), 7.27-7.35 (m, 3H, $H_{b,o}$), 7.71 (t, *J* = 7.6, 1H, H_f), 7.76-7.83 (m, 3H, $H_{c,n}$), 8.18 (d, *J* = 7.6, 1H, H_e), 8.41-8.43 (m, 1H, H_d), 8.65-8.69 (m, 1H, H_a). ^{13}C NMR ($CDCl_3$, 100 MHz): δ 21.5, 25.2, 28.6, 28.7, 29.2, 37.6, 70.5, 118.9, 122.0, 123.5, 124.0, 129.5, 129.7, 132.9, 133.0, 137.8, 138.5, 144.6, 147.8, 154.6, 161.7. LRESI-MS (acetonitrile): *m/z* = 411 $[M+H]^+$. HRESI-MS: *m/z* = 411.1732 $[M+H]^+$ (calc. for $C_{23}H_{27}N_2O_3S_1$, 411.1737).

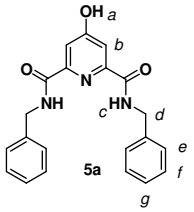

A 250 mL oven dried flask was charged with chelidamic acid monohydrate (6.03 g, 32.5 mmol, 1.0 equiv.) and pentafluorophenol (10.1 g, 55.0 mmol, 2.2 equiv.). CH_2Cl_2 (100 mL) was added to the solids and the resulting suspension was cooled to 0 °C. EDCI (11.1 g, 55.0 mmol, 2.2 equiv.) was added as a solid and the reaction mixture was warmed to RT and stirred for 20 h during which time all the solid materials dissolved yielding a yellow solution. The volume of solvent was then reduced and the residue was chromatographed on silica (3:2 EtOAc:hexane) and the solvents were removed under reduced pressure affording the *bis*-pentafluoroester intermediate as a clear oil (11.2 g, 90%). ^{1}H NMR ($CDCl_3$, 400 MHz): δ 7.98 (s, 2H, Ar-H). LRESI-MS (MeOH): *m/z* = 514 $[M-H]^-$. This oil was immediately dissolved in dry CH_2Cl_2 (200 mL) and cooled to 0 °C. Benzylamine (7.82 g, 70.0 mmol, 3.0 equiv.) and Et_3N (12.3 g, 16.9 mL, 0.120 mol, 5.0 equiv.) were added dropwise *via* syringe and the reaction mixture was stirred at RT for 2 h. The solvents were removed under reduced pressure and the residue redissolved in EtOAc (100 mL) and

washed successively with a 1 M HCl solution (2 x 100 mL), saturated NH_4Cl solution (2 x 50 mL), water (2 x 50 mL), and brine (1 x 100 mL). The organic layer was collected and dried over $MgSO_4$. Filtration, followed by removal of the solvent, yielded the crude product as a tan solid which was recrystallised from acetone/Et_2O to give the title compound as a white solid, m.p. 232 – 234 °C (6.56 g, 75%). ^{1}H NMR (d_6-acetone, 400 MHz): δ 4.56 (d, J = 6.4, 4H, H_d), 7.20-7.30 (m, 10H, $H_{e,f,g}$), 7.78 (s, 2H, H_b), 9.16 (t, J = 6.4, 2H, H_c). ^{13}C NMR (d_6-acetone, 100 MHz): δ 43.3, 112.6, 127.8, 128.1, 129.2, 140.3, 152.6, 164.2, 167.5. LRESI-MS (MeOH/TFA 99:1): *m/z* = 362 $[M+H]^+$. HRESI-MS: *m/z* = 362.1501 $[M+H]^+$ (calc. for $C_{21}H_{20}N_3O_3$ 362.1499 $[M+H]^+$).

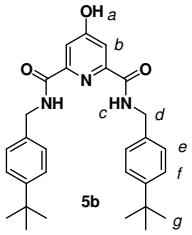

A 250 mL oven dried flask was charged with chelidamic acid monohydrate (1.73 g, 8.62 mmol, 1.0 equiv.) and pentafluorophenol (3.49 g, 18.0 mmol, 2.2 equiv.). CH_2Cl_2 (100 mL) was added to the solids and the resulting suspension was cooled to 0 °C. EDCI (3.79 g, 19.0 mmol, 2.3 equiv.) was added as a solid and the reaction mixture was warmed to RT and stirred for 20 h during which time all the solids dissolved, yielding a yellow solution. The volume of solvent was reduced and the residue was chromatographed on silica (3:2 EtOAc:hexane). The solvents were removed under reduced pressure giving the *bis*-pentafluoroester as a clear oil (4.00 g, 90%). ^{1}H NMR ($CDCl_3$, 400 MHz): δ 7.98 (s, 2H, Ar-H). LRESI-MS (MeOH): *m/z* = 514 $[M-H]^{-1}$. This oil was immediately dissolved in dry CH_2Cl_2 (100 mL) and cooled to 0 °C. 4-(*t*-butyl)benzylamine (3.77 g, 23.0 mmol, 3.0 equiv.) and Et_3N (3.10 g, 4.29 mL, 31.0 mmol, 4.0 equiv.) were dropwise added *via* syringe and the reaction mixture was stirred at RT for 2 h. The solvents were removed under reduced pressure, the residue taken up in ethyl acetate (100 mL), and washed successively with a 1M HCl solution (2 x 100 mL), saturated NH_4Cl solution (2 x 50 mL), water (2 x 50 mL) and brine (1 x 100 mL). The organic layer was collected and dried with $MgSO_4$. Filtration, followed by removal of the solvent, yielded the crude product as a

tan solid which was purified by column chromatography (Et_2O:acetone 1:0 then 1:1) to yield a white solid, m.p. 181-183 °C (3.25 g, 88%). ^{1}H NMR (d_6-acetone, 400 MHz): δ 1.27 (s, 18H, H_g), 2.95 (br, 1H, H_a), 4.51 (d, J = 6.3, 4H, H_d), 7.21 (d, J = 8.4, 4H, H_e), 7.34 (d, J = 8.4, 4H H_f), 7.79 (s, 2H, H_b), 9.17 (t, J = 6.3, 2H, H_c). ^{13}C NMR (d_6-acetone, 100 MHz): δ 31.6, 35.0, 43.0, 112.6, 126.1, 128.0, 137.3, 150.5, 152.3, 164.1, 167.5. LRnanoESI-MS (MeOH/NH_4OAc): *m/z* = 474 $[M+H]^+$. HRESI-MS (MeOH/NH_4OAc): *m/z* = 474.2749 $[M+H]^+$ (calc. for $C_{29}H_{36}N_3O_3$ 474.2751 $[M+H]^+$).

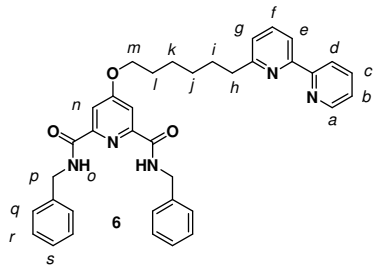

4 (0.524 g, 1.28 mmol, 1.0 equiv.), **5a** (0.463 g, 1.28 mmol, 1.0 equiv.) and K_2CO_2 (0.529 g, 3.83 mmol, 3.0 equiv.) were suspended in butanone (40 mL) and the mixture heated to reflux for 24 h. After this time, the reaction was filtered through celite and the resulting filtrate concentrated under reduced pressure and purified by column chromatography on silica (2:1 hexane:acetone), to give the title compound as a yellow gum (0.428 g, 56%). ^{1}H NMR ($CDCl_3$, 400 MHz): δ 1.42-1.56 (m, 4H, $H_{j,k}$), 1.78-1.88 (m, 4H, $H_{i,l}$), 2.87 (t, J = 7.6, 2H, H_h), 4.09 (t, J = 6.5, 2H, H_m), 4.59 (d, J = 6.2, 4H, H_p), 7.15 (dd, J_1 = 7.7, J_2 = 0.8, 1H, H_g), 7.21-7.28 (m, 11H, $H_{b,q,r,s}$), 7.70 (t, J = 7.7, 1H, H_f), 7.78-7.82 (m, 1H, H_c), 7.84 (s, 2H, H_n), 8.15-8.20 (m, 3H, $H_{e,o}$), 8.41-8.44 (m, 1H, H_d), 8.63-8.66 (m, 1H, H_a). ^{13}C NMR ($CDCl_3$, 100 MHz): δ 25.6, 28.5, 28.8, 29.4, 38.1, 43.2, 68.7, 111.2, 118.1, 121.2, 122.7, 123.4, 127.1, 127.4, 128.3, 136.9, 137.0, 138.0, 148.8, 150.5, 155.1, 156.4, 161.5, 163.7, 167.6. LRESI-MS (MeOH/TFA, 99/1): *m/z* = 600 $[M+H]^+$. HRESI-MS: *m/z* = 600.2975 $[M+H]^+$ (calc. for $C_{37}H_{38}N_5O_3$ 600.2969 $[M+H]^+$).

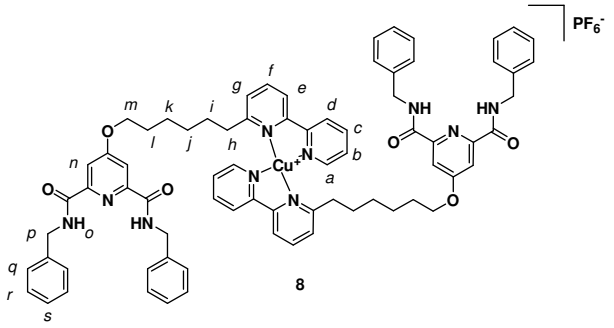

7 (0.054 g, 0.090 mmol, 1.0 equiv.) was dissolved in dry CH_3CN (10 mL) and then added *via* cannula to a stirred solution of $[Cu(CH_3CN)_4](PF_6)$ (0.017 g, 0.045 mmol, 0.5 equiv.) in dry CH_3CN (5 mL), and the resulting deep red solution stirred at RT for 30 minutes. After this time, the solvent was removed under reduced pressure, giving **8** as a dark red solid (0.060 g, 99%). ^{1}H NMR (CD_3CN, 400 MHz): δ 0.73-0.91 (m, 8H, $H_{j,k}$), 1.26-1.42 (m, 8H, $H_{i,l}$), 2.50 (t, *J* = 7.8, 4H, H_h), 3.83 (t, *J* = 6.3, 4H, H_m), 4.56 (d, *J* = 6.5, 8H, H_p), 7.16-7.22 (m, 4H, H_s), 7.24-7.32 (m, 16H, $H_{q,r}$), 7.50 (d, *J* = 7.8, 2H, H_g), 7.55-7.57 (m, 2H, H_b), 7.64 (s, 4H, H_n), 8.01 (t, *J* = 7.8, 2H, H_f), 8.07-8.09 (m, 2H, H_c), 8.25 (d, *J* = 7.8, 2H, H_e), 8.38-8.40 (m, 2H, H_d), 8.51-8.53 (m, 2H, H_a), 8.98 (t, *J* = 6.5, 4H, H_o). LRESI-MS (MeOH/TFA, 99/1): *m/z* = 1262 $[M\text{-}PF_6]^+$.

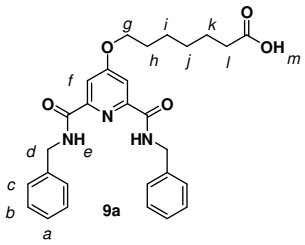

To a solution of **5a** (2.65 g, 7.34 mmol, 1.0 equiv.) and ethyl 7-bromoheptanoate (2.60 g, 2.15 mL, 11.0 mmol, 1.5 equiv.) in butanone (60 mL) was added K_2CO_3 (5.06 g, 36.7 mmol, 5.0 equiv.). The suspension was heated at reflux for 20 h. Subsequently, the reaction mixture was filtered through celite, washed with acetone, and the resulting filtrate concentrated under reduced pressure. The residue obtained was redissolved in THF (30 mL) and a solution of LiOH (3.13 g, 76.8 mmol, 10.0 equiv.) in water (10 mL) was added and the suspension was stirred at RT for 36 h. The solvents were then removed under reduced pressure and the residue suspended in EtOAc (50 mL), cooled in an ice bath, and acidified with 1 M HCl until the pH =

1. The organic layer was separated and washed successively with a 1 M HCl solution (1 x 100 mL), saturated NH_4Cl solution (2 x 50 mL), water (2 x 50 mL), and brine (1 x 100 mL). The organic layer was collected and dried (Na_2SO_4). The resulting yellow oil was purified by column chromatography (solvent gradient, CH_2Cl_2:acetone 9:1 to 6:4) to yield **9a** as a white solid, m.p. 110-112 ˚C (3.30 g, 92%). ^{1}H NMR ($CDCl_3$, 400 MHz): δ 1.24-1.30 (m, 4H, $H_{i,j}$), 1.46-1.50 (m, 2H, H_h), 1.61-1.69 (m, 2H, H_k), 2.16 (t, *J* = 7.3, 2H, H_l), 3.91 (t, *J* = 6.5, 2H, H_g), 4.42 (d, *J* = 6.1, 4H, H_d), 7.06-7.21 (m, 10H, $H_{a,b,c}$), 7.64 (s, 2H, H_f), 7.86 (t, *J* = 6.1, 2H, H_e), 10.24 (br, 1H, H_m). ^{13}C NMR ($CDCl_3$, 100 MHz): δ 24.5, 25.5, 28.5, 28.6, 33.9, 43.3, 68.7, 111.4, 127.3, 127.5, 128.5, 138.0, 150.4, 164.1, 167.8, 178.8. LRESI-MS (MeOH/TFA, 99/1): *m/z* = 490 $[M+H]^+$. HRESI-MS: *m/z* = 490.2338 $[M+H]^+$ (calc. for $C_{28}H_{32}N_3O_5$ 490.2336 $[M+H]^+$).

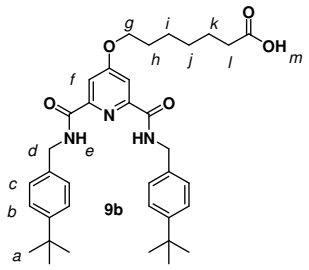

To a solution of **5b** (2.15 g, 4.54 mmol, 1.0 equiv.) and ethyl 7-bromoheptanoate (1.61 g, 1.32 mL, 6.81 mmol, 1.5 equiv.) in butanone (40 mL) was added K_2CO_3 (3.13 g, 22.7 mmol, 5.0 equiv.). The suspension was heated at reflux for 20 h. Subsequently, the reaction mixture was filtered through celite, washed with acetone, and the resulting filtrate concentrated under reduced pressure. The residue thus obtained was redissolved in THF (30 mL) and a solution of LiOH (1.91 g, 45.4 mmol, 10.0 equiv.) in water (10 mL) was added and the suspension was stirred at RT for 36 h. The solvents were then removed under reduced pressure and the residue suspended in EtOAc (50 mL), cooled in an ice bath, and acidified with 1 M HCl until the pH = 1. The organic layer was separated and washed successively with a 1 M HCl solution (1 x 100 mL), saturated NH_4Cl solution (2 x 50 mL), water (2 x 50 mL), and brine (1 x 100 mL). The organic layer was collected and dried (Na_2SO_4). The resulting yellow oil was purified by column chromatography (hexanes:Et_2O 1:3) to yield **9b** as a white solid, m.p. 79-81 ˚C (1.70 g, 65%). ^{1}H NMR ($CDCl_3$, 400

MHz): δ 1.29 (s, 18H, H_a), 1.38-1.52 (m, 4H, $H_{i,j}$), 1.64-1.71 (m, 2H, H_h), 1.79-1.85 (m, 2H, H_k), 2.37 (t, *J* = 7.2, 2H, H_l), 4.11 (t, *J* = 6.4, 2H, H_g), 4.61 (d, *J* = 6.2, 4H, H_d), 7.25 (d, *J* = 8.8, 4H, H_c), 7.33 (d, *J* = 8.8, 4H, H_b), 7.86 (s, 2H, H_f), 8.12 (t, *J* = 6.2, 2H, H_e). ^{13}C NMR ($CDCl_3$, 100 MHz): δ 24.5, 25.4, 28.4, 28.6, 31.3, 33.8, 34.5, 43.1, 68.8, 111.6, 125.6, 127.6, 135.0, 150.6, 150.7, 163.6, 167.9, 178.2. LRESI-MS (acetonitrile): *m/z* = 624 $[M+Na]^+$. HRESI-MS: *m/z* = 602.3583 $[M+H]^+$ (calc. for $C_{36}H_{48}N_3O_5$ 602.3588 $[M+H]^+$).

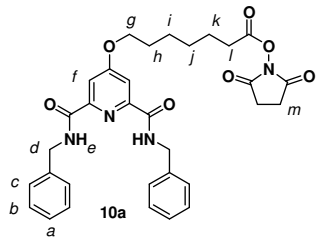

To a solution of **9a** (2.99 g, 5.10 mmol, 1.0 equiv.), N-hydroxysuccinimide (620 mg, 5.36 mmol, 1.05 equiv.) and DMAP (620 mg, 5.10 mmol, 1.0 equiv.) in CH_2Cl_2 (50 mL) was added EDCI (1.07 g, 5.61 mmol, 1.1 equiv.) and the resulting solution stirred at RT for 20 h. Subsequently, the reaction mixture was concentrated under reduced pressure and purified by column chromatography on silica (CH_2Cl_2:acetone 9:1 then 8:2). Removal of the solvents *in vacuo* yielded **10a** as a colourless oil (2.30 g, 92%). ^{1}H NMR ($CDCl_3$, 400 MHz): δ 1.50-1.56 (m, 4H, $H_{i,j}$), 1.79-1.91 (m, 4H, $H_{h,k}$), 2.65 (t, *J* = 7.3, 2H, H_l), 2.85 (s, 4H, H_m), 4.18 (t, *J* = 6.4, 2H, H_g), 4.69 (d, *J* = 6.2, 4H, H_d), 7.28-7.36 (m, 10H, $H_{a,b,c}$), 7.90 (s, 2H, H_f), 8.02 (t, *J* = 6.2, 2H, H_e). ^{13}C NMR ($CDCl_3$, 100 MHz): δ 24.4, 25.3, 25.5, 28.2, 28.4, 30.8, 43.3, 68.7, 111.4, 127.3, 127.6, 128.6, 138.2, 150.6, 163.7, 167.8, 168.5, 169.4. LRESI-MS (MeOH/TFA, 99/1): *m/z* = 587 $[M+H]^+$. HRESI-MS: *m/z* = 587.2500 $[M+H]^+$ (calc. for $C_{32}H_{35}N_4O_7$ 587.2490 $[M+H]^+$).

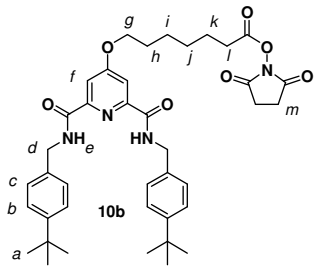

To a solution of **9b** (1.71 g, 2.80 mmol, 1.0 equiv.), N-hydroxysuccinimide (350 mg, 3.04 mmol, 1.05 equiv.) and DMAP (355 mg, 2.80 mmol, 1.0 equiv.) in CH_2Cl_2 (15 mL) was added EDCI (611 mg, 3.08 mmol, 1.1 equiv.). The resulting solution was stirred at RT for 20 h. Subsequently, the reaction mixture was concentrated under reduced pressure and purified by column chromatography on silica (CH_2Cl_2). Removal of the solvents *in vacuo* yielded **10b** as a white solid, m.p. 74-76 ˚C (1.23 g, 63%). ^{1}H NMR ($CDCl_3$, 400 MHz): δ 1.29 (s, 18H, H_a), 1.49-1.51 (m, 4H, $H_{i,j}$), 1.77-1.87 (m, 4H, $H_{h,k}$), 2.63 (t, J = 7.2, 2H, H_l), 2.81 (s, 4H, H_m), 4.13 (t, J = 6.4, 2H, H_g), 4.61 (d, J = 6.0, 4H, H_d), 7.26 (d, J = 8.4, 4H, H_c), 7.34 (d, J = 8.4, 4H, H_b), 7.86 (s, 2H, H_f), 8.08 (t, J = 6.0, 2H, H_e). ^{13}C NMR ($CDCl_3$, 100 MHz): δ 24.5, 25.3, 25.6, 28.2, 28.4, 30.9, 31.3, 34.5, 43.1, 68.7, 111.5, 125.6, 127.5, 135.1, 150.6, 150.8, 163.5, 167.8, 168.5, 169.2. LRESI-MS (acetonitrile): *m/z* = 721 $[M+Na]^+$. HRESI-MS: *m/z* = 699.3747 $[M+H]^+$ (calc. for $C_{40}H_{51}N_4O_7$ 699.3752 $[M+H]^+$).

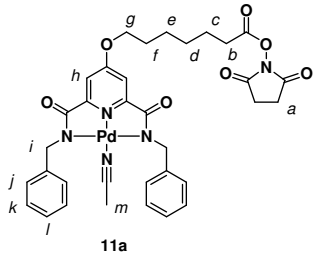

Compound **10a** (0.500 g, 0.0850 mmol, 1.0 equiv.) was dissolved in dry CH_3CN (30 mL) and $Pd(OAc)_2$ (0.219 g, 0.0980 mmol, 1.15 equiv.) was added under a nitrogen atmosphere. After gentle warming for 1 minute (heat gun), the reaction was allowed to stir at RT overnight. The yellow precipitate was then collected by suction filtration, redissolved in boiling CH_3CN and passed (hot) through a plug of celite. Removal of the solvent under reduced pressure followed by recrystallisation from CH_3CN gave the title compound as a yellow gum (0.565 g, 83%). ^{1}H NMR (d_6-DMSO, 400 MHz): δ 1.52-1.56 (m, 4H, $H_{d,e}$), 1.73-1.77 (m, 2H, H_c), 1.82-1.88 (m,

2H, H_f), 2.18 (s, 3H, H_m), 2.78 (t, J = 7.1, 2H, H_b), 2.90 (s, 4H, H_a), 4.35 (t, J = 6.3, 2H, H_g), 4.39 (s, 4H, H_i), 7.20 (s, 2H, H_h), 7.28-7.46 (m, 10H, $H_{j,k,l}$). ^{13}C NMR (d_6-DMSO, 100 MHz): δ 0.0, 23.0, 23.5, 24.3, 26.3, 26.6, 28.9, 46.5, 68.3, 109.1, 117.0, 124.9, 125.7, 126.9, 140.1, 152.6, 167.6, 167.8, 168.4, 169.1. LRFAB-MS (noba): m/z = 691 $[M^{106}Pd\text{-}CH_3CN+H]^+$. HRESI-MS: m/z = 689.1384 $[M\text{-}CH_3CN+H]^+$ (calc. for $C_{32}H_{33}N_4O_7{}^{104}Pd$ 689.1376 $[M\text{-}CH_3CN+H]^+$).

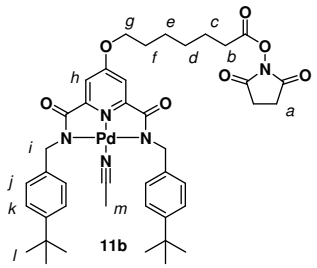

11b

Compound **10b** (0.500 g, 0.0720 mmol, 1.0 equiv.) was dissolved in dry CH_3CN (30 mL) and $Pd(OAc)_2$ (0.223 g, 0.0820 mmol, 1.15 equiv.) was added under a nitrogen atmosphere. After gentle warming for 1 minute (heat gun), the reaction was allowed to stir at RT overnight. Evaporation of the solvent yielded an orange-yellow solid that was redissolved in boiling CH_3CN and passed (hot) through a plug of celite. Removal of the solvent under reduced pressure followed by washing with cold Et_2O gave the title compound as a pale yellow solid, m.p. 150-152 ˚C (0.490 g, 81%). ^{1}H NMR ($CDCl_3$, 400 MHz): δ 1.29 (s, 18H, H_l), 1.49-1.52 (m, 4H, $H_{d,e}$), 1.77-1.87 (m, 4H, $H_{c,f}$), 2.09 (s, 3H, H_m), 2.63 (t, J = 7.2, 2H, H_b), 2.83 (s, 4H, H_a), 4.15 (t, J = 6.4, 2H, H_g), 4.52 (s, 4H, H_i), 7.24-7.31 (m, 10H, $H_{h,j,k}$). ^{13}C NMR (d_6-DMSO, 100 MHz): δ 0.0, 23.0, 23.5, 24.3, 26.3, 26.6, 28.9, 30.0, 32.9, 46.2, 68.2, 109.0, 117.0, 123.5, 125.7, 137.1, 147.2, 152.7, 167.6, 167.8, 168.3, 169.1. LRFAB-MS (noba): m/z = 803 $[M^{106}Pd\text{-}CH_3CN+H]^+$. HRESI-MS: m/z = 801.2637 $[M\text{-}CH_3CN+H]^+$ (calc. for $C_{40}H_{49}N_4O_7{}^{104}Pd$ 801.2636 $[M\text{-}CH_3CN+H]^+$).

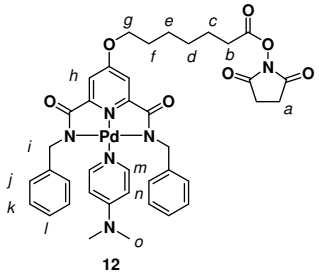

12

11a (0.430 g, 0.587 mmol, 1.0 equiv.) was dissolved in CH_2Cl_2 (20 mL) and DMAP (80.0 mg, 0.656 mmol, 1.1 equiv.) was added and the solution stirred at RT for 15 minutes. After this time, the reaction was passed through a pad of silica to give **12** as a yellow solid, m.p. 165-167 ˚C (0.360 g, 75%). ^{1}H NMR ($CDCl_3$, 400 MHz): δ 1.47-1.60 (m, 4H, $H_{d,e}$), 1.75-1.92 (m, 4H, $H_{c,f}$), 2.64 (t, *J* = 7.2, 2H, H_b), 2.80-2.88 (br, 4H, H_a), 3.01 (s, 6H, H_o), 4.16 (t, *J* = 6.4, 2H, H_g), 4.22 (s, 4H, H_i), 6.09 (d, *J* = 7.2, 2H, H_n), 6.91-6.96 (m, 4H, H_j), 7.05-7.12 (m, 6H, $H_{k,l}$), 7.29 (s, 2H, H_h), 7.47 (d, *J* = 7.2, 2H, H_m). ^{13}C NMR ($CDCl_3$, 100 MHz): δ 24.4, 25.2, 25.5, 28.1, 28.2, 30.8, 39.2, 49.0, 69.3, 107.1, 110.7, 125.8, 127.0, 127.7, 141.3, 149.7, 154.1, 154.2, 168.5, 169.1, 169.2, 171.0. LRESI-MS (MeOH): *m/z* = 713 [M^{106}Pd-DMAP+Na]$^+$. HRESI-MS: *m/z* = 713.1175 [M^{106}Pd-DMAP+Na]$^+$ (calc. for $C_{32}H_{32}N_4O_7{}^{106}$PdNa, 713.1198 [M^{106}Pd-DMAP+Na]$^+$).

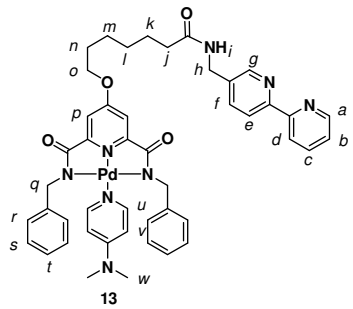

13

To a solution of **12** (0.275 g, 0.265 mmol, 1.0 equiv.) in CH_2Cl_2 (5 mL) was added a solution of 5-(aminomethyl)-2,2'-bipyridine (48.0 mg, 0.265 mmol, 1.0 equiv.) in CH_2Cl_2 (2 mL) dropwise over 30 minutes. After addition was complete, the reaction was stirred at RT overnight. The solvent was then removed under reduced pressure and the crude residue purified by column chromatography on silica (CH_2Cl_2:MeOH 15:1) to give **13** as a yellow solid (0.150 g, 64%). ^{1}H NMR ($CDCl_3$, 400 MHz): δ 1.33-1.48 (m, 4H, $H_{l,m}$), 1.63-1.82 (m, 4H, $H_{k,n}$), 2.22-2.29 (m, 2H, H_j), 2.99 (s, 6H, H_w), 4.03 (t, *J* = 6.5, 2H, H_o), 4.15 (s, 4H, H_q), 4.53 (d, *J* = 6.0, 2H, H_h), 6.07 (d, *J* =

7.2, 2H, H_v), 6.80 (t, J = 6.0, 1H, H_i), 6.87-6.98 (m, 4H, H_r), 7.04-7.11 (m, 6H, $H_{s,t}$), 7.21 (s, 2H, H_p), 7.27-7.31 (m, 1H, H_b), 7.44 (d, J = 7.2, 2H, H_u), 7.74-7.77 (m, 2H, $H_{c,f}$), 8.27-8.34 (m, 2H, $H_{d,e}$), 8.55 (d, J = 2.0, 1H, H_g), 8.63-8.70 (m, 1H, H_a). LRESI-MS (MeOH/TFA): *m/z* = 657 $[M\text{-Pd-DMAP+H}]^+$.

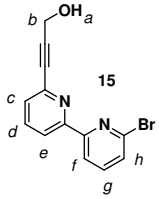

6,6'-Dibromobipyridine (**14**) (4.06 g, 12.9 mmol, 1.0 equiv.) was dissolved in a mixture of toluene (200 mL) and Et_3N (100 mL) and CuI (246 mg, 1.29 mmol, 0.1 equiv.), $Pd(dppf)Cl_2$ (527 mg, 0.650 mmol, 0.05 equiv.) and propargyl alcohol (0.197 g, 0.207 mL, 3.51 mmol, 1.1 equiv.) were added and the reaction mixture heated to 110 °C for 36 h. Subsequently, the reaction mixture was filtered through celite and then concentrated under reduced pressure. The resulting brown solid was redissolved in a toluene/acetone mixture and purified by column chromatography (silica, CH_2Cl_2:acetone 1:0 then 9:1) to yield **15** as a white solid, 190 °C (dec.) (1.49 g, 40%). ^{1}H NMR ($CDCl_3$, 400 MHz): δ 2.85 (s, 1H, H_a), 4.48 (s, 2H, H_b), 7.56 (dd, J_1 = 7.7, J_2 = 0.9, 1H, H_c), 7.68 (dd, J_1 = 7.9, J_2 = 0.8, 1H, H_h), 7.91 (t, J = 7.7, 1H, H_d), 7.97 (t, J = 7.9, 1H, H_g), 8.34 (dd, J_1 = 7.7, J_2 = 0.9, 1H, H_e), 8.45 (dd, J_1 = 7.9, J_2 = 0.8, 1H, H_f). ^{13}C NMR (d_6-acetone, 100 MHz): δ 51.9, 85.3, 90.7, 121.7, 122.0, 129.5, 130.4, 139.6, 142.0, 143.1, 144.7, 156.4, 158.4. LRnanoESI-MS (MeOH/NH_4OAc): *m/z* = 289 $[M^{79}Br+H]^+$. HRESI-MS (MeOH/NH_4OAc): *m/z* = 288.9969 $[M+H]^+$ (calc. for $C_{13}H_{10}{}^{79}BrN_2O$ 288.9971 $[M+H]^+$).

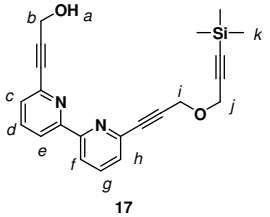

To a solution of **15** (0.760 g, 2.63 mmol, 1.0 equiv.), CuI (50.0 mg, 0.260 mmol, 0.1 equiv.) and $Pd(dppf)Cl_2$ (0.107 g, 0.130 mmol, 0.05 equiv.) in toluene (40 mL) and Et_3N (20 mL) was added trimethyl-(3-prop-2-ynyloxy-prop-1-ynyl)-silane (**16**)

(0.656 g, 3.94 mmol, 1.5 equiv.). The resulting mixture was heated to 100 °C for 20 minutes at atmospheric pressure in a CEM microwave reactor (power level = 150 W). Subsequently, the reaction was quenched with aqueous NH_4Cl (25 mL) and the organic phase washed with water (20 mL) and brine. After drying (Na_2SO_4) and removal of the solvents under reduced pressure, the crude residue was subjected to column chromatography on silica (7:3 Et_2O:hexane) to give the title compound as a tan solid, m.p. 83-85 ºC (0.808 g, 82%). ^{1}H NMR ($CDCl_3$, 400 MHz): δ 0.10 (s, 9H, H_k), 1.77 (t, *J* = 6.3, 1H, H_a), 4.35 (s, 2H, H_j), 4.54 (s, 2H, H_i), 4.56 (d, *J* = 6.3, 2H, H_b), 7.46-7.50 (m, 2H, $H_{c,h}$), 7.75-7.82 (m, 2H, $H_{d,g}$), 8.39-8.43 (m, 2H, $H_{e,f}$). ^{13}C NMR ($CDCl_3$, 100 MHz): δ 0.0, 51.8, 57.4, 57.9, 84.5, 85.3, 86.3, 87.3, 92.6, 100.6, 121.3 (x 2), 127.7, 127.8, 137.4 (x 2), 142.2 (x 2), 155.9, 156.0 LRESI-MS (MeOH/TFA, 99:1): *m/z* = 375 $[M+H]^+$, 397 $[M+Na]^+$. HRESI-MS: *m/z* = 375.1528 $[M+H]^+$ (calc. for $C_{22}H_{23}N_2O_2Si$ 375.1523 $[M+H]^+$).

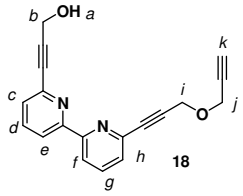

18

To a solution of **17** (1.08 g, 2.87 mmol, 1.0 equiv.) in MeOH (20 mL) and THF (20 mL) was added finely ground K_2CO_3 (0.400 g, 2.87 mmol, 1.0 equiv.). The resulting reaction mixture was stirred at 0 °C for 1 h. The reaction mixture was then quenched by addition of a saturated aqueous NH_4Cl solution (30 mL) followed by extraction with EtOAc (3 x 50 mL). The combined organic layers were washed with water and brine and dried over $MgSO_4$. Evaporation of the solvent yielded the title compound as a white solid, m.p. 113-115 °C (0.850 g, 98%). ^{1}H NMR ($CDCl_3$, 400 MHz): δ 2.43 (t, *J* = 2.4, 1H, H_k), 4.30 (d, *J* = 2.4, 2H, H_j), 4.49-4.50 (m, 4H, $H_{b,i}$), 7.39-7.43 (m, 2H, $H_{c,h}$), 7.70-7.74 (m, 2H, $H_{d,g}$), 8.32-8.36 (m, 2H, $H_{e,f}$). ^{13}C NMR ($CDCl_3$, 100 MHz): δ 56.8, 57.2, 65.9, 75.3, 78.8, 84.1, 85.1, 86.2, 87.2, 121.1 (x 2), 127.5, 129.6, 137.2 (x 2), 141.9, 142.1, 155.7, 171.2. LRESI-MS (acetonitrile): *m/z* = 325 $[M+Na]^+$. HRESI-MS (MeOH/NH_4OAc): *m/z* = 303.1128 $[M+H]^+$ (calc. for $C_{19}H_{15}N_2O_2$ 303.1128 $[M+H]^+$).

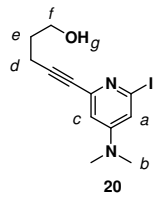

20

To a solution of 2,6-diiodoDMAP (**19**, 3.75 g, 10.0 mmol, 1.0 equiv.) in THF (30 mL) and Et_3N (20 mL) were added CuI (0.380 g, 2.00 mmol, 0.2 equiv.) and $Pd(PPh_3)_2Cl_2$ (0.701 g, 1.00 mmol, 0.1 equiv.). 4-Pentyn-1-ol (0.925 g, 1.02 mL, 11.0 mmol, 1.1 equiv.) was then added and the mixture was stirred at RT for 20 h. The reaction mixture was then quenched by addition of a saturated aqueous NH_4Cl solution (30 mL) followed by extraction with CH_2Cl_2 (3 x 50 mL). The combined organic layers were washed with water and brine and dried (Na_2SO_4). The solvent was then removed under reduced pressure and the resulting residue purified by column chromatography on silica (CH_2Cl_2 to CH_2Cl_2:acetone, 4:1) giving the title compound as a yellow oil (2.64 g, 80%). ^{1}H NMR ($CDCl_3$, 400 MHz): δ 1.76-1.80 (m, 2H, H_e), 2.46 (t, *J* = 7.0, 2H, H_d), 2.68 (br, 1H, H_g) 2.89 (s, 6H, H_b), 3.73 (t, *J* = 6.2, 2H, H_f), 6.49 (d, *J* = 2.4, 1H, H_c), 6.73 (d, *J* = 2.4, 1H, H_a). ^{13}C NMR ($CDCl_3$, 100 MHz): δ 15.9, 31.0, 39.3, 61.3, 80.4, 90.0, 109.6, 115.8, 118.1, 143.2, 154.5. LRESI-MS (MeOH/TFA, 99/1): *m/z* = 331 $[M+H]^+$. HRESI-MS: *m/z* = 331.0300 $[M+H]^+$ (calc. for $C_{12}H_{16}IN_2O$ 331.0302 $[M+H]^+$).

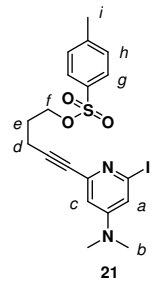

21

A solution of **20** (3.18 g, 9.63 mmol, 1.0 equiv.) and Et_3N (1.94 g, 2.66 mL, 19.0 mmol, 2.0 equiv.) in anhydrous CH_2Cl_2 (50 mL) was cooled to 0 °C. *p*-toluenesulfonyl chloride (2.20 g, 11.5 mmol, 1.2 equiv.) was added and the solution was stirred at RT for 18 h. The reaction was then quenched with water (100 mL) and the organic layer was separated and dried ($MgSO_4$). After filtration and concentration under reduced pressure, the resulting crude oil was purified by column chromatography on silica (solvent gradient, hexane:EtOAc 9:1, 8:2 then 6:4) to yield

21 as a yellow oil (4.03 g, 84%). ^{1}H NMR (400 MHz, $CDCl_3$): δ 1.90-1.94 (m, 2H, H_e), 2.41 (s, 3H, H_i), 2.44-2.48 (m, 2H, H_d), 2.97 (s, 6H, H_b), 4.16 (t, *J* = 6.1, 2H, H_f), 6.55 (d, *J* = 2.4, 1H, H_c), 6.82 (d, *J* = 2.4, 1H, H_a), 7.32 (d, *J* = 8.3, 2H, H_h), 7.79 (d, *J* = 8.3, 2H, H_g). ^{13}C NMR (100 MHz, $CDCl_3$): δ = 15.7, 21.7, 27.5, 39.3, 69.0, 81.0, 87.7, 109.8, 115.9, 118.3, 127.9, 129.9, 132.8, 142.9, 144.9, 154.5. LRESI-MS (MeOH/TFA, 99/1): *m/z* = 485 $[M+H]^+$. HRESI-MS: *m/z* = 485.0384 $[M+H]^+$ (calc. for $C_{19}H_{22}IN_2O_3S$, 485.0384 $[M+H]^+$).

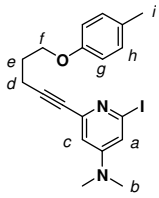

23a

To a solution of **21** (3.10 g, 6.40 mmol, 1.0 equiv.) and 4-methylphenol (**22a**) (80.0 mg, 0.770 mL, 7.36 mmol, 1.15 equiv.) in butanone (50 mL) was added K_2CO_3 (4.00 g, 32.0 mmol, 5.0 equiv.) and the suspension heated at reflux for 20 h. After this time, the reaction mixture was filtered through celite, washed with acetone, and the filtrate concentrated under reduced pressure. The resulting yellow oil was purified by column chromatography on silica (hexane:EtOAc 9:1 to 7:3) to yield **23a** as a white solid, m.p. 68-70 ºC (1.52 g, 56%). ^{1}H NMR ($CDCl_3$, 400 MHz): δ 1.97-2.01 (m, 2H, H_e), 2.21 (s, 3H, H_i), 2.54 (t, *J* = 7.1, 2H, H_d), 2.89 (s, 6H, H_b), 3.99 (t, *J* = 6.1, 2H, H_f), 6.49 (d, *J* = 2.4, 1H, H_c), 6.72-6.76 (m, 3H, $H_{a,g}$), 7.00 (d, *J* = 8.2, 2H, H_h). ^{13}C NMR ($CDCl_3$, 100 MHz): δ 16.2, 20.5, 28.0, 39.2, 66.4, 80.5, 89.3, 109.7, 114.4, 115.8, 118.3, 129.9, 143.2 (x 2), 154.5, 156.7. LRESI-MS (MeOH/TFA, 99/1): *m/z* = 421 $[M+H]^+$. HRESI-MS: *m/z* = 421.0777 $[M+H]^+$ (calc. for $C_{19}H_{22}IN_2O$, 421.0771 $[M+H]^+$).

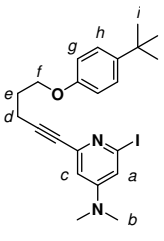

23b

To a solution of **21** (1.84 g, 3.80 mmol, 1.0 equiv.) and 4-*tert*-butylphenol (**22b**) (0.660 g, 4.37 mmol, 1.15 equiv.) in butanone (30 mL) was added K_2CO_3 (2.62 g,

19.0 mmol, 5.0 equiv.). The suspension was heated at reflux for 24 h. After this time, the reaction mixture was filtered through celite, washed with acetone, and the filtrate concentrated under reduced pressure. The resulting yellow oil was purified by column chromatography on silica (hexane:EtOAc 9:1) to yield **23b** as a colourless oil (1.40 g, 80%). ^{1}H NMR ($CDCl_3$, 400 MHz): δ 1.29 (s, 9H, H_i), 2.06 (m, 2H, H_e), 2.60 (t, *J* = 7.1, 2H, H_d), 2.94 (s, 6H, H_b), 4.06 (t, *J* = 6.0, 2H, H_f), 6.55 (d, *J* =2.4, 1H, H_c), 6.80 (d, *J* = 2.4, 1H, H_a), 6.84 (d, *J* = 8.8, 2H, H_g), 7.29 (d, *J* = 8.8, 2H, H_h). ^{13}C NMR ($CDCl_3$, 100 MHz): δ 16.2, 28.1, 31.6, 34.1, 39.2, 66.3, 80.5, 89.3, 109.7, 114.0, 115.8, 118.3, 126.2, 143.2, 143.3, 154.5, 156.6. LRESI-MS (acetonitrile): *m/z* = 463 $[M+H]^+$. HRESI-MS: *m/z* = 463.1246 $[M+H]^+$ (calc. for $C_{22}H_{28}IN_2O$, 463.1241 $[M+H]^+$).

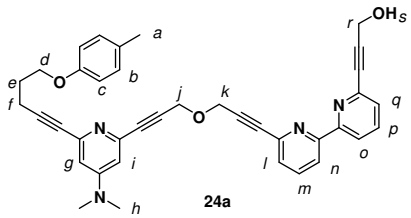

18 (0.400 g, 1.32 mmol, 1.0 equiv.) and **23a** (0.556 g, 1.32 mmol, 1.0 equiv.) were dissolved in toluene (30 mL) and Et_3N (20 mL). $Pd(dppf)Cl_2$ (54.0 mg, 66.0 μmol, 0.05 equiv.) and CuI (25.0 mg, 0.132 mmol, 0.1 equiv.) were then added as solids and the resulting reaction mixture was heated to 100 °C for 20 minutes at atmospheric pressure in a CEM microwave reactor (power level = 150 W). The reaction was then quenched with aqueous NH_4Cl (25 mL) and extracted with CH_2Cl_2 (2 x 100 mL). The organic phase was washed with water (20 mL), brine (20 mL) and then dried (Na_2SO_4). The solvent was removed under reduced pressure and the crude residue was subjected to column chromatography on silica (CH_2Cl_2:acetone 9:1 to 7:3). Removal of the solvents *in vacuo* then gave **24a** as a white solid, m.p. 62-64 ºC (0.580 g, 74%). ^{1}H NMR ($CDCl_3$, 400 MHz): δ 2.03-2.10 (m, 2H, H_e), 2.27 (s, 3H, H_a), 2.61 (t, *J* = 7.0, 2H, H_f), 2.96 (s, 6H, H_h), 4.06 (t, *J* = 6.0, 2H, H_d), 4.54-4.62 (m, 6H, $H_{j,k,r}$), 6.55 (d, *J* = 2.5, 1H, H_i), 6.62 (d, *J* = 2.5, 1H, H_g), 6.78-6.83 (m, 2H, H_c), 7.04-7.08 (m, 2H, H_b), 7.43-7.49 (m, 2H, $H_{l,q}$), 7.74-7.79 (m, 2H, $H_{m,p}$), 8.38-8.43 (m, 2H, $H_{n,o}$). ^{13}C NMR ($CDCl_3$, 100 MHz): δ 16.1, 20.5, 28.2, 39.1, 51.1, 57.4, 57.5, 66.4, 81.0, 82.7, 84.3, 84.4, 86.2, 86.8, 88.2, 88.5, 109.2 (x 2), 114.3, 120.9, 121.0,

127.4, 127.6, 129.8 (x 2), 137.2 (x 2), 141.9, 142.2, (x 2), 143.5, 154.3, 155.2, 155.6, 156.7. LRESI-MS (MeOH/TFA, 99:1): *m/z* = 595 $[M+H]^+$, 617 $[M+Na]^+$. HRESI-MS (MeOH/NH_4OAc): *m/z* = 595.2713 $[M+H]^+$ (calc. for $C_{38}H_{35}N_4O_3$ 595.2704 $[M+H]^+$).

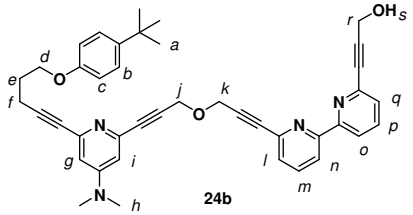

24b

18 (0.682 g, 2.26 mmol, 1.0 equiv.) and **23b** (1.05 g, 2.26 mmol, 1.0 equiv.) were dissolved in toluene (30 mL) and Et_3N (20 mL). $Pd(dppf)Cl_2$ (92.0 mg, 0.110 mmol, 0.05 equiv.) and CuI (43.0 mg, 0.230 mmol, 0.1 equiv.) were then added as solids and the resulting reaction mixture was heated to 100 °C for 40 minutes at atmospheric pressure in a CEM microwave reactor (power level = 150 W). The reaction was then quenched with aqueous ammonia (20% b/w, 25 mL) and extracted with CH_2Cl_2 (4 x 70 mL). The organic phase was washed with water (20 mL) and brine (20 mL) and then dried ($MgSO_4$). The solvent was removed under reduced pressure and the crude residue was subjected to column chromatography on silica (CH_2Cl_2:acetone 9:1), giving **24b** as a white solid, m.p. 80-82 ºC (0.838 g, 60%). ^1H NMR ($CDCl_3$, 400 MHz): δ 1.28 (s, 9H, H_a), 2.05-2.09 (m, 2H, H_e), 2.61 (t, *J* = 6.4, 2H, H_f), 2.60-2.75 (br, 1H, H_s), 2.95 (s, 6H, H_h), 4.07 (t, *J* = 6.0, 2H, H_d), 4.57 (s, 4H, $H_{j,k}$), 4.60 (s, 2H, H_r), 6.54 (d, *J* = 2.4, 1H, H_i), 6.61 (d, *J* = 2.4, 1H, H_g), 6.83-6.85 (m, 2H, H_c), 7.27-7.29 (m, 2H, H_b), 7.43-7.48 (m, 2H, $H_{l,q}$), 7.75 (t, *J* = 7.6, 2H, $H_{m,p}$), 8.36-8.40 (m, 2H, $H_{n,o}$). ^{13}C NMR ($CDCl_3$, 100 MHz): δ 16.1, 28.2, 31.5, 34.0, 39.2, 51.4, 57.4, 57.5, 66.3, 81.1, 82.6, 84.4, 84.9, 86.2, 86.9, 87.5, 88.5, 109.2, 109.3, 114.0, 121.0, 121.1, 126.2, 127.4, 127.7, 137.2 (x 2), 142.0, 142.1, 142.3, 143.3, 143.6, 154.3, 155.6, 155.7, 156.6. LRESI-MS (acetonitrile): *m/z* = 637 $[M+H]^+$. HRESI-MS: *m/z* = 637.3176 $[M+H]^+$ (calc. for $C_{41}H_{41}N_4O_3$ 637.3173 $[M+H]^+$).

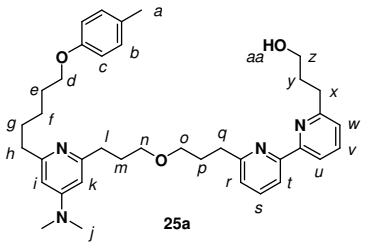

25a

24a (0.540 g, 0.910 mmol, 1.0 equiv.) was dissolved in THF (40 mL) and $Pd(OH)_2/C$ (20% b/w, 0.108 g) was added. The mixture was thoroughly degassed and then stirred at RT under a hydrogen atmosphere for 5 h. Then the reaction was filtered through celite, washing with acetone and the resulting filtrate concentrated under reduced pressure to give the title compound as a pale brown oil (0.536 g, 97%). ^{1}H NMR ($CDCl_3$, 400 MHz): δ 1.52 (m, 2H, H_f), 1.68-1.85 (m, 4H, $H_{e,g}$), 1.94-2.16 (m, 6H, $H_{m,p,y}$), 2.26 (s, 3H, H_a), 2.63-2.68 (m, 2H, H_h), 2.71-2.77 (m, 2H, H_l), 2.91-2.95 (m, 8H, $H_{j,q}$), 3.01-3.04 (m, 2H, H_x), 3.46-3.52 (m, 4H, $H_{n,o}$), 3.74 (t, *J* = 5.9, 2H, H_z), 3.90 (t, *J* = 6.6, 2H, H_d), 6.20 (d, *J* = 2.4, 1H, H_i), 6.24 (d, *J* = 2.4, 1H, H_k), 6.75-6.79 (m, 2H, H_c), 7.02-7.06 (m, 2H, H_b), 7.14-7.17 (m, 2H, $H_{t,u}$), 7.69-7.72 (m, 2H, $H_{s,v}$), 8.12 (d, *J* = 7.4, 1H, H_r), 8.25 (d, *J* = 7.8, 1H, H_w). ^{13}C NMR ($CDCl_3$, 100 MHz): δ 20.4, 25.9, 29.2, 29.5, 30.1, 30.3, 31.1, 34.8, 35.3, 35.4, 38.8, 39.3, 62.4, 67.9, 70.2, 70.4, 102.9, 103.0, 114.3, 118.3, 119.0, 122.9, 123.0, 129.6, 129.8, 137.2, 137.6, 155.3 (x 2), 155.9, 156.9 160.7, 161.2 (x 2), 161.7. LRESI-MS (MeOH/TFA 99:1): *m/z* = 611 $[M+H]^+$. HRESI-MS (MeOH/NH_4OAc): *m/z* = 633.3770 $[M+Na]^+$ (calc. for $C_{38}H_{50}N_4O_3Na$ 633.3775 $[M+Na]^+$).

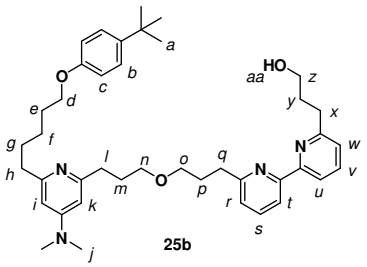

25b

24b (0.544 g, 0.850 mmol, 1.0 equiv.) was dissolved in THF (40 mL) and $Pd(OH)_2/C$ (20% b/w, 0.108 g) was added. The mixture was thoroughly degassed and then stirred at RT under a hydrogen atmosphere for 5 h. Then, the reaction was filtered through celite, washing with acetone and the resulting filtrate concentrated under reduced pressure to give the title compound as pale brown oil (0.559 g, 99%). ^{1}H

NMR ($CDCl_3$, 400 MHz): δ 1.29 (s, 9H, H_a), 1.48-1.56 (m, 2H, H_f), 1.71-1.82 (m, 4H, $H_{e,g}$), 1.98-2.14 (m, 6H, $H_{m,p,y}$), 2.65-2.67 (m, 2H, H_h), 2.72-2.74 (m, 2H, H_l), 2.91-2.98 (m, 8H, $H_{j,q}$), 3.02-3.08 (m, 2H, H_x), 3.48-3.53 (m, 4H, $H_{n,o}$), 3.76 (t, *J* = 5.6, 2H, H_z), 3.93 (t, *J* = 6.4, 2H, H_d), 6.21 (d, *J* = 2.4, 1H, H_i), 6.24 (d, *J* = 2.4, 1H, H_k), 6.79-6.83 (m, 2H, H_c), 7.17 (t, *J* = 7.6, 2H, $H_{t,u}$), 7.26-7.30 (m, 2H, H_b), 7.71-7.75 (m, 2H, $H_{s,v}$), 8.11 (d, *J* = 8.0, 1H, H_r), 8.26 (d, *J* = 8.0, 1H, H_w). ^{13}C NMR ($CDCl_3$, 100 MHz): δ 26.0, 29.3, 29.5, 30.2, 30.3, 31.2, 31.5, 34.0, 34.8, 35.3, 35.4, 38.9, 39.2, 62.4, 67.8, 70.2, 70.5, 102.9, 103.0, 113.9, 118.2, 119.0, 122.9, 123.0, 125.5, 126.2, 137.3, 137.7, 143.0, 155.2, 155.3, 155.9, 156.8, 160.7, 161.2, 161.7. LRESI-MS (acetonitrile): *m/z* = 653 $[M+H]^+$. HRESI-MS: *m/z* = 653.4423 $[M+H]^+$ (calc. for $C_{41}H_{57}N_4O_3$ 653.4425 $[M+H]^+$).

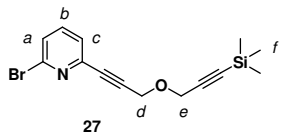

27

To a solution of 2-bromo-6-iodopyridine (**26**, 1.99 g, 7.03 mmol, 1.0 equiv.) in THF (50 mL) and Et_3N (25 mL) were added CuI (0.260 g, 1.40 mmol, 0.2 equiv.) and $Pd(PPh_3)_2Cl_2$ (0.490 g, 0.700 mmol, 0.1 equiv.). Trimethyl-(3-prop-2-ynyloxy-prop-1-ynyl)-silane (**16**, 1.16 g, 7.03 mmol, 1.0 equiv.) was then added to the reaction mixture *via* syringe and the solution was stirred at RT for 16 h. Subsequently, the solvents were removed under reduced pressure, the resulting residue redissolved in EtOAc and washed with aqueous NH_4Cl (2 x 50 mL) and brine (50 mL). The organic extracts were collected and dried with Na_2SO_4. After concentration under reduced pressure, the crude residue was purified by column chromatography on silica (9:1 then 8:2 hexane:Et_2O) yielding **27** as a white solid, m.p. 64-66 ºC (2.04 g, 90%). ^{1}H NMR ($CDCl_3$, 400 MHz): δ 0.00 (s, 9H, H_f), 4.12 (s, 2H, H_e), 4.30 (s, 2H, H_d), 7.21 (dd, J_1 = 7.4, J_2 = 1.0, 1H, H_c), 7.26 (dd, J_1 = 8.0, J_2 = 1.0, 1H, H_a), 7.29-7.36 (m, 1H, H_b). ^{13}C NMR ($CDCl_3$, 100 MHz): δ 0.0, 57.1, 58.0, 84.8, 86.4, 92.8, 100.5, 126.3, 128.1, 138.6, 142.0, 143.2. LRESI-MS (MeOH/TFA, 99/1): *m/z* = 322 $[M^{79}Br+H]^+$, 324 $[M^{81}Br+H]^+$. HRESI-MS (MeOH/TFA 99:1): *m/z* = 322.0258 $[M^{79}Br+H]^+$ (calc. for $C_{14}H_{17}{}^{79}BrNOSi$ 322.0257 $[M+H]^+$).

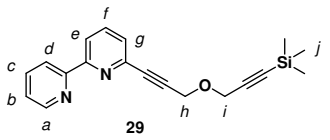

29

To a solution of **27** (2.80 g, 8.69 mmol, 1.0 equiv.) in THF (20 mL) was added $Pd(PPh_3)_4$ (1.00 g, 0.869 mmol, 0.1 equiv.). 2-Pyridylzinc bromide (**28**, 0.5 M in THF, 23.0 mL, 11.5 mmol, 1.3 equiv.) was added *via* syringe, and the reaction mixture was then heated to reflux for 20 h. The THF was then removed under reduced pressure and the resulting residue was redissolved in EtOAc and washed with aqueous EDTA/K_2CO_3 (2 x 100 mL). The layers were separated, the aqueous phase extracted with EtOAc (3 x 100 mL) and the combined organic extracts washed with brine and dried with Na_2SO_4. After concentration under reduced pressure, the crude residue was purified by column chromatography on silica (hexane:Et_2O, 8:2 then 6:4) providing **29** as a orange oil (1.81 g, 65%). ^{1}H NMR ($CDCl_3$, 400 MHz): δ 0.20 (s, 9H, H_j), 4.36 (s, 2H, H_i), 4.54 (s, 2H, H_h), 7.30-7.34 (m, 1H, H_b), 7.48 (dd, J_1 = 7.7, J_2 = 1.0, 1H, H_g), 7.79-7.83 (m, 2H, $H_{c,f}$), 8.36-8.38 (m, 1H, H_e), 8.42-8.44 (m, 1H, H_d), 8.67-8.69 (m, 1H, H_a). ^{13}C NMR ($CDCl_3$, 100 MHz): δ 0.0, 57.4, 57.9, 84.4, 86.4, 92.6, 100.7, 120.9, 121.7, 124.3, 127.5, 137.1, 137.3, 142.2, 149.3, 155.5, 156.7. LRESI-MS (MeOH/TFA, 99/1): *m/z* = 321 $[M+H]^+$, 343 $[M+Na]^+$. HRESI-MS (MeOH/TFA 99:1): *m/z* = 321.1419 $[M+H]^+$ (calc. for $C_{19}H_{21}N_2OSi$ 321.1418 $[M+H]^+$).

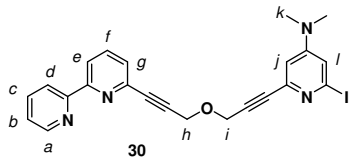

30

2,6-DiiodoDMAP (**19**, 1.86 g, 5.00 mmol, 1.0 equiv.) and **29** (1.60 g, 5.00 mmol, 1.0 equiv.) were dissolved in degassed benzene (50 mL). $Pd(PPh_3)_2Cl_2$ (0.350 g, 0.490 mmol, 0.1 equiv.) and CuI (0.200 g, 1.05 mmol. 0.2 equiv.) were then added as solids. Subsequently, DBU (4.57 g, 4.48 mL, 30.0 mmol, 6.0 equiv.) and water (0.100 g, 0.100 mL, 5.55 mmol, 1.1 equiv.) were added to the reaction mixture and the resulting brown solution was stirred at RT for 36 h, during which time a white precipitate formed and the solution became black. The reaction mixture was quenched with water (10 mL) and extracted with EtOAc (3 x 50 mL). The organic

layer was then washed with an aqueous saturated NH_4Cl solution (2 x 50 mL), and brine (2 x 50 mL). The combined organic fractions were dried (Na_2SO_4), filtered, concentrated under reduced pressure, and then subjected to column chromatography on silica (solvent gradient, EtOAc:hexane, 1:1 to 7:3) to give **30 as** a yellow oil (1.56 g, 65%). ^{1}H NMR (400 MHz, $CDCl_3$): δ 2.87 (s, 6H, H_k), 4.49 (s, 2H, H_i), 4.52 (s, 2H, H_h), 6.58 (d, *J* = 2.3, 1H, H_j), 6.76 (d, *J* = 2.3, 1H, H_l), 7.30-7.28 (m, 1H, H_b), 7.41 (d, *J* = 7.4, 1H, H_g), 7.75-7.70 (m, 2H, $H_{c,f}$), 8.30 (d, *J* = 7.8, 1H, H_e), 8.37 (d, *J* = 8.0, 1H, H_d), 8.59 (d, *J* = 4.7, 1H, H_a). ^{13}C NMR (100 MHz, $CDCl_3$): δ 39.2, 57.5, 57.6, 83.8, 84.1, 85.9, 86.5, 111.0, 116.3, 118.3, 120.7, 121.5, 124.1, 127.3, 136.9, 137.2, 141.9, 142.0, 149.1, 154.4, 155.3, 156.5. LRESI-MS (MeOH/TFA): *m/z* = 495 $[M+H]^+$. HRESI-MS: *m/z* = 495.0673 $[M+H]^+$ (calc. for $C_{23}H_{20}IN_4O$ 495.0676 $[M+H]^+$).

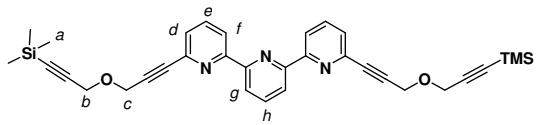

32

A suspension of 6,6''-dibromo-2,2':6',2''-terpyridine (**31**, 1.00 g, 2.30 mmol, 1.0 equiv.) in toluene (50 mL) and Et_3N (15 mL) was degassed with nitrogen for 30 minutes. Subsequently, $Pd(dppf)_2Cl_2$ (56.0 mg, 70.0 μmol, 0.03 equiv.), CuI (26.0 mg, 0.140 mmol, 0.06 equiv.), and trimethyl-(3-prop-2-ynyloxy-prop-1-ynyl)-silane (**16**, 1.15 g, 6.90 mmol, 3.0 equiv.) were added and the reaction mixture stirred at 105 ˚C for 6 h. The reaction mixture was then cooled to RT, filtered through celite, and the solvents were removed *in vacuo* to give 1.50 g of crude product which was purified by means of a short column (alumina (basic, activity II), hexane:Et_2O 1:1) to yield **32** as a tan solid, m.p. 110-112 ˚C (1.20 g, 93%). ^{1}H NMR (400 MHz, $CDCl_3$): δ 0.20 (s, 18H, H_a), 4.37 (s, 4H, H_b), 4.55 (s, 4H, H_c), 7.50 (dd, J_1 = 8.0, J_2 = 1.0, 2H, H_d), 7.83 (t, *J* = 8.0, 2H, H_e), 7.95 (t, *J* = 8.0, 1H, H_h), 8.50 (d, *J* = 8.0, 2H, H_g), 8.57 (dd, J_1 = 8.0, J_2 = 1.0, 2H, H_f). ^{13}C NMR (100 MHz, $CDCl_3$): δ 0.0, 57.4, 57.9, 84.4, 86.4, 92.6, 100.7, 121.0, 121.9, 127.6, 137.2, 138.2, 142.2, 154.7, 156.7. LRESI-MS (acetonitrile): *m/z* = 562 $[M+H]^+$. HRESI-MS: *m/z* = 562.2347 $[M+H]^+$ (calc. for $C_{33}H_{36}O_2N_3Si_2$ 562.2341$[M+H]^+$).

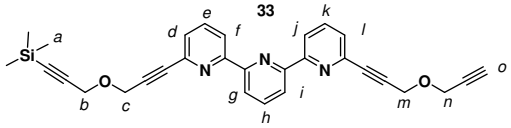

33

To a solution of **32** (1.08 g, 1.92 mmol, 1.0 equiv.) in THF (15 mL) and MeOH (70 mL) at 0 ˚C was added finely ground K_2CO_3 (1.52 g, 1.10 mmol, 1.0 equiv.). After 30 minutes, TLC analysis (alumina, hexanes:Et_2O, 1:1) showed that traces of the doubly-deprotected species had begun to form, and so the reaction was quenched by adding saturated aqueous NH_4Cl (30 mL). The mixture was then extracted with EtOAc (3 x 100 mL), the combined organic layers washed with brine (100 mL) and dried over $MgSO_4$. After evaporation of the solvents the crude product was dissolved in 1 mL CH_2Cl_2, and subjected to column chromatography on silica (15% EtOAc in hexanes with 5% Et_3N) to yield unreacted starting material **32** (0.484 g, 45%), the completely de-silylated *bis*-terminal acetylene (80.0 mg, 10 %) and the desired mono-deprotected alkyne **33** as a white solid, m.p. 106-108 ˚C (0.421 g, 45 %). ^{1}H NMR (400 MHz, $CDCl_3$): δ 0.22 (s, 9H, H_a), 2.50 (t, J = 2.4, 1H, H_o), 4.34 (s, 2H, H_b), 4.38 (d, J = 2.4, 2H, H_n), 4.55 (s, 2H, H_c), 4.57 (s, 2H, H_m), 7.50 (dd, J_1 = 8.0, J_2 = 1.0, 2H, $H_{d,l}$), 7.83 (dt, J_1 = 8.0, J_2 = 1.0, 2H, $H_{e,k}$), 7.95 (t, J = 8.0, 1H, H_h), 8.53 (d, J = 8.0, 2H, $H_{g,i}$), 8.57 (dt, J_1 = 8.0, J_2 = 1.0, 2H, $H_{f,j}$). ^{13}C NMR (100 MHz, $CDCl_3$): δ 0.0, 57.0, 57.4 (x 2), 57.9, 75.4, 79.0, 84.1, 84.4, 86.3, 86.5, 92.5, 100.6, 120.8, 120.9, 121.9 (x 2), 127.5 (x 2), 137.2 (x 2), 138.1, 142.1 (x 2), 154.6 (x 2), 156.6 (x 2). LRESI-MS (acetonitrile): *m/z* = 512 $[M+Na]^+$. HRESI-MS: *m/z* = 490.1952 $[M+H]^+$ (calc. for $C_{30}H_{28}N_3O_2Si$ 490.1945 $[M+H]^+$).

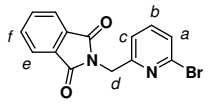

35

To a solution of PPh_3 (0.950 g, 3.62 mmol, 1.2 equiv.) in dry THF (30 mL) was added DIAD (0.650 mL, 3.30 mmol, 1.1 equiv.) dropwise at 0 ˚C. The mixture was stirred for 15 minutes at this temperature during which time a creamy white suspension formed. 2-Bromo-6-(hydroxymethyl)-pyridine (**34**, 0.567 g, 3.02 mmol, 1.0 equiv.) in THF (2 mL) was then added dropwise at 0 ˚C and the mixture stirred for another 20 minutes at 0 ˚C. After this, phthalimide (0.485 g, 3.30 mmol, 1.1 equiv.) was added as a solid in one portion. The mixture became an orange

solution and was stirred for 16 h without further cooling. Subsequently, the solution was concentrated to give an orange oil which was purified by means of a short silica column (CH_2Cl_2) to give the pure title compound as a cream solid, m.p. 124-126 ˚C (0.813 g, 85 %). ^{1}H NMR (400 MHz, $CDCl_3$): δ 4.99 (s, 2H, H_d), 7.16 (d, *J* = 7.6, 1H, H_c), 7.37 (d, *J* = 7.6, 1H, H_a), 7.48 (t, *J* = 7.6, 1H, H_b), 7.74-7.78 (m, 2H, H_f), 7.88-7.92 (m, 2H, H_e). ^{13}C NMR (100 MHz, $CDCl_3$): δ 42.5, 119.9, 123.6, 127.0, 132.1, 134.2, 139.0, 141.9, 156.9, 167.9. LRESI-MS (acetonitrile): *m/z* = 317 $[M^{79}Br+H]^+$, 319 $[M^{81}Br+H]^+$. HRESI-MS: *m/z* = 316.9923 $[M^{79}Br+H]^+$ (calc. for $C_{14}H_{10}{}^{79}BrN_2O_2$ 316.9920 $[M^{79}Br+H]^+$).

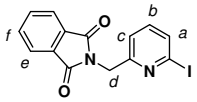

36

A solution of N,N'-dimethylethylenediamine (41.0 mg, 50.0 μL, 0.470 mmol, 0.1 equiv.) in dry dioxane (35 mL) was degassed with nitrogen for 30 minutes. Subsequently, CuI (45.0 mg, 0.240 mmol, 0.05 equiv.), NaI (8.90 g, 59.0 mmol, 12.5 equiv.), and **35** (1.50 g, 4.73 mmol, 1.0 equiv.) were added and the mixture stirred vigorously at 105 ˚C for 48 h. The reaction mixture was then allowed to cool to RT, before aqueous ammonia (20 % b/w, 25 mL) was added and the mixture extracted into EtOAc (3 x 50 mL). The combined organic layers were washed with brine, then water, and dried with $MgSO_4$. The crude product thus obtained was then purified by column chromatography on alumina (basic, activity II, eluting in CH_2Cl_2), to give the title compound as a white solid, m.p. 138-140 ˚C (1.55 g, 90%). ^{1}H NMR (400 MHz, $CDCl_3$): δ 4.98 (s, 2H, H_d), 7.15 (d, *J* = 7.8, 1H, H_c), 7.25 (t, *J* = 7.8, 1H, H_b), 7.60 (t, *J* = 7.8, 1H, H_a), 7.74-7.78 (m, 2H, H_f), 7.88-7.92 (m, 2H, H_e). ^{13}C NMR (100 MHz, $CDCl_3$): δ 42.5, 117.8, 120.1, 123.6, 132.1, 133.8, 134.2, 138.0, 157.3, 167.9. LRESI-MS (acetonitrile): *m/z* = 365 $[M+H]^+$. HRESI-MS: *m/z* = 364.9784 $[M+H]^+$ (calc. for $C_{14}H_{10}IN_2O_2$ 364.9781 $[M+H]^+$).

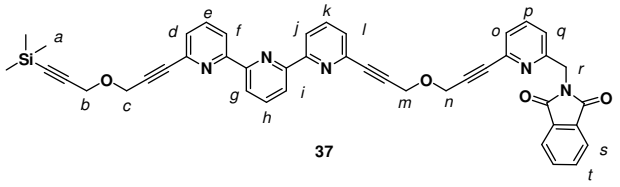

37

A solution of **36** (0.280 g, 0.770 mmol, 0.95 equiv.) in a mixture of THF (10 mL) and Et_3N (7 mL) was degassed with nitrogen for 30 minutes at 35 ˚C. After addition of $Pd(PPh_3)_4$ (36.0 mg, 30.0 μmol, 0.04 equiv.) and CuI (6.00 mg, 30.0 μmol, 0.04 equiv.), acetylene **33** (0.402 g, 0.820 mmol, 1.0 equiv.) in THF (7.5 mL) was added over 2 h at 35 ˚C *via* syringe. The reaction mixture was then stirred for 5 days at 35 ˚C until TLC analysis (alumina, hexane:Et_2O, 1:1) showed complete consumption of **36**. After cooling to RT and filtering through celite, the solvents were evaporated, the residue washed with aqueous ammonia (15 % b/w, 30 mL) and extracted with EtOAc (3 x 70 mL). The combined organic layers were washed with brine, then water and dried with $MgSO_4$. The crude product was purified by column chromatography on silica (CH_2Cl_2 then CH_2Cl_2:MeOH, 100:2) to yield **37** (0.505 g, 85%) as a cream foam. ^{1}H NMR (400 MHz, $CDCl_3$): δ 0.20 (s, 9H, H_a), 4.36 (s, 2H, H_b), 4.55 (s, 2H, H_n), 4.60 (s, 4H, $H_{c,m}$), 5.02 (s, 2H, H_r), 7.15 (d, *J* = 8.0, 1H, H_q), 7.36 (d, *J* = 8.0, 1H, H_o), 7.50 (d, *J* = 7.6, 2H, $H_{d,l}$), 7.59 (t, *J* = 8.0, 1H, H_p), 7.72-7.76 (m, 2H, H_t), 7.83 (t, *J* = 7.6, 2H, $H_{e,k}$), 7.87-7.91 (m, 2H, H_s), 7.94 (t, *J* = 7.6, 1H, H_h), 8.48-8.52 (m, 2H, $H_{g,i}$), 8.57 (d, *J* = 7.6, 2H, $H_{f,j}$). ^{13}C NMR (100 MHz, $CDCl_3$): δ 0.0, 43.2, 57.4, 57.7 (x 2), 57.9, 84.3, 84.4, 84.8, 86.3, 86.4, 86.5, 92.6, 100.7, 120.7, 120.9, 121.9, 122.0, 123.8, 123.9 126.3, 127.6 (x 2), 132.3, 134.4 (x 2), 137.2, 137.3, 138.2, 142.1, 142.2, 142.5, 154.7 (x 2), 156.3, 156.7 (x 2), 168.2. LRESI-MS (acetonitrile): *m/z* = 726 $[M+H]^+$, 748 $[M+Na]^+$, 764 $[M+K]^+$. HRESI-MS: *m/z* = 726.2527 $[M+H]^+$ (calc. for $C_{44}H_{36}N_5O_4Si$ 726.2531 $[M+H]^+$).

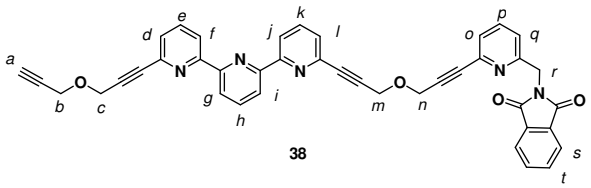

38

To a stirred solution of **37** (0.505 g, 0.697 mmol, 1.0 equiv.) in MeOH (50 mL) and THF (25 mL) at 0 ºC was added K_2CO_3 (96.0 mg, 0.697 mmol, 1.0 equiv.) in one portion. After 3 h, TLC analysis (alumina, Et_2O) showed complete consumption of

the starting material and so the reaction mixture was quenched with saturated aqueous NH_4Cl (50 mL) and extracted with EtOAc (3 x 75 mL). The combined organic layers were washed with brine, then water and dried with $MgSO_4$. Evaporation of the solvents yielded **38** (0.432 g, 95%) as a yellow oil. ^{1}H NMR (400 MHz, $CDCl_3$): δ 2.50 (t, *J* = 2.4, 1H, H_a), 4.38 (d, *J* = 2.4, 2H, H_b), 4.57 (s, 2H, H_n), 4.60 (s, 4H, $H_{c,m}$), 5.02 (s, 2H, H_r), 7.15 (d, *J* = 7.6, 1H, H_q), 7.36 (d, *J* = 7.6, 1H, H_o), 7.48-7.52 (m, 2H, $H_{d,l}$), 7.59 (t, *J* = 7.6, 1H, H_p), 7.72-7.77 (m, 2H, H_t), 7.83 (t, *J* = 7.8, 2H, $H_{e,k}$), 7.87-7.91 (m, 2H, H_s), 7.94 (t, *J* = 7.8, 1H, H_h), 8.48-8.52 (m, 2H, $H_{g,i}$), 8.58-8.54 (m, 2H, $H_{f,j}$). ^{13}C NMR (100 MHz, $CDCl_3$): δ 43.0, 56.9, 57.2, 57.5 (x 2), 75.3, 78.9, 84.0, 84.1, 84.6, 86.1, 86.3, 86.5, 120.5, 120.7, 120.8, 121.7, 121.8, 123.6, 126.2, 127.4 (x 2), 132.1, 134.2, 137.0, 137.1 (x 2), 138.0, 141.9, 142.0, 142.3, 154.5 (x 2), 156.1, 156.5 (x 2), 168.0. LRESI-MS (acetonitrile): *m/z* = 654 $[M+H]^+$, 676 $[M+Na]^+$, 692 $[M+K]^+$. HRESI-MS: *m/z* = 654.2130 $[M+H]^+$ (calc. for $C_{41}H_{28}N_5O_4$ 654.2136 $[M+H]^+$).

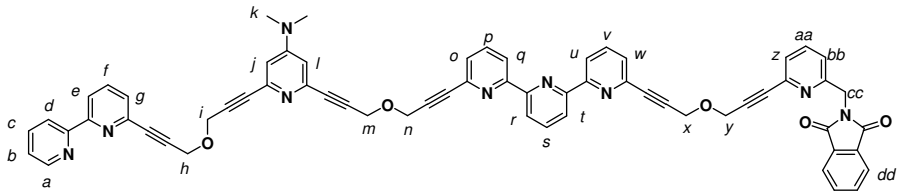

39

A solution of **30** (0.327 g, 0.662 mmol, 1.0 equiv.) in a mixture of THF (10 mL) and Et_3N (7 mL) was degassed with nitrogen for 30 minutes at 35 ˚C. After addition of $Pd(PPh_3)_4$ (33.0 mg, 27.0 μmol, 0.04 equiv.) and CuI (5.10 mg, 27.0 μmol, 0.04 equiv.), the acetylene **38** (0.432 g, 0.662 mmol, 1.0 equiv.) in THF (7.5 mL) was added over 2 h at 35 ˚C *via* syringe. The reaction mixture was then stirred for 5 days at 35 ˚C until TLC analysis (alumina, hexane:Et_2O, 1:1) showed complete consumption of the starting materials. After cooling to RT and filtering through celite, the solvents were evaporated, the residue washed with aqueous ammonia (15 % b/w, 30 mL) and extracted with EtOAc (3 x 70 mL). The combined organic layers were washed with brine, then water and dried with $MgSO_4$. The crude product was purified by column chromatography on silica (CH_2Cl_2 then CH_2Cl_2:MeOH, 100:2) to yield **39** as a creamy-white solid, 100 ºC (dec.) (0.438 g, 65%). ^{1}H NMR (400 MHz, $CDCl_3$): δ 2.97 (s, 6H, H_k), 4.57-4.62 (m, 12H, $H_{h,i,m,n,x,y}$), 5.01 (s, 2H,

H_{cc}), 6.65 (s, 2H, $H_{j,l}$), 7.14 (d, *J* = 8.0, 1H, H_{bb}), 7.28-7.31 (m, 1H, H_b), 7.35 (d, *J* = 8.0, 1H, H_z), 7.46-7.50 (m, 3H, $H_{g,o,w}$), 7.58 (t, *J* = 8.0, 1H, H_{aa}), 7.73-7.90 (m, 8H, $H_{c,f,p,v,dd,ee}$), 7.93 (t, *J* = 7.8, 1H, H_s), 8.35 (d, *J* = 8.0, 1H, H_e), 8.44 (d, *J* = 8.0, 1H, H_d), 8.49 (d, *J* = 7.8, 2H, $H_{r,t}$), 8.55 (d, *J* = 8.0, 2H, $H_{q,u}$), 8.66-8.63 (m, 1H, H_a). ^{13}C NMR (100 MHz, $CDCl_3$): δ 39.2, 43.0, 57.4 (x 4), 57.5 (x 2), 82.8 (x 2), 84.1, 84.2 (x 2), 84.6, 86.2 (x 2), 86.4, 86.5, 86.8 (x 2), 109.7, 120.5 (x 2), 120.7 (x 2), 121.5, 121.8, 123.6, 124.1, 126.2, 127.4 (x 2), 128.5, 128.6, 132.0 (x 3), 132.1 (x 2), 134.2, 137.0 (x 3), 137.1, 138.0, 141.9 (x 2), 142.3, 142.6, 149.1, 154.3, 154.5 (x 2), 155.3, 156.1, 156.5 (x 3), 168.0 LRESI-MS (acetonitrile): *m/z* = 1020 $[M+H]^+$, 1042 $[M+Na]^+$, 1058 $[M+K]^+$. HRESI-MS: *m/z* = 1020.3611 $[M+H]^+$ (calc. for $C_{64}H_{46}N_9O_5$ 1020.3616 $[M+H]^+$).

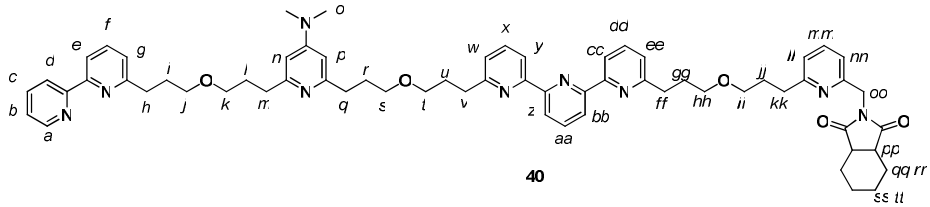

40

39 (0.378 g, 0.371 mmol, 1.0 equiv.) was dissolved in THF/EtOH (40 mL/40 mL) and PtO_2 (84.0 mg, 0.371 mmol, 1.0 equiv.) was added. The solution was then thoroughly saturated with hydrogen, and left to stir under a hydrogen atmosphere overnight. The reaction mixture was then filtered through a plug of celite, washing succesively with acetone and THF. After evaporation of the solvents, the crude product was purified by column chromatography (alumina IV, CH_2Cl_2:MeOH, slow gradient 100:0.2 to 100:2), giving **40** as a brown oil (0.250 g, 63%). ^{1}H NMR (400 MHz, $CDCl_3$): δ 1.50-1.41 (m, 4H, $H_{ss,tt}$), 1.82-2.16 (m, 16H, $H_{i,l,r,u,gg,jj,qq,rr}$), 2.72-2.81 (m, 6H, $H_{m,q,kk}$), 2.88-3.00 (m, 14H, $H_{h,o,v,ff,pp}$), 3.38-3.53 (m, 12H, $H_{j,k,s,t,hh,ii}$), 4.76 (s, 2H, H_{oo}), 6.23 (s, 2H, $H_{n,p}$), 6.95-7.01 (m, 2H, $H_{ll,nn}$), 7.14-7.18 (m, 3H, $H_{g,w,ee}$), 7.24-7.27 (m, 1H, H_b), 7.48 (t, *J* = 7.7, 1H, H_{mm}), 7.67-7.79 (m, 4H, $H_{c,f,x,dd}$), 7.89 (t, *J* = 7.8, 1H, H_{aa}), 8.17 (d, *J* = 7.8, 1H, H_e), 8.39-8.48 (m, 5H, $H_{d,y,z,bb,cc}$), 8.63-8.65 (m, 1H, H_a). ^{13}C NMR (100 MHz, $CDCl_3$): δ 21.7, 23.7, 29.4 (x 3), 30.2, 34.6, 34.7 (x 3), 35.3 (x 2), 39.1, 39.7, 42.8, 53.4, 70.0 (x 2), 70.1 (x 3), 70.4 (x 2), 102.9, 117.9, 118.1, 118.2 (x 2), 120.7 (x 2), 121.1, 121.3, 122.7 (x 2), 122.8, 123.3, 123.4, 132.1, 133.9, 136.6, 136.7, 136.8, 136.9, 137.5, 148.9, 153.9, 155.1 (x 2),

155.3, 155.5 (x 3), 156.4, 160.9 (x 2), 161.0 (x 2), 161.3, 179.5. LRESI-MS (acetonitrile): *m/z* = 1051 $[M+H]^+$. HRESI-MS: *m/z* = 1050.5980 $[M+H]^+$ (calc. for $C_{64}H_{76}N_9O_5$ 1050.5964 $[M+H]^+$).

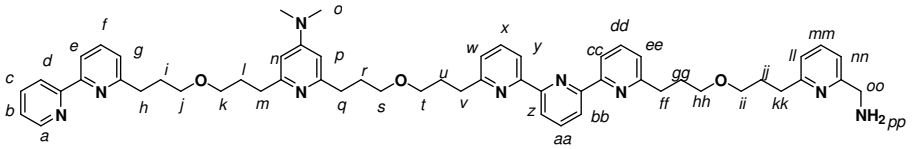

41

40 (0.035 g, 0.030 mmol, 1.0 equiv) was dissolved in EtOH (2 mL) and hydrazine monohydrate (8.0 mg, 8.0 µL, 0.15 mmol, 5.0 equiv.) was added *via* microsyringe. The reaction was heated to reflux for 6 days, at which point TLC analysis (alumina, CH_2Cl_2:MeOH, 20:1) showed no starting material present. The crude mixture was concentrated under reduced pressure and subjected to column chromatography (alumina grade IV, CH_2Cl_2:MeOH 100:0.2 to 100:5 (slow gradient)), giving **41** as a yellow gum (5.0 mg, 18%). ^{1}H NMR (400 MHz, $CDCl_3$): δ 1.70-1.90 (br, 2H, H_{pp}), 1.96-2.17 (m, 12H, $H_{i,l,r,u,gg,jj}$), 2.71-2.76 (m, 4H, $H_{m,q}$), 2.84-2.88 (m, 2H, H_{kk}), 2.92-2.98 (m, 12H, $H_{h,o,v,ff}$), 3.44-3.54 (m, 12H, $H_{j,k,s,t,hh,ii}$), 3.92 (s, 2H, H_{oo}), 6.27 (s, 2H, $H_{n,p}$), 7.02 (d, *J* = 7.6, 1H, H_{ll}), 7.06 (d, *J* = 7.6, 1H, H_{nn}), 7.15-7.19 (m, 3H, $H_{g,w,ee}$), 7.25-7.29 (m, 1H, H_b), 7.52 (t, *J* = 7.6, 1H, H_{mm}), 7.67-7.80 (m, 4H, $H_{c,f,x,dd}$), 7.90 (t, *J* = 7.8, H_{aa}), 8.18 (d, *J* = 7.4, 1H, H_e), 8.40-8.49 (m, 5H, $H_{d,y,z,bb,cc}$), 8.63-8.67 (m, 1H, H_a). LRESI-MS (acetonitrile): *m/z* = 915 $[M+H]^+$.

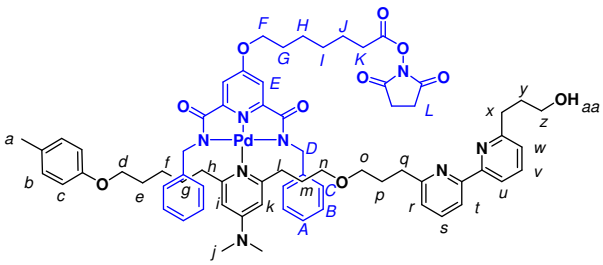

42

To a solution of **25a** (0.217 g, 0.355 mmol, 1.0 equiv.) in d_7-DMF (2 mL) was added a solution of **11a** (0.260 g, 0.355 mmol, 1.0 equiv.) in d_7-DMF (1 mL), and the solution stirred at RT for 1 h. The initially yellow solution was seen to turn dark brown. After this time, the reaction mixture was poured into CH_2Cl_2 (300 mL), and

washed with water (2 x 150 mL) and then brine (2 x 150 mL). After drying over Na_2SO_4, the crude reaction mixture was concentrated under reduced pressure to afford a brown residue, which was columned on silica (eluting in 1:1 CH_2Cl_2:acetone) to give the title compound as a yellow gum (0.413 g, 89%). ^{1}H NMR (400 MHz, $CDCl_3$): δ 1.25-1.39 (m, 4H, $H_{f,g}$), 1.45-1.54 (m, 4H, $H_{H,I}$), 1.60-1.70 (m, 4H, $H_{e,m}$), 1.74-1.88 (m, 4H, $H_{G,J}$), 2.02-2.10 (m, 4H, $H_{p,y}$), 2.27 (s, 3H, H_a), 2.63 (t, *J* = 7.2, 2H, H_K), 2.74-2.93 (m, 10H, $H_{h,l,q,L}$), 3.02-3.10 (m, 8H, $H_{j,x}$), 3.23 (t, *J* = 6.7, 2H, H_n), 3.46 (t, *J* = 6.4, 2H, H_o), 3.75 (t, *J* = 5.7, 2H, H_z), 3.86 (t, *J* = 6.4, 2H, H_d), 3.97-4.12 (m, 6H, $H_{D,F}$), 6.11 (d, *J* = 2.5, 2H, H_i), 6.17 (d, *J* = 2.5, 2H, H_k), 6.71-6.80 (m, 6H, $H_{c,C}$), 7.01-7.09 (m, 8H, $H_{b,A,B}$), 7.13-7.19 (m, 2H, $H_{t,u}$), 7.27 (s, 2H, H_E), 7.75-7.84 (m, 2H, $H_{s,v}$), 8.12 (d, *J* = 7.5, 1H, H_r), 8.26 (d, *J* = 7.5, 1H, H_w). ^{13}C NMR (100 MHz, $CDCl_3$): δ 20.4, 24.4, 25.2, 25.5, 25.9, 27.4, 28.0, 28.1, 28.2, 29.0, 29.3, 30.8, 31.2, 34.6, 35.2 (x 2), 38.6, 39.4, 49.7, 62.3, 67.6, 69.3, 70.0, 70.2, 103.4, 103.6, 110.7, 114.2, 118.2, 118.9, 122.8, 123.0, 126.1, 127.5, 127.8, 129.6, 129.8, 137.2, 137.6, 141.3, 154.1, 155.2, 155.4, 155.8, 156.8, 160.6, 161.0, 161.4, 161.9, 168.5, 168.9, 169.2, 171.3. LRESI-MS (MeOH): *m/z* = 1302 $[M^{106}Pd+H]^+$.

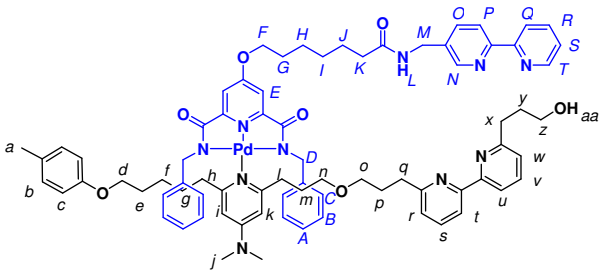

43

42 (0.240 g, 0.184 mmol, 1.0 equiv.) was dissolved in dry CH_2Cl_2 (10 mL) and added to a solution of 5-(aminomethyl)-2,2'-bipyridine (34.0 mg, 0.184 mmol, 1.0 equiv.) in dry CH_2Cl_2 (10 mL), and the reaction mixture stirred at RT overnight. After this time, the crude mixture was concentrated *in vacuo* to give a yellowish oil, which was subjected to column chromatography (basic alumina, activity IV, CH_2Cl_2:MeOH, 99:1) to yield **43** as a yellow solid, m.p. 48-50 °C (0.179 g, 71%). ^{1}H NMR (400 MHz, $CDCl_3$): δ 1.18-1.50 (m, 8H, $H_{f,g,H,I}$), 1.52-1.81 (m, 8H, $H_{e,m,G,J}$), 2.00-2.08 (m, 4H, $H_{p,y}$), 2.22-2.30 (m, 5H, $H_{a,K}$), 2.73-2.77 (m, 2H, H_h), 2.83-2.92 (m, 4H, $H_{l,q}$), 3.00-3.11 (m, 8H, $H_{j,x}$), 3.23 (t, *J* = 6.6, 2H, H_n), 3.45 (t, *J* = 6.4, 2H,

H_o), 3.78 (t, J = 5.9, 2H, H_z), 3.86 (t, J = 6.4, 2H, H_d), 3.96-4.08 (m, 6H, $H_{D,F}$), 4.49 (d, J = 5.7, 2H, H_M), 6.11 (d, J = 2.3, 1H, H_i), 6.17 (d, J = 2.3, 1H, H_k), 6.40 (t, J = 5.7, 1H, H_L), 6.72-6.78 (m, 6H, $H_{c,C}$), 7.01-7.08 (m, 8H, $H_{b,A,B}$), 7.12-7.18 (m, 2H, $H_{t,u}$), 7.22 (s, 2H, H_E), 7.27-7.32 (m, 1H, H_S), 7.67-7.76 (m, 3H, $H_{s,v,O}$), 7.80 (dt, J_1 = 7.8, J_2 = 1.8, 1H, H_R), 8.11 (d, J = 7.7, 1H, H_r), 8.26 (d, J = 7.7, 1H, H_w), 8.31-8.37 (m, 2H, $H_{P,Q}$), 8.58 (d, J = 1.9, 1H, H_N), 8.66 (d, J = 4.1, 1H, H_T). ^{13}C NMR (100 MHz, $CDCl_3$): δ 20.4, 25.3, 25.4 (x 2), 25.9, 27.4, 28.0, 28.6, 29.0, 29.3, 31.2, 34.6, 35.2 (x 3), 36.4, 39.4, 40.8, 49.8, 62.3, 67.6, 69.3, 70.0, 70.1, 103.4, 103.6, 110.7, 114.2, 118.2 (x 2), 118.9, 120.9, 121.0, 122.8, 123.0, 123.6, 123.7, 124.8, 126.1, 127.5, 127.6, 127.8, 128.6, 129.8, 143.3, 134.5, 136.4, 136.5, 136.9, 137.2, 137.6, 141.3, 148.6, 149.1, 154.1, 155.5, 155.8, 161.0, 161.9, 168.8, 171.3, 173.0. LRESI-MS (MeOH): *m/z* = 1372 $[M+H]^+$, 1394 $[M+Na]^+$. HRESI-MS: *m/z* = 1371.5960 $[M+H]^+$ (calc. for $C_{77}H_{89}N_{10}O_7{}^{106}Pd$ 1371.5969 $[M+H]^+$), 686.3018 $[M+2H]^{2+}$ (calc. for $C_{77}H_{90}N_{10}O_7{}^{106}Pd$ 686.3020 $[M+2H]^{2+}$.

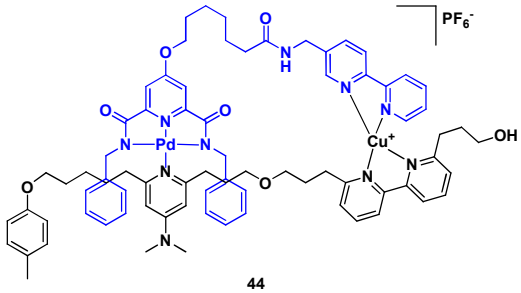

44

43 (0.022 g, 0.016 mmol, 1.0 equiv.) was suspended in dry CH_3CN (20 mL), and a solution of $[Cu(CH_3CN)_4](PF_6)$ (6.0 mg, 0.016 mmol, 1.0 equiv.) in dry CH_3CN (1 mL) was added dropwise over 10 minutes. Upon complete addition, all the ligand was seen to have dissolved and the previously yellow solution was deep red. The reaction mixture was stirred at RT for 30 minutes, before being concentrated *in vacuo* to give **44** as a dark red solid (0.025 g, 99%). LRESI-MS (MeOH/TFA, 99:1): *m/z* = 1434 $[M^{106}Pd\text{-}PF_6]^+$.

4.7 References and Notes

(1) Crowley, J. D.; Leigh, D. A.; Lusby, P. J.; McBurney, R. T.; Perret-Aebi, L. E.; Petzold, C.; Slawin, A. M. Z.; Symes, M. D. *J. Am. Chem. Soc.* **2007**, *129,* 15085-15090.

(2) Cárdenas, D. J.; Livoreil, A.; Sauvage, J.-P. *J. Am. Chem. Soc.* **1996**, *118,* 11980-11981.

(3) Livoreil, A.; Dietrich-Buchecker, C. O.; Sauvage, J.-P. *J. Am. Chem. Soc.* **1994**, *116,* 9399-9400.

(4) Livoreil, A.; Sauvage, J.-P.; Armaroli, N.; Balzani, V.; Flamigni, L.; Ventura, B. *J. Am. Chem. Soc.* **1997**, *119,* 12114-12124.

(5) Armaroli, N.; Balzani, V.; Collin, J.-P.; Gaviña, P.; Sauvage, J.-P.; Ventura, B. *J. Am. Chem. Soc.* **1999**, *121,* 4397-4408.

(6) Durola, F.; Sauvage, J.-P. *Angew. Chem. Int. Ed.* **2007**, *46,* 3537-3540.

(7) Gaviña, P.; Sauvage, J.-P. *Tetrahedron Lett.* **1997**, *38,* 3521-3524.

(8) Jiménez, M. C.; Dietrich-Buchecker, C.; Sauvage, J.-P. *Angew. Chem. Int. Ed.* **2000***, 39,* 3284-3287.

(9) Jimenez-Molero, M. C.; Dietrich-Buchecker, C.; Sauvage, J.-P. *Chem. Eur. J.* **2002***, 8,* 1456-1466.

(10) Letinois-Halbes, U.; Hanss, D.; Beierle, J. M.; Collin, J.-P.; Sauvage, J.-P. *Org. Lett.* **2005**, *7,* 5753-5756.

(11) Poleschak, I.; Kern, J.-M.; Sauvage, J.-P. *Chem. Commun.* **2004**, 474-476.

(12) Raehm, L.; Kern, J.-M.; Sauvage, J.-P. *Chem. Eur. J.* **1999***, 5,* 3310-3317.

(13) Kalsani, V.; Schmittel, M.; Listorti, A.; Accorsi, G.; Armaroli, N. *Inorg. Chem.* **2006***, 45,* 2061-2067.

(14) The lowest energy state at thermodynamic equilibrium is that in which the walker forms the smallest macrocyclic chelate with the track, as this structure allows the highest number of degrees of freedom to the track as a whole. The thermodynamics associated with the reversible formation of large (30-60 member) macrocycles has been modelled by Dua and Cherayil, using parameters intended to

mimic "semi-rigid" molecular structures, where some degrees of freedom are restricted in the acyclic starting materials. Such parameters seem well-suited to the current system, which contains both flexible and rigid components. Dua and Cherayil find that the standard free energy of cyclisation varies linearly with the chain length, *N*, with the formation of macrocycles becoming less favourable as *N* gets larger, see: Dua, A.; Cherayil, B. J. *J. Chem. Phys.* **2002**, *117*, 7765-7773.

(15) Sonogashira, K.; Tohda, Y.; Hagihara, N. *Tetrahedron Lett.* **1975**, *16,* 4467-4470.

(16) Fang, Y.-Q.; Hanan, G. *Synlett.* **2003**, 852-854.

(17) Newkome, G. R.; Hager, D. C.; Kiefer, G. E. *J. Org. Chem.* **1986***, 51,* 850-853.

(18) Cai, D.; Hughes, D. L.; Verhoeven, T. R. *Tetrahedron Lett.* **1996***, 37,* 2537-2540.

(19) Hideg, K.; Hankovszky, H. O.; Lex, L.; Kulcsár, G. *Synthesis* **1980**, 911-914.

(20) Fuller, A.-M.; Leigh, D. A.; Lusby, P. J.; Oswald, I. D. H.; Parsons, S.; Walker, D. B. *Angew. Chem. Int. Ed.* **2004**, *43,* 3914-3918.

(21) Furusho, Y.; Matsuyama, T.; Takata, T.; Moriuchi, T.; Hirao, T. *Tetrahedron Lett.* **2004**, *45,* 9593-9597.

(22) Leigh, D. A.; Lusby, P. J.; Slawin, A. M. Z.; Walker, D. B. *Angew. Chem. Int. Ed.* **2005**, *44,* 4557-4564.

(23) Dwyer, A. N.; Grossel, M. C.; Horton, P. N. *Supramol. Chem.* **2004***, 16,* 405-410.

(24) Milani, B.; Alessio, E.; Mestroni, G.; Sommazzi, A.; Garbassi, F.; Zangrando, E.; Bresciani-Pahor, N.; Randaccio, L. *J. Chem. Soc., Dalton Trans.,* **1994**, *13,* 1903-1911.

(25) For a recent review on the use of similar pyridine-based Pd(II) coordination motifs to create various highly stable extended structures, see: Tominaga, M.; Fujita, M. *Bull. Chem. Soc. Jpn.* **2007**, *80,* 1473-1482.

(26) Panetta, C. A.; Kumpaty, H. J.; Heimer, N. E.; Leavy, M. C.; Hussey, C. L. *J. Org. Chem.* **1999***, 64,* 1015-1021.

(27) The coupling of **12** and 5-amino-2,2'-bipyridine was also attempted, but no reaction was observed. CPK modelling suggested that increasing the linker length by one CH_2 unit (by using 5-(aminomethyl)-2,2'-bipyridine instead) would not have any detrimental effects with regards to the walker's coordination to the track.

(28) Bai, X.-L.; Liu, X.-D.; Wang, M.; Kang, C.-Q.; Gao, L.-X. *Synthesis* **2005**, 458-464.

(29) Chang, H.-T.; Jeganmohan, M.; Cheng, C. H. *Org. Lett.* **2007**, *9,* 505-508.

(30) Failure to hydrogenate the acetylene spacers was found to greatly reduce the solubility of the track and led to the Pd(II)-containing foot becoming labile in coordinating solvents at room temperature.

(31) Trécourt, F.; Breton, G.; Bonnet, V.; Mongin, F.; Marsais, F.; Quéguiner, G. *Tetrahedron Lett.* **1999**, *40,* 4339-4342.

(32) Trécourt, F.; Breton, G.; Bonnet, V.; Mongin, F.; Marsais, F.; Quéguiner, G. *Tetrahedron* **2000**, *56,* 1349-1360.

(33) Negishi, E.; King, A. O.; Okukado, N. *J. Org. Chem.* **1977**, *42,* 1821-1823.

(34) Mitsunobu, O.; Yamada, M. *Bull. Chem. Soc. Jpn.* **1967**, *40,* 2380-2382.

(35) Klapars, A.; Buchwald, S. L. *J. Am. Chem. Soc.* **2002**, *124,* 14844-14845.

CHAPTER FIVE

Towards a Molecular Walking System Based on Co(II)/Co(III) Redox Chemistry

Acknowledgements and Declaration

The syntheses of compounds **9-12**, **15-17**, **19**, **20** and **22-32** were performed by Dr. Daniel D'Souza and Dr. Romen Carrillo.

Synopsis

The apparent dynamic exchange shown by the Cu(I) complex of the putative molecular walker in Chapter Four means that a new switch orthogonal to the Pd(II) ligand exchange chemistry must be found. Given this, it was decided to try and keep the existing track if possible, and to screen other metals in the search for improved kinetic stability of the track/walker ensembles.

Complexes of cobalt seemed to present an attractive alternative to the Cu(I)/Cu(II) redox switch in this regard. When the metal is in its divalent oxidation state, cobalt complexes are generally quite labile, exchanging ligands readily under mild conditions. However, oxidation to Co(III) slows ligand exchange markedly, to the extent that Co(III) complexes are often said to be inert *to exchange. Both Co(II) and Co(III) are kinetically stable oxidation states under standard laboratory conditions, but conversion between the two can be achieved using very mild procedures. Hence it was envisaged that Co(III) complexes could act as effective ratchets under the rather forcing conditions necessary for the Pd(II)-containing foot to step, but that reduction to Co(II) would allow for the second foot to move without affecting the state of the Pd(II) centre. This Chapter addresses the search for suitable ligand sets for cobalt displaying the desired switchable kinetics, along with a discussion of how a thermodynamic bias might be incorporated into such systems to allow directional walking. An improved walker design based on these considerations will then be proposed, and details given of the progress towards this new target to date.*

5.1 Introduction

Following the disappointing results obtained in Chapter Four using Cu(I), it was decided that the processivity of stepping should be a paramount consideration in any new walking system design. Hence a highly reliable "on/off" kinetic switch was sought, which could be easily converted between its labile and inert forms. The Co(II)/Co(III) redox system seemed well suited to this task for several reasons. Firstly and most importantly, Co(III) polypyridyl complexes are well known for their extremely slow rates of ligand exchange,[1] whilst Co(II) polypyridyl complexes are rather more labile. Hence when in its divalent oxidation state, stepping of the cobalt-containing foot would be possible, whilst oxidation to Co(III) should give highly stable walker/track complexes that would allow processive stepping of the Pd(II)-containing foot. Secondly, the stimuli for switching between Co(II) and Co(III) would still rely on redox chemistry, and so would be orthogonal to the switching mechanism for the palladium complexes used as the other foot/foothold combination.

The issue of directionality was initially considered secondary to making sure that the walker stayed on the track. However, it was hoped that some measure of bias could be introduced during stepping by altering the nature and number of auxiliary ligands on the cobalt (Scheme 5.1). Hence it was envisioned that adding a Co(II) source such as $CoCl_2.6H_2O$ would favour formation of $Co(bipy)_2Cl_2$-type complexes, with the anionic chlorides remaining bound to the metal centre and disfavouring the formation of $[Co(terpy)(bipy)Cl]^+$-type systems. Oxidation to Co(III) would then give kinetically inert complexes of the generic type $[Co(bipy)_2Cl_2]^+$, stable enough to anchor the walker to the track whilst the Pd(II)-containing foot moved. Subsequent reduction of Co(III) to Co(II) would then make these complexes more labile, at which point washing the walker system with an aqueous EDTA solution would remove the cobalt salt entirely. By then adding a Co(II) salt lacking any coordinating anions, such as $Co(ClO_4)_2.6H_2O$, it was hoped to bias the system in favour of the higher-valency chelating coordination site, giving complexes of the form $[Co(terpy)(bipy)L]^{2+}$, where L is a solvent molecule or an additional equivalent of coordinating anion. Literature precedents for compounds of the type $Co(bipy)_2Cl_2$,[2] $[Co(bipy)_2Cl_2]^+$ [2,3] and $[Co(terpy)(bipy)L]^{2+}$ [4-6] gave cause for some optimism that

such an approach would prove profitable, especially as the existing track and walker unit seemed ideal structures for such a system.

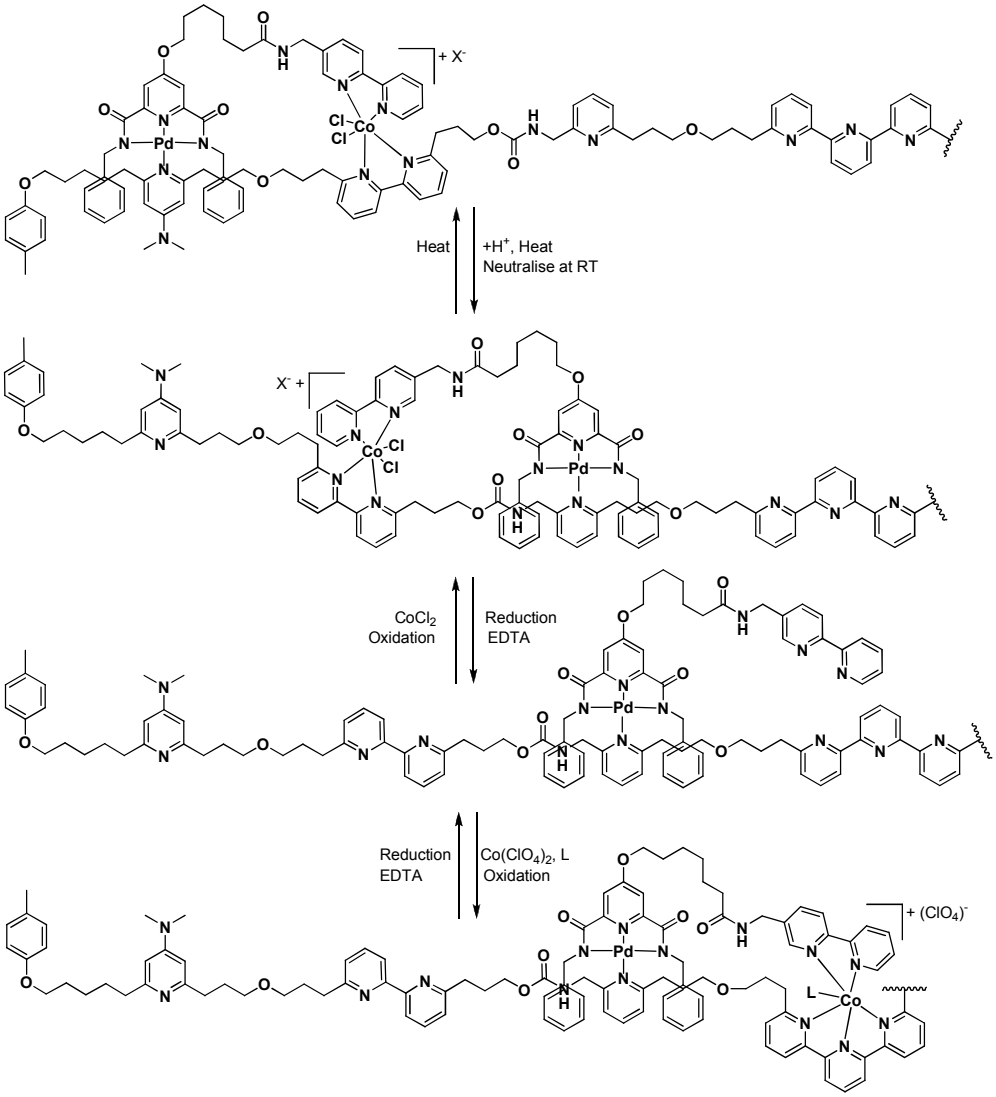

Scheme 5.1 Proposed operation of the walker based on cobalt chemistry. Both Co(II) and Co(III) favour octahedral coordination environments, and so additional auxiliary ligands must be added to encourage the cobalt to take the quadra-dentate walker/track chelating binding site. Only the first four stations of the methylphenol-labelled ensemble are shown for clarity.

5.2 Model Studies

To this end, the walker/track system **1** was suspended in acetonitrile and treated with one equivalent of $CoCl_2.6H_2O$ with gentle heating (Scheme 5.2). A marked colour change from yellow to blue accompanied the complete dissolution of the ligand, and the formation of the hetero-bimetallic species **2** was supported by ESI-MS (*m/z* = 1465, 1467 = $[\mathbf{2}\text{-}^{37}Cl]^+$, $[\mathbf{2}\text{-}^{35}Cl]^+$).

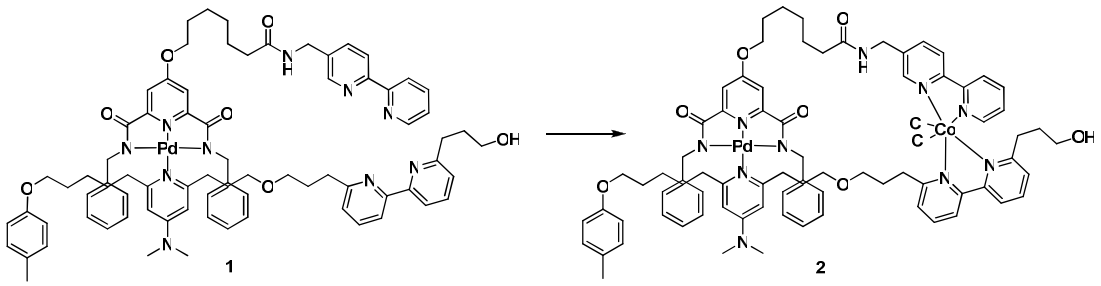

Scheme 5.2 Synthesis of **2**. Reagents and conditions: (i) $CoCl_2.6H_2O$, CH_3CN, 30 mins, 40 ˚C.

However, cyclic voltammetry studies on **2** in DMF with 0.1 M TBABF as supporting electrolyte revealed no wave corresponding to oxidation of Co(II) to Co(III) in the region -1.5 to +1.5 V *vs*. (Ag/AgCl) (Figure 5.2), despite the redox couple of similar species being reported to lie well within this range.[7]

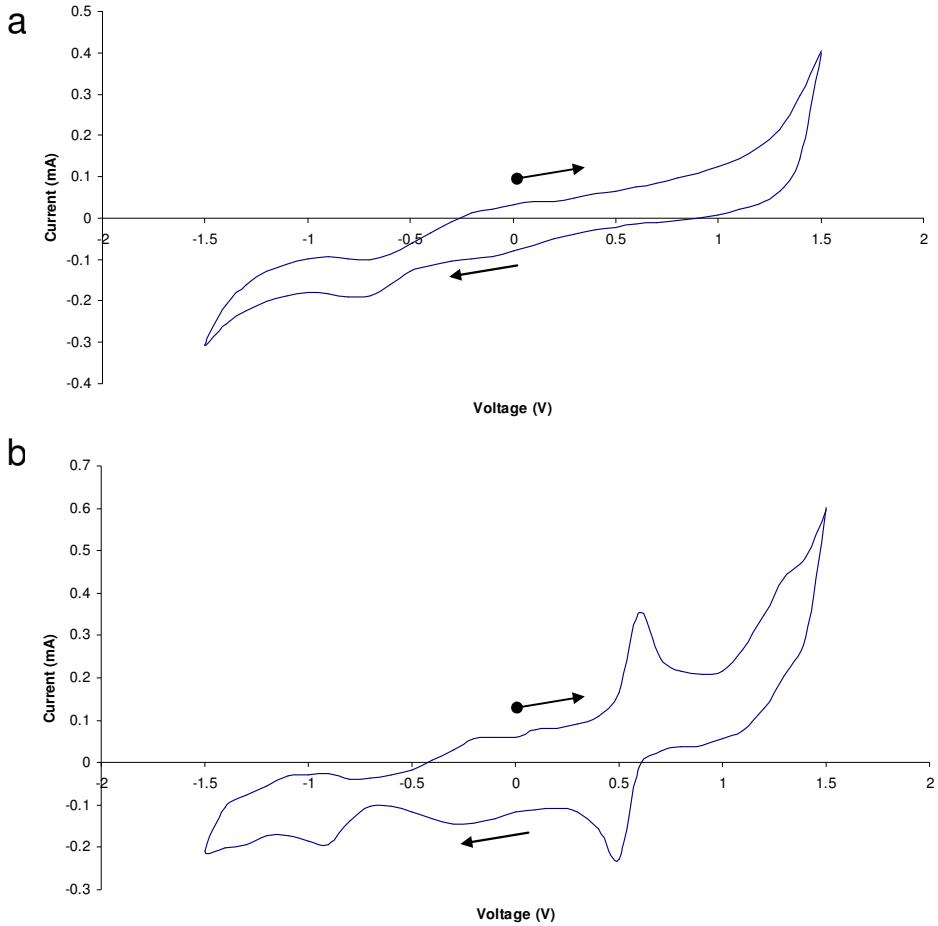

Figure 5.2a Cyclic voltammogram of a 1 mM solution of **2** in DMF, with 0.1 M TBABF as the supporting electrolyte. **b** Cyclic voltammogram of the same solution, in the presence of 1 mM ferrocene for reference. The reversible oxidation wave at ~ +0.55 V corresponds to the ferrocene/ferrocinium redox couple. Both voltammograms were recorded at 298 K under an N_2 atmosphere at a scan rate of 200 mV s^{-1}. ● denotes the start/end point of the scan.

In order to uncover the reason for this lack of redox activity, the two substituted bipyridyls **3** and **5** were added to solutions of $CoCl_2.6H_2O$ and the reactivity of the resulting complexes towards the mild oxidants ferrocinium hexafluorophosphate and iodine probed by ^{1}H NMR (Scheme 5.3).

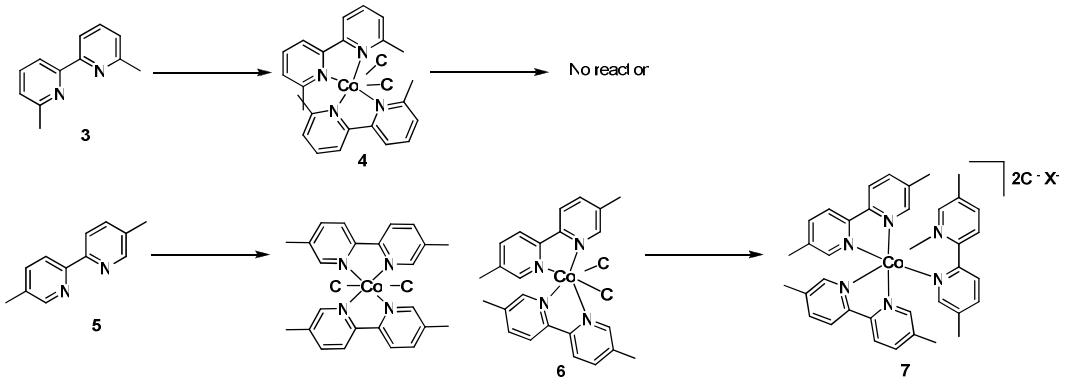

Scheme 5.3 Preparation and attempted oxidation of the model compounds **4** and **6**. Reagents and conditions: (i) $CoCl_2.6H_2O$, MeOH, 15 mins, RT, (ii) ferrocinium hexafluorophosphate, MeOH, 1 h, RT *or* I_2, MeOH, 5 mins, RT. X = I or PF_6.

Surprisingly, although formation of complex **4** seemed to proceed rapidly, producing a turquoise solid with only the molecular ion visible by ESI-MS (*m/z* = 214 = $[Co(6,6'\text{-dimethyl-}2,2'\text{-bipyridine})_2]^{2+}$), all subsequent attempts to oxidise the metal centre proved unsuccessful, as judged by ^{1}H NMR (only broad signals, indicative of paramagnetic species were observed in the range -5 to +15 ppm relative to tetramethylsilane) and the naked eye (the complex did not change colour). When the substitution pattern of the bipyridyl ligand was changed from 6,6'-dimethyl (as in the track fragment of **1**) to 5,5'-dimethyl (as for the foot of the walker), reaction with $CoCl_2.6H_2O$ gave an orange solution, which was treated with ferrocinium hexafluorophosphate in methanol at room temperature. Within seconds the colour of the reaction mixture had changed to brown and a green precipitate was seen to form. After filtering off the precipitate, the brown filtrate was extracted with hexane (to remove any reduced ferrocene formed during the reaction) until the hexane layer was colourless, and concentrated to give a brown solid. The mass spectrum of this solid (**6**) was identical to that found for **4**, and ^{1}H NMR analysis again evinced the presence of paramagnetic species, indicating that oxidation of Co(II) to Co(III) had not occurred. However, the green precipitate (**7**) did give a clean ^{1}H NMR spectrum, consistent with a highly symmetrical diamagnetic species containing 5,5'-dimethyl-

2,2'-bipyridine, but with the peaks greatly shifted compared with the free ligand. Hence it initially appeared that the Co(III) compound *trans*-[Co(5,5'-dimethyl-2,2'-bipyridine)$_2$Cl$_2$]PF$_6$ had been produced.[2,3] CPK modelling of **4** and **6** gave some indication as to the difference in behaviour of these compounds upon oxidation. Oxidation of Co(II) to Co(III) brings about a marked reduction in the ionic radius of the metal (from 0.65 to 0.55 Å),[8,9] drawing the surrounding ligands closer in space. In the case of **4**, the bulky methyl groups only just allow formation of *cis*-Co(6,6'-dimethyl-2,2'-bipyridine)$_2$Cl$_2$, and any further contraction of the structure in response to oxidation of the metal centre is not possible (*trans*-Co(6,6'-dimethyl-2,2'-bipyridine)$_2$Cl$_2$ cannot form at all). However, CPK modelling of **6** suggested that whilst formation of *cis*-Co(5,5'-dimethyl-2,2'-bipyridine)$_2$Cl$_2$ was somewhat disfavoured on steric grounds, formation of *trans*-Co(5,5'-dimethyl-2,2'-bipyridine)$_2$Cl$_2$ should be *even less favourable*, and so any oxidation of either of these species to give stable Co(III) complexes was highly unlikely. On the other hand, CPK suggested that formation of complexes of the type [Co(5,5'-dimethyl-2,2'-bipyridine)$_3$]$^{2+}$ was facile, with apparently no steric factors preventing contraction of the metal centre within that ligand set. Moreover, the resulting oxidised complexes of the type [Co(5,5'-dimethyl-2,2'-bipyridine)$_3$]$^{3+}$ should display highly symmetrical ^{1}H NMR spectra, consistent with that already obtained. This supposition was given further credence by ESI-MS on the green precipitate, which gave mass ions at *m/z* = 204, 214 and 305 corresponding to [Co(5,5'-dimethyl-2,2'-bipyridine)$_3$]$^{3+}$, [Co(5,5'-dimethyl-2,2'-bipyridine)$_2$]$^{2+}$, and [Co(5,5'-dimethyl-2,2'-bipyridine)$_3$]$^{2+}$ respectively. Repeating these reactions using iodine as the oxidant instead of ferrocinium hexafluorophosphate (in either methanol or acetonitrile) also proved efficacious for preparing [Co(5,5'-dimethyl-2,2'-bipyridine)$_3$]$^{3+}$ moieties, but gave no diamagnetic species corresponding to any *bis*-bipy Co(III)-dichloride compounds of either 6,6'-dimethyl-2,2'-bipyridine or 5,5'-dimethyl-2,2'-bipyridine.

To confirm the unexpected formation and oxidation of **7**, it was decided to prepare the same complex by a different route and compare the spectroscopic data obtained. Hence, three equivalents of 5,5'-dimethyl-2,2'-bipyridine were dissolved in deuterated methanol, and a methanolic solution containing one equivalent of

$Co(ClO_4)_2.6H_2O$ was added, gving a bright yellow solution. A solution of iodine in deuterated methanol was then added to this solution until the colour of iodine was seen to persist in the reaction mixture, at which point ^1H NMR analysis of the crude mix indicated the quantitative formation of a highly symmetrical diamagnetic species containing 5,5'-dimethyl-2,2'-bipyridine, with peak shifts identical to those seen for complex **7**. ESI-MS of this mixture evinced the presence of mass peaks (corresponding to *m/z* = 204, 214 and 305) consistent with the formation of $[Co(5,5'\text{-dimethyl-2,2'-bipyridine})_3]^{3+}$.

The failure to make any stable Co(III)-dichloride *bis*-bipyridyl species, coupled with the remarkable ease with which $[Co(5,5'\text{-dimethyl-2,2'-bipyridine})_3](ClO_4)_2I$ could be synthesised, led to the idea of using some sort of bipyridyl moiety in place of the two auxiliary ligands on Co(III) in the first instance (Scheme 5.1). Model studies carried out on $[Co(phen)_3](ClO_4)_2I$ (prepared *via* oxidation of $[Co(phen)_3](ClO_4)_2$ with iodine[10]) showed that there was no exchange of ligands around the Co(III) centre when this complex was heated in deuterated acetonitrile in the presence of excess 2,2'-bipyridine or 2,2':6',2''-terpyridine (terpy), as judged by variable temperature ^1H NMR, and ^1H NMR and ESI-MS of the reaction mixture after 12 hours at 100 ˚C (Scheme 5.4).

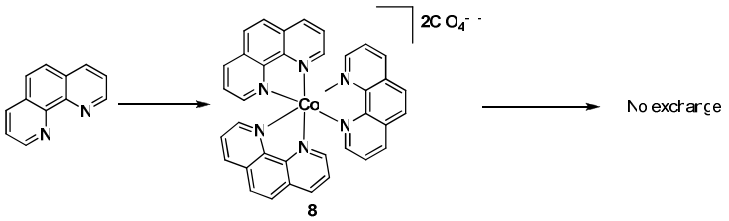

Scheme 5.4 The high kinetic stability of $[Co(phen)_3](ClO_4)_2I$, as shown by its lack of ligand exchange in coordinating solvents at elevated temperatures in the presence of competing ligands. Reagents and conditions: (i) $Co(ClO_4)_2.6H_2O$, CD_3CN, I_2, 5 mins, RT, (ii) *either* excess 2,2'-bipyridine, CD_3CN, 12 h, 100 ˚C, *or* excess 2,2':6',2''-terpyridine, CD_3CN, 12 h, 100 ˚C.

Furthermore, in the course of these model studies, an unexpected thermodynamic bias in favour of $[Co(phen)_3](ClO_4)_2I$ over $[Co(terpy)_2](ClO_4)_2I$ was discovered (Scheme 5.5). Treatment of two equivalents of terpy in deuterated acetonitrile with one equivalent of $Co(ClO_4)_2.6H_2O$ led to formation of a dark red solution of $[Co(terpy)_2](ClO_4)_2.H_2O$, as previously reported.[10-12] However, addition of three equivalents of 1,10-phenanthroline to this solution immediately produced a change in

colour from deep red to orange. Oxidation of this mixture with iodine then gave an orange solid after extraction with hexane, showing major peaks in its ^{1}H NMR spectrum corresponding to uncomplexed terpy and $[Co(phen)_3](ClO_4)_2I$, with $[Co(terpy)_2](ClO_4)_2I$ present only in small amounts and no uncomplexed phen visible at all. Again, heating this mixture to 100 ˚C overnight in CD_3CN produced no further ligand exchange. Hence it seemed that the complex $[Co(phen)_3](ClO_4)_2I$ showed the required kinetic stability necessary to act as one foot/foothold combination, and that a high level of thermodynamic bias was possible in favour of the *tris*-phen complex when the cobalt was in its divalent oxidation state. Oxidation would then "freeze" this thermodynamic distribution as the analogous inert Co(III) complexes.

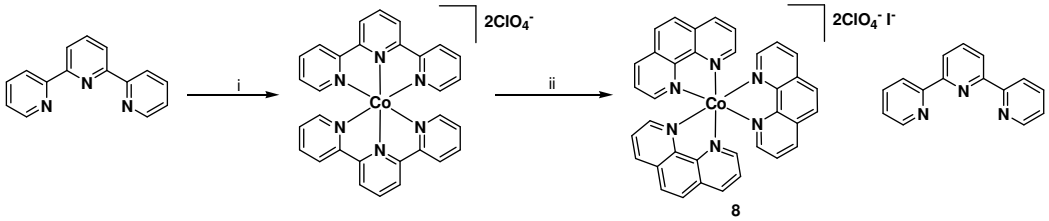

Scheme 5.5 Co(II) shows a thermodynamic bias for $[Co(phen)_3](ClO_4)_2I$ over $[Co(terpy)_2](ClO_4)_2I$. Reagents and conditions: (i) $Co(ClO_4)_2.6H_2O$, CD_3CN, <5 mins, RT, (ii) 1,10-phenanthroline; then I_2, 5 mins, RT.

Removal of the cobalt from $[Co(phen)_3](ClO_4)_2I$ was achieved by dissolving the complex in methanol and adding five equivalents of activated zinc powder as a solid. After stirring for 15 minutes at room temperature the initial orange colour had disappeared from the solution phase, which was almost colourless. At this point the reaction mixture was poured into dichloromethane and washed with an aqueous EDTA solution, giving a pale blue aqueous layer and a colourless organic fraction, from which uncomplexed phen was recovered in quantitative yield. In contrast, if $[Co(phen)_3](ClO_4)_2I$ was dissolved in a 1:1 mixture of methanol and an aqueous EDTA solution, no colour change was observed and no uncomplexed phen could be recovered by extraction with dichloromethane. These results served to confirm the high stability of $[Co(phen)_3](ClO_4)_2I$ with respect to ligand dissociation from the metal, as well as providing a mild route to reduction and removal of cobalt from such complexes.

Given the lower steric demands of a *tris*-bipyridyl ligand set on the metal centre compared with a $(bipy)_2Cl_2$ ligand set, the analogous model reactions were carried out on the original walker/track ligand **1**, to see if the species $[Co\mathbf{1}(phen)](ClO_4)_2I$ could be prepared. To this end, **1** was suspended in deuterated acetonitrile and one equivalent of $Co(ClO_4)_2.6H_2O$ was added, giving a deep yellow solution. One equivalent of 1,10-phenanthroline was then added as the auxiliary ligand, causing the solution to brighten significantly, before oxidation with a solution of excess iodine in acetonitrile was attempted. However, the resulting ^1H NMR spectrum of the crude reaction mixture showed $[Co(phen)_3](ClO_4)_2I$ as the only identifiable diamagnetic species, serving as final confirmation that the original track design (substitution at the 6,6' positions) did not constitute a suitable ligand environment for Co(III). However, it was noted during the course of these reactions that the Pd(II) complex in unit **1** was stable to both the oxidation and reduction/removal conditions developed for the Co(II)/Co(III) redox switch (i.e. oxidation with iodine, followed by reduction with activated zinc and removal of the Co(II) with EDTA). It was also noted that after removal of the Co(II) with EDTA, the auxilliary bidentate ligand could be easily removed from the reaction mixture by recrystallisation from an acetonitrile / diethyl ether solvent system.

On account of this apparent chemical orthogonality between the two switches, as well as the excellent kinetic and thermodynamic properties shown by $[Co(phen)_3]X_3$ complexes, it was decided to change the substitution pattern of the track bidentate binding sites to the 5,5'-isomers in order to accommodate Co(III). 5,5'-Disubstituted bipyridine was chosen for the track in preference to 3,8-disubstituted phenanthroline due to the relative ease of synthesis of the 5,5'-dibromo-2,2'-bypridyl starting material.[13] It was also decided at this point to change the amine protecting group on the four-station track unit from phthalimide to *tert*-butoxycarbonyl (BOC), which should be more stable to hydrogenation and hence present fewer problems with removal compared to phthalimide (see Chapter Four and Section 5.3). Furthermore, it was resolved to reduce the acetylenes in the first two-station block of the track with deuterium gas, so that the two almost identical DMAP stations could be distinguished from one another. This would allow the chemical shifts and integration

of the ^{1}H NMR signals of the methylene protons adjacent to the DMAP stations to be used to assign which DMAP station (if either) the walker was on.

After the first step of the Pd(II)-containing foot, the cobalt-containing foot would be required to assume a quasi-five coordinate binding site between the bidentate walker ligand and the terpyridyl station of the track (Scheme 5.1). CPK modelling indicated that there should be few steric constraints to oxidation with this site, with room for an auxiliary sixth ligand such as a pyridine or halide around the Co(III) centre. Preliminary studies with $Co(ClO_4)_2.6H_2O$ and two equivalents of terpy in deuterated acetonitrile showed that clean conversion to diamagnetic $[Co(terpy)_2](ClO_4)_2I$ occurred upon addition of iodine, which had spectroscopic properties matching that of the analogous compound reported by Constable and co-workers.[8] However, all attempts to prepare model compounds of the general formula $[Co(terpy)(bipy)L]^{3+}$ (where L is a coordinating solvent, halide or monodentate pyridyl ligand) in order to measure their stability proved unsuccessful. Whilst Co(II) precursors of the type $[Co(terpy)(bipy)L]^{2+}$ could be prepared by well-established literature procedures,[4-6] oxidation with either iodine or ferrocinium hexafluorophosphate gave only the two homoleptic species $[Co(bipy)_3]^{3+}$ and $[Co(terpy)_2]^{3+}$. Heteroleptic $[Co(terpy)(bipy)L]^{3+}$ complexes should be easier to form in the walker system itself however, as the bidentate foot and terpyridyl station together will present a penta-dentate chelating ligand to cobalt. Hence it was decided to address the issue of the precise nature of the required monodentate auxiliary ligand at such a time as the penta-dentate binding site was in hand. A retrosynthetic analysis for the revised target ensemble based on these Co(II)/Co(III) redox chemistry model studies is given in Section 5.3.

5.3 Retrosynthesis

The retrosynthesis of the proposed first two-station block of the track is shown in Scheme 5.6. Starting from 5,5'-dibromo-2,2'-bipyridine,[13] two Sonogashira couplings (first with propargyl ether and then with trimethyl-(3-prop-2-ynyloxy-prop-1-ynyl)-silane[14] were proposed to furnish the unsymmetrical bipyridyl unit of this section of

the track. Removal of the trimethylsilyl group of this moiety would then allow a further Sonogashira coupling to either of the mass-labelled DMAP-derived first stations of the track, as described in Chapter Four. Finally, deuteration of the acetylenes would afford the desired two-station block, ready for complexation to the walker unit.

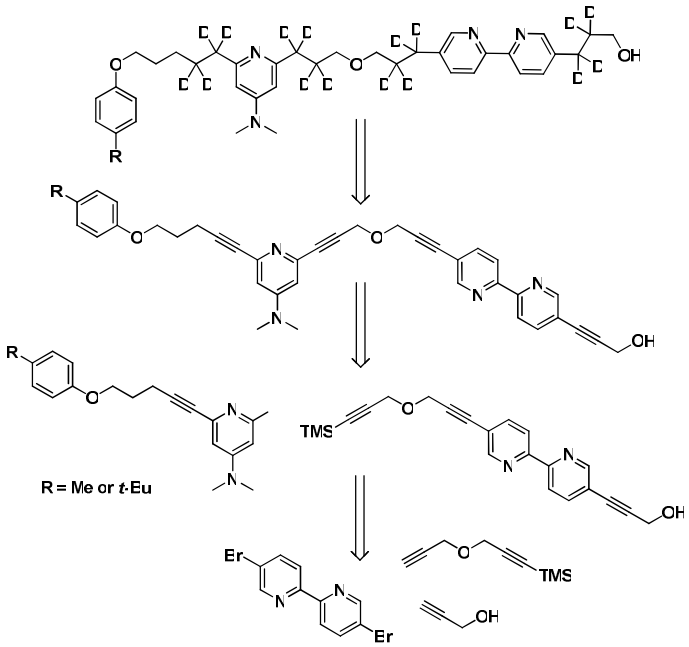

Scheme 5.6 Retrosynthesis of the first two stations of the track.

The complexation of the walker to this section of track was to be performed in an analogous fashion to the coordination of the track and walker detailed in Section 4.4. Hence it was proposed to stir the tracks with the appropriate walker/activated ester modules in DMF at room temperature, and then to couple the products of these reactions with 5-(aminomethyl)-2,2'-bipyridine[15] (Scheme 5.7). Addition of one equivalent of $Co(ClO_4)_2.6H_2O$ and bipyridine, followed by oxidation with iodine would then generate the bi-metallic walker/track ensembles for subsequent connection to the rest of the track.

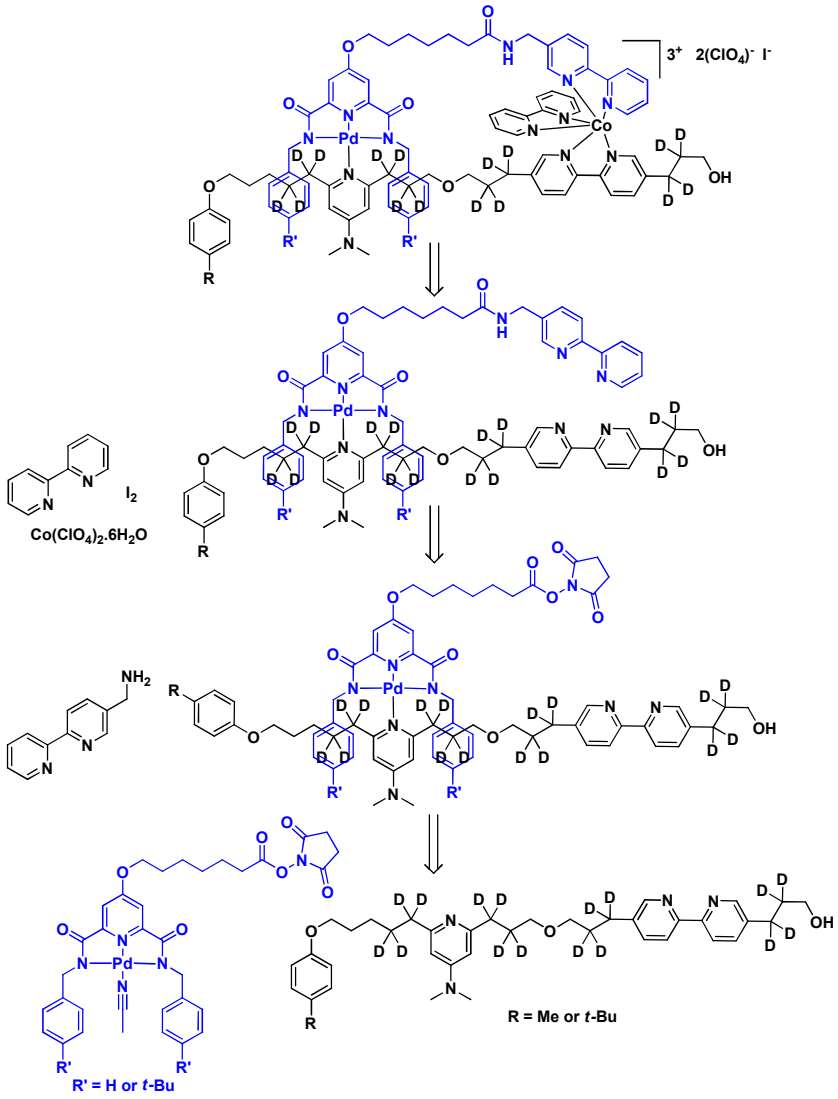

Scheme 5.7 Retrosynthesis of the bimetallic walker/first-two-station-track complexes. The walker unit has been coloured for clarity.

The retrosynthesis of the final two stations of the track is shown in Scheme 5.8. Again following a Sonogashira coupling strategy, it was proposed to react 5-bromo-2,2'-bipyridine[13] with propargyl ether to generate the final station of the track bearing a terminal acetylene group. Reaction of this bipyridyl station unit with 2,6-diiodoDMAP[16] under Sonogashira conditions would then afford the final two-station block of the track.

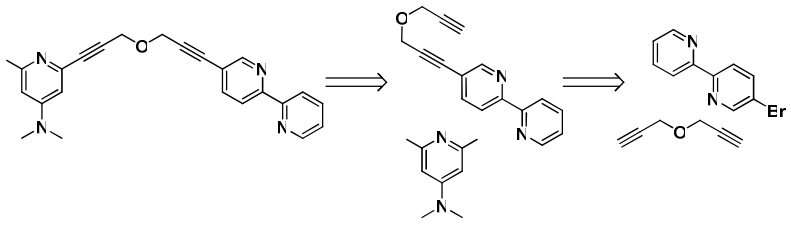

Scheme 5.8 Retrosynthesis of the final two-station block of the track.

The middle two stations of the track were to be synthesised from the mono-trimethylsilyl-protected terpyridyl moiety described in Chapter Four and a BOC-protected aminomethyl-pyridine derivative as shown in Scheme 5.9. This protected pyridine station was to be prepared from the analogous free amine compound, which could in turn be obtained from the phthalimide-protected aminomethyl-pyridine station encountered in Chapter Four.

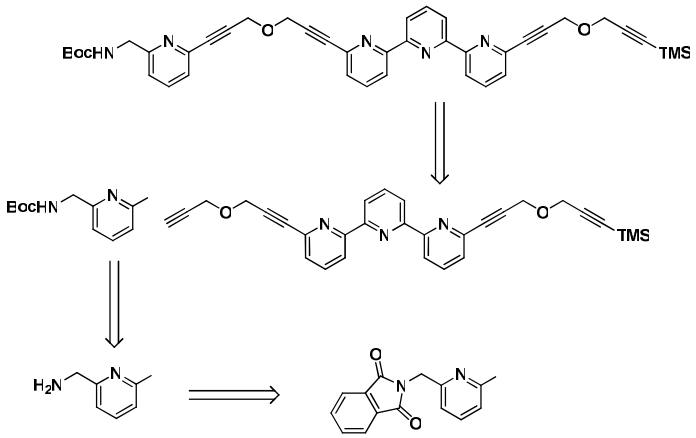

Scheme 5.9 Retrosynthesis of the middle two stations of the track.

Sonogashira coupling of the final and middle two-station blocks followed by hydrogenation of the acetylenes would then furnish the completed four-station track segment, ready for isocyanate formation and subsequent urethane-coupling to either of the walker/first-two-station-track ensembles to give the completed walker/track systems as shown in Scheme 5.10.

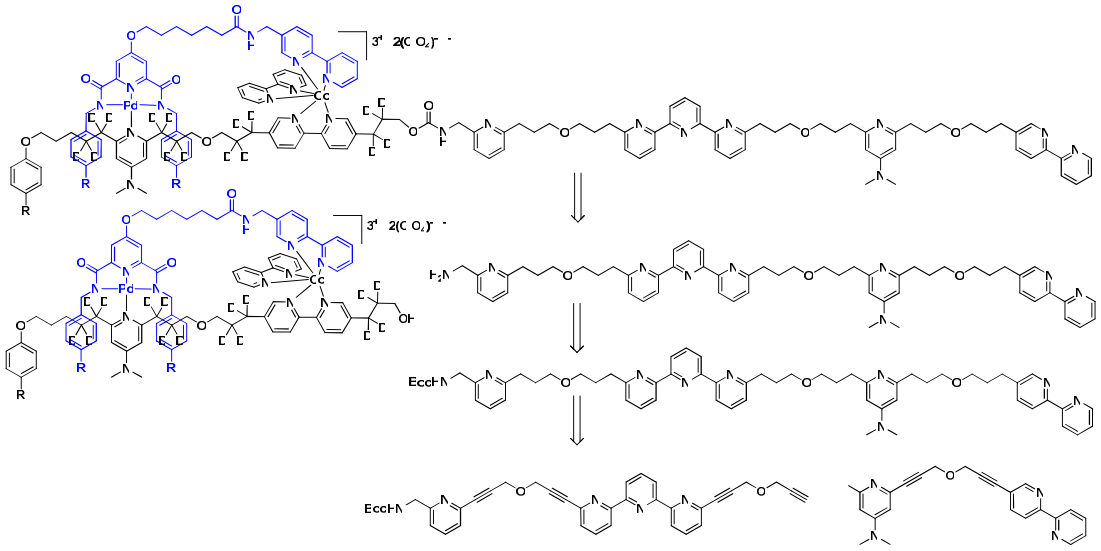

Scheme 5.10 Retrosynthesis of the completed walker/track systems. The walker unit has been coloured for clarity.

5.4 Synthesis

The syntheses of new bidentate binding sites of the track (substituted at the 5,5'-positions) are outlined in Schemes 5.11-5.13. For the final (right-hand-end in Scheme 5.10) bipyridyl binding site, 5-bromo-2,2'-bipyridine (**9**) was coupled with an excess of commercially available propargyl ether *via* a Sonogashira coupling to give bipyridine **10** in excellent yield. A further Sonogashira coupling with 2,6-diiodoDMAP (**11**) then generated the final two station block **12**.

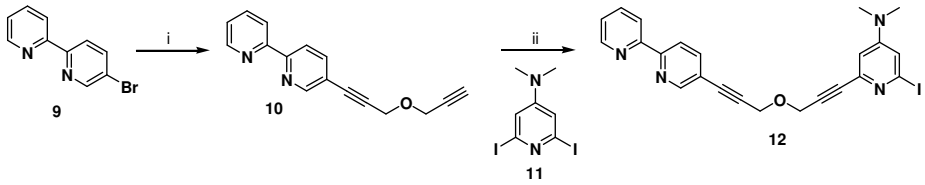

Scheme 5.11 Synthesis of the final two stations of the track. Reagents and conditions: (i) propargyl ether, $Pd(PPh_3)_4$, CuI, THF/Et_3N, 22 h, 55 ˚C, 87%, (ii) $Pd(PPh_3)_4$, CuI, THF/Et_3N, 22 h, 55 ˚C, 73%.

Initially, it was hoped to synthesise the first two-station block of the track from 5,5'-dibromo-2,2'-bipyridine (**13**) using an analogous Sonogashira strategy, as similar transformations on bipyridine **13** were known from the literature.[17-19] However, reaction of bipyridine **13** with one equivalent of propargyl alcohol gave the desired alcohol **14** in only poor yield, and all subsequent attempts to couple **14** with

propargyl ether returned only starting material from the reaction mixture, even with extended heating in the presence of a large excess of the acetylene and high catalyst loading (Scheme 5.12). To circumvent this unexpected lack of reactivity under Sonogashira conditions, a strategy employing *Stille* couplings[20] was devised. Firstly, propargyl alcohol was protected as its paramethoxybenzyl derivative *via* a literature procedure to give known acetylene **15**.[21] This compound was then converted to the tri-butyltin derivative **16** in near quantitative yield, before Stille coupling with bipyridine **13** to furnish mono-substituted bipyridinyl, **17**. Attempts to couple bipyridine **17** with the mono-protected propargyl ether moiety **18** under Sonogashira conditions gave similarly disappointing results to those seen with bipyridine **14**, and so propargyl ether **18** was activated for Stille coupling as its tri-butyltin analogue, **19**. Gratifyingly, Stille coupling of stannane **19** and bipyridine **17** followed by desilylation of the crude mixture with NaOH/methanol furnished the desired *bis*-substituted bipyridinyl **20** in 85% yield from bipyridine **17**.

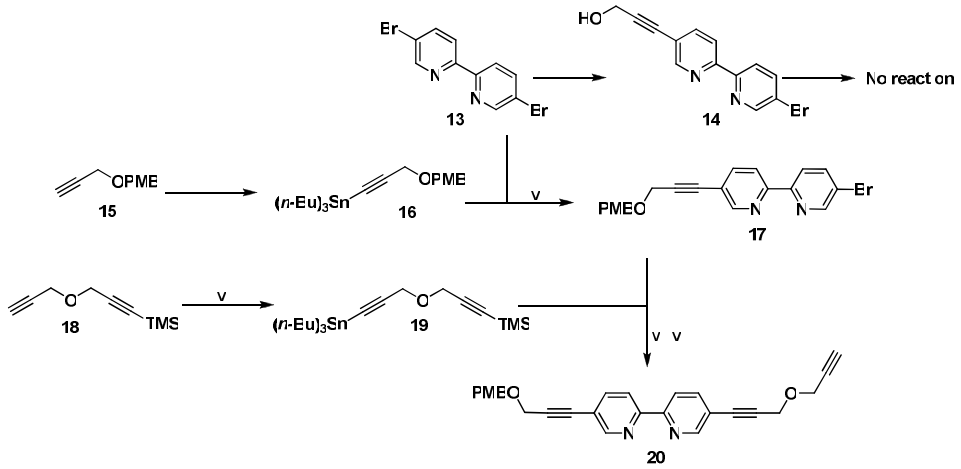

Scheme 5.12 Synthesis of the unsymmetrical bipyridyl station **20**. Reagents and conditions: (i) Propargyl alcohol, $Pd(dppf)Cl_2$, CuI, MeOH/toluene/Et_3N, microwave, 20 mins, 70 ˚C, 26%, (ii) propargyl ether, $Pd(dppf)Cl_2$, CuI, MeOH/toluene/Et_3N, microwave, 20 mins, 70 ˚C *or* $Pd(PPh_3)_4$, CuI, MeOH/toluene/Et_3N, reflux, 20 h, (iii) *n*-BuLi, Bu_3SnCl, THF, 16 h, -78 ˚C → RT, 98%, (iv) $Pd(PPh_3)_4$, DMF, 16 h, 110 ˚C, 42%, (v) *n*-BuLi, Bu_3SnCl, THF, 1 h, -78 ˚C → RT, quant., (vi) $Pd(PPh_3)_4$, DMF, 16 h, 110 ˚C, (vii) 1 M NaOH/MeOH, 1 h, 0 ˚C, 85% (over two steps).

Bipyridine **20** then proved a suitable substrate for Sonogashira coupling to the methylphenol-labelled first station of the track, **21** (see Chapter Four), giving the rigid two-station block **22** in excellent yield (Scheme 5.13). Deuteration of the acetylenes present in two-station block **22** under neutral conditions (D_2, THF,

$Pd(OH)_2/C$; no evidence of any *hydrogenation* of the acetylenes by ^1H NMR) was found to lead to a small but significant amount of ether cleavage (~10% by ^1H NMR).[22] This could be avoided by performing the reaction under mildly basic conditions (by adding solid K_2CO_3 to the reaction or by using a 95:5 THF/Et_3N solvent system), although the rate of reaction was slowed considerably (reduction of the acetylenes is complete within three hours under neutral conditions, or 16 hours under basic conditions with the same catalyst loading). In addition to this, the addition of base prevented the removal of the paramethoxybenzyl protecting group on the alcohol, as would normally be expected under standard hydrogenation conditions.[23] The product of reduction was therefore the paramethoxybenzyl-bearing two-station unit **23**, which was obtained in quantitative yield. Removal of the paramethoxybenzyl protecting group with concentrated hydrochloric acid in the presence of triisopropylsilane as a cation scavenger then gave the completed two-station block, **24**, ready for complexation to the walker units.

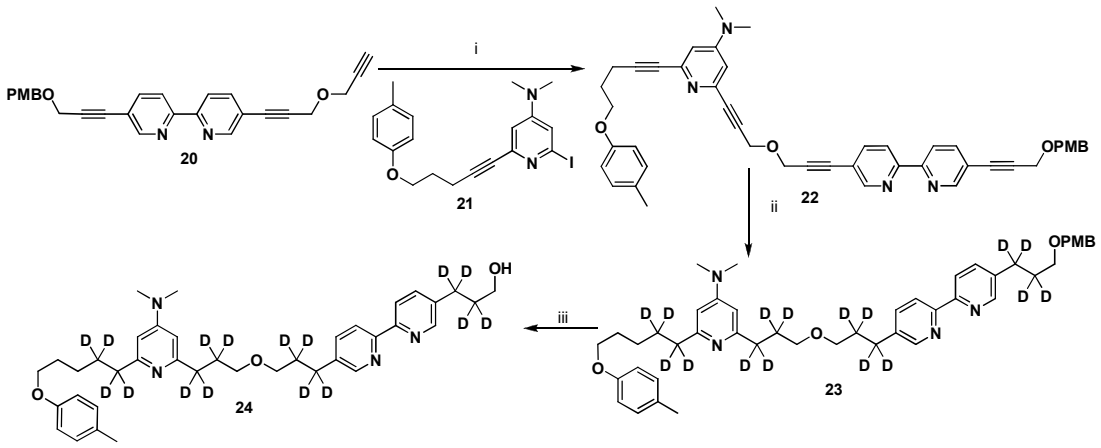

Scheme 5.13 Synthesis of the first two-station block of the track. Reagents and conditions: (i) $Pd(PPh_3)_4$, CuI, THF/Et_3N, 16 h, 55 °C, 87%, (ii) $Pd(OH)_2/C$, D_2, K_2CO_3, D_2O/THF, 16 h, RT, quant., (iii) conc. HCl, triisopropylsilane, dioxane, 0.5 h, RT, 86%.

The synthesis of the BOC-protected middle two-station block of the track is shown in Scheme 5.14. Starting from the phthalimide-protected iodo-pyridine moiety, **25** (see Chapter Four), free amine **26** was generated in excellent yield. Amine **26** was then converted to its mono-BOC derivative (**27**), in order to prevent decomposition and ease purification in subsequent steps. Sonogashira coupling of pyridine **27** and terpyridyl unit **28** (see Chapter Four) then afforded two-station unit **29** in very good yield. Subsequent deprotection of the terminal acetylene using K_2CO_3 in a

tetrahydrofuran/methanol mixed solvent system gave two-station block **30** in nearly quantitative yield.

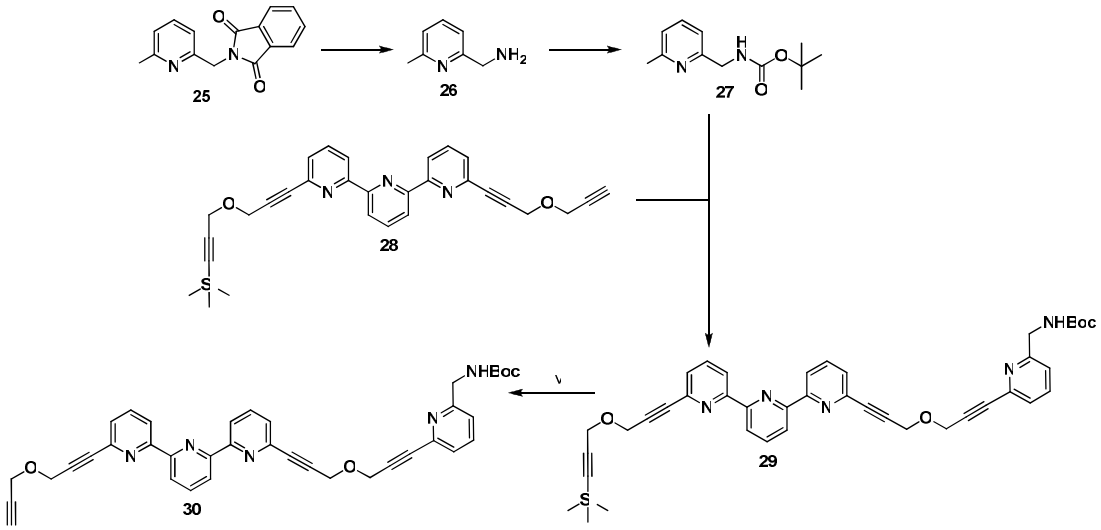

Scheme 5.14 Synthesis of the middle two-station block of the track. Reagents and conditions: (i) hydrazine monohydrate, EtOH, 4 h, reflux, 92%, (ii) BOC anhydride, CH_2Cl_2, 16 h, 0 ˚C → RT, 97%, (iii) $Pd(PPh_3)_4$, CuI, THF/Et_3N, 5 days, 45 ˚C, 81%, (iv) K_2CO_3, MeOH/THF, 30 mins, 0 ˚C, 99%.

The synthetic approach taken towards the free-amine four-station block **33** is shown in Scheme 5.15. Terminal acetylene **30** was coupled to iodoDMAP-derivative **12** under Sonogashira conditions, requiring five days' gentle heating under an inert atmosphere but providing the four-station unit **31** in excellent yield. Subsequent hydrogenation of the acetylenes under basic conditions proceeded smoothly, giving the BOC-protected four-station block **32** in 97% yield.

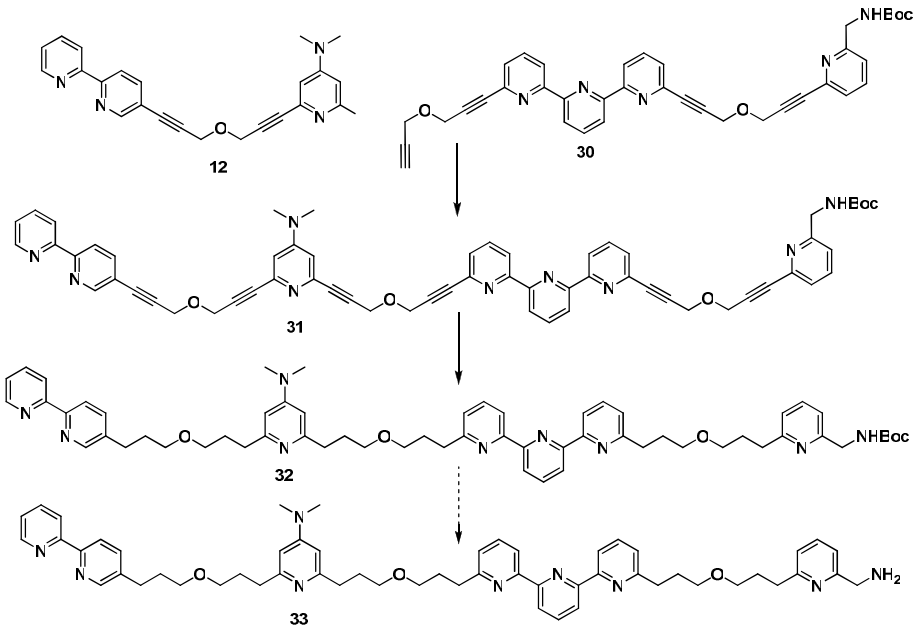

Scheme 5.15 Synthesis of the four-station block of the track. Reagents and conditions: (i) $Pd(PPh_3)_4$, CuI, THF/Et_3N, 5 days, 45 ˚C, 83%, (ii) $Pd(OH)_2$/C, K_2CO_3, H_2, THF/EtOH, 16 h, RT, 97%.

5.5 Ongoing and Future Work

Removal of the BOC unit should then afford the free-amine four-station block **33**. To test the efficacy of this proposed deprotection, a small amount of two-station unit **29** (Scheme 5.14) was dissolved in a 5:1 CH_2Cl_2:TFA mixed solvent system and the solution stirred for one hour at 0 °C. After removal of the solvents, ^{1}H NMR analysis of the crude reaction mixture showed that deprotection of the amine had occurred quantitatively, with no evidence of unwanted side-reactions. Deprotection of four-station block **32** should therefore proceed equally as smoothly, generating track segment **33**. It is then proposed to react amine **33** with phosgene to generate the analogous isocyanate, which will then be coupled to the bi-metallic walker/two-station unit **37** (see Scheme 5.16) to give the completed methylphenol-labelled walker track ensemble as depicted in Scheme 5.10. It will also be necessary to couple a small amount of amine **33** to the first two-station block **24** in order to generate the six station track with no walker unit on it for comparison with the walker/track ensemble.

The route towards the walker/first-two-station-block ensemble, **37**, is outlined in Scheme 5.16. Complexation of methylphenol-labelled two-station unit **24** with walker precursor **34** (see Chapter Four) was accomplished by stirring the two reactants in DMF at room temperature overnight, giving complex **35** in good yield. Subsequent coupling of complex **35** and 5-(aminomethyl)-2,2'-bipyridine in CH_2Cl_2 afforded the cobalt-free walker unit **36** in 78% yield.

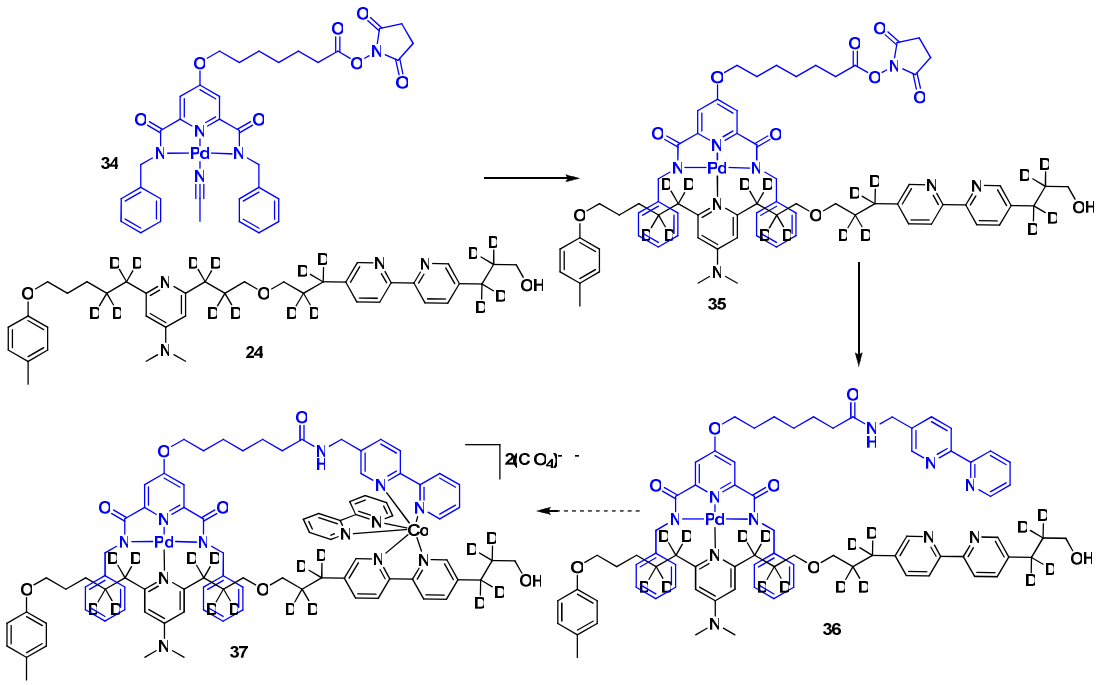

Scheme 5.16 Synthesis of the walker on the first two station block of the track. Reagents and conditions: (i) d_7-DMF, 16 h, RT, 60%, (ii) 5-(aminomethyl)-2,2'-bipyridine, CH_2Cl_2, 20 h, RT, 78%. The walker unit has been coloured for clarity.

The synthesis of bimetallic walker/two-station complex **37** is currently under active investigation. It is hoped that iodine oxidation of a solution containing **36** and one equivalent each of 2,2'-bipyridine and $Co(ClO_4)_2.6H_2O$ will generate species akin to compound **37**. Alternatively, a suspension of **36** in acetonitrile can be treated with one equivalent of $CoCl_2.6H_2O$ to give the turquoise complex **38** as the only product detectable by ESI-MS (see Scheme 5.17). Addition of one equivalent of 2,2'-bipyridine to a solution of complex **38** in 9:1 acetonitrile:methanol produced a rapid colour change from turquoise to yellow, indicative of the formation of Co(II) *tris*-bipy species such as the reduced form of complex **37**. However, subsequent attempts to oxidise this Co(II) complex with iodine to give the Co(III) homologue **37** have so

far proved unsuccessful. Reagents and conditions suitable for this oxidation step are now being pursued.

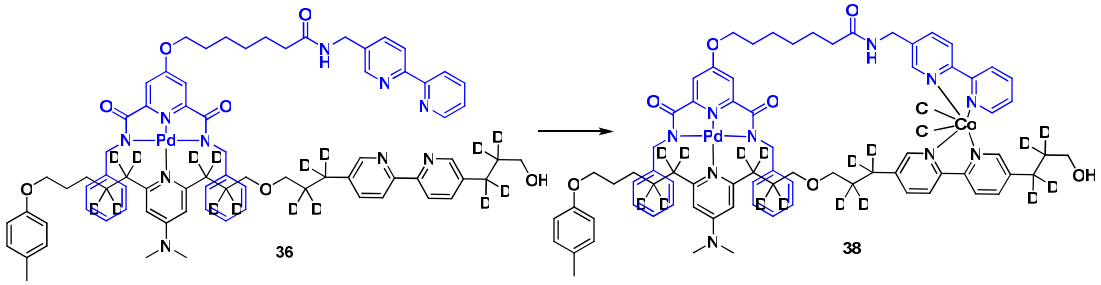

Scheme 5.17 Formation of Co(II) complex **38**. Reagents and conditions: (i) $CoCl_2.6H_2O$, CH_3CN, MeOH, 5 mins, RT. The walker unit has been coloured for clarity.

With the completed methylphenol-labelled walker/track ensemble in hand, the sequence of walking steps shown in Scheme 5.1 will be attempted. If these prove to be successful (as judged by ^{1}H NMR), the synthesis of the analogous *tert*-butylphenol-labelled walker/track ensemble will be undertaken and its operation investigated. Should the behaviour of this system also be satisfactory, equimolar amounts of the methylphenol- and *tert*-butylphenol-labelled ensembles will be mixed together and the processivity of walking will be probed by analysing mass spectra of this mixture after each step of the sequence of operations outlined in Scheme 5.1.[24]

The demonstration of processive, unidirectional walking in such a system would represent a major milestone in metal-ligand coordination chemistry. From a scientific point of view, comparing the efficiency of walking in solution with that acheived when the track is attached to a surface (Figure 5.3) would offer unique insights into how molecular machines operate at solid/liquid interfaces (where most of the natural motor proteins operate).

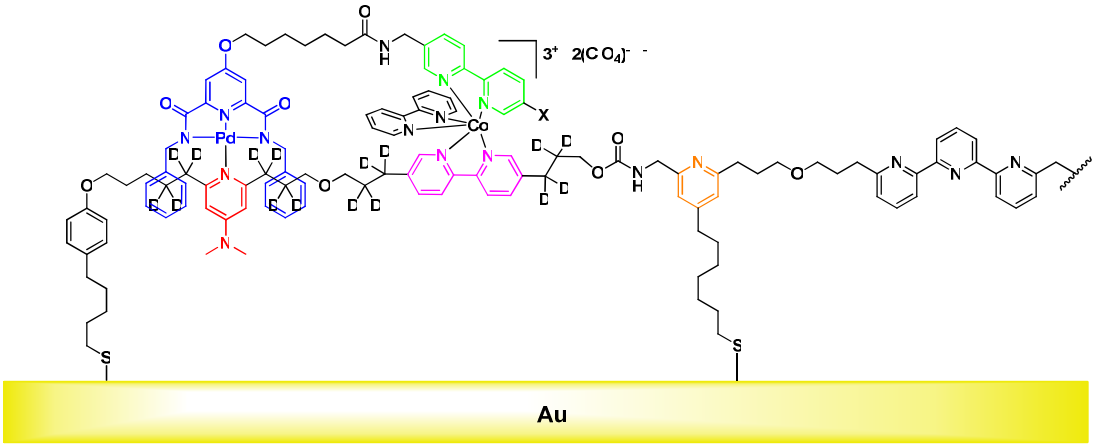

Figure 5.3 A hand-over-hand molecular walker mounted on (e.g.) a gold surface. "X" indicates a potential attachment point for flourescence labels and/or molecular cargo. In order to discourage the heterocycles from interacting with the Au surface it may prove necessary to cover the surface with long chain alkyl thiols (not shown for clarity).[25]

Furthermore, it is proposed to synthesise an analogous walking ensemble that would operate using an inchworm mechanism. A putative design for such a system, based on a pseudo-[3]rotaxane is shown in Figure 5.4.

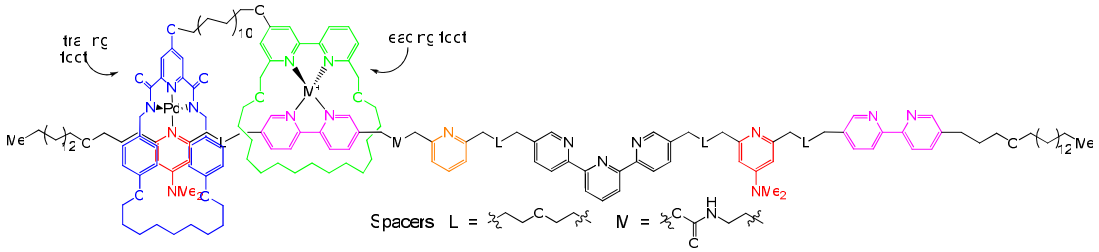

Figure 5.4 An inchworm walking system. The ligand exchange reactions necessary for directional walking with this ensemble could be the same as with the hand-over-hand system, or could employ a different second metal ("M^{+n}"). The feet would also have to move in a different order – the leading foot would have to move first as drawn. An inchworm mode of locomotion is enforced by the fact that the two macrocyles are interlocked with the track, thereby providing *vertical confinement* to the system.[26]

As they are confined to only one track, inchworm walkers of the type shown in Figure 5.4 are not compatible with branched tracks. The same is not true, however, of hand-over-hand systems, which raises the intriguing possibility of designing walkers that are able to "choose" one pathway over another at track branching points, with potential applications in fields as diverse as medicine, molecular logic and advanced molecular machines.

5.6 Experimental Section

General

5,5'-Dimethyl-2,2'-bipyridine, 6,6'-Dimethyl-2,2'-bipyridine, 3,8-phenanthroline, propargyl ether, propargyl alcohol, tri-n-butyltin chloride and all Co(II) salts were purchased from the Aldrich Co. 5-Bromo-2,2'-bipyridine (**9**),[13] 2,6-diiodo-4-(dimethylamino)pyridine (**11**),[16] 5,5'-bromo-2,2'-bipyridine (**13**),[13] 1-methoxy-4-prop-2-ynyloxymethyl-benzene (**15**),[21] trimethyl-(3-prop-2-ynyloxy-prop-1-ynyl)-silane (**18**)[14] and 5-(aminomethyl)-2,2'-bipyridine[15] were prepared *via* literature methods.

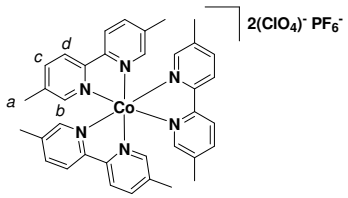

7

To a solution of 5,5'-dimethyl-2,2'-bipyridine (10 mg, 0.054 mmol, 3.0 equiv.) in CH_3CN (2 mL) was added a pink solution of $Co(ClO_4)_2.6H_2O$ (7.0 mg, 0.018 mmol, 1.0 equiv.) in CH_3CN (1 mL). The reaction turned yellow at once, and was then stirred at RT for 10 minutes. After this time, ferrocinium hexafluorophosphate (12 mg, 0.037 mmol, 2.0 equiv.) was added as a solid and the reaction turned greenish/brown. After stirring at RT for another 30 minutes, the reaction was extracted with hexanes (which turned yellow) and the CH_3CN fraction concentrated *in vacuo*, giving **7** as a brown/red solid, 210 °C (dec.) (50 mg, 98%). ^{1}H NMR (CD_3CN, 400 MHz): δ 2.31 (s, 18H, H_a), 6.86 (s, 6H, H_b), 8.25 (d, J = 8.3, 6H, H_c), 8.50 (d, J = 8.3, 6H, H_d). ^{13}C NMR (CD_3CN, 100 MHz): δ 19.5, 127.0, 143.4, 144.6, 151.6, 154.2. LRESI-MS (acetonitrile): m/z = 204 $[M\text{-}PF_6\text{-}2(ClO_4)]^{3+}$.

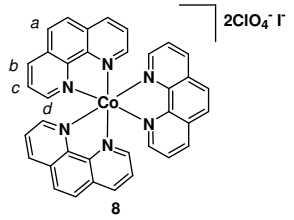

8

To a stirred solution of 3,8-phenanthroline (20 mg, 0.11 mmol, 3.0 equiv.) in CH_3CN (2 mL) was added a pink solution of $Co(ClO_4)_2.6H_2O$ (14 mg, 0.037 mmol, 1.0 equiv.) in CH_3CN (3 mL). The reaction turned yellow at once, and was then stirred at RT for 10 minutes. After this time, a solution of I_2 (9.0 mg, 0.037 mmol, 1.0 equiv.) in CH_3CN (1 mL) was added and the reaction turned orange/brown. After stirring at RT for another 5 minutes, the reaction was extracted exhaustively with hexanes (until such time as no more colour was extracted from the reaction) and the CH_3CN fraction was concentrated under reduced pressure to yield **8** as a tan solid, 220 °C (dec.) (0.10 g, 98%). ^{1}H NMR (CD_3CN, 400 MHz): δ 7.39 (d, J = 5.5, 6H, H_d), 7.76 (dd, J_1 = 8.3, J_2 = 5.5, 6H, H_c), 8.31 (s, 6H, H_a), 8.86 (dd, J_1 = 8.3, J_2 = 1.0, 6H, H_b). ^{13}C NMR (CD_3CN, 100 MHz): δ 129.7, 129.9, 133.4, 143.0, 146.8, 154.3. LRESI-MS (acetonitrile): m/z = 200 $[M\text{-}I\text{-}2(ClO_4)]^{3+}$.

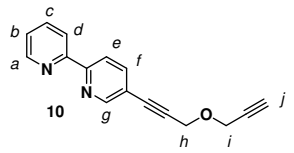

10

A 250 mL RBF was charged with THF (120 mL), Et_3N (14 mL), **9** (3.00 g, 12.8 mmol, 1.0 equiv.) and propargyl ether (5.00 g, 53.1 mmol, 4.2 equiv.) and degassed for 30 minutes. $Pd(PPh_3)_4$ (1.50 g, 1.28 mmol, 0.1 equiv.) and CuI (0.120 g, 0.640 mmol, 0.05 equiv.) were then added and the reaction heated to 55 ˚C for 22 h. After this time, the reaction was allowed to cool to RT, quenched with a saturated solution of NH_4Cl (100 mL) and extracted with CH_2Cl_2 (3 x 100 mL). The combined organic layers were washed with brine and dried over Na_2SO_4. Column chromatography on silica (1% MeOH in CH_2Cl_2) gave **10** as a tan solid, m.p. 60-62 ˚C (2.77 g, 87%). ^{1}H NMR ($CDCl_3$, 400 MHz): δ 2.50 (t, J = 2.4, 1H, H_j), 4.40 (d, J = 2.4, 2H, H_i), 4.53 (s, 2H, H_h), 7.29-7.33 (m, 1H, H_b), 7.79-7.87 (m, 2H, $H_{c,f}$), 8.36-8.40 (m, 2H, $H_{d,e}$), 8.66-8.69 (m, 1H, H_a), 8.72-8.74 (m, 1H, H_g). ^{13}C NMR ($CDCl_3$, 100 MHz): δ 56.7, 57.2, 75.2, 78.7, 83.7, 88.3, 119.3, 120.2, 121.3, 123.9, 136.9, 139.6, 149.2,

151.7, 155.1, 155.2. LRESI-MS (acetonitrile): *m/z* = 249 $[M+H]^+$, 271 $[M+Na]^+$. HRESI-MS: *m/z* = 249.1025 $[M+H]^+$ (calc. for $C_{16}H_{13}N_2O$, 249.1022 $[M+H]^+$).

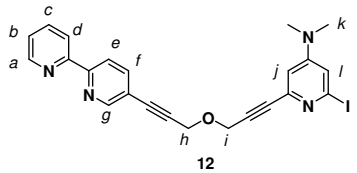

12

A 250 mL RBF was charged with THF (120 mL), Et_3N (14 mL), **10** (1.30 g, 5.20 mmol, 1.0 equiv.) and **11** (5.82 g, 15.6 mmol, 3.0 equiv.) and degassed for 30 minutes. $Pd(PPh_3)_4$ (0.600 g, 0.520 mmol, 0.1 equiv.) and CuI (0.100 g, 0.520 mmol, 0.1 equiv.) were then added and the reaction heated to 55 ˚C for 22 h. After this time, the reaction was allowed to cool to RT, quenched with a saturated solution of NH_4Cl (100 mL) and extracted with CH_2Cl_2 (3 x 100 mL). The combined organic layers were washed with brine and dried over Na_2SO_4. Column chromatography on silica (1% MeOH in CH_2Cl_2) gave **12** as a orange solid, m.p. 128-130 ˚C (1.88 g, 73%). ^{1}H NMR ($CDCl_3$, 400 MHz): δ 2.92 (s, 6H, H_k), 4.52 (s, 2H, H_i), 4.55 (s, 2H, H_h), 6.62 (d, *J* = 2.3, 1H, H_j), 6.82 (d, *J* = 2.3, 1H, H_l), 7.27-7.32 (m, 1H, H_b), 7.77-7.87 (m, 2H, $H_{c,f}$), 8.32-8.41 (m, 2H, $H_{d,e}$), 8.65 (d, *J* = 4.7, 1H, H_a), 8.71 (d, *J* = 1.4, 1H, H_g). ^{13}C NMR ($CDCl_3$, 100 MHz): δ 39.1, 57.3, 57.5, 83.5, 83.8, 85.8, 88.5, 110.1, 116.2, 118.2, 119.3, 120.1, 121.2, 123.9, 136.8, 139.6, 141.9, 149.1, 151.7, 154.3, 155.0, 155.2. LRESI-MS (MeOH): *m/z* = 495 $[M+H]^+$. HRESI-MS: *m/z* = 495.0688 $[M+H]^+$ (calc. for $C_{23}H_{20}IN_4O$, 495.0676 $[M+H]^+$).

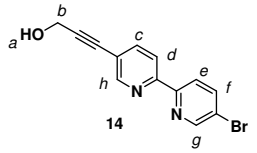

14

13 (0.333 g, 1.06 mmol, 1.0 equiv.) was dissolved in a mixture of MeOH (20 mL), toluene (10 mL) and Et_3N (10 mL) and $Pd(dppf)_2Cl_2$ (43.0 mg, 53.0 µmol, 0.05 equiv.) and CuI (20.0 mg, 0.106 mmol, 0.1 equiv.) were added. Propargyl alcohol (65.0 mg, 68.0 µL, 1.17 mmol, 1.1 equiv.) was then added to this mixture *via* syringe, and the reaction heated to 70 °C for 20 minutes at atmospheric pressure in a CEM microwave reactor (power level = 150 W). After this time, the solvents were removed *in vacuo* and the resulting brown residue purified by column

chromatography on silica (2% MeOH in CH_2Cl_2) to give **14** as a tan solid (80.0 mg, 26%). ^{1}H NMR ($CDCl_3$, 400 MHz): δ 1.80-1.88 (br, 1H, H_a), 4.55 (d, J = 3.7, 2H, H_b), 7.84 (dd, J_1 = 8.2, J_2 = 2.1, 1H, H_c), 7.94 (dd, J_1 = 8.5, J_2 = 2.4, 1H, H_f), 8.30-8.36 (m, 2H, $H_{d,e}$), 8.69-8.73 (m, 2H, $H_{g,h}$). ^{13}C NMR ($CDCl_3$, 100 MHz): δ 51.6, 82.6, 91.6, 119.8, 120.2, 121.4, 122.5, 139.5, 139.6, 150.3, 151.7, 153.8, 154.1. LRESI-MS (MeOH): *m/z* = 289 $[M^{79}Br+H]^+$, 291 $[M^{81}Br+H]^+$. HRESI-MS: *m/z* = 288.9966 $[M+H]^+$ (calc. for $C_{13}H_{10}{}^{79}BrN_2O$, 288.9971 $[M+H]^+$).

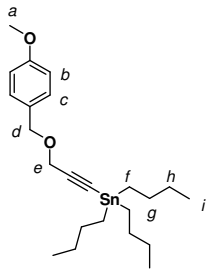

16

To a solution of **15** (9.52 g, 54.0 mmol, 1.0 equiv.) in THF (150 mL) was added *n*-BuLi (20.0 mL of a 2.7 M solution in hexanes, 54.0 mmol, 1.0 equiv.) dropwise at -78 ˚C and the solution stirred at this temperature for 1 h. After this time, Bu_3SnCl (17.6 g, 14.7 mL, 54.0 mmol, 1.0 equiv.) was added dropwise over 20 minutes and the solution allowed to stir at RT overnight. The reaction mixture was then poured into brine (500 mL), extracted with Et_2O (3 x 200 mL), dried over Na_2SO_4 and concentrated *in vacuo* to afford **16** as a pale yellow oil (24.7 g, 98%). ^{1}H NMR ($CDCl_3$, 400 MHz): δ 0.93 (t, J = 7.4, 9H, H_i), 1.00-1.07 (m (with Sn satellites), 6H, H_f), 1.30-1.43 (m, 6H, H_h), 1.57-1.65 (m (with Sn satellites), 6H, H_g), 3.79 (s, 3H, H_a), 4.17 (s (with Sn satellites), 2H, H_e), 4.57 (s, 2H, H_d), 6.86-6.90 (m, 2H, H_b), 7.28-7.32 (m, 2H, H_c). ^{13}C NMR ($CDCl_3$, 100 MHz): δ 10.9, 13.5, 26.8, 28.7, 55.0, 57.5, 70.4, 89.6, 105.8, 113.6, 129.6 (x 2), 159.1. LRESI-MS (FAB 3-Noba): *m/z* = 409 $[M-Bu]^+$. HRESI-MS: *m/z* = 409.1185 $[M-Bu]^+$ (calc. for $C_{19}H_{29}O_2Sn$, 409.1184 $[M-Bu]^+$).

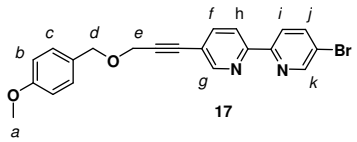

17

13 (340 mg, 1.00 mmol, 1.0 equiv.) and $Pd(PPh_3)_4$ (58.0 mg, 50.0 µmol, 0.05 equiv.) were suspended in DMF (8 mL) and the mixture heated to 110 ˚C, at which temperature all the solids dissolved. To this solution was added **16** (512 mg, 1.10 mmol, 1.1 equiv.) *via* syringe and the solution heated to 110 ˚C overnight. In the morning, the reaction was cooled to 0 ˚C, quenched with a 1 M solution of NaOH in MeOH (8 mL) and stirred at 0 ˚C for 1 h. The mixture was then poured into brine (150 mL) and extracted with CH_2Cl_2 (5 x 50 mL). The combined organic extracts were then dried over Na_2SO_4 and concentrated *in vacuo*. The resulting crude residue was subjected to column chromatography on silica (CH_2Cl_2) to give **17** as a white solid, m.p. 105-107 ˚C (173 mg, 42%). ^{1}H NMR ($CDCl_3$, 400 MHz): δ 3.81 (s, 3H, H_a), 4.40 (s, 2H, H_e), 4.62 (s, 2H, H_d), 6.88-6.93 (m, 2H, H_b), 7.31-7.35 (m, 2H, H_c), 7.85 (dd, J_1 = 8.3, J_2 = 2.1, 1H, H_f), 7.94 (dd, J_1 = 8.5, J_2 = 2.4, 1H, H_j), 8.30-8.37 (m, 2H, $H_{h,i}$), 8.71-8.73 (m, 2H, $H_{g,k}$). ^{13}C NMR ($CDCl_3$, 100 MHz): δ 55.2, 57.4, 71.6, 83.1, 89.8, 113.8, 119.9, 120.1, 121.4, 122.5, 129.2, 129.8, 139.5, 139.6, 150.2, 151.8, 153.8, 154.0, 159.4. LRESI-MS (MeOH): *m/z* = 431 $[M^{79}Br+Na]^+$, 433 $[M^{81}Br+Na]^+$. HRESI-MS: *m/z* = 409.0543 $[M^{79}Br+H]^+$ (calc. for $C_{21}H_{18}{}^{79}BrN_2O_2$, 409.0546 $[M^{79}Br+H]^+$).

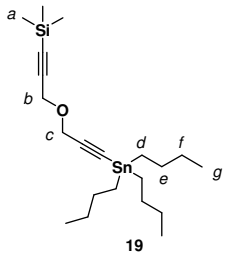

19

To a solution of **18** (9.27 g, 55.7 mmol, 1.0 equiv.) in THF (250 mL) was added *n*-BuLi (20.6 mL of a 2.7 M solution in hexanes, 55.7 mmol, 1.0 equiv.) dropwise at -78 ˚C and the solution stirred at this temperature for 30 minutes. After this time, Bu_3SnCl (18.1 g, 55.7 mmol, 1.0 equiv.) was added dropwise over 20 minutes and the solution then allowed to stir at RT for 1 h. The reaction mixture was then poured into brine (500 mL), extracted with Et_2O (3 x 200 mL), dried over Na_2SO_4 and concentrated *in vacuo* to afford **19** as a yellow oil (25.1 g, 99%). ^{1}H NMR ($CDCl_3$,

400 MHz): δ 0.14 (s, 9H, H_a), 0.87 (t, *J* = 7.3, 9H, H_g), 0.93-0.99 (m (with Sn satellites), 6H, H_d), 1.24-1.36 (m, 6H, H_f), 1.49-1.57 (m (with Sn satellites), 6H, H_e), 4.19-4.24 (m (with Sn satellites) 4H, $H_{b,c}$). ^{13}C NMR ($CDCl_3$, 100 MHz): δ -0.3, 10.9, 13.5, 26.8, 28.7, 56.7, 57.3, 90.3, 91.3, 100.8, 104.7. LRESI-MS (FAB 3-Noba): *m/z* = 399 $[M-Bu]^+$. HRESI-MS: *m/z* = 399.1167 $[M-Bu]^+$ (calc. for $C_{17}H_{31}OSiSn$, 399.1161 $[M-Bu]^+$).

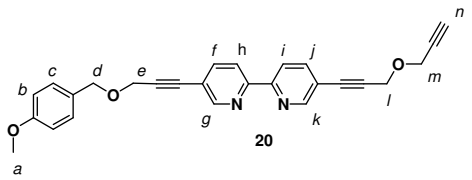

20

13 (1.32 g, 3.20 mmol, 1.0 equiv.), $Pd(PPh_3)_4$ (280 mg, 0.256 mmol, 0.08 equiv.) and **19** (2.91 g, 6.40 mmol, 2.0 equiv.) were suspended in DMF (60 mL) and the mixture heated to 110 ˚C overnight. After this time, the reaction mixture was cooled to 0 ˚C and a 1 M solution of NaOH in MeOH (60 mL) was added and the resulting mixture stirred at 0 ˚C for 1 h. This was then poured into brine (500 mL) and extracted with CH_2Cl_2 (5 x 100 mL). The combined organic extracts were then washed with brine and dried over Na_2SO_4, before concentration under reduced pressure. The crude residue was then purified by column chromatography on silica (2% MeOH in CH_2Cl_2) to give **20** as a white solid, m.p. 74-76 ˚C (1.15 g, 85%). ^{1}H NMR ($CDCl_3$, 400 MHz): δ 2.51 (t, *J* = 2.4, 1H, H_n), 3.81 (s, 3H, H_a), 4.35 (d, *J* = 2.4, 2H, H_m), 4.40 (s, 2H, H_e), 4.54 (s, 2H, H_l), 4.62 (s, 2H, H_d), 6.89-6.93 (m, 2H, H_b), 7.31-7.35 (m, 2H, H_c), 7.86 (dd, J_1 = 8.2, J_2 = 2.1, 2H, $H_{f,j}$), 8.38 (d, *J* = 8.2, 2H, $H_{h,i}$), 8.71-8.75 (m, 2H, $H_{g,k}$). ^{13}C NMR ($CDCl_3$, 100 MHz): δ 55.2, 56.8, 57.2, 57.4, 71.5, 75.2, 78.7, 83.2, 83.7, 88.6, 89.8, 113.8, 119.6, 119.9, 120.5 (x 2), 129.2, 129.8, 139.6 (x 2), 151.8 (x 2), 154.2, 154.4, 159.4. LRESI-MS (MeOH): *m/z* = 423 $[M+H]^+$, 445 $[M+Na]^+$. HRESI-MS: *m/z* = 423.1712 $[M+H]^+$ (calc. for $C_{27}H_{23}N_2O_3$, 423.1703 $[M+H]^+$).

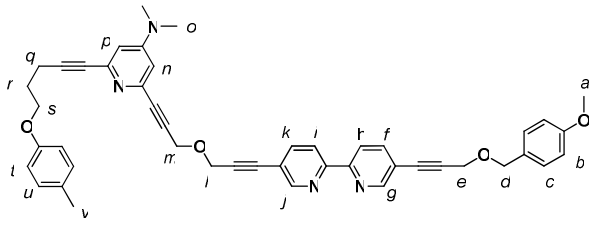

22

To a solution of **20** (400 mg, 0.95 mmol, 1.0 equiv.) in THF (8 mL) and Et_3N (2 mL) was added $Pd(PPh_3)_4$ (56 mg, 0.048 mmol, 0.05 equiv.) and CuI (18 mg, 0.095 mmol, 0.1 equiv.) at RT. To this was added **21** (480 mg, 1.1 mmol, 1.2 equiv.) as a solid and the mixture heated to 55 ˚C overnight. After this time, the reaction was poured into CH_2Cl_2 (50 mL), quenched with an aqueous NH_4Cl solution (25 mL) and the organic phase washed with water (20 mL) and brine. After drying (Na_2SO_4) and removal of the solvents under reduced pressure, the crude residue was subjected to column chromatography on silica (1% MeOH in CH_2Cl_2) to give **22** as a yellow gum (0.590 g, 87%). ^{1}H NMR ($CDCl_3$, 400 MHz): δ 2.04-2.10 (m, 2H, H_r), 2.27 (s, 3H, H_v), 2.61 (t, J = 7.0, 2H, H_q), 2.98 (s, 6H, H_o), 3.81 (s, 3H, H_a), 4.06 (t, J = 6.1, 2H, H_s), 4.40 (s, 2H, H_e), 4.54 (s, 2H, H_m), 4.59 (s, 2H, H_l), 4.62 (s, 2H, H_d), 6.56 (d, J = 2.5, 1H, H_n), 6.62 (d, J = 2.5, 1H, H_p), 6.78-6.83 (m, 2H, H_t), 6.88-6.93 (m, 2H, H_b), 7.04-7.09 (m, 2H, H_u), 7.30-7.35 (m, 2H, H_c), 7.86 (dt, J_1 = 8.2, J_2 = 2.3, 2H, $H_{f,k}$), 8.37 (dd, J_1 = 8.2, J_2 = 2.0, 2H, $H_{h,i}$), 8.71-8.74 (m, 2H, $H_{g,j}$). ^{13}C NMR ($CDCl_3$, 100 MHz): δ 16.0, 20.4, 28.1, 39.1, 55.2, 57.4 (x 3), 66.3, 71.5, 80.9, 82.4, 83.2, 83.7, 86.8, 88.4, 88.9, 89.7, 109.1, 109.2, 113.8, 114.3, 119.7, 119.8, 120.5 (x 2), 129.2 (x 2), 129.8 (x 2), 139.6, 139.7, 142.1, 143.5, 151.8 (x 2), 154.2, 154.3 (x 2), 156.6, 159.4. LRESI-MS (MeOH): *m/z* = 715 $[M+H]^+$. HRESI-MS: *m/z* = 715.3270 $[M+H]^+$ (calc. for $C_{46}H_{43}N_4O_4$, 715.3279).

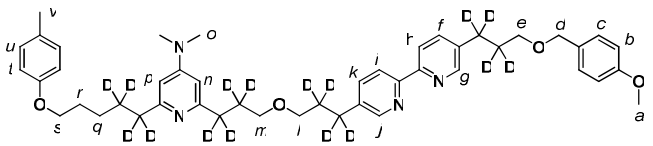

23

To a solution of **22** (320 mg, 0.448 mmol, 1.0 equiv.) in THF (5 mL) and D_2O (0.1 mL) was added $Pd(OD)_2/C$ (20% b/w, 64.0 mg) and K_2CO_3 (622 mg, 4.50 mmol, 10.0 equiv.) and the mixture thoroughly degassed with nitrogen and then deuterium. The mixture was then allowed to stir under a deuterium atmosphere at RT overnight and subsequent filtration through Mg_2SO_4 and concentration of the reaction mixture *in vacuo* gave **23** as an analytically pure pale brown oil (325 mg, 99%). ^{1}H NMR ($CDCl_3$, 400 MHz): δ 1.49-1.57 (m, 2H, H_q), 1.78-1.86 (m, 2H, H_r), 2.29 (s, 3H, H_v), 2.99 (s, 6H, H_o), 3.42-3.52 (m, 6H, $H_{e,l,m}$), 3.82 (s, 3H, H_a), 3.94 (t, *J* = 6.6, 2H, H_s), 4.46 (s, 2H, H_d), 6.24 (d, *J* = 2.3, 1H, H_p), 6.27 (d, *J* = 2.3, 1H, H_n), 6.77-6.83 (m, 2H, H_t), 6.91 (d, *J* = 8.6, 2H, H_b), 7.05-7.10 (m, 2H, H_u), 7.29 (d, *J* = 8.6, 2H, H_c), 7.60-7.67 (m, 2H, $H_{f,k}$), 8.26-8.32 (m, 2H, $H_{h,i}$), 8.50-8.55 (m, 2H, $H_{g,j}$). ^{13}C NMR ($CDCl_3$, 100 MHz): δ 20.3, 25.6, 28.1-30.3 (br, 6 x **C**D_2), 29.1, 34.4 (br, **C**D_2), 37.9 (br, **C**D_2), 39.1, 55.1, 67.8, 68.4, 69.2, 70.3, 72.6, 102.8 (x 2), 113.6, 114.2, 120.3 (x 2), 129.2, 129.4, 129.7, 130.3, 136.7 (x 2), 136.9, 137.0, 149.2 (x 2), 153.9, 154.0, 155.1, 156.8, 159.0, 160.9, 161.5. LRESI-MS (MeOH): *m/z* = 748 $[M+H]^+$. HRESI-MS: *m/z* = 747.5538 $[M+H]^+$ (calc. for $C_{46}H_{43}{}^2H_{16}O_4N_4$, 747.5535 $[M+H]^+$).

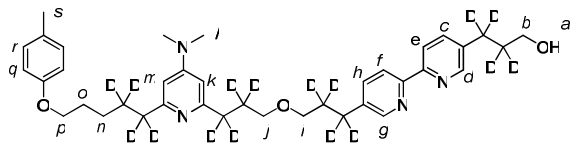

24

To a solution of **23** (1.04 g, 1.39 mmol, 1.0 equiv.) in dioxane (50 mL) and conc. HCl (10 mL) was added triisopropylsilane (6.60 g, 8.54 mL, 41.7 mmol, 30 equiv.) and the reaction stirred at RT for 30 minutes. After this time, $KHCO_3$ was added until no more bubbling was observed and pH = 7. The reaction was filtered through celite, concentrated *in vacuo* and the crude residue purified by column chromatography on alumina (Bockmann type I, neutral, activated), eluting in EtOAc:MeOH (95:5) to give **24** as a viscous colourless gum (0.750 g, 86%). ^{1}H NMR ($CDCl_3$, 400 MHz): δ 1.48-1.54 (m, 2H, H_n), 1.75-1.85 (m, 2H, H_o), 2.27 (s, 3H, H_s), 2.97 (s, 6H, H_l), 3.43 (s, 2H, H_i), 3.46 (s, 2H, H_j), 3.69 (s, 2H, H_b), 3.91 (t, *J* = 6.6, 2H, H_p), 6.21 (d, *J* = 2.3, 1H, H_m), 6.24 (d, *J* = 2.3, 1H, H_k), 6.77 (d, *J* = 8.4, 2H, H_q), 7.05 (d, *J* = 8.4, 2H, H_r), 7.60-7.67 (m, 2H, $H_{c,h}$), 8.23-8.29 (m, 2H, $H_{e,f}$), 8.47-8.54 (m, 2H, $H_{g,d}$). ^{13}C NMR ($CDCl_3$, 100 MHz): δ 20.3, 25.6, 27.8-30.3 (br, 5 x **C**D_2), 29.1, 32.8 (br, **C**D_2), 34.0 (br, **C**D_2), 37.2 (br, **C**D_2), 39.2, 61.2, 67.8, 69.3, 70.2, 102.9, 103.0, 114.2, 120.4 (x 2), 129.5, 129.7, 136.7, 136.8, 137.0, 137.1, 149.1, 149.2, 153.9 (x 2), 155.4, 156.8, 160.4, 161.0. LRESI-MS (MeOH): *m/z* = 627 $[M+H]^+$. HRESI-MS: *m/z* = 627.4949 $[M+H]^+$ (calc. for $C_{38}H_{35}{}^2H_{16}O_3N_4$, 627.4965 $[M+H]^+$).

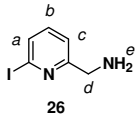

26

25 (2.18 g, 6.00 mmol, 1.0 equiv.) and hydrazine monohydrate (0.350 mL, 6.00 mmol, 1.0 equiv.) were suspended in EtOH (50 mL) and the mixture heated to reflux, at which point all the reactants dissolved. After 2 h reflux, additional hydrazine monohydrate (50.0 µL, 0.860 mmol, 0.15 equiv.) was added and the solution stirred at reflux for a further 2 h. At this time, the reaction mixture was allowed to cool to RT, diluted with Et_2O (300 mL) and the solids removed *via* filtration. The filtrate was concentrated under reduced pressure and the resulting crude residue purified by column chromatography on silica (20% MeOH in CH_2Cl_2 with 1% Et_3N) to give **26**

as a yellow solid, m.p. 30-32 ˚C (1.29 g, 92%). ^{1}H NMR ($CDCl_3$, 400 MHz): δ 3.92 (s, 2H, H_d), 7.24-7.30 (m, 2H, $H_{a,b}$), 7.58 (dd, J_1 = 6.5, J_2 = 2.1, 1H, H_c). ^{13}C NMR ($CDCl_3$, 100 MHz): δ 47.2, 117.8, 120.2, 132.8, 137.9, 164.2. LRESI-MS (acetonitrile): *m/z* = 235 $[M+H]^+$, 257 $[M+Na]^+$. HRESI-MS: *m/z* = 234.9726 $[M+H]^+$ (calc. for $C_6H_8IN_2$, 234.9727 $[M+H]^+$).

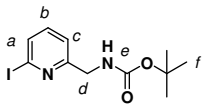

27

BOC anhydride (3.60 g, 16.5 mmol, 1.1 equiv.) was dissolved in CH_2Cl_2 (35 mL) and the solution cooled to 0 ˚C. To this was added **26** (3.51 g, 15.0 mmol, 1.0 equiv.) as a solid in one portion and the reaction mixture stirred at RT overnight. Removal of the solvents *in vacuo*, followed by column chromatography on silica (20% EtOAc in CH_2Cl_2) yielded **27** as a white solid m.p. 84-86 ˚C (4.86 g, 97%). ^{1}H NMR ($CDCl_3$, 400 MHz): δ 1.46 (s, 9H, H_f), 4.38 (d, *J* = 5.8, 2H, H_d), 5.34-5.48 (br, 1H, H_e), 7.23-7.32 (m, 2H, $H_{a,b}$), 7.59-7.63 (m, 1H, H_c). ^{13}C NMR ($CDCl_3$, 100 MHz): δ 28.4, 45.4, 79.7, 117.4, 120.8, 133.4, 138.1, 155.9, 159.9. LRESI-MS (acetonitrile): *m/z* = 335 $[M+H]^+$, 357 $[M+Na]^+$. HRESI-MS: *m/z* = 335.0250 $[M+H]^+$ (calc. for $C_{11}H_{16}IN_2O_2$, 335.0251 $[M+H]^+$).

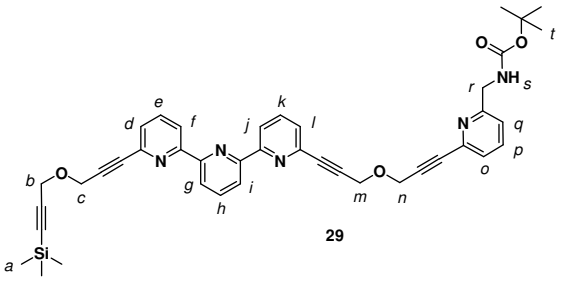

29

27 (281 mg, 0.840 mmol, 0.95 equiv.) was dissolved in THF (10 mL) and Et_3N (7 mL) and the solution heated to 45 ˚C. At this temperature, $Pd(PPh_3)_4$ (39.0 mg, 34.0 µmol, 0.04 equiv.) and CuI (6.40 mg, 34.0 µmol, 0.04 equiv.) were added as solids, and then **28** (435 mg, 0.884 mmol, 1.0 equiv.) was added as a solution in THF (10 mL) dropwise over the course of 4 h. The reaction mixture was then stirred at 45 ˚C for 5 days, before being allowed to cool to RT and poured into concentrated NH_4OH (150 mL). The aqueous phase was extracted with EtOAc (5 x 50 mL) and the

combined organic fractions dried over Na_2SO_4. The crude residue was then purified by column chromatography on silica (25% EtOAc in CH_2Cl_2) to afford **29** as a white solid, m.p. 88-90 ˚C (475 mg, 81%). ^{1}H NMR ($CDCl_3$, 400 MHz): δ 0.20 (s, 9H, H_a), 1.45 (s, 9H, H_t), 4.36 (s, 2H, H_b), 4.43 (d, *J* = 5.5, 2H, H_r), 4.55 (s, 2H, H_c), 4.63 (s, 4H, $H_{m,n}$), 5.42-5.54 (br, 1H, H_s), 7.25 (d, *J* = 6.5, 1H, H_q), 7.37 (d, *J* = 7.6, 1H, H_o), 7.48-7.52 (m, 2H, $H_{d,l}$), 7.60-7.65 (m, 1H, H_p), 7.80-7.85 (m, 2H, $H_{e,k}$), 7.94 (t, *J* = 7.8, 1H, H_h), 8.48-8.52 (m, 2H, $H_{g,i}$), 8.56 (d, *J* = 8.0, 2H, $H_{f,j}$). ^{13}C NMR ($CDCl_3$, 100 MHz): δ -0.2, 28.3, 29.6, 45.7, 57.1, 57.4, 57.5, 57.7, 84.0, 84.2, 84.5, 86.0, 86.1, 86.4, 92.3, 100.4, 120.6, 120.7, 121.4, 121.7, 125.8, 127.3, 128.4, 128.5, 131.8, 131.9, 132.0, 132.1, 136.9, 137.0, 137.9, 141.8, 141.9 (x 2), 154.4, 156.4, 158.2. LRESI-MS (acetonitrile): *m/z* = 697 $[M+H]^+$, 719 $[M+Na]^+$. HRESI-MS: *m/z* = 696.3004 $[M+H]^+$ (calc. for $C_{41}H_{42}N_5O_4Si$, 696.3001 $[M+H]^+$).

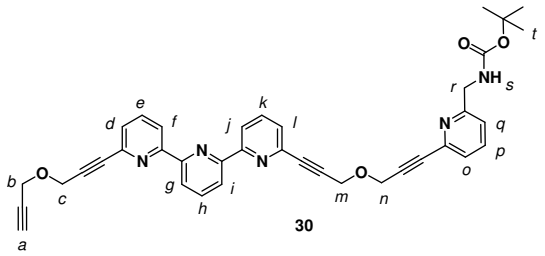

30

29 (562 mg, 0.810 mmol, 1.0 equiv.) were dissolved in MeOH (40 mL) and THF (30 mL) and cooled to 0 ˚C. Powdered K_2CO_3 (138 mg, 1.00 mmol, 1.2 equiv.) was added at this temperature and the reaction monitored by TLC on silica (25% EtOAc in CH_2Cl_2). When TLC analysis showed complete consumption of **29**, the reaction mixture was poured into a saturated NH_4Cl solution (250 mL) and extracted with CH_2Cl_2 (5 x 100 mL). The combined organic extracts were then washed with brine (200 mL) and dried over Na_2SO_4. Removal of the solvents *in vacuo* followed by column chromatography on silica (25% EtOAc in CH_2Cl_2) gave **30** as a white solid, m.p. 115-117 ˚C (500 mg, 99%). ^{1}H NMR ($CDCl_3$, 400 MHz): δ 1.45 (s, 9H, H_t), 2.50 (t, *J* = 2.4, 1H, H_a), 4.37 (d, *J* = 2.4, 2H, H_b), 4.42 (d, *J* = 5.6, 2H, H_r), 4.56 (s, 2H, H_c), 4.63 (s, 4H, $H_{m,n}$), 5.40-5.53 (br, 1H, H_s), 7.25 (d, *J* = 7.7, 1H, H_q), 7.37 (d, *J* = 7.7, 1H, H_o), 7.47-7.52 (m, 2H, $H_{d,l}$), 7.63 (t, *J* = 7.7, 1H, H_p), 7.82 (t, *J* = 7.8, 2H, $H_{e,k}$), 7.94 (t, *J* = 7.8, 1H, H_h), 8.48-8.52 (m, 2H, $H_{g,i}$), 8.54-8.59 (m, 2H, $H_{f,j}$). ^{13}C NMR ($CDCl_3$, 100 MHz): δ 28.3, 45.7, 56.8, 57.1, 57.4, 57.5, 75.2, 78.8, 79.6,

83.9, 84.0, 84.4, 86.0, 86.3, 86.4, 120.7 (x 2), 121.4, 121.7 (x 2), 125.8, 127.3 (x 2), 136.9, 137.0 (x 2), 137.9, 141.8, 141.9, 154.4 (x 2), 155.9, 156.4 (x 2), 157.0, 158.2. LRESI-MS (MeOH): *m/z* = 624 $[M+H]^+$, 646 $[M+Na]^+$. HRESI-MS: *m/z* = 624.2605 $[M+H]^+$ (calc. for $C_{38}H_{34}N_5O_4$, 624.2605 $[M+H]^+$).

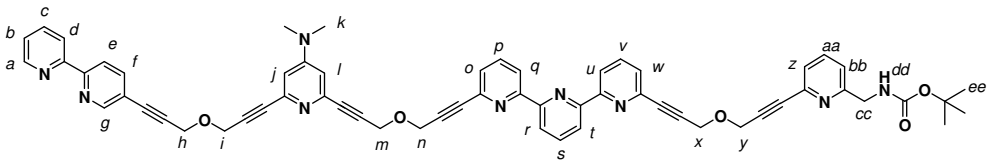

31

30 (220 mg, 0.350 mmol, 1.0 equiv.) was dissolved in THF (10 mL) and Et_3N (7 mL) and the solution heated to 45 ˚C. At this temperature, $Pd(PPh_3)_4$ (25.0 mg, 22.0 µmol, 0.04 equiv.) and CuI (4.00 mg, 22.0 µmol, 0.04 equiv.) were added as solids, and then **12** (208 mg, 42.0 µmol, 1.2 equiv.) was added as a solution in THF (10 mL) dropwise over the course of 3 h. The reaction mixture was then stirred at 45 ˚C for 5 days, allowed to cool to RT and then poured into a concentrated NH_4OH solution (150 mL). The aqueous phase was extracted with EtOAc (5 x 50 mL) and the combined organic fractions dried over Na_2SO_4. The crude residue was then purified by column chromatography on silica (25% EtOAc in CH_2Cl_2, followed by 25% EtOAc in CH_2Cl_2 with 3% Et_3N) to afford **31** as a white solid, 75 ˚C (dec.) (289 mg, 83%). ^{1}H NMR ($CDCl_3$, 400 MHz): δ 1.45 (s, 9H, H_{ee}), 2.97 (s, 6H, H_k), 4.41 (d, *J* = 5.6, 2H, H_{cc}), 4.54-4.63 (m, 12H, $H_{h,i,m,n,x,y}$), 5.43-5.59 (br, 1H, H_{dd}), 6.63-6.67 (m, 2H, $H_{j,l}$), 7.24 (d, *J* = 7.7, 1H, H_{bb}), 7.27-7.32 (m, 1H, H_b), 7.36 (d, *J* = 7.7, 1H, H_z), 7.47-7.52 (m, 2H, $H_{o,w}$), 7.61 (t, *J* = 7.7, 1H, H_{aa}), 7.77-7.89 (m, 4H, $H_{c,f,p,v}$), 7.92 (t, *J* = 7.8, 1H, H_s), 8.34-8.40 (m, 2H, $H_{d,e}$), 8.47-8.51 (m, 2H, $H_{r,t}$), 8.53-8.57 (m, 2H, $H_{q,u}$), 8.64-8.68 (m, 1H, H_a), 8.72 (d, *J* = 1.6, 1H, H_g). ^{13}C NMR ($CDCl_3$, 100 MHz): δ 28.3, 29.6, 39.1, 45.7, 57.3, 57.4 (x 3), 57.5, 79.6, 82.6, 82.7, 83.7, 83.9, 84.1, 84.4, 86.0, 86.3, 86.4, 86.6, 86.7, 88.6, 109.6 (x 2), 119.3, 120.2, 120.6, 120.7, 121.3 (x 2), 121.6, 121.7, 123.9, 125.8, 127.3 (x 2), 136.8, 136.9 (x 3), 137.8, 139.6, 141.8 (x 2), 141.9, 142.5 (x 2), 149.2, 151.7, 154.2, 154.4 (x 3), 155.1, 155.2, 156.3, 156.4, 158.2. LRESI-MS (MeOH): *m/z* = 991 $[M+H]^+$, 1013 $[M+Na]^+$. HRESI-MS: *m/z* = 990.4063 $[M+H]^+$ (calc. for $C_{61}H_{52}N_9O_5$, 990.4086 $[M+H]^+$).

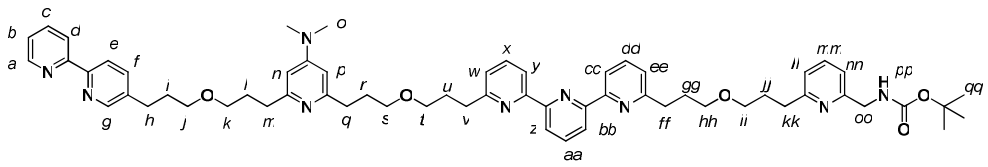

32

31 (0.600 g, 0.606 mmol, 1.0 equiv.) was dissolved in THF/EtOH (20 mL/20 mL) and K_2CO_3 (0.168 g, 1.21 mmol, 2.0 equiv.) was added. To this was added $Pd(OH_2)/C$ (25% b/w, 0.150 g) and the suspension thoroughly degassed with nitrogen and then hydrogen. The reaction was then stirred under an hydrogen atmosphere overnight. After this time, fitration through celite followed by removal of the solvents from the filtrate under reduced pressure afforded **32** as a viscous brown gum, which was used without further purification (0.595 g, 97%). ^{1}H NMR ($CDCl_3$, 400 MHz): δ 1.46 (s, 9H, H_{qq}), 1.88-2.05 (m, 8H, $H_{i,l,r,jj}$), 2.09-2.18 (m, 4H, $H_{u,gg}$), 2.70-2.79 (m, 6H, $H_{h,m,q}$), 2.82-2.88 (m, 2H, H_{kk}), 2.92-2.99 (m, 10H, $H_{o,v,ff}$), 3.42-3.55 (m, 12H, $H_{j,k,s,t,hh,ii}$), 4.40 (d, *J* = 5.1, 2H, H_{oo}), 5.56-5.66 (br, 1H, H_{pp}), 6.23-6.26 (m, 2H, $H_{n,p}$), 7.04 (t, *J* = 7.7, 2H, $H_{ll,nn}$), 7.18 (d, *J* = 7.6, 2H, $H_{w,ee}$), 7.26-7.30 (m, 1H, H_b), 7.53 (t, *J* = 7.7, 1H, H_{mm}), 7.62-7.66 (m, 1H, H_f), 7.71-7.82 (m, 3H, $H_{c,x,dd}$), 7.90 (t, *J* = 7.8, 1H, H_{aa}), 8.29 (d, *J* = 8.1, 1H, H_e), 8.33-8.36 (m, 1H, H_d), 8.40-8.44 (m, 2H, $H_{y,cc}$), 8.47 (d, *J* = 7.8, 2H, $H_{z,bb}$), 8.51 (d, *J* = 1.7, 1H, H_g), 8.64-8.67 (m, 1H, H_a). ^{13}C NMR ($CDCl_3$, 100 MHz): δ 28.4, 29.3, 29.5 (x 2), 29.7, 30.2 (x 2), 31.0, 34.7, 34.8 (x 2), 35.4 (x 2), 39.2, 45.7, 69.5, 70.1, 70.2 (x 2), 70.4, 70.5, 79.4, 103.0 (x 2), 118.3 (x 2), 118.7, 120.7, 120.8 (x 4), 121.1, 122.8 (x 2), 123.4, 136.9 (x 4), 137.5, 137.6, 149.1, 149.4, 153.9, 155.3, 155.6 (x 4), 156.0, 156.2, 156.5, 157.2, 161.0 (x 2), 161.1, 161.2. LRESI-MS (MeOH): *m/z* = 1014 $[M+H]^+$. HRESI-MS: *m/z* = 1014.5963 $[M+H]^+$ (calc. for $C_{61}H_{76}N_9O_5$, 1014.5969 $[M+H]^+$).

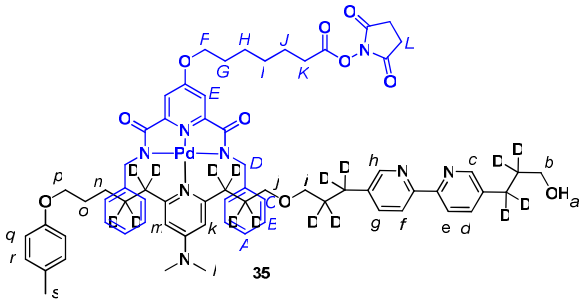

35

To a solution of **24** (0.361 g, 0.576 mmol, 1.0 equiv.) in DMF (10 mL) was added **34** (0.422 g, 0.576 mmol, 1.0 equiv.) as a solid in one portion and the solution stirred at RT for 16 h. After this time, the reaction was poured into CH_2Cl_2 (200 mL), washed with water (2 x 500 mL) and brine (100 mL) and dried over Na_2SO_4. After removal of the solvents under reduced pressure, the crude residue was purified by column chromatography on silica (CH_2Cl_2:acetone 1:1, then straight acetone) to afford **35** as a yellow foam, m.p. 64-66 °C (0.456 g, 60%). ^{1}H NMR ($CDCl_3$, 400 MHz): δ 1.26-1.32 (m, 2H, H_n), 1.43-1.53 (m, 4H, $H_{H,I}$), 1.60-1.84 (m, 6H, $H_{o,G,J}$), 2.28 (s, 3H, H_s), 2.63 (t, J = 7.1, 2H, H_K), 2.80-2.88 (m, 4H, H_L), 3.09 (s, 6H, H_l), 3.22 (s, 2H, H_j), 3.36 (s, 2H, H_i), 3.69 (s, 2H, H_b), 3.86 (t, J = 6.4, 2H, H_p), 3.98-4.09 (m, 6H, $H_{D,F}$), 6.11 (d, J = 2.7, 1H, H_m), 6.16 (d, J = 2.7, 1H, H_k), 6.74-6.81 (m, 6H, $H_{q,C}$), 7.02-7.10 (m, 8H, $H_{r,A,B}$), 7.23 (s, 2H, H_E), 7.59 (dd, J_1 = 8.1, J_2 = 2.0, 1H, H_g), 7.65 (dd, J_1 = 8.1, J_2 = 2.0, 1H, H_d), 8.24 (d, J = 8.1, 1H, H_f), 8.28 (d, J = 8.1, 1H, H_e), 8.47 (d, J = 2.0, 1H, H_h), 8.51 (d, J = 2.0, 1H, H_c). ^{13}C NMR ($CDCl_3$, 100 MHz): δ 20.3, 24.3, 25.1. 25.4, 25.6, 27.7-30.5 (br, 6 x **C**D_2), 28.0, 28.1, 28.9, 30.7, 34.5 (br, **C**D_2), 37.5 (br, **C**D_2), 39.3, 49.6, 61.3, 67.5, 69.0, 69.1, 69.8, 103.4 (x 2), 110.6, 114.1, 120.3, 120.4, 126.0, 127.4, 127.7, 129.5, 129.7, 136.7 (x 2), 136.8, 137.0, 141.2, 149.1 (x 2), 153.8 (x 2), 153.9, 155.3, 156.7, 161.2, 161.8, 168.4, 168.8, 169.2, 171.2. LRESI-MS (acetonitrile): *m/z* = 1318 $[M^{106}Pd+H]^+$.

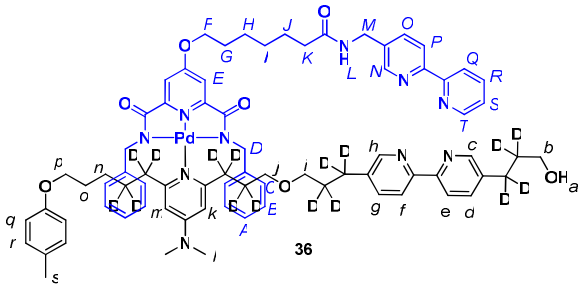

36

To a solution of 5-(aminomethyl)-2,2'-bipyridine (85.0 mg, 0.459 mmol, 1.5 equiv.) in CH_2Cl_2 (10 mL) was added a solution of **35** (0.402 g, 0.305 mmol, 1.0 equiv.) in CH_2Cl_2 (20 mL), and the resulting yellow solution stirred at RT for 20 h. After this time, the reaction was concentrated under reduced pressure and the resulting crude foam purified by column chromatography on alumina (Bockmann type I, neutral, activated; acetone then 95:5 acetone/MeOH) to give **36** as a viscous yellow gum (0.332 g, 78%). ^{1}H NMR ($CDCl_3$, 400 MHz): δ 1.24-1.37 (m, 6H, $H_{n,H,I}$), 1.57-1.84 (m, 6H, $H_{o,G,J}$), 2.23-2.29 (m, 5H, $H_{s,K}$), 3.09 (s, 6H, H_l), 3.22 (s, 2H, H_j), 3.33 (s, 2H, H_i), 3.63 (s, 2H, H_b), 3.86 (t, *J* = 6.4, 2H, H_p), 3.96-4.10 (m, 6H, $H_{D,F}$), 4.50 (d, *J* = 5.9, 2H, H_M), 6.11 (d, *J* = 2.6, 1H, H_m), 6.16 (d, *J* = 2.6, 1H, H_k), 6.43-6.50 (br, 1H, H_L), 6.74-6.80 (m, 6H, $H_{q,C}$), 7.01-7.09 (m, 8H, $H_{r,A,B}$), 7.17 (s, 2H, H_E), 7.27-7.32 (m, 1H, H_S), 7.56 (dd, J_1 = 8.0, J_2 = 2.0, 1H, H_g), 7.64 (dd, J_1 = 8.1, J_2 = 2.0, 1H, H_d), 7.75 (dd, J_1 = 8.0, J_2 = 1.9, 1H, H_O), 7.81 (dt, J_1 = 8.0, J_2 = 1.4, 1H, H_R), 8.21 (d, *J* = 8.0, 1H, H_f), 8.28 (d, *J* = 8.1, 1H, H_e), 8.34 (t, *J* = 8.0, 2H, $H_{Q,P}$), 8.44 (d, *J* = 2.0, 1H, H_h), 8.48 (d, *J* = 2.0, 1H, H_c), 8.56-8.59 (m, 1H, H_N), 8.66 (d, *J* = 4.5, 1H, H_T). ^{13}C NMR ($CDCl_3$, 100 MHz): δ 20.3, 25.2, 25.4, 25.6, 26.5 (br, **C**D_2), 27.7-28.6 (br, 3 x **C**D_2), 28.0, 28.9, 29.1, 29.7 (br, **C**D_2), 32.8 (br, **C**D_2), 34.5 (br, **C**D_2), 36.3, 37.7 (br, **C**D_2), 39.3, 40.6, 49.7, 61.2, 67.5, 68.8, 69.4, 69.7, 103.4 (x 2), 110.5, 114.1, 120.2, 120.4, 120.8, 120.9, 123.6, 126.1, 127.4, 127.7, 129.5, 129.7, 134.4, 136.4, 136.7 (x 2), 136.8 (x 2), 137.1, 141.1, 148.5, 149.0, 149.1, 149.2, 153.8 (x 2), 153.9, 155.0, 155.4, 155.7, 156.7, 161.2, 161.8, 168.7, 171.2, 173.2. LRESI-MS (acetonitrile): *m/z* = 1388 $[M^{106}Pd+H]^+$, 1410 $[M^{106}Pd+Na]^+$. HRESI-MS: *m/z* = 1387.6979 $[M+H]^+$ (calc. for $C_{77}H_{73}{}^2H_{16}N_{10}O_7{}^{106}Pd$, 1387.6955 $[M+H]^+$).

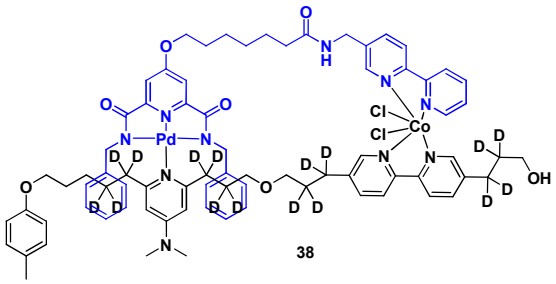

38

To a suspension of **36** (29 mg, 0.021 mmol, 1.0 equiv.) in CH_3CN (10 mL) was added a solution of $CoCl_2.6H_2O$ (5.0 mg, 0.021 mmol, 1.0 equiv.) in MeOH (1 mL) and the resulting turquoise solution stirred at RT for 5 minutes. The formation of **38** as the sole coordination product of the reaction was confirmed by ESI-MS; LRESI-MS (MeOH): m/z = 722 $[M^{106}Pd\text{-}2Cl]^{2+}$.

5.7 References and Notes

(1) Cotton, F. A.; Wilkinson, G. *Advanced Inorganic Chemistry - A Comprehensive Text*; 4th. ed.; John Wiley & Sons Inc.: New York, 1980, pp 773-775.

(2) Vlcek, A. A. *Inorg. Chem.* **1967**, *6*, 1425-1427.

(3) Ghosh *et al.* have reported the ^1H NMR of *cis*-$[Co(bipy)Cl_2]Cl$, which shows no symmetry and contains 16 distinct signals, see: Ghosh, S.; Barve, A. C.; Kumbhar, A. A.; Kumbhar, A. S.; Puranik, V. G.; Datar, P. A.; Sonawane, U. B.; Joshi, R. R. *J. Inorg. Biochem.* **2006**, *100*, 331-343.

(4) Huchital, D. H.; Martell, A. E. *Inorg. Chem.* **1974**, *13*, 2966-2969.

(5) Mizuno, K.; Imamura, S.; Lunsford, J. H. *Inorg. Chem.* **1984**, *23*, 3510-3514.

(6) Ramprasad, D.; Gilicinski, A. G.; Markley, T. J.; Pez, G. P. *Inorg. Chem.* **1994**, *33*, 2841-2847.

(7) Crumbliss *et al*. report the $Co(bipy)_3^{2+/3+}$ redox couple at $E_{1/2}$ = +0.128 V (*vs*. Ag/AgCl) for $Co(bipy)_3^{3+}$ cations immobilised in carrageenan hydrogels. Buttry and Anson give values of the $Co(bipy)_3^{2+/3+}$ redox couple of +0.15 V (*vs*. Ag/AgCl) for the complex in acetonitrile solution and +0.30 V (*vs*. Ag/AgCl) when the cations are incorporated in a Nafion coating on a graphite electrode, whilst Winkler and co-workers give an oxidation potential at +0.1 V (*vs*.

Ag/Ag(ClO_4)) for $Co(bipy)_3^{2+}$ in a mixed toluene/acetonitrile solvent system, see: (a) Crumbliss, A. L.; Perine, S. C.; Kirk Edwards, A.; Rillema, D. P. *J. Phys. Chem.* **1992**, *96*, 1388-1394. (b) Buttry, D. A.; Anson, F. C. *J. Am. Chem. Soc.* **1983**, *105*, 685-689. (c) Winkler, K.; Płonska, M. E.; Rećko, K.; Dobrzyński, L. *Electochem. Acta* **2006**, *51*, 4544-4553. Vlček[2] reports that both the *cis* and *trans* isomers of $Co(bipy)_2Cl_2$ can be oxidised to $[Co(bipy)_2Cl_2]Cl$ by treatment with chlorine gas. The couple $Cl_2 + 2e^- \rightarrow 2Cl^-$ has $E^\ominus = +1.14$ V (*vs.* Ag/AgCl) implying that both $Co(bipy)_2Cl_2$ isomers have oxidation potentials below this value. No such potentials were observed during cyclic voltammetry on **2**, however, suggesting that oxidation of Co(II) to Co(III) in this ligand set is not possible, see: (d) Atkins, P. W. *Physical Chemistry*; Oxford University Press, Oxford, United Kingdom, 1987, pp 267-269, 825.

(8) Constable and co-workers have determined that $[Co(terpy)_2](PF_6)_2$ is low spin. However, $[Co(terpy)_2]^{2+}$ salts can be either high- or low-spin, with the counterions and solvent playing important roles in determining the spin state. A high spin Co(II) ion has an ionic radius of 0.75 Å. $[Co(terpy)_2]^{3+}$ salts are invariably low spin and diamagnetic, with an ionic radius of the Co(III) of 0.55 Å, see: Chow, H. S.; Constable, E. C.; Housecroft, C. E.; Kulicke, K. J.; Tao, Y. *Dalton Trans.* **2005**, 236-237.

(9) Blasse, G. *J. Inorg. Nucl. Chem.* **1965**, *27*, 748-750.

(10) Baker, B. R.; Basolo, F.; Neumann, H. M. *J. Phys. Chem.* **1959**, *63*, 371-378.

(11) Farina, R. D.; Wilkins, R. G. *Inorg. Chem.* **1968**, *7*, 514-518.

(12) A small portion of this mixture was taken and oxidised with iodine, giving a compound with an ESI-MS spectrum containing peaks corresponding to $[Co(terpy)_2]^{3+}$. ^1H NMR of the oxidation product confirmed the presence of a diamagnetic species with six signals in its spectrum, all showing significant shifts compared to the uncomplexed ligand. This shows that $[Co(terpy)_2](ClO_4)_2.H_2O$ can be oxidised by iodine and gives good reason to infer that the initial yellow solution was indeed $[Co(terpy)_2](ClO_4)_2.H_2O$.

(13) Zdravkov, A.; Khimich, N. *Russ. J. Org. Chem.* **2006**, *42*, 1200-1202.

(14) Chang, H.-T.; Jeganmohan, M.; Cheng, C.-H. *Org. Lett.* **2007**, *9*, 505-508.

(15) Panetta, C. A.; Kumpaty, H. J.; Heimer, N. E.; Leavy, M. C.; Hussey, C. L. *J. Org. Chem.* **1999**, *64*, 1015-1021.

(16) Crowley, J. D.; Leigh, D. A.; Lusby, P. J.; McBurney, R. T.; Perret-Aebi, L. E.; Petzold, C.; Slawin, A. M. Z.; Symes, M. D. *J. Am. Chem. Soc.* **2007**, *129*, 15085-15090.

(17) De Nicola, A.; Goeb, S.; Ziessel, R. *Tetrahedron Lett.* **2004**, *45*, 7963-7967.

(18) Khatyr, A.; Ziessel, R. *J. Org. Chem.* **2000**, *65*, 7814-7824.

(19) Khatyr, A.; Ziessel, R. *Tetrahedron Lett.* **2000**, *41*, 3837-3841.

(20) Scott, W. J.; Crisp, G. T.; Stille, J. K. *J. Am. Chem. Soc.* **1984**, *106*, 4630-4632.

(21) Organ, M. G.; Bratovanov, S. *Tetrahedron Lett.* **2000**, *41*, 6945-6949.

(22) No evidence was found to suggest that the analogous reactions performed with $Pd(OH)_2/C$ in Chapter Four suffered from any ether cleavage of this sort. However, hydrogenation of the four-station block (Molecule **39** in Chapter Four) with PtO_2 did lead to significant amounts of decomposition, consistent with cleavage of some of the track spacer ethers.

(23) Heathcock, C. H.; Ratcliffe, R. *J. Am. Chem. Soc.* **1971**, *93*, 1746-1757.

(24) It may also be necessary to prepare both completed walker/track ensembles as mono-metallic species – i.e. containing no cobalt at all. Performing the first cycle of the operations in Scheme 5.1 upon a mixture of these two mono-metallic ensembles would then give a "pure scrambling" benchmark against which to compare the processivity of the bi-metallic species.

(25) Berna, J.; Leigh, D. A.; Lubomska, M.; Mendoza, S. M.; Perez, E. M.; Rudolf, P.; Teobaldi, G.; Zerbetto, F. *Nat. Mater.* **2005**, *4*, 704-710.

(26) For discussions on using vertical confinement to enforce an inchworm mechanism of walking, see: (a) Li, D.; Fan, D.; Wang, Z. *J. Chem. Phys.* **2007**, *126,* 245105. (b) Li, D.; Fan, D.; Zheng, W.; Le, Y.; Wang, Z. *Chem. Phys.* **2008**, *352,* 235-240.

APPENDIX

Published Papers

A Switchable Palladium-Complexed Molecular Shuttle and Its Metastable Positional Isomers J. D. Crowley, D. A. Leigh, P. J. Lusby, R. T. McBurney, L.-E. Perret-Aebi, C. Petzold, A. M. Z. Slawin, and M. D. Symes, *J. Am. Chem. Soc.*, **2007**, *129*, 15085–15090.

Cadiot-Chodkiewicz Active Template Synthesis of Rotaxanes and Switchable Molecular Shuttles with Weak Intercomponent Interactions J. Berná, S. M. Goldup, A.-L. Lee, D. A. Leigh, M. D. Symes, G. Teobaldi, F. Zerbetto, *Angew. Chem. Int. Ed.* **2008**, *47*, 4392-4396.

Rotaxanes

DOI: 10.1002/anie.200800891

Cadiot–Chodkiewicz Active Template Synthesis of Rotaxanes and Switchable Molecular Shuttles with Weak Intercomponent Interactions**

José Berná, Stephen M. Goldup, Ai-Lan Lee, David A. Leigh, Mark D. Symes, Gilberto Teobaldi, and Francesco Zerbetto**

The noncovalent binding motifs used to template the synthesis of mechanically interlocked architectures are generally retained in the final products.[1] This feature has been widely exploited to make molecular shuttles,[2] rotaxanes with two or more discrete binding sites or "stations" on the thread between which the macrocycle incessantly shuttles through Brownian motion. However, the noncovalent interactions used to maximize the rotaxane yield and localize the position of the ring on the thread also provide the major contribution to the activation energy to shuttling.[3] To achieve faster moving rotaxane-based molecular machines, it will be necessary to make molecular shuttles with much weaker intercomponent interactions than are typically introduced with classical template methods.[4] Here we report on a new rotaxane-forming reaction that can produce rotaxanes with unsymmetrical threads (as required for switchable molecular shuttles) but does not leave strong intercomponent binding motifs in the rotaxane product. Instead the active template[5] Cadiot–Chodkiewicz[6] reaction is compatible with building blocks that can provide relatively modest macrocycle–thread binding motifs in the rotaxane, but which are still strong enough to afford good positional integrity of the ring. The methodology is exemplified through the synthesis of a "weak interaction" molecular shuttle in which a single hydrogen bond between the components determines the predominant position of the macrocycle in each of two well-defined states which can be switched between by reversible complexation with Li^+ or protonation.

[*] Dr. J. Berná, Dr. S. M. Goldup, Dr. A.-L. Lee, Prof. D. A. Leigh, M. D. Symes
School of Chemistry, The University of Edinburgh
The King's Buildings, West Mains Road, Edinburgh EH9 3JJ (UK)
Fax: (+44) 131-650-6453
E-mail: David.Leigh@ed.ac.uk
Homepage: http://www.catenane.net
Dr. G. Teobaldi, Prof. F. Zerbetto
Dipartimento di Chimica "G. Ciamician", Università di Bologna
via F. Selmi 2, 40126 Bologna (Italy)
Fax: (+39) 051-209-9456
E-mail: Francesco.Zerbetto@unibo.it
Homepage: http://www.ciam.unibo.it/sitcon/

[**] This work was supported by the European Union project *STAG* and the EPSRC. D.A.L. is an EPSRC Senior Research Fellow and holds a Royal Society-Wolfson Research Merit Award.

Supporting information for this article is available on the WWW under http://www.angewandte.org or from the author.

Active template syntheses differ from classical "passive-template" reactions in that a single species acts as both the template for the product architecture and the catalyst for the formation of the covalent bond(s) that captures it.[5] Although combining these two roles has several potential advantages,[5a] controlling the positions of the metal-ligated building blocks during the reaction to template the product puts additional demands (which can provide insight into the reaction pathway)[5d] on the mechanism of catalysis. Accordingly, successful combinations of ligands and metal-catalyzed reactions for active template syntheses are still rare and the development of new systems challenging.[5e]

The active metal template homodimerization of acetylenes to form rotaxanes[5b,c] introduces a relatively rigid linear connector which inhibits folding—potentially desirable for fully exploiting the spatial separation of the ring between different states[7]—but can only be used to make [2]rotaxanes with symmetrical axles. The coupling of two different building blocks is necessary to produce bistable molecular shuttles in which the macrocycle can be switched between two different positions on the thread. The Cu^I-mediated Cadiot–Chodkiewicz[6] heterocoupling of a terminal alkyne with an alkyne halide appeared a suitable candidate reaction for such studies (Table 1).

Promisingly, [2]rotaxane was produced (Table 1) using appropriately "stoppered" alkyne halide (**1a** or **1b**) and aryl alkyne (**2**) derivatives and a bidentate macrocycle (**3**) under typical conditions[6] used for the Cadiot–Chodkiewicz reaction in nonaqueous solvents. However, in these initial studies poor selectivity for the heterocoupled rotaxane (**4**) versus the homocoupled rotaxanes (**5** and **6**) was observed together with low overall conversion of the alkyne starting materials to bis-acetylene products. In an attempt to improve both the reaction yield and the selectivity for the heterocoupled rotaxane, we investigated changing the traditional Cadiot–Chodkiewicz procedure of mixing the alkyne and alkyne halide components with neutral amine bases, to preforming the copper acetylide by treatment of terminal alkyne **2** with *n*BuLi, followed by transmetalation with CuI (Table 2).[8]

Following this protocol, we were delighted to find that subsequent addition of bipyridine macrocycle **3** and bromoacetylene **1b** led to the desired [2]rotaxane **4** in high yield (84%) and with excellent selectivity (>98%) for the heterocoupled product (Table 2, entry 1).[9] Although the procedure did not prove compatible with reversing the reactive bromine/hydrogen functionalities of the alkyl and aryl acetylene building blocks (**7** with **8**, Table 2, entry 2),[10] when coupling

Table 1: Preliminary solvent screen for the bis-acetylene rotaxane forming active template Cadiot–Chodkiewicz reaction.[6]

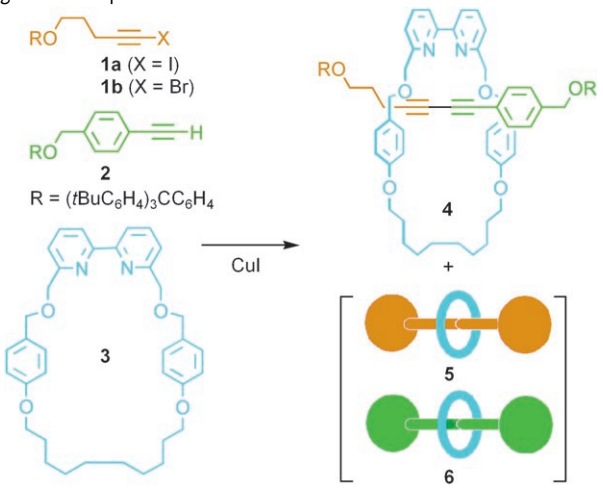

Entry	Alkyne halide	Solvent	Rotaxane yield **1**+**2**+**3**→**4**+**5**+**6**	Selectivity **4**:**5**:**6**
1	**1a**	$(i\text{Pr})_2\text{NH}$	40%	10:9:1
2	**1a**	NEt_3	20%	2:15:1
3	**1a**	pyrrolidine	<2%	no rotaxane
4	**1a**	benzene[b]	35%	1.7:1:1
5	**1b**	$(i\text{Pr})_2\text{NH}$	<5%	2:5:1

[a] A solution of **1**, **2**, **3**, and CuI (all 1 equiv) was allowed to stir at 298 K under an atmosphere of N_2 for 18 h. [b] Plus 2 equiv of $(i\text{Pr})_2\text{NH}$.

Table 2: Substrate scope of the Cadiot–Chodkiewicz active metal template synthesis of heterocoupled [2]rotaxanes.

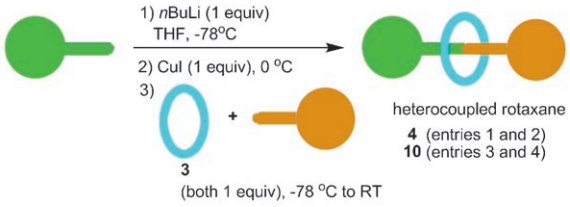

Entry	Terminal acetylene[a]	Bromo-acetylene	Rotaxane yield [%]	Selectivity
1	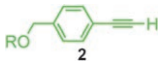	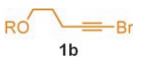	84	>98%[b]
2		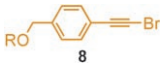	32	1.7:8:1 (**4**:**5**:**6**)
3		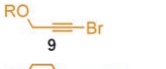	85	>98%[b]
4	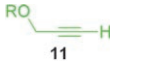	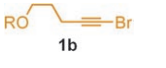	74	>98%[b]

[a] R = $(t\text{BuC}_6\text{H}_4)_3\text{CC}_6\text{H}_4$. [b] No homocoupled rotaxanes observed.

two different alkyl alkynes (**7** with **9** or **11** with **1b** to give **10**) either could be used successfully as the bromoacetylene partner whilst maintaining high yields and apparent exclusive selectivity for the heterocoupled rotaxane (Table 2, entries 3 and 4).

The Cadiot–Chodkiewicz reaction is thought to proceed via a different mechanism to the (also Cu-catalyzed) Glaser homocoupling of alkynes,[11] and the proposed pathway for the active-metal template rotaxane assembly of **4** is shown in Scheme 1. The preformed copper(I)–acetylide **I** is sequestered by bipyridine macrocycle **3**.[12] Oxidative addition across the C–Br bond of the bromoacetylene occurs from the opposite face of the macrocycle to produce Cu^{III} intermediate **II** and subsequent reductive elimination furnishes the heterocoupled [2]rotaxane.

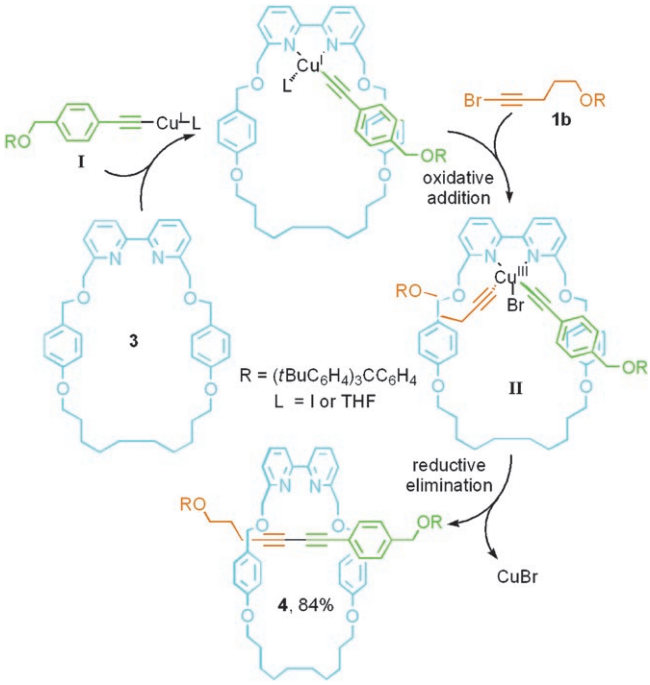

Scheme 1. Proposed mechanism for the Cadiot–Chodkiewicz active metal template formation of [2]rotaxane **4**.[11]

To demonstrate the utility of this new active template reaction, we synthesized a stimuli-switchable molecular shuttle **12** which has modest strength intercomponent interactions of a type that would be difficult or impossible to access by traditional template methods. The single contact H-bond that molecular modeling (see the Supporting Information) indicates (Figure 2) exists between the aniline unit of the thread and bipyridine group of the macrocycle in **12** is too weak to template rotaxane formation through "stoppering" or "clipping" strategies[1] and no passive metal templates which utilize a 1+2 donor ligand set have been reported to date. However, the modified Cadiot–Chodkiewicz active metal template method readily produced molecular shuttle **12** in good yield (61%) from functionalized building blocks **13** and **14** with no homocoupled rotaxane products being detected (Scheme 2).

^{1}H NMR Spectroscopy clearly shows the macrocycle to be predominantly held over the axle aniline unit in neutral molecular shuttle **12** at 300 K in CD_2Cl_2. The ^{1}H NMR spectrum of the rotaxane (Figure 1b) displays significant upfield shifts (H_d 0.2 ppm, H_e 0.4 ppm, H_g 0.6 ppm) of signals associated with the aniline station relative to those in the free thread (Figure 1a). Calculations on the macrocycle-station

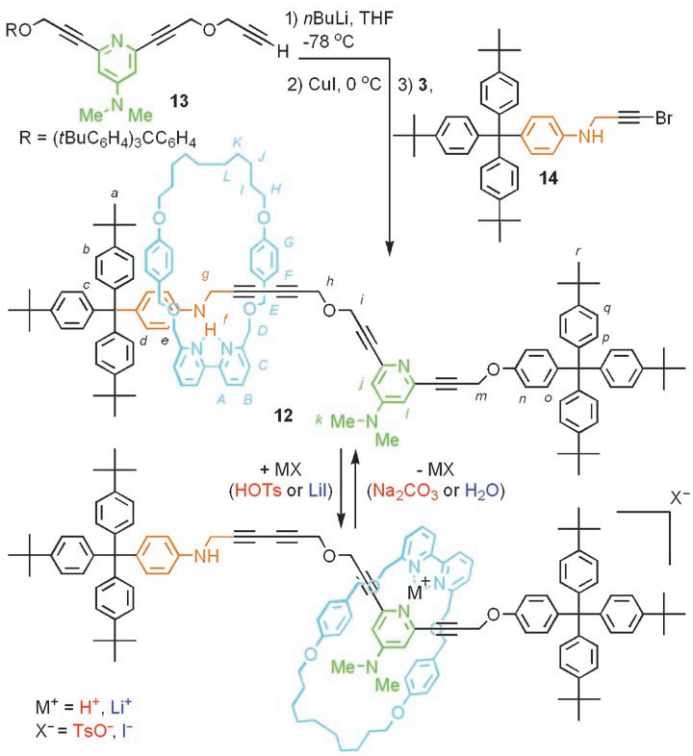

Scheme 2. Active template synthesis and stimuli-induced [by protonation (MX = HOTs) or complexation with Li^+ (MX = LiI)] translocation of the macrocycle in molecular shuttle **12**.

fragments for **12** in CH_2Cl_2 at B3LYP/3-21G* level[13] (see the Supporting Information) show that the minimum structure intercomponent binding energy, ΔG_{bind}, of -3.9 kcal mol^{-1} is largely attributable to a single contact H-bond of 2.1 Å between the (N)H of the aniline and one nitrogen atom of the macrocycle bipyridine unit (Figure 2a). A review of the Cambridge Structural Database (CSD) reveals a range of 2.1–2.4 Å for similar aniline-to-pyridine contacts in the solid state.[14]

Addition of 1 equivalent of TsOH to a solution of rotaxane **12** in CD_2Cl_2 causes significant shifts in several of the axle signals in the ^{1}H NMR spectrum (Figure 1c).[15] Protons H_d, H_e, and H_g associated with the aniline unit return to the position they occupy in the non-interlocked thread in the presence of TsOH (Figure 1d), while those of the DMAP station shift to higher field (H_j and H_l each 0.5 ppm, H_k 0.2 ppm). This is consistent with protonation of the DMAP nitrogen and translocation of the macrocycle along the thread so that the pyridinium NH hydrogen bonds strongly with the bipyridine moiety of the macrocycle (Scheme 2, MX = HOTs). B3LYP/3-21G* level calculations (see the Supporting Information) indicate that the protonated-DMAP-bound co-conformation is now favored by ca. 0.9 kcal mol^{-1} (Figure 2b). A search of the CSD finds that the calculated H-bond contact distance of 1.8 Å is in the 1.4–1.9 Å range found for pyridinium-to-pyridine H-bonds in the solid state.[16] Treating a solution of rotaxane **12**·H^+ with solid Na_2CO_3 quantitatively regenerates the neutral molecular shuttle **12**, returning the macrocycle to its original position on the thread.

A similar change in co-conformation could be generated by shaking a solution of rotaxane **12** in CD_2Cl_2 with excess LiI (Scheme 2, MX = LiI). The ^{1}H NMR spectrum of the shuttle after treatment with LiI (Figure 1f) displays significant upfield shifts and broadening of the resonances of the DMAP station (H_j and H_k) compared with the corresponding protons in the non-interlocked thread in the presence of excess LiI (Figure 1e).[17] As was seen with protonation, the signals of the rotaxane aniline station H_d, H_e, and H_g return to the positions they occupy in the non-interlocked thread. These changes are consistent with the mechanically interlocked components of rotaxane **12** coordinating Li^+ through the bipyridine moiety of the macrocycle and the DMAP station of the axle. A simple aqueous wash removes the metal salt and regenerates rotaxane **12** in its original form.

The utility of the Cadiot–Chodkiewicz active template strategy has been exemplified through the construction and operation of a switchable molecular shuttle which features a single hydrogen bond between the

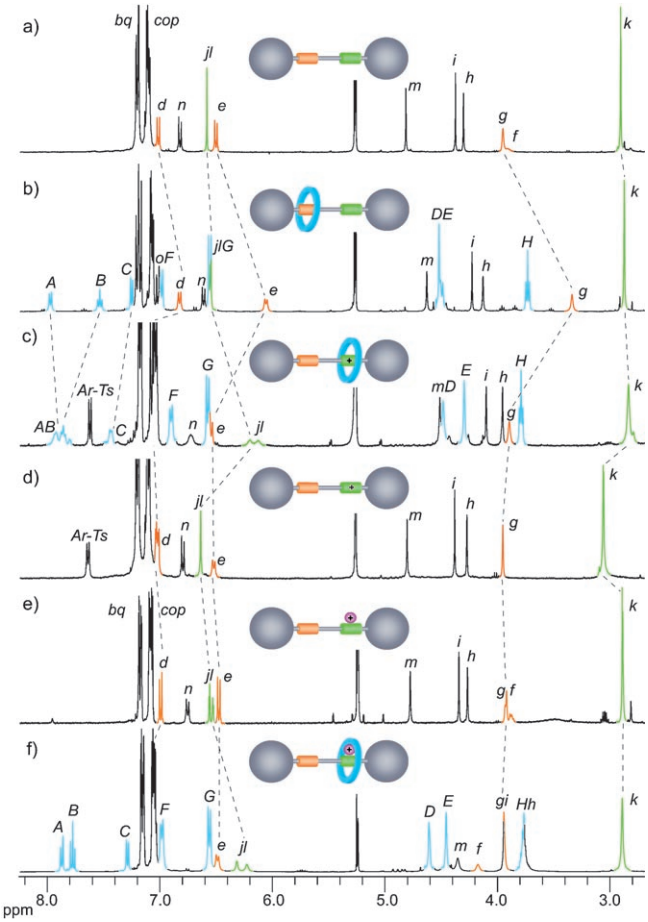

Figure 1. ^{1}H NMR spectra (400 MHz, CD_2Cl_2, 300 K) of a) non-interlocked thread, b) rotaxane **12**, c) rotaxane **12** + 1 equiv TsOH, d) non-interlocked thread + 1 equiv TsOH, e) non-interlocked thread in the presence of excess LiI, f) rotaxane **12** in the presence of excess LiI.

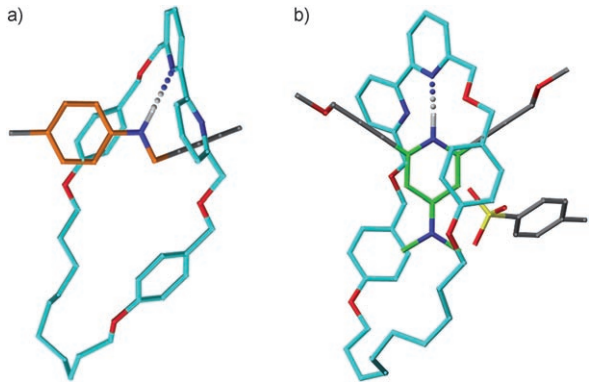

Figure 2. B3LYP/3-21G* level quantum chemical calculated minimum-energy macrocycle-station structures in CH_2Cl_2 at 298 K showing the single hydrogen-bond interactions between the macrocycle and a) aniline and b) protonated DMAP (dimethylaminopyridine; tosylate counterion) stations present in molecular shuttle **12** and **12**·H^+.[13] Hydrogen atoms not attached to N atoms are not shown for clarity. Intercomponent NH···N distances and angles: **12** 2.1 Å (153.6°); **12**·H^+ 1.8 Å (170.3°). Intercomponent binding energies (kcal mol^{-1}): electronic, ΔE_{bind}, **12** −8.0 (±0.05), **12**·H^+ −14.1 (±0.05); enthalpic, ΔH_{bind}, **12** −6.7 (±0.04), **12**·H^+ −11.4 (±1); free energy, ΔG_{bind}, **12** −3.9 (±0.1), **12**·H^+ −4.8 (±1). The errors in the calculations were estimated by increasing the solvent cavity radius by 0.5 Å.

mechanically interlocked components in each state, much less than half the intercomponent binding energy found in typical molecular shuttles yet still strong enough to ensure a high degree of positional integrity of the macrocycle in both forms. The methodology paves the way for faster moving, faster responding, mechanically interlocked molecular machines which can be designed to feature only the weakest non-covalent interactions necessary for their function.

Experimental Section

Procedure for the Cadiot–Chodkiewicz active template synthesis of rotaxane **4**: A solution of acetylene **2** (20 mg, 0.032 mmol) in THF (0.4 mL) was cooled to −78 °C. To this solution was added *n*BuLi (0.32 mL, 0.1 M in THF) at −78 °C. The resulting solution was allowed to warm to 0 °C over 15 min. CuI (6.2 mg, 0.032 mmol) was added at 0 °C and the resulting yellow solution allowed to warm to room temperature over 15 min. The reaction mixture was recooled to −78 °C and bipyridine macrocycle **3** (18 mg, 0.032 mmol) and bromoacetylene **1b** (22 mg, 0.032 mmol) were added as a solution in THF (0.6 mL). The resulting orange solution was allowed to stir at room temperature for 20 h before the reaction was quenched by addition of an aqueous solution of 17.5% NH_3 saturated with ethylenediaminetetraacetic acid (EDTA). The layers were allowed to stir in air for 40 min during which time the aqueous layer turned blue. The aqueous layer was extracted with CH_2Cl_2 (×3) and the combined organic layers were washed with brine and dried over anhydrous $MgSO_4$. Chromatography (silica gel, 7:2.5:0.5 hexane:CH_2Cl_2:MeCN as eluent) yielded [2]rotaxane **4** as a colorless film (47 mg, 84%).

Full details of the experimental procedures, compound characterization and molecular modelling are given in the Supporting Information.

Received: February 25, 2008
Published online: April 29, 2008

Keywords: Cadiot–Chodkiewicz reaction · heterocoupling · molecular shuttles · rotaxanes · template synthesis

[1] a) D. B. Amabilino, J. F. Stoddart, *Chem. Rev.* **1995**, *95*, 2725–2828; b) *Molecular Catenanes, Rotaxanes and Knots: A Journey Through the World of Molecular Topology* (Eds.: J.-P. Sauvage, C. Dietrich-Buchecker), Wiley-VCH, Weinheim, **1999**.

[2] a) For the first molecular shuttle with degenerate stations, see: P. L. Anelli, N. Spencer, J. F. Stoddart, *J. Am. Chem. Soc.* **1991**, *113*, 5131–5133; b) for the first switchable molecular shuttle, see: R. A. Bissell, E. Córdova, A. E. Kaifer, J. F. Stoddart, *Nature* **1994**, *369*, 133–136; c) for a recent review on molecular shuttles, see: H. Tian, Q.-C. Wang, *Chem. Soc. Rev.* **2006**, *35*, 361–374.

[3] The intercomponent binding interactions employed in classical template reactions—typically 12–30 kcal mol^{-1} or more[1]—are much stronger than is necessary to give good positional discrimination of the ring on the thread in a rotaxane. For an unsymmetrical thread featuring two different stations, a 2 kcal mol^{-1} difference in binding affinity is sufficient to ensure 95% occupancy of the preferred binding site at room temperature, see: a) A. Altieri, G. Bottari, F. Dehez, D. A. Leigh, J. K. Y. Wong, F. Zerbetto, *Angew. Chem.* **2003**, *115*, 2398–2402; *Angew. Chem. Int. Ed.* **2003**, *42*, 2296–2300. The length of the thread only accounts for ca. 1 kcal mol^{-1} of the activation energy in a typical 1.5 nm molecular shuttle, see: b) A. S. Lane, D. A. Leigh, A. Murphy, *J. Am. Chem. Soc.* **1997**, *119*, 11092–11093.

[4] E. R. Kay, D. A. Leigh, F. Zerbetto, *Angew. Chem.* **2007**, *119*, 72–196; *Angew. Chem. Int. Ed.* **2007**, *46*, 72–191.

[5] a) V. Aucagne, K. D. Hänni, D. A. Leigh, P. J. Lusby, D. B. Walker, *J. Am. Chem. Soc.* **2006**, *128*, 2186–2187; b) S. Saito, E. Takahashi, K. Nakazono, *Org. Lett.* **2006**, *8*, 5133–5136; c) J. Berná, J. D. Crowley, S. M. Goldup, K. D. Hänni, A.-L. Lee, D. A. Leigh, *Angew. Chem.* **2007**, *119*, 5811–5815; *Angew. Chem. Int. Ed.* **2007**, *46*, 5709–5713; d) V. Aucagne, J. Berná, J. D. Crowley, S. M. Goldup, K. D. Hänni, D. A. Leigh, P. J. Lusby, V. E. Ronaldson, A. M. Z. Slawin, A. Viterisi, D. B. Walker, *J. Am. Chem. Soc.* **2007**, *129*, 11950–11963; e) J. D. Crowley, K. D. Hänni, A.-L. Lee, D. A. Leigh, *J. Am. Chem. Soc.* **2007**, *129*, 12092–12093; f) S. M. Goldup, D. A. Leigh, P. J. Lusby, R. T. McBurney, A. M. Z. Slawin, *Angew. Chem.* **2008**, *120*, 3429–3432; *Angew. Chem. Int. Ed.* **2008**, *47*, 3381–3384.

[6] a) W. Chodkiewicz, *Ann. Chim.* **1957**, *2*, 819–869; b) P. Cadiot, W. Chodkiewicz in *Chemistry of Acetylenes* (Ed.: H. G. Viehe), Marcel Dekker, New York, **1969**, pp. 597–647; c) M. Alami, F. Ferri, *Tetrahedron Lett.* **1996**, *37*, 2763–2766; d) J. M. Montierth, D. R. DeMario, M. J. Kurth, N. E. Schore, *Tetrahedron* **1998**, *54*, 1174–11748.

[7] S. Nygaard, B. W. Laursen, T. S. Hansen, A. D. Bond, A. H. Flood, J. O. Jeppesen, *Angew. Chem.* **2007**, *119*, 6205–6209; *Angew. Chem. Int. Ed.* **2007**, *46*, 6093–6097.

[8] a) R. F. Curtis, J. A. Taylor, *J. Chem. Soc. C* **1971**, 186–188; b) U. Niedballa in *Methoden der Organischen Chemie. Houben Weyl, Vol. V/2a* (Ed.: E. Müller), Thieme, Stuttgart, **1977**, pp. 925–937; c) C. Hartbaum, H. Fisher, *Chem. Ber.* **1997**, *130*, 1063–1067.

[9] Employing an iodoacetylene in place of the bromoacetylene led to poor selectivity (8:2:5 of **4**:**5**:**6**) and reduced (78%) conversion.

[10] As well as producing only 32% rotaxane (the majority arising from homodimerization of the bromoacetylene; Table 2, entry 2), **8** is prone to decomposition. To ensure high yields and selectivity of the heterocoupled rotaxane, it appears that aryl acetylenes should only be employed as the terminal acetylene coupling partner in such reactions.

[11] The mechanism of the Cadiot–Chodkiewicz coupling is generally held to proceed in an analogous fashion to the Castro–Stephens

reaction, see: a) R. D. Stephens, C. E. Castro, *J. Org. Chem.* **1963**, *28*, 3313 – 3315; b) P. Siemsen, R. C. Livingston, F. Diederich, *Angew. Chem.* **2000**, *112*, 2740 – 2767; *Angew. Chem. Int. Ed.* **2000**, *39*, 2632 – 2657; c) R. Brückner in *Advanced Organic Chemistry: Reaction Mechanisms*, Harcourt/Academic Press, San Diego, **2002**, p. 538. This differs markedly from the accepted mechanism of the Glaser Cu-catalyzed homocoupling of alkynes in that 1) the key intermediate is monometallic and 2) the oxidation state of copper formally changes from Cu^{I} to Cu^{III} during the key step of the Cadiot–Chodkiewicz and Castro–Stephens reactions, whereas in the Glaser homocoupling it switches between Cu^{I} and Cu^{II}.

[12] The heterocoupling does not proceed in the absence of the bipyridine macrocycle ligand **3** under these conditions. A control reaction repeating this procedure in the absence of **3** resulted in no heterocoupled thread (by ^{1}H NMR analysis). The high yields of the active template rotaxane forming reaction without the need for excess reactants can be attributed to the absence of background reactivity.

[13] Geometry optimizations and frequency calculations for the macrocycle-station fragments of **12** and **12**·HOTs were carried out at B3LYP/3-21G* level with the Gaussian03 program (M. J. Frisch, et al. Gaussian 03, revision C.02; Gaussian, Inc., Wallingford CT, **2004**). The hybrid exchange-correlation B3LYP (A. D. J. Becke, *J. Chem. Phys.* **1993**, *98*, 5648 – 5652) functional was adopted on the basis of its reported suitability in describing both hydrogen bonding interactions and aromatic stacking interactions (Y. Zhao, D. G. Truhlar, *J. Chem. Theory Comput.* **2005**, *1*, 415 – 432), particularly in the presence of N-based π-electron systems such as those considered here (G. Bouchoux, *Mass Spectrom. Rev.* **2007**, *26*, 775 – 835). Specifically, it has been shown to properly account for the geometry and proton and hydrogen bonding affinity of both aniline (N. Russo, M. Toscano, A. Grand, T. Mineva, *J. Phys. Chem. A* **2000**, *104*, 4017 – 4020; V. Q. Nguyen, F. Tureček, *J. Mass Spectrom.* **1997**, *32*, 55 – 63) and pyridinium based systems (H. Szatyłowicz, T. M. Krygowski, J. E. Zachara-Horeglad, *J. Chem. Inf. Model.* **2007**, *47*, 875 – 886). Solvent phase (CH_2Cl_2) calculations were performed with the self-consistent reaction field method (SCRF) (M. W. Wong, K. B. Wiberg, M. J. Frisch, *J. Am. Chem. Soc.* **1992**, *114*, 1645 – 1652, and references therein) implemented in the Gaussian program.

[14] a) N. Haider, K. Mereiter, R. Wanko, *Heterocycles* **1995**, *41*, 1445 – 1459; b) Q. Ye, X. S. Wang, H. Zhao, R. G. Xiong, *Tetrahedron: Asymmetry* **2005**, *16*, 1595 – 1602; c) C. D. Hopkins, H. C. Malinakova, *Org. Lett.* **2006**, *8*, 5971 – 5974.

[15] For examples of molecular shuttles that are reversibly switchable by protonation, see Ref. [2b] and: a) M.-V. Martínez-Díaz, N. Spencer, J. F. Stoddart, *Angew. Chem.* **1997**, *109*, 1991 – 1994; *Angew. Chem. Int. Ed. Engl.* **1997**, *36*, 1904 – 1907; b) P. R. Ashton, R. Ballardini, V. Balzani, I. Baxter, A. Credi, M. C. T. Fyfe, M. T. Gandolfi, M. Gómez-López, M.-V. Martínez-Díaz, A. Piersanti, N. Spencer, J. F. Stoddart, M. Venturi, A. J. P. White, D. J. Williams, *J. Am. Chem. Soc.* **1998**, *120*, 11932 – 11942; c) A. M. Elizarov, S.-H. Chiu, J. F. Stoddart, *J. Org. Chem.* **2002**, *67*, 9175 – 9181; d) J. D. Badjić, V. Balzani, A. Credi, S. Silvi, J. F. Stoddart, *Science* **2004**, *303*, 1845 – 1849; e) C. M. Keaveney, D. A. Leigh, *Angew. Chem.* **2004**, *116*, 1242 – 1244; *Angew. Chem. Int. Ed.* **2004**, *43*, 1222 – 1224; f) S. Garaudée, S. Silvi, M. Venturi, A. Credi, A. H. Flood, J. F. Stoddart, *ChemPhysChem* **2005**, *6*, 2145 – 2152; g) J. D. Badjić, C. M. Ronconi, J. F. Stoddart, V. Balzani, S. Silvi, A. Credi, *J. Am. Chem. Soc.* **2006**, *128*, 1489 – 1499; h) Y. Tokunaga, T. Nakamura, M. Yoshioka, Y. Shimomura, *Tetrahedron Lett.* **2006**, *47*, 5901 – 5904; i) D. A. Leigh, A. R. Thomson, *Org. Lett.* **2006**, *8*, 5377 – 5379; j) J. D. Crowley, D. A. Leigh, P. J. Lusby, R. T. McBurney, L.-E. Perret-Aebi, C. Petzold, A. M. Z. Slawin, M. D. Symes, *J. Am. Chem. Soc.* **2007**, *129*, 15085 – 15090.

[16] a) K. Biradha, R. E. Edwards, G. J. Foulds, W. T. Robinson, G. R. Desiraju, *J. Chem. Soc. Chem. Commun.* **1995**, 1705 – 1707; b) D. Braga, S. L. Giaffreda, M. Polito, F. Grepioni, *Eur. J. Inorg. Chem.* **2005**, 2737 – 2746; c) A. R. Kennedy, M. Kittner, *Acta Crystallogr. Sect. E* **2005**, *61*, o333 – o334.

[17] For molecular shuttles that are reversibly switchable by complexation with Li^{+}, see Ref. [15h] and: a) S. A. Vignon, T. Jarrosson, T. Iijima, H.-R Tseng, J. K. M. Sanders, J. F. Stoddart, *J. Am. Chem. Soc.* **2004**, *126*, 9884 – 9885; b) Y. Nagawa, J.-I. Suga, K. Hiratani, E. Koyama, M. Kanesato, *Chem. Commun.* **2005**, 749 – 751; c) N.-C. Chen, P.-Y. Huang, C.-C. Lai, Y.-H. Liu, Y. Wang, S.-M. Peng, S.-H. Chiu, *Chem. Commun.* **2007**, 4122 – 4124.

Article

A Switchable Palladium-Complexed Molecular Shuttle and Its Metastable Positional Isomers

James D. Crowley, David A. Leigh, Paul J. Lusby, Roy T. McBurney, Laure-Emmanuelle Perret-Aebi, Christiane Petzold, Alexandra M. Z. Slawin, and Mark D. Symes

J. Am. Chem. Soc., **2007**, 129 (48), 15085-15090• DOI: 10.1021/ja076570h • Publication Date (Web): 09 November 2007

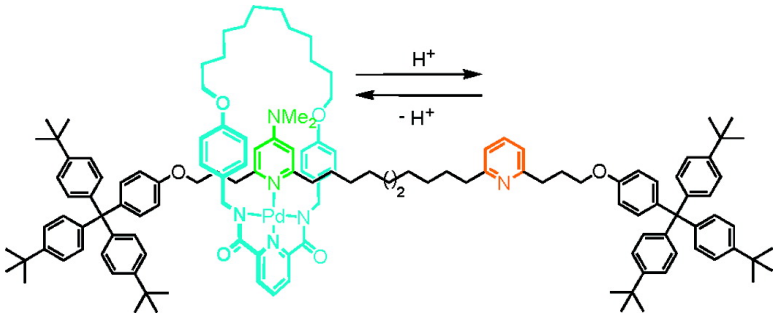

More About This Article

Additional resources and features associated with this article are available within the HTML version:

- Supporting Information
- Links to the 16 articles that cite this article, as of the time of this article download
- Access to high resolution figures
- Links to articles and content related to this article
- Copyright permission to reproduce figures and/or text from this article

View the Full Text HTML

J|A|C|S
ARTICLES
Published on Web 11/09/2007

A Switchable Palladium-Complexed Molecular Shuttle and Its Metastable Positional Isomers

James D. Crowley,[†] David A. Leigh,*[,†] Paul J. Lusby,[†] Roy T. McBurney,[†] Laure-Emmanuelle Perret-Aebi,[†] Christiane Petzold,[†] Alexandra M. Z. Slawin,[‡] and Mark D. Symes[†]

Contribution from the School of Chemistry, University of Edinburgh, The King's Buildings, West Mains Road, Edinburgh EH9 3JJ, United Kingdom, and the School of Chemistry, University of St. Andrews, Purdie Building, St. Andrews, Fife KY16 9ST, United Kingdom

Received August 31, 2007; E-mail: David.Leigh@ed.ac.uk

Abstract: We report the design, synthesis, characterization, and operation of a [2]rotaxane in which a palladium-complexed macrocycle can be translocated between 4-dimethylaminopyridine and pyridine monodentate ligand sites via reversible protonation, the metal remaining coordinated to the macrocycle throughout. The substitution pattern of the ligands and the kinetic stability of the Pd−N bond means that changing the chemical state of the thread does not automatically cause a change in the macrocycle's position in the absence of an additional input (heat and/or coordinating solvent/anion). Accordingly, under ambient conditions any of the four sets of protonated and neutral, stable, and metastable co-conformers of the [2]rotaxane can be selected, manipulated, isolated, and characterized.

Introduction

Despite the success and influence of the redox-responsive Cu(I)/Cu(II) catenane and rotaxane systems developed in Strasbourg,[1,2] there are no other examples of stimuli-switchable molecular shuttles[3] based on the manipulation of metal−ligand interactions between the components.[4,5] This lack of switchable metal coordination motifs for interlocked molecules may be set to change, however, following the recognition of the need to vary the kinetics of binding events and transportation pathways (e.g., ratcheting and escapement[6]) in any mechanical molecular machine more sophisticated than a switch,[7] and the crucial role played by metastability in the functioning of rotaxanes currently being investigated for molecular electronics.[8] Here we describe a simple-to-assemble-and-operate [2]rotaxane in which a palladium-complexed macrocycle can be translocated between 4-dimethylaminopyridine (DMAP) and pyridine (Py) ligand sites via reversible protonation (the metal remaining coordinated to

[†] University of Edinburgh.

[‡] University of St Andrews.

(1) For macrocycle translocation in Cu(I)/Cu(II)-coordinated rotaxanes, see: (a) Gaviña, P.; Sauvage, J.-P. *Tetrahedron Lett.* **1997**, *38*, 3521−3524. (b) Armaroli, N.; Balzani, V.; Collin, J.-P.; Gaviña, P.; Sauvage, J.-P.; Ventura, B. *J. Am. Chem. Soc.* **1999**, *121*, 4397−4408. (c) Durola, F.; Sauvage, J.-P. *Angew. Chem., Int. Ed.* **2007**, *46*, 3537−3540. For macrocycle translocation in Cu(I)/Cu(II)-coordinated catenanes, see: (d) Livoreil, A.; Dietrich-Buchecker, C. O.; Sauvage, J.-P. *J. Am. Chem. Soc.* **1994**, *116*, 9399−9400. (e) Cárdenas, D. J.; Livoreil, A.; Sauvage, J.-P. *J. Am. Chem. Soc.* **1996**, *118*, 11980−11981. (f) Livoreil, A.; Sauvage, J.-P.; Armaroli, N.; Balzani, V.; Flamigni, L.; Ventura, B. *J. Am. Chem. Soc.* **1997**, *119*, 12114−12124. For macrocycle rotation in Cu(I)/Cu(II)-coordinated rotaxanes, see: (g) Raehm, L.; Kern, J.-M.; Sauvage, J.-P. *Chem.—Eur. J.* **1999**, *5*, 3310−3317. (h) Weber, N.; Hamann, C.; Kern, J.-M.; Sauvage, J.-P. *Inorg. Chem.* **2003**, *42*, 6780−6792. (i) Poleschak, I.; Kern, J.-M.; Sauvage, J.-P. *Chem. Commun.* **2004**, 474−476. (j) Létinois-Halbes, U.; Hanss, D.; Beierle, J. M.; Collin, J.-P.; Sauvage, J.-P. *Org. Lett.* **2005**, *7*, 5753−5756. For a recent review of transition metal complexed molecular machines, see: (k) Bonnet, S.; Collin, J.-P.; Koizumi, M.; Mobian, P.; Sauvage, J.-P. *Adv. Mater.* **2006**, *18*, 1239−1250.

(2) For contraction/stretching in a rotaxane dimer through Cu(I)−Zn(II) exchange, see: (a) Jiménez, M. C.; Dietrich-Buchecker, C.; Sauvage, J.-P. *Angew. Chem., Int. Ed.* **2000**, *39*, 3284−3287. (b) Jiménez-Molero, M. C.; Dietrich-Buchecker, C.; Sauvage, J.-P. *Chem.—Eur. J.* **2002**, *8*, 1456−1466.

(3) (a) Bissell, R. A.; Córdova, E.; Kaifer, A. E.; Stoddart, J. F. *Nature* **1994**, *369*, 133−136. For other examples of pH-responsive molecular shuttles see: (b) Martínez-Díaz, M.-V.; Spencer, N.; Stoddart, J. F. *Angew. Chem., Int. Ed. Engl.* **1997**, *36*, 1904−1907. (c) Ashton, P. R.; Ballardini, R.; Balzani, V.; Baxter, I.; Credi, A.; Fyfe, M. C. T.; Gandolfi, M. T.; Gómez-López, M.; Martínez-Díaz, M.-V.; Piersanti, A.; Spencer, N.; Stoddart, J. F.; Venturi, M.; White, A. J. P.; Williams, D. J. *J. Am. Chem. Soc.* **1998**, *120*, 11932−11942. (d) Elizarov, A. M.; Chiu, S.-H.; Stoddart, J. F. *J. Org. Chem.* **2002**, *67*, 9175−9181. (e) Badjić, J. D.; Balzani, V.; Credi, A.; Silvi, S.; Stoddart, J. F. *Science* **2004**, *303*, 1845−1849. (f) Keaveney, C. M.; Leigh, D. A. *Angew. Chem., Int. Ed.* **2004**, *43*, 1222−1224. (g) Garaudée, S.; Silvi, S.; Venturi, M.; Credi, A.; Flood, A. H.; Stoddart, J. F. *ChemPhysChem.* **2005**, *6*, 2145−2152. (h) Badjić, J. D.; Ronconi, C. M.; Stoddart, J. F.; Balzani, V.; Silvi, S.; Credi, A. *J. Am. Chem. Soc.* **2006**, *128*, 1489−1499. (i) Tokunaga, Y.; Nakamura, T.; Yoshioka, M.; Shimomura, Y. *Tetrahedron Lett.* **2006**, *47*, 5901−5904. (j) Leigh, D. A.; Thomson, A. R. *Org. Lett.* **2006**, *8*, 5377−5379.

(4) For ruthenium-coordinated catenanes and rotaxanes which undergo photoinduced decomplexation of the components, see: (a) Mobian, P.; Kern, J.-M.; Sauvage, J.-P. *Angew. Chem., Int. Ed.* **2004**, *43*, 2392−2395. (b) Collin, J.-P.; Jouvenot, D.; Koizumi, M.; Sauvage, J.-P. *Eur. J. Inorg. Chem.* **2005**, 1850−1855. For other types of rotaxanes and catenanes which feature intercomponent metal−ligand coordination, see: (c) Hutin, M.; Schalley, C. A.; Bernardinelli, G.; Nitschke, J. R. *Chem.—Eur. J.* **2006**, *12*, 4069−4076. (d) Blight, B. A.; Wisner, J. A.; Jennings, M. C. *Chem. Commun.* **2006**, 4593−4595. (e) Blight, B. A.; Wisner, J. A.; Jennings, M. C. *Angew. Chem., Int. Ed.* **2007**, *46*, 2835−2838.

(5) For examples of rotaxanes and catenanes which utilize transition metal ions to switch on/off other types of intercomponent interaction, see: (a) Korybut-Daszkiewicz, B.; Więckowska, A.; Bilewicz, R.; Domagała, S.; Woźniak, K. *Angew. Chem., Int. Ed.* **2004**, *43*, 1668−1672. (b) Jiang, L.; Okano, J.; Orita, A.; Otera, J. *Angew. Chem., Int. Ed.* **2004**, *43*, 2121−2124. (c) Leigh, D. A.; Lusby, P. J.; Slawin, A. M. Z.; Walker, D. B. *Angew. Chem., Int. Ed.* **2005**, *44*, 4557−4564. (d) Leigh, D. A.; Lusby, P. J.; Slawin, A. M. Z.; Walker, D. B. *Chem. Commun.* **2005**, 4919−4921. (e) Marlin, D. S.; González Cabrera, D.; Leigh, D. A.; Slawin, A. M. Z. *Angew. Chem., Int. Ed.* **2006**, *45*, 77−83. (f) Marlin, D. S.; González Cabrera, D.; Leigh, D. A.; Slawin, A. M. Z. *Angew. Chem., Int. Ed.* **2006**, *45*, 1385−1390.

(6) Chatterjee, M. N.; Kay, E. R.; Leigh, D. A. *J. Am. Chem. Soc.* **2006**, *128*, 4058−4073.

(7) (a) Kay, E. R.; Leigh, D. A. *Nature* **2006**, *440*, 286−287. (b) Kay, E. R.; Leigh, D. A.; Zerbetto, F. *Angew. Chem., Int. Ed.* **2007**, *46*, 72−191.

Scheme 1. Reversible Substitution of Pyridine and DMAP Ligands in Macrocycle−Pd Complex **L1**PdPy/DMAP in DMF-d_7 at 298 K[a]

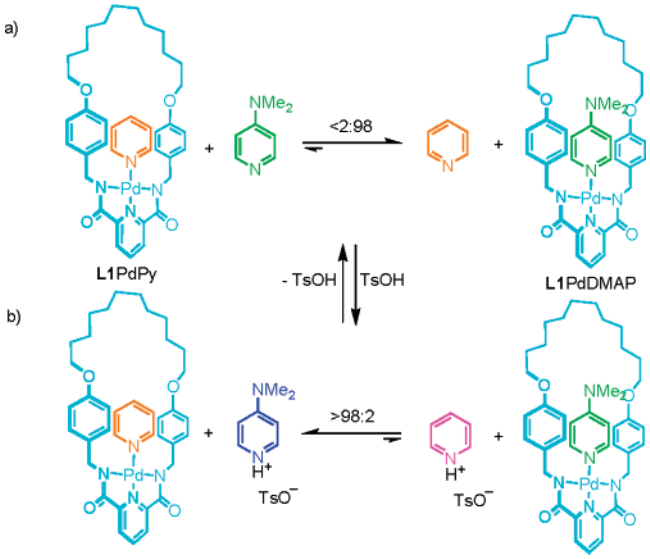

[a] Upon mixing the substrates, equilibrium is reached within the time taken to acquire a ^{1}H NMR spectrum. (a) Neutral conditions; (b) in the presence of TsOH (1 equiv).

the macrocycle throughout). The substitution pattern of the ligands and the kinetic stability of the Pd−N bond means that changing the chemical state of the thread (adding or removing protons) does not automatically cause a change in the macrocycle's position in the absence of an additional input (heat and/or coordinating solvent/anion). Accordingly, under ambient conditions any of the four sets of protonated and neutral, stable, and metastable co-conformers of the [2]rotaxane can be selected, manipulated, isolated, and characterized.

Results and Discussion

Basis of the Design: Protonation/Deprotonation-Driven Ligand Exchange Experiments. The shuttle is based on a recognition motif previously used to assemble rotaxanes and catenanes by organizing tridentate pyridine 2,6-dicarboxamide and appropriately derivatized monodentate pyridine ligands about a square planar Pd(II) template.[9] In a simple exchange experiment with non-interlocked versions of these ligands (Scheme 1a), we found that the pyridine group of **L1**PdPy was rapidly[10] and quantitatively substituted for DMAP.[11] By adding an equivalent of *p*-toluenesulfonic acid (TsOH), the process could be reversed (Scheme 1b).[12] The reasons for the selectivity in Scheme 1b are quite subtle: although both heterocycles are "coordinated"—one to Pd(II) and one to H^+—on both sides of the equation (Scheme 1b), protonation of the more basic heterocycle determines the position of equilibrium because the N−H bond is significantly stronger than the Pd−N bond.[13] In other words, a proton differentiates DMAP and Py more effectively than does Pd(II). The results suggested that a palladium-complexed [2]rotaxane incorporating both DMAP and Py binding sites in the thread could operate as a pH-switchable molecular shuttle.

Synthesis and Characterization of Palladium-Coordinated Molecular Shuttle L2Pd. A candidate [2]rotaxane, **L2**Pd, was synthesized in nine steps using a "threading-followed-by-stoppering" strategy[14] (Scheme 2). 2,6-Diiodo-4-dimethylaminopyridine, **1**, was prepared via a modified literature procedure[15] (Scheme 2, step a) and subjected to consecutive Sonogashira cross-coupling reactions,[16] first with propargyl alcohol (1 equiv) and then with decadiyne (5 equiv), to afford the unsymmetrical *DMAP*-station[17] intermediate **3** (Scheme 2, step c). The synthesis of the *Py*-station fragment was achieved by desymmetrization of commercially available 2,6-dibromopyridine through a Sonogashira cross-coupling with 1 equiv of propargyl alcohol to give **2** (Scheme 2, step b), hydrogenation (over PtO_2), and Mitsunobu reaction[18] with bulky phenol **4**[19] to give **5** (Scheme 2, step d). The coupling of **3** and **5** via another Pd-catalyzed Sonogashira reaction, and subsequent hydrogenation over Pd(OH)$_2$/C, afforded the saturated monostoppered thread, **6** (Scheme 2, step e). Coordination of the macrocycle−palladium complex to the *DMAP* site of **6** occurred upon simple stirring with **L1**Pd(CH_3CN)[9c] in dichloromethane (298 K, 1 h). The resulting threaded pseudo-rotaxane complex was covalently

(8) (a) Tseng, H.-R.; Wu, D.; Fang, N. X.; Zhang, X.; Stoddart, J. F. *ChemPhysChem* **2004**, *5*, 111−116. (b) Steuerman, D. W.; Tseng, H.-R.; Peters, A. J.; Flood, A. H.; Jeppesen, J. O.; Nielsen, K. A.; Stoddart, J. F.; Health, J. R. *Angew. Chem., Int. Ed.* **2004**, *43*, 6486−6491. (c) Flood, A. H.; Peters, A. J.; Vignon, S. A.; Steuerman, D. W.; Tseng, H. -R.; Kang, S.; Heath, J. R.; Stoddart, J. F. *Chem.—Eur. J.* **2004**, *10*, 6558−6564. (d) Flood, A. H.; Stoddart, J. F.; Steuerman, D. W.; Heath, J. R. *Science* **2004**, *306*, 2055−2056. (e) Choi, J. W.; Flood, A. H.; Steuerman, D. W.; Nygaard, S.; Braunschweig, A. B.; Moonen, N. N. P.; Laursen, B. W.; Luo, Y.; Delonno, E.; Peters, A. J.; Jeppesen, J. O.; Xe, K.; Stoddart, J. F.; Heath, J. R. *Chem.—Eur. J.* **2006**, *12*, 261−279.

(9) (a) Fuller, A.-M.; Leigh, D. A.; Lusby, P. J.; Oswald, I. D. H.; Parsons, S.; Walker, D. B. *Angew. Chem., Int. Ed.* **2004**, *43*, 3914−3918. (b) Furusho, Y.; Matsuyama, T.; Takata, T.; Moriuchi, T.; Hirao, T. *Tetrahedron Lett.* **2004**, *45*, 9593−9597. (c) Fuller, A.-M. L.; Leigh, D. A.; Lusby, P. J.; Slawin, A. M. Z.; Walker, D. B. *J. Am. Chem. Soc.* **2005**, *127*, 12612−12619. (d) Leigh, D. A.; Lusby, P. J.; Slawin, A. M. Z.; Walker, D. B. *Angew. Chem., Int. Ed.* **2005**, *44*, 4557−4564. (e) Fuller, A.-M. L.; Leigh, D. A.; Lusby, P. J. *Angew. Chem., Int. Ed.* **2007**, *46*, 5015−5019.

(10) Exchange of the unsubstituted heterocycles in $CDCl_3$, $C_2D_2Cl_4$, or DMF-d_7 was complete within the time frame of mixing the **L1**PdPy complex with DMAP and acquiring a ^{1}H NMR spectrum, as was the reverse proton-driven exchange upon adding TsOH. However, the 2,6-dipropyl substituted heterocycles did not exchange in $CDCl_3$ even over extended periods (7 d) or upon heating at reflux. In DMF-d_7 at 358 K equilibrium was reached after 60 min (neutral conditions) or 130 min (in the presence of TsOH). For full details of the exchange experiments, see the Supporting Information.

(11) For the exchange of various 4-substituted pyridine ligands at the fourth coordination site of Pd−pincer complexes, see: (a) van Manen, H.-J.; Nakashima, K.; Shinkai, S.; Kooijman, H.; Spek, A. L.; van Veggel, F. C. J. M.; Reinhoudt, D. N. *Eur. J. Inorg. Chem.* **2000**, 2533−2540. The exchange of DMAP for poly(4-vinylpyridine) at the fourth coordination site of bimetallic Pd− and Pt−pincer complexes has been exploited in the chemoresponsive viscosity switching of a metallo-supramolecular network; see: (b) Loveless, D. M.; Jeon, S. L.; Craig, S. L. *J. Mater. Chem.* **2007**, *17*, 56−61.

(12) A proton-driven ligand exchange of diethylamine and lutidine coordinated to Pd(II) has previously been reported; see: (a) Hamann, C.; Kern, J.-M.; Sauvage, J.-P. *Dalton Trans.* **2003**, 3770−3775. For the proton-driven exchange of one amine for another within copper-coordinated imine ligands, see: (b) Nitschke, J. R. *Angew. Chem., Int. Ed.* **2004**, *43*, 3073−3075. (c) Nitschke, J. R.; Schultz, D.; Bernardinelli, G.; Gérard, D. *J. Am. Chem. Soc.* **2004**, *126*, 16538−16543. (d) Schultz, D.; Nitschke, J. R. *Proc. Natl. Acad. Sci. U.S.A.* **2005**, *102*, 11191−11195. (e) Nitschke, J. R. *Acc. Chem. Res.* **2007**, *40*, 103−112.

(13) (a) Sanderson, R. T. *Chemical Bonds & Bond Energy*; Academic Press: New York, 1976. (b) Cotton, F. A.; Wilkinson, G.; Murillo, C.; Bochmann, M.; Grimes, R.; Murillo, C. A.; Bochmann M. *Advanced Inorganic Chemistry: A Comprehensive Text*, 6th ed.; John Wiley & Sons: New York, 1999. A contributing reason as to why the proton discriminates DMAP and pyridine better than the Pd−macrocycle complex may be because the proton is charged while the Pd−macrocycle is not. However, since this is not the situation in ref 12a, where proton-driven ligand exchange at Pd(II) also occurs, it is presumably not a major factor in the present system either.

(14) Amabilino, D. B.; Stoddart, J. F. *Chem. Rev.* **1995**, *95*, 2725−2828.

(15) Wayman, K. A.; Sammakia, T. *Org. Lett.* **2003**, *5*, 4105−4108.

(16) Sonogashira, K.; Tohda, Y.; Hagihara, N. *Tetrahedron Lett.* **1975**, *16*, 4467−4470.

(17) The italicized prefixes *DMAP-* and *Py-* denote the position of the macrocycle on the thread in the rotaxane.

(18) Mitsunobu, O.; Yamada, Y. *Bull. Chem. Soc. Jpn.* **1967**, *40*, 2380−2382.

(19) Gibson, H. W.; Lee, S. H.; Engen, P. T.; Lecavalier, P.; Sze, J.; Shen, Y. X.; Bheda, M. *J. Org. Chem.* **1993**, *58*, 3748−3756.

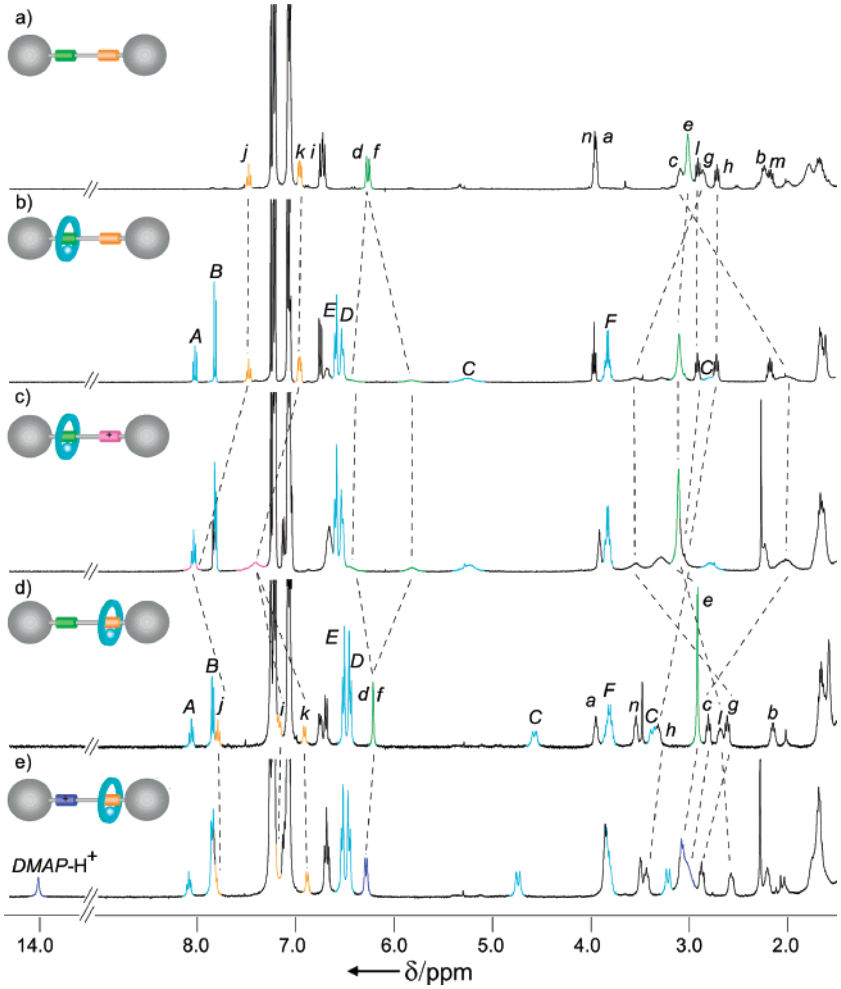

Figure 1. ^{1}H NMR spectra (400 MHz, $CDCl_3$, 300 K) of palladium rotaxane **L2**Pd in its four different protonated and co-conformational states, and for comparison the free thread: (a) Thread **8**; (b) *DMAP*-**L2**Pd; (c) *DMAP*-[**L2**HPd]OTs; (d) *Py*-**L2**Pd; (e) *Py*-[**L2**HPd]OTs. The lettering in the figure refers to the assignments in Scheme 2.

captured with **4** (DIAD, PPh_3, THF) to give the [2]rotaxane, **L2**Pd, in 26% yield[20] after column chromatography (Scheme 2, step f).

Mass spectrometry confirmed the product's constitution as **L2**Pd, and ^{1}H NMR spectroscopy (Figure 1b) showed the co-conformation formed to be exclusively *DMAP*-**L2**Pd;[17] i.e., the Pd−macrocycle fragment, **L1**Pd, was solely coordinated to the *DMAP* binding site. A comparison of the spectra of free thread **8** (Figure 1a) and *DMAP*-**L2**Pd in $CDCl_3$ (Figure 1b) shows significant differences between the signals of the *DMAP* station (H_{d-f}) for the rotaxane and thread, while the *Py* station signals (H_{i-k}) of the rotaxane occur at very similar values to those of the free thread. Interestingly, and for reasons that would become apparent later, attempting the threading protocol with **7**, a close analogue of **6** in which the positions of the two stations were reversed (i.e., the *Py* binding site was closest to the unstoppered end of the thread; Scheme 2, step g), led exclusively to the formation of *Py*-**L2**Pd! The outcomes of the two threading reactions indicate that the pyridine and DMAP binding sites are both astonishingly efficient at capturing the Pd−macrocycle component from **L1**Pd(CH_3CN) on its initial pass over the heterocycle at the open end of the thread, irrespective of relative orientation, solvation, or other factors.

Macrocycle-to-Py-Station Protonation-Driven Shuttling Experiments. Switching of the macrocycle position in *DMAP*-**L2**Pd was attempted by the addition of 1 equiv of TsOH in $CDCl_3$ (Scheme 3). The ^{1}H NMR spectrum of the resulting adduct (Figure 1c) showed significant changes in the *Py* resonances, H_{i-k}, but no discernible shift of the *DMAP* signals, H_{d-f}, indicating that protonation of the *Py* station had occurred but the position of the macrocycle had not changed; i.e., the chemical structure was now *DMAP*-[**L2**HPd]OTs (Scheme 3). No changes to the ^{1}H NMR spectrum of the sample were observed over several days, indicating that the co-conformer is effectively stable at room temperature in $CDCl_3$. Somewhat surprisingly, however, given the results of the exchange experiments reported in Scheme 1,[10] even in neat coordinating solvents (DMSO-d_6 or DMF-d_7) no evidence of translocation of the ring in *DMAP*-[**L2**HPd]OTs was observed at room temperature. Translocation of the palladium macrocycle sub-component (**L1**Pd) only takes place at elevated temperatures (383 K), in both coordinating (DMF-d_7) and non-coordinating solvents ($C_2D_2Cl_4$), in both cases reaching an equilibrium 89:11 ratio of *Py*:*DMAP*-[**L2**HPd]OTs (Scheme 3) after 16 h (DMF-d_7) or 36 h ($C_2D_2Cl_4$).

(20) The modest yield of rotaxane in the stoppering step is probably a consequence of using a triphenylphosphine-mediated reaction with a Pd-complexed pseudo-rotaxane. Alternative methodologies are currently being investigated.

Scheme 2. Synthesis of Palladium-Complexed Molecular Shuttle **L2**Pd[a]

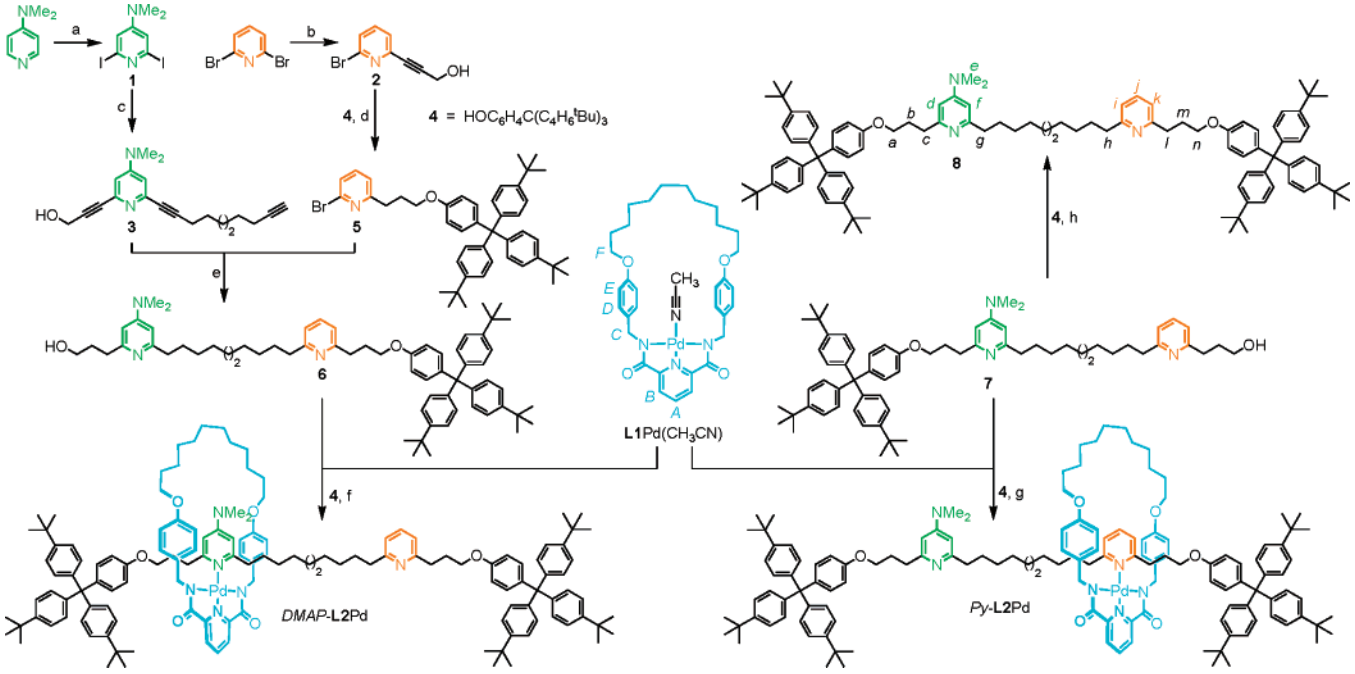

[a] Reagents and conditions: (a) $BF_3{\cdot}OEt_2$, LDA, I_2, THF, 40%; (b) propargyl alcohol, $Pd(PPh_3)_4$, CuI, Et_3N/THF (1:2), 60%; (c) (i) propargyl alcohol, $Pd(PPh_3)_4$, CuI, Et_3N/THF, 75%, (ii) 1,9-decadiyne (5 equiv), $Pd(PPh_3)_4$, CuI, Et_3N/THF, 77%; (d) (i) H_2, PtO_2, EtOH/Et_3N, 94%, (ii) **4**, DIAD, PPh_3, THF, 61%; (e) (i) $Pd(PPh_3)_4$, CuI, Et_3N/THF, 66%, (ii) H_2, $Pd(OH)_2$/C, THF, 88%; (f) (i) **L1**Pd(CH_3CN), CH_2Cl_2 (90%), (ii) **4**, DIAD, PPh_3, THF, 26% (from **6**); (g) (i) **L1**Pd(CH_3CN), CH_2Cl_2 (67%), (ii) **4**, DIAD, PPh_3, THF, 21% (from **7**); (h) **4**, DIAD, PPh_3, THF, 25%.

Scheme 3. Operation of the Palladium-Complexed Molecular Shuttle **L2**Pd[a]

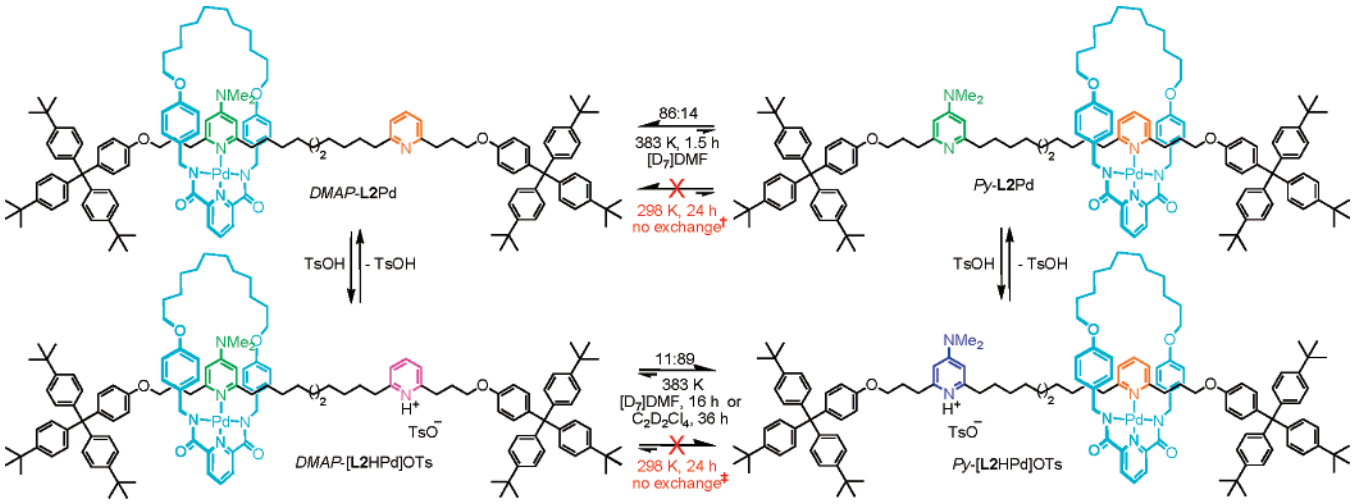

[a] † No macrocycle translocation observed over 24 h in DMF-d_7 at 298 K or in $C_2D_2Cl_4$ over 24 h at 383 K; ‡ No macrocycle translocation observed in either DMF-d_7 or $C_2D_2Cl_4$ at 298 K over 24 h.

Ligand Exchange Experiments and X-ray Crystallography Using 2,6-Dialkyl-Substituted Heterocycles. The dramatic kinetic stability of the *DMAP*−Pd bond in the protonated [2]-rotaxane led us to re-examine the kinetics of non-interlocked ligand exchange, this time using 2,6-dialkyl-substituted heterocycles (Scheme 4). Indeed, using 2,6-dipropylPy and 2,6-dipropylDMAP as the monodentate components of the **L1**Pd−heterocycle complex (Scheme 4) produced the same extremely slow exchange of ligands observed in the [2]rotaxane. Single crystals of both **L1**Pd(2,6-dipropylPy) and **L1**Pd(2,6-dipropylDMAP) were subsequently grown by vapor diffusion of diethyl ether into saturated solutions of the complexes in dichloromethane. The X-ray crystal structures of these two complexes (Figure 2a and 2b) are indicative of the likely coordination mode and geometry of the macrocycle at the two different binding sites in the [2]rotaxane. The crystal structures suggest that the reason for the enhanced kinetic stability of the Pd-coordinated 2,6-dialkylheterocycle units is that the α-hydrogen atoms of the alkyl substituents block the pathway of incoming nucleophiles to the Pd center.[21]

Macrocycle-to-DMAP-Station Deprotonation-Driven Shuttling Experiments. Deprotonation of the 89:11 *Py*:*DMAP* equilibrium mixture of [**L2**HPd]OTs (Na_2CO_3, CH_2Cl_2, 30 min) generated the neutral co-conformers which were readily sepa-

(21) Similar effects have been observed upon increasing the steric bulk about the coordination sphere in other Pd and Pt complexes. For examples, see: (a) Atwood, J. D. *Inorganic and Organometallic Reaction Mechanisms*, 2nd ed.; Wiley-VCH: New York, 1997. (b) Yount, W. C.; Loveless, D. M.; Craig, S. L. *J. Am. Chem. Soc.* **2005**, *127*, 14488−14496.

Scheme 4. Reversible Substitution of 2,6-Dipropylpyridine and 2,6-DipropylDMAP Ligands in Macrocycle−Pd Complex **L1**Pd(2,6-dipropylPy)/(2,6-dipropylDMAP) in DMF-d_7[a]

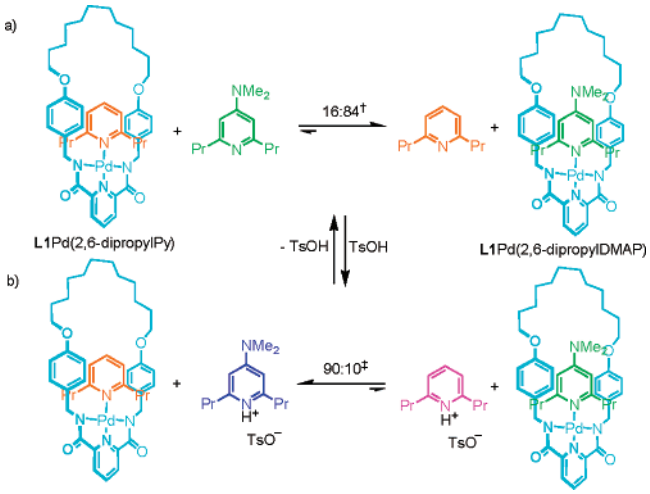

[a] (a) Neutral conditions; (b) in the presence of TsOH (1 equiv). Time required to reach equilibrium:[10] † 60 min at 358 K; ‡ 130 min at 358 K. No exchange of the 2,6-dipropylheterocycle ligands was observed in $CDCl_3$, under either neutral conditions or in the presence of TsOH, even under heating at reflux over 7 d.

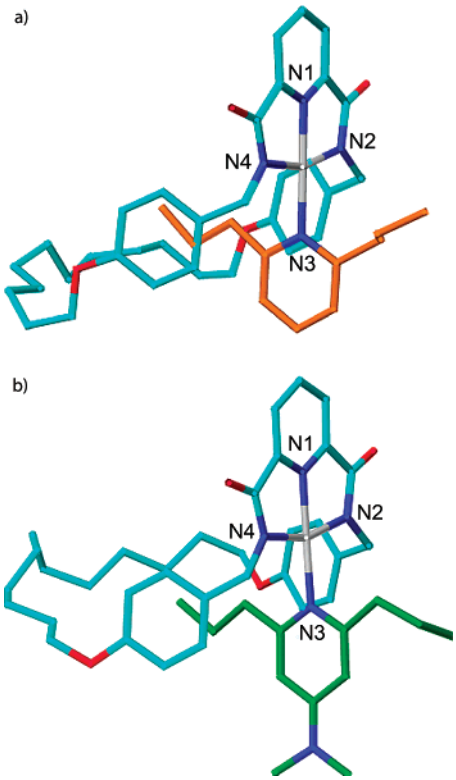

Figure 2. X-ray crystal structures of (a) **L1**Pd(2,6-dipropylPy) and (b) **L1**Pd(2,6-dipropylDMAP). Carbon atoms of the macrocycle are shown in light blue, and those of the monodentate ligands, in orange and green, respectively; oxygen atoms are red; nitrogen, dark blue; and palladium, gray. Selected bond lengths [Å] and angles [deg]: (a) N1−Pd 1.94, N2−Pd 2.03, N3−Pd 2.06, N4−Pd 2.03, N2−Pd−N4 161.6; (b) N1−Pd 1.93, N2−Pd 2.03, N3−Pd 2.06, N4−Pd 2.02, N2−Pd−N4 161.4.

rated by column chromatography to give pure, kinetically stable samples of both *DMAP*-**L2**Pd (minor product) and *Py*-**L2**Pd (major product). Their ^{1}H NMR spectra are shown in Figure 1b and 1d, respectively. As before, the relative shifts of the resonances of the *DMAP* and *Py* stations unambiguously confirmed the position of the macrocycle in the *Py*-**L2**Pd isomer. Reprotonation of *Py*-**L2**Pd (1 equiv of TsOH in $CDCl_3$) quantitatively generated *Py*-[**L2**HPd]OTs (^{1}H NMR spectrum, Figure 1e), as another kinetically stable, out-of-equilibrium co-conformer.

To complete the cycle of operations on **L2**Pd, pure *Py*-**L2**Pd and the nonequilibrium, 11:89, mixture of *DMAP*/*Py*-**L2**Pd were each heated at 383 K in DMF-d_7. After 90 min both had reached identical 86:14 ratios of *DMAP*/*Py*-**L2**Pd which did not change upon further heating (Scheme 3). Unlike the proton-driven translocation, no macrocycle translational isomerization was observed when *Py*-**L2**Pd was heated in $C_2D_2Cl_4$. Similarly, 2,6-dipropylDMAP did not undergo a substitution reaction with **L1**Pd(2,6-dipropylPy) in non-coordinating solvents (Scheme 4).

Conclusions

The practical realization and mechanistic investigation of molecular-level systems in which both the kinetics and thermodynamics of binding events can be varied and controlled is profoundly important for the development of sophisticated molecular machine systems.[7b] Although nature is clearly able to achieve this through the rapid manipulation of hydrogen bonding and electrostatic interactions, the transient nature of such weak binding events makes it hard to see how to emulate this in synthetic systems given current levels of understanding and expertise. We anticipate that metal−ligand coordination (and dynamic covalent chemistry) will play a prominent role in the early development of synthetic molecular machine systems.

Experimental Section

Synthesis of *DMAP*-L2Pd from 6 and Selected Spectroscopic Data: To a solution of **6** (0.043 g, 0.046 mmol, 1.0 equiv) in CH_2Cl_2 (30 mL) was added **L1**Pd(CH_3CN) (0.032 g, 0.046 mmol, 1.0 equiv), and the solution stirred at RT for 1 h. The solvent was removed under reduced pressure, and the crude residue was purified by column chromatography (MeOH/CH_2Cl_2, 4:96) to give the threaded pseudo-rotaxane (0.066 g, 90%). To a solution of the pseudo-rotaxane (0.054 g, 0.0304 mmol, 1.0 equiv), PPh_3 (0.013 g, 0.0509 mmol, 1.5 equiv), and **4** (0.026 g, 0.0509 mmol, 1.5 equiv) in THF (10 mL) was added DIAD (0.010 mL, 0.0509 mmol, 1.5 equiv) *via* microsyringe, and the resulting solution was stirred at RT for 36 h. After removal of the solvent under reduced pressure, the crude residue was purified by column chromatography on silica (EtOAc:CH_2Cl_2 2:3) and washed with ice-cold CH_3CN to yield *DMAP*-**L2**Pd as a yellow solid (0.025 g, yield = 29% from the pre-rotaxane, 26% from **6**). Mp 170−172 °C; ^{1}H NMR (400 MHz, $CDCl_3$): δ = 1.01−1.43 (m, 84H, *^{t}Bu-Stopper*-H + *thread-alkyl*-H + *macrocycle-alkyl*-H + H_b), 1.61−1.79 (m, 6H, *thread-alkyl*-H + *macrocycle-alkyl*-H), 2.01 (br, 4H, *thread-alkyl*-H + H_c), 2.15−2.25 (m, 2H, H_m), 2.65−3.38 (m, 14H, $H_{a+e+h+l+C}$), 3.55 (br, 2H, H_g), 3.80−3.89 (m, 4H, H_F), 3.98 (t, J = 6.3, 2H, H_n), 5.25 (br, 2H, $H_{C'}$), 5.82 (br, 1H, H_f), 6.40−6.80 (m, 13H, *stopper*-H + H_{D+E+d}), 6.93−7.02 (m, 2H, H_{i+k}), 7.05−7.11 (m, 16H, *stopper*-H), 7.19−7.25 (m, 12H, *stopper*-H), 7.45−7.53 (m, 1H, H_j), 7.83 (d, J = 7.8, 2H, H_B), 8.04 (t, J = 7.8, 1H, H_A); LRESI-MS (MeOH/CH_2Cl_2/TFA): m/z = 2075 [M^+]; HR-FABMS (3-NOBA matrix): m/z = 2075.20724 [M^+] (calcd for $C_{135}H_{168}N_6O_6{}^{106}Pd$, 2075.20601).

Preparation of *DMAP*-[L2HPd]OTs: To a solution of *DMAP*-**L2**Pd (0.0295 g, 0.0142 mmol, 1.0 equiv) in $CDCl_3$ (2 mL) was added TsOH (0.00270 g, 0.0142 mmol, 1.0 equiv), and the reaction stirred at RT until all the TsOH had dissolved (5 min). ^{1}H NMR spectroscopy revealed quantitative formation of *DMAP*-[**L2**HPd]OTs. ^{1}H NMR (400 MHz, $CDCl_3$): δ = 1.00−1.40 (m, 82H, *stopper*-H + *alkyl-thread*-H + *alkyl-macrocycle*-H), 1.59−1.77 (m, 10H, *thread-alkyl*-H + H_b), 2.03

(br, 2H, H_c), 2.19−2.31 (m, 5H, *tosyl*-H + H_m), 2.69−3.42 (m, 14H, $H_{a+e+h+l+C'}$), 3.56 (br, 2H, H_g), 3.79−3.94 (m, 6H, H_{n+F}), 5.23 (br, 2H, $H_{C'}$), 5.82 (br, 1H, H_f), 6.39−6.71 (m, 13H, *stopper*-H + H_{d+D+E}), 7.05−7.14 (m, 18H, *stopper*-H + *tosyl*-H), 7.21−7.24 (m, 12H, *stopper*-H), 7.44 (br, 2H, H_{i+k}), 7.82−7.85 (m, 4H, *tosyl*-H + H_B), 8.02−8.14 (m, 2H, H_{j+A}).

Preparation of *Py*-L2Pd *via* the Protonation-Driven Translational Isomerization and Subsequent Deprotonation of *DMAP*-[L2HPd]-OTs: *DMAP*-[**L2**HPd]OTs (0.0322 g, 0.0142 mmol) was dissolved in DMF-d_7 (1 g), and a control ^{1}H NMR spectrum acquired before the sample was heated at 383 K. The sample was monitored regularly by ^{1}H NMR spectroscopy. An equilibrium ratio of 89:11 *Py*:*DMAP*-[**L2**HPd]OTs was reached after 16 h and remained unchanged upon further heating. (Similarly, heating *DMAP*-[**L2**HPd]OTs at 383 K in $C_2D_2Cl_4$ for 36 h gave the same ratio of isomers, and subsequent heating did not alter the product distribution.) After removal of DMF-d_7 under reduced pressure, the reaction mixture was redissolved in CH_2Cl_2 (10 mL) and stirred with a large excess of Na_2CO_3 (5 g) for 30 min. Filtration through celite followed by removal of the solvent under reduced pressure gave a yellow solid. ^{1}H NMR (400 MHz, $CDCl_3$) analysis revealed that the crude residue was comprised of a mixture of *Py*:*DMAP*-**L2**Pd in an (unchanged) 89:11 ratio. The two co-conformers were separated by column chromatography on silica gel (MeOH/CH_2Cl_2 1:19) to give pure samples of both *DMAP*-**L2**Pd (identical spectroscopic and other physical data to the sample previously obtained) and *Py*-**L2**Pd. ^{1}H NMR (400 MHz, $CDCl_3$): δ = 1.07−1.43 (m, 82H, *stopper*-H + *thread-alkyl*-H + *macrocycle-alkyl*-H), 1.47−1.72 (m, 10H, *thread alkyl*-H + *macrocycle-alkyl*-H + H_g), 2.14−2.23 (m, 2H, H_b), 2.57−3.00 (m, 12H, $H_{c+e+g+l}$), 3.29−3.43 (m, 4H, H_{h+C}), 3.52−3.59 (m, 2H, H_n), 3.78−3.88 (m, 4H, H_F), 3.93−4.00 (m, 2H, H_a), 4.59 (d, J = 12.5, 2H, $H_{C'}$), 6.21−6.23 (m, 2H, H_{d+f}), 6.44−6.47 (m, 4H, H_D), 6.49−6.56 (m, 4H, H_E), 6.68−6.79 (m, 4H, *stopper*-H), 6.92 (d, J = 7.6, 1H, H_k), 7.05−7.11 (m, 16H, *stopper*-H), 7.17−7.24 (m, 13H, *stopper*-H + H_h), 7.79−7.82 (m, 1H, H_j), 7.84−7.87 (m, 2H, H_B), 8.05−8.09 (m, 1H, H_A).

Preparation of Pure *Py*-[L2HPd]OTs: To a solution of *Py*-**L2**Pd (0.0221 g, 0.0106 mmol, 1.0 equiv) in $CDCl_3$ (2 mL) was added TsOH (0.00202 g, 0.0106 mmol, 1.0 equiv), and the reaction stirred at RT until all the TsOH had dissolved (5 min). ^{1}H NMR spectroscopy revealed quantitative formation of *Py*-[**L2**HPd]OTs. ^{1}H NMR (400 MHz, $CDCl_3$): δ = 1.47−1.66 (m, 82H, *stopper*-H + *thread-alkyl*-H + *macrocycle-alkyl*-H), 1.58−1.81 (m, 10H, *thread-alkyl*-H + *macrocycle-alkyl*-H + H_m), 2.16−2.32 (m, 5H, *tosyl*-H + H_b), 2.53−2.63 (m, 2H, H_l), 2.83−3.26 (m, 12H, $H_{c+e+g+C}$), 3.40−3.53 (m, 4H, H_{h+n}), 3.79−3.90 (m, 6H, H_{a+F}), 4.74 (d, J = 13.9, 2H, $H_{C'}$), 6.28 (d, J = 7.6, 2H, H_{d+f}), 6.42−6.57 (m, 8H, H_{D+E}), 6.66−6.71 (m, 4H, *stopper*-H), 6.88 (d, J = 7.3, 1H, H_k), 7.02−7.15 (m, 19H, *stopper*-H + *tosyl*-H + H_i), 7.18−7.26 (m, 12H, *stopper*-H), 7.80−7.86 (m, 5H, tosyl-*H* + H_{j+B}), 8.06−8.10 (m, 1H, H_A), 14.00 (br, 1H, *DMAP*-H).

Preparation of *DMAP*-L2Pd *via* Translational Isomerization of *Py*-L2Pd: Rotaxane *Py*-**L2**Pd was heated to 110 °C in DMF-d_7 (1 g) and monitored *via* ^{1}H NMR spectroscopy at regular intervals. A ratio of 86:14 *DMAP*:*Py*-**L2**Pd was established after 1.5 h, and further heating did not alter this ratio. Upon heating pure *Py*-**L2**Pd to 110 °C in $C_2D_2Cl_4$, no isomerization was observed, even after 7 days of heating at 383 K.

X-ray Crystallographic Structure Determinations. Single crystals of **L1**Pd(2,6-dipropylPy) and **L1**Pd(2,6-dipropylDMAP) of suitable quality for X-ray diffraction studies were grown by the vapor diffusion of Et_2O into CH_2Cl_2 solutions of the complexes. Structural data for both **L1**Pd(2,6-dipropylPy) and **L1**Pd(2,6-dipropylDMAP) were collected at 93 K using a Rigaku Mercury diffractometer (MM007 high-flux RA/Mo Kα radiation, confocal optic). All data collections employed narrow frames (0.3−1.0) to obtain at least a full hemisphere of data. Intensities were corrected for Lorentz polarization and absorption effects (multiple equivalent reflections). The structures were solved by direct methods, and non-hydrogen atoms were refined anisotropically with CH protons being refined in riding geometries (SHELXTL) against F^2. **L1**Pd(2,6-dipropylDMAP): $C_{46}H_{61}N_5O_4Pd$, M_r = 854.40, yellow prism, crystal size = 0.08 × 0.08 × 0.08 mm^3, monoclinic, $P2_1/c$, a = 18.098(2) Å, b = 18.151(2) Å, c = 12.7405(14) Å, β = 91.62(3)°, V = 4183.6(8) Å^3, Z = 4, ρ_{calcd} = 1.357 Mg m^{-3}; μ = 0.493 mm^{-1}, 27 337 data (7572 unique, R_{int} = 0.0510), R = 0.0512 for 6199 observed data, wR_2 0.1268, S = 1.125 for 506 parameters. Residual electron density 1.273 and −1.090 eÅ^{-3}. **L1**Pd(2,6-dipropylPy): $C_{44}H_{56}N_4O_4Pd$, M_r = 811.33, yellow prism, crystal size = 0.05 × 0.03 × 0.03 mm^3, monoclinic, $P2_1/c$, a = 14.437(6) Å, b = 18.314(6) Å, c = 16.522(6) Å, β = 112.17(9)°, V = 4045(3) Å^3, Z = 4, ρ_{calcd} = 1.332 Mg m^{-3}; μ = 0.505 mm^{-1}, 26 021 data (7361 unique R_{int} = 0.2872), R = 0.0937 for 3061 observed data, wR_2 = 0.1982 S = 0.953 for 479 parameters. Residual electron density 1.263 and −0.812 eÅ^{-3}. CCDC 651736 and 651737 contain the supplementary crystallographic data for this paper. These data can be obtained free of charge from the Cambridge Crystallographic Data Centre via www.ccdc.cam.ac.uk/data_request/cif.

Acknowledgment. This work was financed by the EU project SingleMotor-FLIN and the EPSRC. We also thank the Ramsay Memorial Trust (J.D.C.), EPSRC (D.A.L.), Royal Society (P.J.L.), Deutscher Akademischer Austausch Dienst (C.P.), and the Swiss National Science Foundation (L.-E.P.-A.) for their generous support through various fellowship schemes.

Supporting Information Available: Experimental procedures and spectroscopic data for all new compounds, details of the model heterocycle exchange experiments, the protonation/deprotonation-driven shuttling experiments, and full crystallographic details of **L1**Pd(2,6-dipropylPy) and **L1**Pd(2,6-dipropylDMAP). This material is available free of charge via the Internet at http://pubs.acs.org.

JA076570H